UNIVERSITÀ
DEGLI STUDI
DI PADOVA

UNIVERSITA' DEGLI STUDI DI PADOVA

DIPARTIMENTO DI MEDICINA MOLECOLARE

SCUOLA DI DOTTORATO DI RICERCA IN MEDICINA MOLECOLARE

INDIRIZZO DI MEDICINA RIGENERATIVA

CICLO XXVIII

CARDIOMYOCYTES GENERATION BY PROGRAMMING HUMAN PLURIPOTENT STEM CELL FATE IN MICROFLUIDICS: FROM WNT PATHWAY MODULATORS TO SYNTHETIC MODIFIED mRNA

Direttore della Scuola : Ch.mo Prof. Stefano Piccolo

Supervisore :Ch.mo Prof. Stefano Piccolo

Co-Supervisore: Ch.mo Prof. Nicola Elvassore

Dottoranda : Anna Contato

La cosa migliore che tu possa fare
è credere in te stessa.
Non avere paura di tentare.
Non avere paura di cadere.
E se capitasse,
levati la polvere di dosso,
rialzati e prova ancora.

The greatest thing you could ever do,
is believing in yourself.
Don't be afraid of trying.
Don't be afraid of falling.
And if that happens,
Dust yourself off,
Raise and try again.

Mother Teresa of Calcutta

Table of Contents

Sommario

Le malattie cardiovascolari rappresentano ad oggi una delle principali cause di morbidità e mortalità nel mondo, tra le quali la patologia ischemica è responsable del maggior numero di decessi negli ultimi 10 anni. L'elevato impatto determinato da tali patologie, sia acute che croniche, e gli elevati costi per i sistemi sanitari, richiedono lo sviluppo di nuove strategie terapeutiche.

La questione principale riguardante gli attuali approcci terapeutici, sia farmacologici sia interventistici, è rappresentata dalla loro incapacità di compensare l'elevata ed irreversibile perdita di cardiomiociti funzionali. A causa della limitata capacità rigenerativa dei cardiomiociti post-natali e della difficoltà di reperire ed isolare tessuto cardiaco bioptico, scarse sono le fonti di tali cellule disponibili per uno studio dedicato. Tra l'altro, anche se i modelli animali ancora oggi rappresentano sicuramente lo stumento migliore per studiare e comprendere *in vivo* i meccanismi alla base dello sviluppo di specifiche patologie umane, nel constesto di un organismo complesso, essi non sono completamente predittivi e rappresentativi della condizione umana analizzata; da un punto di vista economico, il mantenimento di tali animali e le relative sperimentazioni, richiedono molto tempo e costi elevati.

In questo scenario, le cellule staminali umane pluripotenti (hPSCs), comprese le cellule staminali embrionali (hESCs) e le cellule staminali pluripotenti indotte (hiPSCs), rivestono un ruolo importante nella ricerca cardiovascolare perché possono essere espanse in coltura indefinitamente, senza perdere la loro staminalità, e differenziare nelle cellule che componogono i tre foglietti germinativi, come ad esempio i cardiomiociti. Un'importante svolta nella ricerca scientifica è avvenuta nel 2007, con la scoperta delle hiPSCs da parte del Premio Nobel Shinya Yamanaka. Ciò ha rappresentato il punto di partenza per derivare hiPSCs paziente-specifiche attraverso il reprogramming di cellule somatiche ottenute con procedure mini- o non-invasive (derivate da biopsie cutanee, sangue, urina…), utili per generare tessuti per una riparazione autologa, evitando i prblemi etici e politici relativi alla derivazione delle hESCs. Notevoli studi sono stati condotti dai ricercatori nel tentativo di sviluppare strategie che efficientemente ed in maniera robusta guidino il differenziamento cardiaco delle hPSCs, basate sulla perturbazione stadio-specifica di differenti vie di segnalazione, mediante l'uso di fattori di crescita e piccole molecole, che ricapitolano i punti essenziali dello sviluppo cardiaco osservato *in vivo*. Tuttavia, questi metodi sono accompagnati da

alcune limitazioni, quali: elevata variabilità intra ed inter-sperimentale, presenza di xeno-contaminanti, componenti indefinite nei medium di coltura e differenze nei livelli di espressione di citochine endogene. Altre strategie si basano invece sulla conversione diretta di cellule somatiche, specialmente fibroblasti, attraverso l'overespressione di una combinazione di fattori di trascrizione cardiaci mediante vettori integrativi e non-integrativi; tuttavia, anche tali approcci sono caratterizzati da basse efficienze nella generazione di cardiomiociti, associate al rischio di integrazioni genomiche e mutagenesi inserzionale nel caso dei vettori integrativi, o alla necessità di effettuare diversi step di purificazione quando si ultilizzano sistemi non-integrativi. Pertanto, a causa delle difficoltà dei sistemi convenzionali di coltura nel dirigere specificamente ed in maniera robusta il differenziamento cardiaco delle hPSCs, assieme alla scarsa capacità di riprodurre *in vitro* l'ambiente in cui le cellule risiedono *in vivo*, i cardiomiociti prodotti attualmente sono immaturi e più simili allo stadio fetale di sviluppo.

Nel 2010 Warren L. ed il suo gruppo di ricerca ha sperimentato per la prima volta una tecnologia innovativa di tipo non-integrativo basata su trasfezioni ripetute con lipidi cationici di RNA messaggeri modificati sinteticamente (mmRNA) per evitare la risposta immunitaria innata da parte delle cellule; egli ha dimostrato la possibilità sia di riprogrammare cellule somatiche allo stato pluripotente, sia di programmare il differenziamento miogenico di hiPSCs.

Pertanto, lo scopo di questa tesi di dottorato è quello di sviluppare un metodo robusto ed efficiente per il differenziamento cardiaco di hPSCs combinando gli mmRNA con la tecnologia microfluidica. Ripetute trasfezioni di mmRNA codificanti per 6 fattori di trascrizione coinvolti nello sviluppo e nel funzionamento cardiaco, vengono impiegate per forzare l'espressione proteica endogena delle cellule e per guidare il differenziamento verso la maturazione funzionale dei cardiomiociti. L'integrazione del differenziamento cardiaco in una piattaforma microfluidica *ad hoc*, prodotta nel laboratorio BioERA, consente un controllo più preciso delle condizioni di coltura garantendo un'elevata efficienza di trasfezione degli mmRNA grazie all'elevato rapporto superficie/volume e permette la riproduzione *in vitro* di nicchie fisiologiche. Infatti, la miniaturizzazione consente di mimare al meglio le dinamiche cellulari che avvengono *in vivo* nel microambiente solubile. Le tecnologia microfluidica offre la possibilità di effettuare esperimenti combinati, multiparametrici e paralleli in una sola volta e con elevato rendimento a costi ridotti, non realizzabili nei macroscopici e costosi sistemi di coltura convenzionali.

Il Capitolo 1 inizia con la definizione di medicina rigenerativa e introduce la complessità dello sviluppo cardiaco ed il network di fattori di trascrizione che cooperano durante questo processo. Viene poi descritto lo stato dell'arte relativo alle strategie per l'ottenimento di cardiomiociti da hPSCs e al transdifferenziamento cardiaco di cellule somatiche, insieme alle relative limitazioni e alle problematiche attuali da risolvere. Infine viene presentato lo scopo generale di questa tesi di dottorato.

Il Capitolo 2 si focalizzerà sulle hPSCs (sia hES sia hiPS) impiegate durante questo progetto, descrivendo le caratterisatiche principali di tali cellule. Verrà inoltre presentato un protocollo di differenziamento cardiaco di hPSCs in monostrato che attualmente è considerato il gold standard per ottenere velocemente un'elevata resa di cardiomiociti contrattili in supporti di coltura convenzionali. Tale protocollo si basa sulla modulazione del pathway canonico di Wnt attraverso l'applicazione di due piccole molecole. Inoltre, una linea di hES, doppio reporter per 2 fattori di trascrizione cardiaci, verrà descritta ed impiegata in tutti gli esperimenti come strumento per monitorare l'andamento del differenziamento cardiaco delle hPSC. I risultati ottenuti in colture standard verranno mostrati.

Il Capitolo 3 esaminerà lo stato dell'arte della tecnologia microfluidica nelle applicazioni di medicina rigenerativa, sottolineando i vantaggi derivanti dalla combinazione della microtecnologia con la biologia cellulare. Verrà successivamente descritta la fabbricazione della piattaforma microfluidica utilizzata, con la successiva ottimizzazione della coltura, espansione e differenziamento cardiaco gold standard delle hPSCs conseguenti alla conversione dalla macro- alla microscala.

Il Capitolo 4 introdurrà la nuova strategia degli mmRNA per la riprogrammazione e la programmazione cellulare: anche in tal caso verrà discusso lo stato dell'arte. In seguito, verranno presentate le strategie sperimentali sviluppate per programmare il differenziamento cardiaco delle hPSCs verso un fenotipo più maturo dei cardiomiociti, insieme ai risultati ottenuti con le relative caratterizzazioni strutturali, funzionali e molecolari. In questo lavoro, per la prima volta, è stato possibile ottenere cardiomiociti da hPSCs attraverso ripetute trasfezioni di mmRNA per 6 fattori di trascrizione cardiaci in microfluidica, con efficienze superiori rispetto ai metodi presenti attualmente in letteratura, svolti in sistemi convenzionali.

Il Capitolo 5 infine presenterà la discussione e le conclusioni generali, assieme alle prospettive future riguardanti l'uso degli mmRNA combinati con la

microfluidica per ottenere diversi fenotipi di cardiomiociti, variando la combinazione di fattori di trascrizione veicolati. In conclusione, gli esperimenti sviluppati in questo progetto di dottorato forniscono un proof-of-principle della possibilità di programmare con gli mmRNA il destino delle hPSCs verso il differenziamento e la maturazione di cardiomiociti funzionali in microfluidica; inoltre, essendo gli mmRNA una strategia non-integrativa , i cardiomiociti ottenuti in questo modo possono essere impiegati nel prossimo futuro per applicazioni cliniche di ricostruzione tissutale autologa e per screening farmacologici personalizzati.

Summary

Cardiovascular disease (CVD) is still one of the major cause of morbidity and mortality in the world, with ischemic heart disease representing the majority of deaths over the past 10 years. The high burden of the disease, both immediate and chronic, associated with the high costs for the healthcare systems, claim for the development of novel therapeutic strategies. The main issue of current pharmacological and interventional therapeutic approaches is their inability to compensate the great and irreversible loss of functional cardiomycytes (CMs). Because of the limited regenerative capacity of post-natal CMs and the difficulty to obtain and isolate heart bioptic tissue, very limited supplies of these cells are available at present for dedicated studies. Moreover, even if animal models are surely the best tool to study and understand *in vivo* the mechanisms of specific human pathologies in a complex organism, they are not fully predictive and representative of the human condition; from an economic point of view, animal maintenance and the related experimentations are time consuming and very expensive.

In this scenario, human pluripotent stem cells (hPSCs), including human embryonic (hESCs) and human induced pluripotent stem cells (hiPSCs), play an important role in the cardiovascular research field, because they can be indefinitely expanded in culture without loosing their stemness, and differentiated into cells of the three germ layers, such as CMs. A great breakthrough in science has occurred in 2007 with the discovery of hiPSCs by the Nobel Prize Shinya Yamanaka. This has been the starting point for deriving patient-specific hiPSCs from the reprogramming of somatic cells obtained with less- or non-invasive procedures (skin biopsies, blood, urine…), useful for the generation of tissues for autologous-repair, bypassing the ethical and political debates surrounding the hESCs derivation.

The researchers have made several efforts to develop strategies to efficiently direct hPSCs cardiac differentiation and the existing methods for deriving CMs involve stage-specific perturbations of different signaling pathways using growth factors (GFs) or small molecules that recapitulate key steps of the cardiac development observed *in vivo*. However, these strategies are accompanied by some limitations including: high intra- and inter-experimental variability, low efficiencies, presence of xeno-contaminants, undefined medium components and differences in the expression of cytokines of endogenous signaling pathways.

Other strategies are based on the direct lineage conversion of somatic cells, especially fibroblasts, *via* the overexpression of cardiac transcription factors (TFs) combinations through integrating and non-integrating vectors. However, also these approaches are characterized by low efficiencies, combined with the risk of genomic integration and insertional mutagenesis when using integrating vectors or the need for stringent steps of purification when using non-integrating techniques. Because of the difficulty to specifically direct hPSCs cardiac fate in a robust way, combined with the scarce ability of conventional culture systems to reproduce *in vitro,* the environment in which cells reside *in vivo*, the CMs produced to date are immature and more similar to fetal cardiac cells.

In 2010, Warren L. and co-workers pioneered a novel, non-integrating strategy based on repeated transfection with cathionic vehicles of synthetic modified messenger RNA (mmRNA), specifically designed to avoid innate immune response from the cell, demonstrating the possibility to both reprogram somatic cells to pluripotency and to programm hPSCs fate into terminally differentiated myogenic cells.

Hence, the aim of this PhD thesis is the development of an efficient and robust method for cardiac differentiation of hPSCs by combining the mmRNA with the microfluidic technology. Repeated transfections with mmRNA encoding 6 cardiac TFs are employed to force the endogenous protein expression in the cells and to drive the differentiation toward functional maturation of CMs. The integration of cardiac differentiation within an *ad hoc* microfluidic platform, facbricated in BioERA laboratory, allows a more precise control of culture conditions, enabling a high mmRNA transfection efficiency, thanks to the high volume/surface ratio, and the *in vitro* reproduction of physiological niches. In fact, the small scale offered by microfluidics, best mimics the cellular dynamics, which occur in the soluble microenvironment *in vivo*. Moreover, the microfluidic technology offers the possibility to perform combinatorial, multiparametric, parallelized and highthroughput experiments at one time in a cost-effective manner, not achievable and not economically sustainable in macroscopic conventional culture systems.

Chapter 1 starts with the definition of regenerative medicine and introduces the complexity of cardiac development, with the network of TFs that cooperate in this process. The state of the art regarding the derivation of CMs from hPSCs and from the transdifferentiation of somatic cells is described, together with the

current limitations and challenges. Finally, the general aim of this PhD thesis is presented.

Chapter 2 will focus on hPSCs (hES and hiPS) employed during this project, describing their most important characteristics. It will be also presented a monolayer-based cardiac differentiation protocol of hPSCs that, to date is considered the gold standard for the fast generation of a high yield of beating CMs in conventional culture systems. This protocol relies on the temporal modulation of Wnt pathway via the administration of small molecules. In addition, a hES line, dual reporter for 2 cardiac TFs will be described and always adopted as a tool to monitor the progression of cardiac differentiation. The results obtained in standard cultures will be showed.

Chapter 3 will review the state of the art of microfluidic technology for cell culture in regenerative medicine applications. Then, the microfluidic platform fabrication will be described and employed, followed by the optimization of culture, expansion and cardiac differentiation of hPSCs with the gold standard protocol deriving form the translation from macro- to micro-scale.

Chapter 4 will introduce the novel mmRNA strategy for reprogramming and programming cell fate: also in this case the state of the art will be discussed. Then, the experimental strategies developed to program cardiac differentiation of hPSCs toward a more mature CM phenotype will be presented, together with the results obtained and the related structural, functional and molecular characterizations. In this work, for the first time, it has been possible to derive CMs from hPSCs with repeated transfections of mmRNA encoding 6 cardiac TFs in microfluidics, with efficiencies higher to current methods described in literature, performed in standard systems.

Finally, Chapter 5 will present the general discussion and conclusions, with the future perspectives regarding the use of mmRNA combined with microfluidic technology for deriving different CMs phenotypes, just varying the combination of TFs delivered.

To conclude, the experiments developed during this project provide proof-of-principle that it is possible to program hPSCs fate toward cardiac lineage and cardiac maturation in microfluidics; moreover, thanks to the non-integrating characteristic of mmRNA, the CMs obtained are clinical-grade and could potentially be employed in the next future for clinical applications of autologous tissue self-repair and for personalized drug screening.

Foreword

The work presented in this PhD thesis was performed at the Department of Industrial Engineering (DII) of the University of Padova and the Venetian Institute of Molecular Medicine (VIMM), "Fondazione per la Ricerca Biomedica Avanzata onlus" of Padova under the supervision of Professor Nicola Elvassore.

I came in BioERA laboratory at the beginning of the 2nd year of PhD, after changing completely my research project. During my time as PhD student, I could apply engineering tools to my medical biotechnological background, having the possibility to explore and enjoy new and unexpercted biology/engineering cross-talks.

I would like to thank my Supervisor, Professor Stefano Piccolo, for the great opportunity to work in this multi- and interdisciplinary environment and to open my mind to challenging situations.

I would also like to thank my PhD co-tutor, Professor Nicola Elvassore, for welcoming me in his research group and for the possibility to test me with this innovative and challenging project, which has represented also a great struggle against time. He made me cry all my tears but this has strengthen myself; I will never forget it.

I thank Dr. Elena Serena for her scientific support.

Mandatory heartfelt thanks are due to the group members of BioERA laboratory, in which I found real friends instead of simple colleagues, with special mentions for:

-Alice Zoso for her sensitivity and her big and generous heart, for always being close to me despite the kilometers of distance;

-Giovanni G. Giobbe for his contagious joy and for made me laugh a lot, especially in grey days;

-Sebastian Martewicz for his precious advice and the great support in all the situations; for made me always work in the safest conditions as possible…and for the funny Rhodigium dialect lessons;

-Lia Prevedello for her inner strength and for being a free spirit as I am;

-Stefano Giulitti for his infinite knowledge and utmost precision… and for all the week-ends spent under the safety cabinet.

-Federica Michielin for supporting me scientifically and personally and for helping diluting my anxiety;

-Massimo Vetralla because he is a good person and a strongman;

-Silvia Galvanin for her trustworthiness and for always helping everyone;
-Ida Maroni for supporting me in a difficult moment of my life;
-Michele Zanatta for all the great moments of fun and laughts, for the "high five" to encourage me to face the bad situations.

A special thanks is for Erika Torchio, one of the most beautiful person I have met in my life, for sharing every instant of these intense PhD years, living closely to one another with "bread, water and transfections", day-dreaming on our future and projects…and for being an excellent cook!

Thanks to Maria Elena "Nena" Ricci Signorini for her wonderful and sparkling personality and for all the reassuring hugs.

Thanks to Giulia Selmin for her kindness, for putting her heart and soul into everything and for all her extraordinary passions.

Finally, many thanks are due to all the students who passed through the BioERA lab; everyone of them is special and gave me so much.

Thanks to everyone of you because, at the end,
It is the Heart that matters.

All the material reported in this dissertation is original unless explicit references to studies carried out by other people are indicated.

During the period of the PhD program, I had the opportunity to present my research results at national congresses:

- Research activity presentation; Macroarea 2- Life Sciences-Medical Area- "Directing hiPSCs fate: strategies for cardiomyocytes differentiation from monolayer-based protocols to synthetic modified mRNA". Aula Magna, Palazzo Carlo Bo, October 20th 2014.
- Abstract and poster presentation, 13th VIMM annaul Meeting: "Directing cardiac and myogenic hiPS differentiation with modified mRNA"; Preganziol (TV), February 6th-7th 2015.
- A manuscript concerning my reseaech activity is in preparation.

Acknowledgements

Last but not least, I take this opportunity to thank the people I love the most, to whom this thesis is dedicated. My mother Graziella and my father Mario for always supporting me in every moment and for every choice I made; for always believeing in me, also when I was going to give up on everything. They are for me an example of life.

Thanks to my grandmother Ida for being there for such important goal in my way and for being an example of serenity and peace of mind.

Heartfelt thanks to my boyfriend Massimiliano who I love in such way that is impossible to describe by words, for making me always happy and for making my life a masterpiece. Without him, probably I would not have finished this intense, diffcult but also constructive experience. Thanks also to his family for always being close to me.

Finally, thanks to my beautiful family, cats included, which represents what really matters in life and which taught me that happiness resides in everyday little things.

For all of these things and even more, I consider myself a very lucky and rich person.

Chapter 1.
Introduction: strategies for cardiac regeneration

This Chapter introduces the concept of Regenerative Medicine, which is the curriculum of my PhD School in Biomedicine, focused on the development of strategies for cardiac regeneration. The Chapter continues describing the complexity of cardiac development and formation, and the network of transcription factors (TFs) involved is studied to better understand cardiogenesis. Then, the evolution of cardiac regeneration approaches and the current state of the art are presented, with the new perspectives offered in this field by the derivation of cardiomyocytes (CMs) from human pluripotent stem cells (hPSCs), which recapitulate in vitro the cardiac development stages. Finally, the principal strategies for the differentiation of hPSCs into CMs are described, highlighting also the current limitation and challenges of hPSC-derived CMs for in vitro studies. Finally, the aim of this thesis is presented.

1.1. Regenerative Medicine

'The development of cell lines that may produce almost every tissue of the human body is an unprecedented scientific breakthrough. It is not too unrealistic to say that stem cell research has the potential to revolutionize the practice of medicine and improve the quality and length of life'.

"Harold Varmus, National Institute of Health and 1989 Nobel Laureate in Physiology or Medicine; testimony before the U.S. Senate Appropriations Subcommittee on Labor, Health and Human Services, Education and Related Agencies, December 2nd, 1998" [1].

Human beings have always been fascinated with tissue regeneration, especially from the observation of this phenomenon in some species of fishes and newts, while they are not able to do the same. In the last decade major advances in stem cell biology, created genuine hope for the emerging discipline of regenerative medicine [2].

Regenerative medicine is a new branch of medicine which studies how to regenerate damaged, tired or failing organ caused by age, diseases, injuries, or genetic defects. This field aims at stimulating the healing of organs considered irreparable and, in order to regenerate tissues suitable for clinical implantation, scientists generate and grow them *in vitro*.

Organ transplantation and autologous tissue transplantation remain a gold standard of treatment in case of severely compromised organ function; however, limited availability is one of the major issue, especially for elderly patients. In the last two decades, as a response to the requirements of these tissues, scientists have made several efforts to grow stem cells for generating new tissues using tissue engineering and regenerative medicine techniques for restoring tissues of the human body.

Regenerative medicine can be considered in fact a multidisciplinary field that requires exchange of knowledge of a wide variety of scientific disciplines: expertise in cell and molecular biology, physiology, chemical engineering, biomaterials, nanotechnologies, pharmacology and clinical sciences have to collaborate. These approaches will use soluble molecules, stem cells, tissue engineering approaches and the reprogramming and programming of cells and tissue types [1]. The development rate of new strategies, together with the decreasing of costs represent a recurring critical point encountered in regenerative medicine. Whitesides G.M. defines microfluidics as "the science and technology of systems that process or manipulate small amounts of fluids

(10^{-9} to 10^{-18} liters), using channels with dimensions of tens to hundreds of micrometres"[3][4]; this technology is a useful tool for developing novel, more representative *in vitro* models. Microfluidic devices have found applications in cell-based screens to deeply understand fundamental biological processes and for drug tests, with advantages over conventional cell culture systems: it allows in fact, a spatiotemporal control of fluid dynamycs and physical parameters, streamlining the regenerative medicine research, thanks to the ability to provide high-throughput multiplexed platforms, allowing the parallelization of the assays as well as automation at the same time [4].

Since the heart is one of the last regenerative organs in the body, cardiac regenerative medicine applications could bring great benefits [2]; for this reason, this work aimed at coupling the potential of pluripotent stem cells field and the cell fate programming with the microtechnologies to allow the development of functional and mature cardiac tissue on-a-chip, as *in vitro* disease model or drug screening and toxicity assays.

1.2. The human heart

Before starting with the analysis of the strategies for cardiac regeneration, it is necessary to have the whole picture of the human heart physiology, cardiomyogenesis with the network of signalling pathways and transcription factors involved. The human heart has the function of pumping blood in the organism in order to provide oxygen and nutrients to tissues and to remove waste products. The heart possesses four chambers, two upper atria, and two lower ventricles. The heart itself can be divided into right heart, formed by the right atrium and right ventricle, and the left heart, constituted by left atrium and ventricle, separated by the septum. The pericardium is a double walled sac that envelops the heart to protect it. Between the parietal pericardium (outer) and the serous pericardium (inner), flows the pericardial fluid, which lubricates the heart to soften contractions and movements of the surrounding lungs and diaphragm. The external wall of the heart is composed by three layers: the outermost is the epicardium (inner face of pericardium); the middle layer is myocardium with its contracting muscles and the inner one is the endocardium in contact with blood [5] (Figure 1.1).

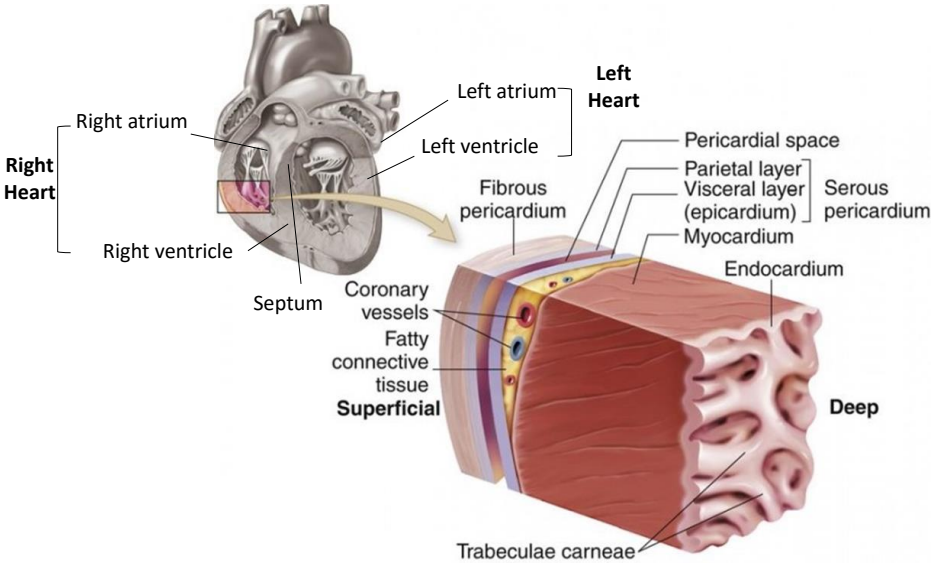

Figure 1.1: *Human heart with the four chambers, atria and ventricles. The magnification shows a section of the heart wall, composed by three layers: the epicardium (outer), the myocardium (middle), and the endocardium (inner (modified from [6]).*

This work focuses on the cardiac muscle, specifically the myocardium, which is a three-dimensional arrangement of rod-shaped cardiomyocytes (CMs) [7] attached to each other and forming myofibers. Only 20-40% of the cells in the heart is represented by CMs but they cover 80-90% of the organ volume [8]. Myofibers are in contact with interstitial fibroblasts, blood vessels and the extracellular matrix, within a proteoglycan gel matrix [9]. The CMs form a three-dimensional syncytium (atrial and ventricular) that enables propagation of electrical signals across the gap junctions to coordinate contractions that pump blood to the body. The contractile apparatus (Figure 1.2) of each CM is the sarcomere that possesses a bundle of myofibrils aligned in parallel in the cytoplasm; it contains several contractile proteins such as actin and myosin and the accessory proteins, troponin and tropomyosin, which form the thin and thick filaments. [10].

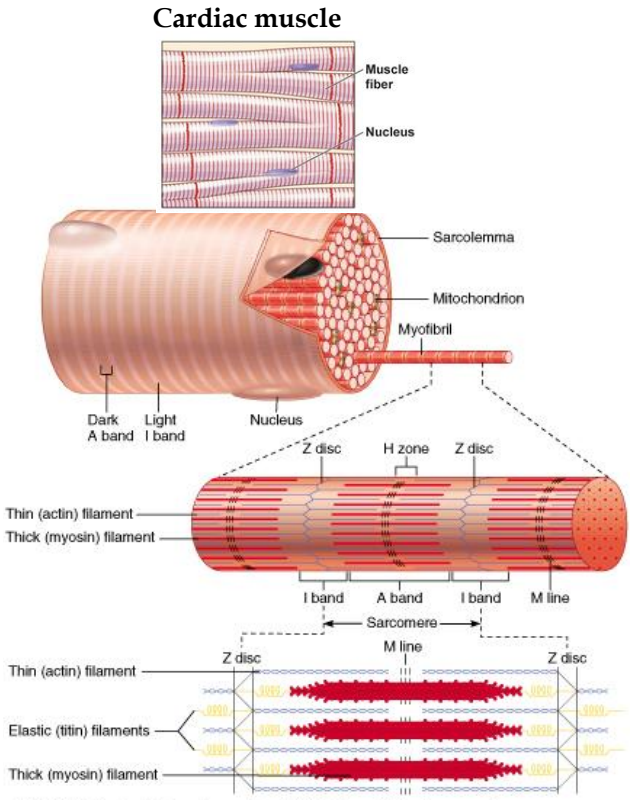

Figure 1.2: *Cardiac myofibril cylinder, with single tandem line of sarcomere (banded pattern). At the top of the image is represented a section of multi-nucleated striated cardiomyocyte. One sarcomere goes from one Z-band to the adjacent one: the thicker myofilaments are composed of myosin, crossing the A bands, while the thinner filaments are mainly represented by of actin, and extends from the Z lines through the I band into the A band (modified from [11]).*

CMs propagate synchronous contractions of the electrical impulse thanks to their connection *via* intercalated discs. Groups of specialized pacemaker CMs generate a wave of electrical excitation from one cell to the adjacent causing a coordinated atrial-ventricular rhythmic contraction. The CM excitation is followed by an increase of cytoplasmic calcium that triggers mechanical contractions, the so-called calcium-induced calcium release (CICR), giving the calcium sparks [12]. Precisely, in a resting phase, a myocardial cell has a negative membrane potential; after the initiation of the action potential by pacemaker cells, the subsequent depolarization determines the extracellular Ca^{2+} influx *via* the voltage-gated ion channels. The following increase in intracellular Ca^{2+} leads to the binding of the ion with troponin C, moving the tropomyosin complex off the actin binding site. The myosin head can now bind to the actin filament [13]. Using ATP hydrolysis, the myosin head pulls the actin filament toward the centre of the sarcomere,

generating the contraction. Intracellular Ca^{2+} is re-uptaken into the sarcoplasmic reticulum (SR), ready to begin a new cycle. After the absolute refractory period, potassium channels reopen, K^+ exits from cells which return the resting state [14] (Figure 1.3).

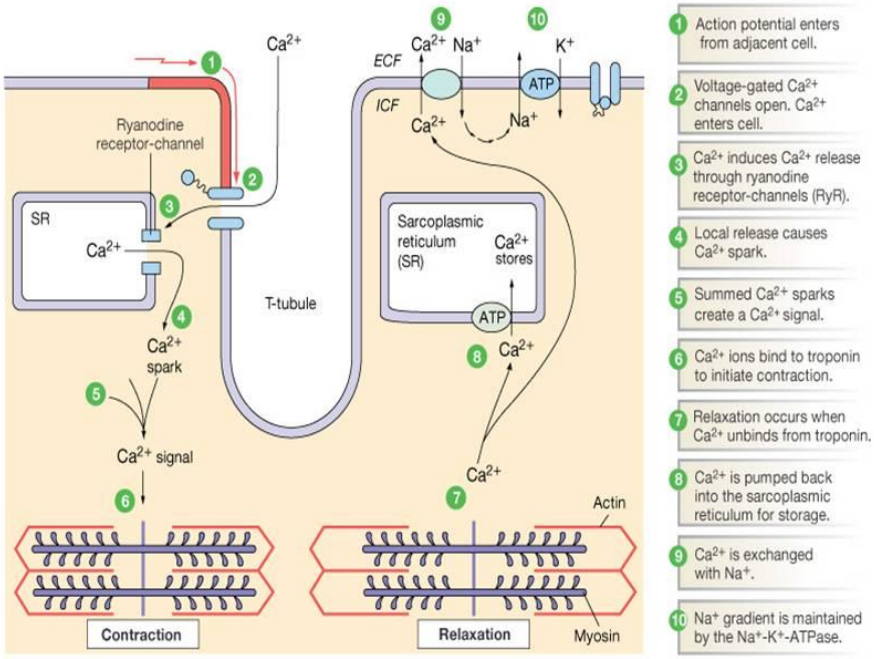

Figure 1.3: *Scheme of excitation-contraction (EC) coupling in CMs. ECF, Extra-Cellular Fluid; ICF, Intra-Cellular Fluid (adapted from [15]).*

As regards the metabolic requirements of the CMs, during the early phase of embryogenesis, the uterine environment in which the fetal heart develops and grows is oxygen-poor, with carbohydrates representing the primary source of energy[16]. The subsequent maturation determines an oxygen increase and oxidative phosphorylation begins to supply additional energy required by the growing and maturing heart, with a shift to long-chain fatty acids as the primary energy source[16][17][18].

1.2.1. Cardiomyogenesis and cardiac Transcription Factors network

The induction and specification of cardiac progenitor cells within the anterior lateral mesoderm is the strating point of the mammalian heart development [19]. Around day 15 of human embryonic development [20], the cardiac mesoderm gives rise to the endocardium, the First Heart Field (FHF,

forming the atria, left ventricle, and the nodal conduction system), the Secondary Heart Field (SHF, which forms the right ventricle, outflow tract, and part of the atria), and the proepicardial mesenchyme [21][22]. The FHF is composed by cells that differentiate, whereas cells of the SHF (expressing the Insulin gene enhancer protein 1, ISL1) maintain an undifferentiated state, because of inhibitory Wingless integrated (Wnt) signals [21][23]. After approximately 3 weeks of human development, a primitive heart tube begins to be formed and undergoes rightward looping, with cells from the SHF added to both the inflow and outflow poles. After this point, approximately during the 6th and 7th weeks of human gestation, the formation of the outflow tract (OFT) and the atrioventricular canal (AVC) begins [19][24]. The early cardiac conduction system also begin to be specified, while neural crest and proepicardium give important contributions to the developing heart. Proceeding to later stages, the heart undergoes extensive remodelling to reach the mature, definitive architecture [19][25]. Figure 1.4 shows the several stages of heart development.

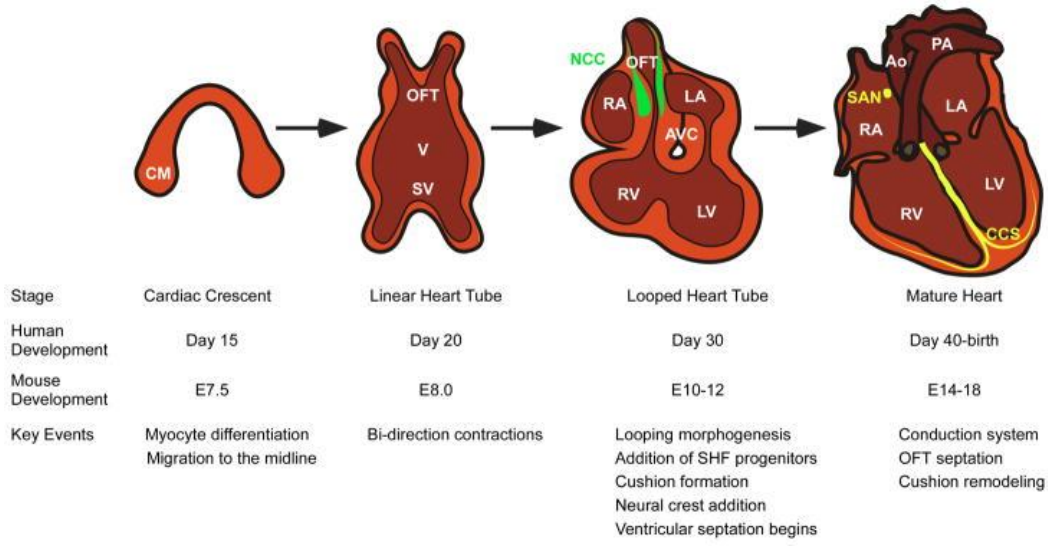

Figure 1.4: *Schematic representation of the stages of mammalian heart development in mouse and human heart shown in parallel. Mouse development is indicated in embryonic days (E). Ao, aorta; AVC, atrioventricular canal; CM, cardiac mesoderm; LA and LV, left atrium and ventricle respectively; NCC, neural crest cells; OFT, outflow tract; PA, pulmonary artery; RA and RV, right atrium and ventricle respectively; SAN, sinoatrial node; SV, sinus venosus; V, ventricle (adapted from [19]).*

The deep comprehension and knowledge of cardiogenesis in the early embryo is of paramount importance for the development of *ad hoc* differentiation strategies for cardiac repair [21]. The study of cardiogenesis in fact allows access to the networking and cooperating genes involved in heart development [21].

The first stage of cardiomyogenesis is the generation of mesoderm via the process of gastrulation, a process deeply studied in the mouse, as a model for human cardiac development [21][22][26].

Three families of extracellular signalling molecules control and orchestrate the induction of mesoderm formation and specification into cardiac mesoderm: Wingless integrated (Wnt), Fibroblastic Growth factor (FGF) and Transforming Growth Factor-beta (TGF-β) superfamily ligands, which include WNT3A, Bone Morphogenetic Protein 4 (BMP4), Nodal and Activin A. These ligands are expressed in gradients, sending activating as well inhibitory signals to the underlying cells, in a spatiotemporal manner [27][28]. Briefly, mesoderm induction firstly starts with Nodal signaling in the proximal epiblast, approximately on human embryonic day 12, confining BMP4 expression in the extraembryonic ectoderm. BMP4 induces the expression of Wnt3a in the proximal epiblast. In the anterior visceral endoderm, the expression of the Wnt antagonist Dikkopf 1 (DKK1) and the Nodal antagonists Lefty 1 and Cer 1, confines Nodal and Wnt signalling to the posterior epiblast. At this developmental stage, Wnt induces the expression of mesendodermal markers such as Brachyury T (T) and Eomesodermin (EOMES). Subsequently, FGF4 and FGF8, which are responsible of mesoderm patterning and epithelial-mesenchymal transitions (EMTs), are expressed in the developing primitive streak. T and EOMES determines the expression of Mesoderm Posterior 1 (MESP1), which has been identified as the "master regulator" of cardiac progenitor specification [21][29][30]. At this point, MESP1 guides cardiac differentiation *via* the DKK1-mediated inhibition of WNT3A signalling [21][31]. So, it becomes clear that canonical WNT/β-catenin signaling has a biphasic effect and its fine spatiotemporal modulation is essential for these early steps in cardiac development[21][32][33]. Downstream of MESP1, cardiogenesis is orchestrated by a complex and interacting networking cascade of transcription factors (TFs) and genes, including GATA binding protein 4 (GATA4), NK2 transcription factor related 5 (NKX2.5), Myocyte Enhancer Factor 2C (MEF2C), TBX transcription factor 3 and 5 (TBX3, TBX5) and other factors that mark both the FHF and the SHF. After the specification of cardiac mesoderm, canonical WNT and NOTCH signaling regulate cardiac progenitor cells maintenance and differentiation [21] [34][35]. Figure 1.5 shows the signaling pathways and TFs guiding heart formation during embryogenesis.

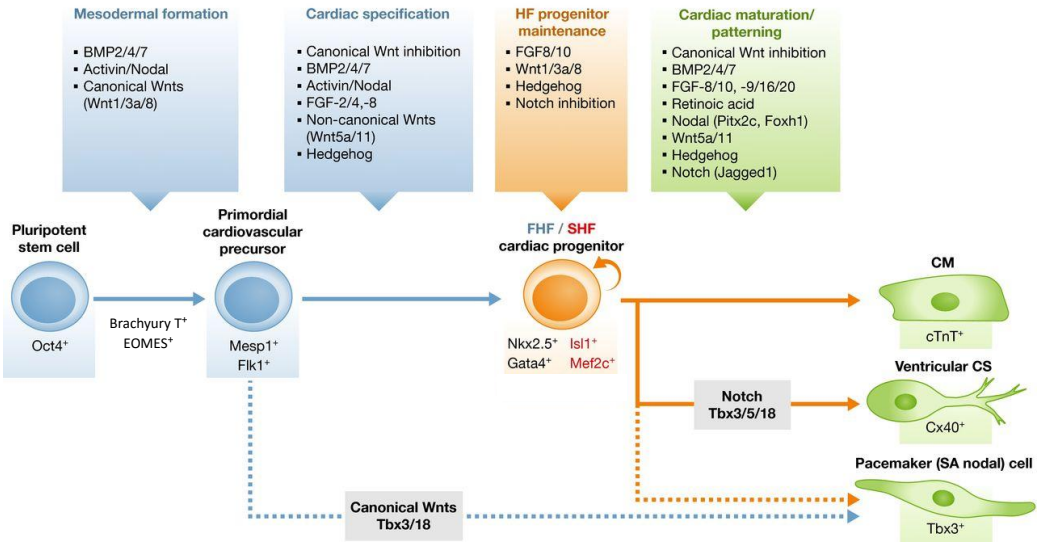

Figure 1.5: *Signaling pathways and TFs that cooperate for programming a CM during embryonic cardiac development. Signaling pathways modulators and TFs work at various stages of cardiac development and cardiac cell differentiation in a spatiotemporal context, from mesodermal formation, cardiac specification, maintenance of heart field (HF) progenitors to cardiac maturation and patterning. The circular arrows indicates the self-renewal process. FHF marker genes is reported in blue and the SHF marker genes in red. CM, cardiomyocyte; CS, conduction system and SA, sino-atrial (adapted from [36]).*

1.3. Cardiovascular Disease and evolution of the strategies for human cardiac regeneration

The heart is one of the first organ formed in the embryo because it is necessary for providing oxygen and nutrients to all the tissues of the body, both in developing embryo and during the entire life of an individual.

Given the crucial role of the heart and the CMs, it is clear how diseases or injuries affecting the heart function are often compromising or fatal; for this reason, scientists are interested in the regenerative medicine of the heart in order to find a strategy to better repair the injured organ [27]. Cardiovascular Disease (CVD) is currently the leading cause of morbidity and mortality in the world, with ischemic heart disease as the principal cause of deaths over the past 10 years. Unfortunately, these conditions are projected to rise in the years to come (Figure 1.6) [16].

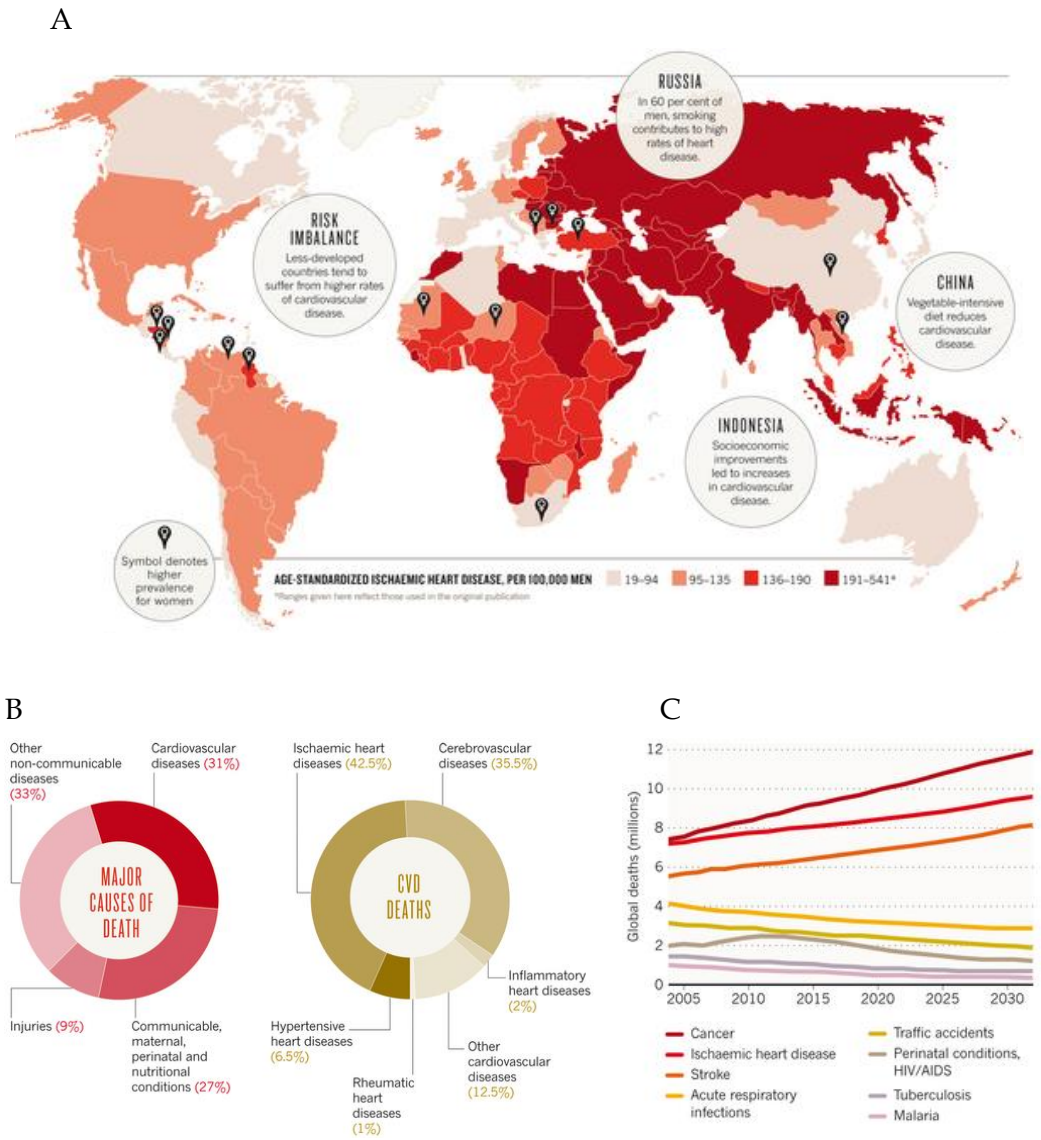

Figure 1.6: ***A.*** *2030 projections of global heart disease burden with the diffusion of ischemic heart disease worldwide.* ***B.*** *Nearly one-third of deaths worldwide is determined by CVD and ischemic heart disease. The number of these fatalities is projected to rise until 2030.* ***C.*** *Over the next 15 years, significant increase in deaths from ischemic heart disease and stroke will only be surpassed by cancer (adapted from [37]).*

This is in part due to the lack of a curative treatment for the damage to myocardium caused by myocardial infarction, aside from left ventricular assist devices (LVADs) and/or organ transplantation, which are an option for a limited number of severe cases; furthermore, over 50% of patients are nonresponsive to the currently available drug therapies. Therefore, there is a huge number of patients experiencing the comprmising and ultimately fatal consequences of heart failure, a condition characterized by CMs death by apoptosis and/or necrosis [16]. The human left ventricle possesses 2-4 billion CMs, and a myocardial infarction can erase 25% of these cells in a few hours [38]. Dead CMs are replaced by fibroblasts that migrate into the damaged area

to form fibrotic scar tissue, with subsequent thinning of the ventricular wall that no longer contracts properly. After the formation of fibroblastic scar, heart failure comes with remodelling and hypertrophy, with further cell death.

The persistence of scar tissue indicates little but insufficient regenerative capacity of the heart to compensate cell death. Shortly after birth, a myocardial cell transitates from a hyperplastic to a hypertrophic phase, with the formation of binucleated CMs that exit from the cell cycle [21].

Over the past 15 years, the major goal of cardiac repair is to generate the myocardium after injury to prevent or treat heart failure. CMs from laboratory animals are currently the most employed tool in the cardiac-related research. Although animal models have provided indispensable insights into systemic whole-organ function *in vivo* as well as *in vitro* disease mechanisms, they are not fully representative of their human counterpart[39][40]. In fact, toxicity studies comparing the drug reactions in human and laboratory animals have shown that only 43% of the toxic effects on humans can be predicted using rodents[39][41]. This suggests the need to use human CMs in drug discovery and cardiovascular research. However, it is currently challenging and complex to utilize human CMs in regular medical research due to the difficulty in isolation of heart bioptic tissue and subsequent primary CMs maintenance, due to their scarce expansion capacity *in vitro*; for these reasons, very limited supplies of these cells are available at present. Therefore, it becomes mandatory to develop alternative, most reliable sources of human CMs: this will require understanding not only the differentiation, but also the physiological maturation of these cells [39].

The discovery of first human Embryonic Stem Cells (hESCs) [42], and more recently, human induced Pluripotent Stem Cells (hiPSCs) [43][44], provides new tools for investigators, who focused their efforts on developing strategies to efficiently direct stem cell to a cardiovascular fate [21]. The majopr exciting advantage is represented by the ability to generate patient-specific hiPSCs, considered a viable, new and ethically less problematic alternative source for studying cardiac diseases, with the unprecedented opportunity to study disease-specific differences in a patient-specific manner [45]. Substantial efforts has been made to improve the efficiency and reproducibility of differentiation, while studying new avenues for establishing more differentiation defined conditions and producing cells on a clinically relevant scale [21].

Directed differentiation approaches of hPSCs into CMs mimic in the conventional dish, the steps of embryonic development, from mesoderm formation to CM specification, taking into account the sensitivity of hPSCs to their

microenvironment, made of signaling pathway and growth factors (GFs) that cooperate to drive the cardiac commitment.

Human Pluripotent Stem Cell-derived CMs (hPSC-CMs) are generally differentiated by tuned timed application of cardiomyogenic GFs and/or small molecules modulating specific stages of cardiac development, with cells cultivated as either Embryoid Bodies (EBs) or in monolayers and these strategies can be grouped into three major approaches that will be described in detail in the next Paragraph 1.4 [21][46].

More recently, new proof-of-concept studies have been developed, based on direct lineage conversion of somatic cells *via* the overexpression of a combination of evolutionarily conserved transcription factors (TFs) involved in cardiac gene expression, heart development and function[27][47]. In literature it is reported that the transgenic expression of a combination of 3 cardiac-specific TFs (GMT, Gata4, Mef2c and Tbx5) resulted in the transdifferentiation of murine fibroblasts into contracting CMs, named for this reason induced CMs (iCMs)[36][48]. Figure 1.7 summarizes the approaches described.

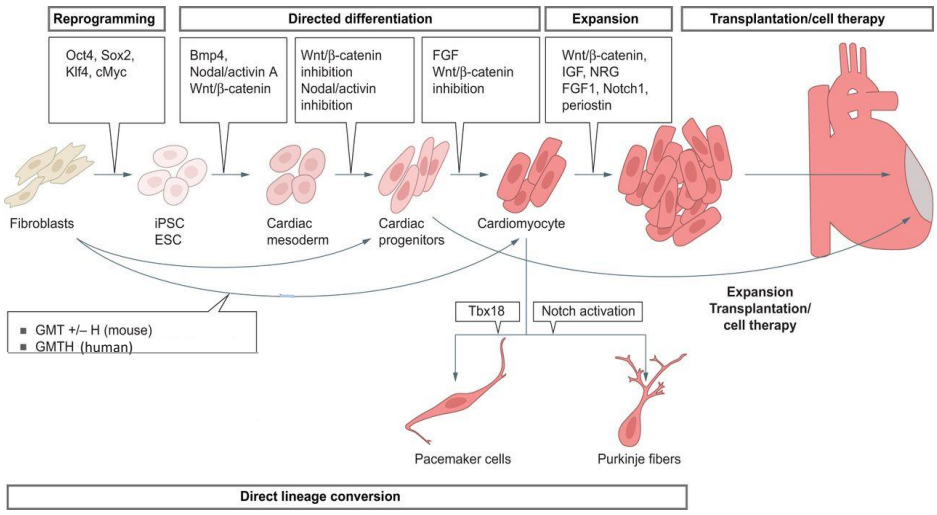

Figure 1.7: *Strategies to generate CMs in vitro that rely on 2 major approaches: directed differentiation from PSCs and direct lineage conversion of fibroblasts. Directed differentiation closely recapitulates the stages of cardiac development with GFs and small molecules. On the other hand, with direct lineage conversion, cells pass directly from one somatic cell type to the cardiac lineage by forced expression of a combination of TFs (adapted from [27]).*

Recently, direct reprogramming of human fibroblasts has also been achieved with the application of randomly integrating vector systems such as oncoretroviaral and lentiviral vectors converting human and murine fibroblasts to CMs, but it resulted in modestly controlled and long-lasting constitutive

transgene expression, with the associated risk of genomic integration and insertional mutagenesis; moreover, all these strategies were characterized by low efficiencies.

Other studies tried repeated administration of transient plasmids, episomal and adenovirus vectors, DNA- or protein- based carrying the TFs, however, also these methods for directing cardiac fate suffered low efficiencies compared to direct iPSC differentiation protocols using GFs and small molecules. Other technologies, described in literature for the generation of iPSCs, used DNA-free methods: serial protein transduction with recombinant proteins incorporating cell-penetrating peptides and transgene delivery with Sendai virus, which has a completely RNA-based reproductive cycle. Despite such progresses, also these approaches present low efficiencies and require stringent steps of purification[49][52][51][52].

In 2010 Warren L. and collaborators described a simple, non-integrating strategy for reprogramming cell fate, based on repeated administration of synthetically modified messenger RNA (mmRNA), specifically designed to bypass innate immune response [49][50]. The details of some of the principal reprogramming approach using TFs is described in Figure 1.8.

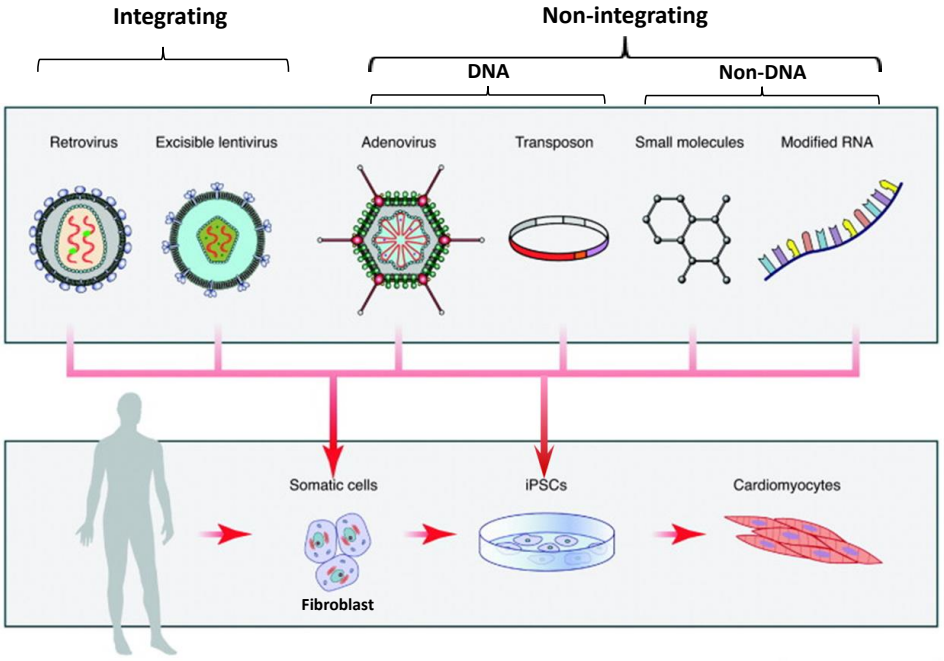

Figure 1.8: *Schematic representation of some of the principal approaches for TFs administration to guide cell fate. Initial approaches of TFs delivery used integrating retroviral or lentiviral vectors while, more recent strategies applied non-integrating methods, using DNA and non-DNA-based procedures. Once reprogrammed to a pluripotent state, iPSC fate could be further programmed to a terminally differentiated cell, as demonstrated by Warren L. and collaborators (modified from [53]).*

Warren's group showed that this approach could reprogram multiple human cell types to pluripotency with conversion efficiencies higher than established viral and non-viral protocols, as reported in Table 1.1. Moreover, they also demonstrated the possibility to use this non-integrating and non-mutagenic technology to direct the differentiation of RNA-induced Pluripotent Stem Cells (RiPSCs) into terminally differentiated myogenic cells, using a MYOD-encoding mmRNA, rendering it applicable to a range of regenerative medicine tasks [49][50].

Table 1.1: *Advantages of using mmRNA delivery of TFs as compared to other reprogramming techniques. mmRNAs provide efficiencies greater than 1% as compared with the other reprogramming strategies, showing efficiencies varying from 0,00001-0,01%. Moreover, mmRNA does not require multi-step passaging or screening for virus or genomic integration once generated the desired cells (modified from Stemgent website).*

	Modified mRNA	Protein	Sendai Virus	Adenovirus	Episomal/ Mini circle	Lentivirus/ Retrovirus
Efficiency	>1%	0,00001%	0,01%	0,0001-0,001%	0,0001%	0,001-0,01%
Integration	NO	NO	NO	Possible	Possible	YES
Screening/ purification	NO	NO	YES	YES	YES	YES
Clinically relevant	YES	Possible	Possible	NO	NO	NO

Taken together, this new approach pioneered and described by Warren's group, provides proof-of-principle that modified mRNAs can be used to both efficiently reprogram and program cell fate. Finally, this technology represents a safe strategy that can be applied for basic research, disease modeling and regenerative medicine, offering key insights into the mechanisms of cardiopoiesis and TFs network, providing hope that in the future injured hearts may be repaired through clinical applications of these cells[49][50]. All these mentioned strategies will be discussed in detail in this work; in Particular, in Chapter 2 will be described and applied a monolayer-based hPSC cardiac differentiation using small molecules that modulate a specific signalling pathway, whereas in Chapter 4 the mmRNA technology was investigated to efficiently drive cardiac hPSCs fate.

1.4. Direct cardiac differentiation of Pluripotent Stem Cells: the three major approaches

As mentioned in the previous Paragraph, the most applied strategies to direct hPSCs differentiation into CMs relied generally on the timed application of cardiomyogenic GFs or small molecules. In the last 10 years, this ability has progressed rapidly. The most reproducible and efficient strategies are based on stage-specific modulation of different signaling pathways in defined culture conditions, recapitulating key events of cardiac development [21].

These strategies can be grouped into three major approaches:

1. hPSCs co-culture on a feeder layer of stromal cells;
2. hPSCs aggregation to form tridimensional colonies known as Embryoid Bodies (EBs)
3. hPSCs differentiation in a monolayer composed of extracellular matrix (ECM) proteins;

The first strategy of direct differentiation involved hESCs co-cultured on a feeder layer of mouse visceral endoderm-like cells (END-2); in developing embryos it was observed, in fact, that visceral endoderm played an important inductive role in the differentiation of cardiogenic precursor cells of the cardiac mesoderm. However, this approach is relatively inefficient even though it generated mostly ventricular-like CMs[21][54][55]. The other two widely applied methods are: the formation of Embryoid Bodies (EBs), and differentiating hPSCs as a monolayer. The EB strategy initially involved the formation of spherical tridimensional aggregates from the suspension culture of hPSCs colonies in media supplemented with 20% FBS [21][56]. This method yielded only a low percentage of CMs, displaying early and immature phenotypes. Additional studies revealed that a higher efficiency of cardiac differentiation could be reached with the timed administration of defined extracellular molecules [28]. In fact, the temporary application of Activin A and BMP4 efficiently induced cardiac mesoderm formation in mouse and human EBs [27][57][58]; furthermore, the addition of FGF2, VEGF and DKK1, and the inhibition of Nodal or TGFβ receptor 2 signaling, enhanced the CMs differentiation efficiency greater that 50%[27][57][59][60]. However, the EBs differentiation methods are technically complex with high intra- and inter-experimental variability in the efficiency of CMs formation while cell phenotype is still immature. The reproducibility of this method is also problematic for reasons such as the undefined medium and serum components and the

constant presence of complex diffusion barriers within the tridimensional EB structure [61]. This leads to the development of monolayer-based methods, the third major approach presented, where hPSCs were cultured at high density on extracellular matrix proteins (e.g. Matrigel), applying sequential exposure to Activin A and then BMP4 in a defined RPMI/B27 supplemented medium. This strategy initially generated ~30% of beating CMs [27][60]. Finally, endogenous canonical Wnt signalling was identified to be indispensable for hPSCs to differentiate into contracting CMs sheets: in fact, as demonstrated by Paige S.L in 2010 [62]. and Lian X in 2012 and 2013 [63][64], the temporal perturbation of canonical Wnt/β-catenin signalling with small molecules, in a completely defined, GFs-free culture settings, determined the production of 80-98% CMs from multiple hPSCs lines [27][63][64].

The three major approaches for the generation of CMs *in vitro* are outlined in Figure 1.9.

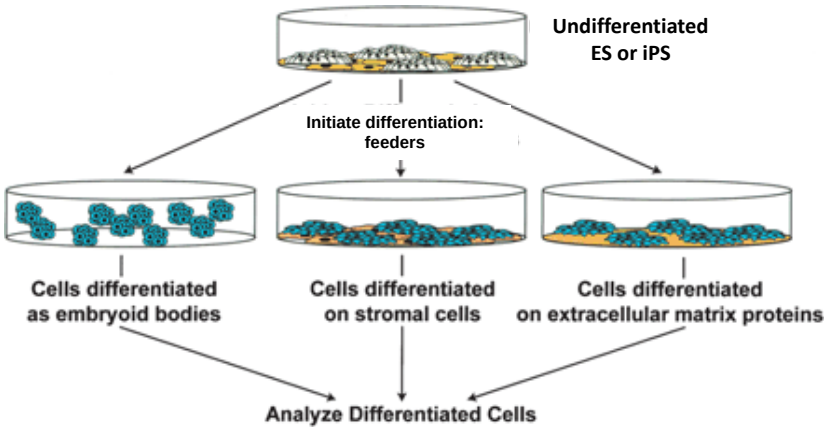

Figure 1.9: *The three major approaches to differentiate PSCs (adapted from [46]).*

These 3 approaches for PSCs differentiation possess specific advantages as well disadvantages. The EBs three-dimensional structure promotes cell-cell interactions needed for the activation of cardiac programs, but their disadvantage is represented by the different levels of expression of cytokines and inducing factors of endogenous pathways from these 3-D structures, leading to a high intra- and inter-experimental variability. Co-culture with stromal feeder cells provides the beneficial effects to cell growth thanks to the feeder cell layer. However, also in this case, the high variability due to undefined components produced by these supportive cells may influence the differentiation of the PSCs to desired cell types. An additional concern with this method is the difficulty to isolate PSCs-CMs from the stromal layer [46]. In

general, the significant variability between cell lines used and experiments performed could be due to differences in the sensitivity of cells to GFs, passage numbers and, in the case of hiPSCs, their retention of the epigenetic memory from the original organ or tissue, which appears to influence the response to extracellular signaling molecules [65].

Differentiation in monolayers on known substrates can lower the influence of neighbouring and feeder stromal cells and is also one of the simplest, fastest and efficient protocol [46]. A recent improvement to this protocol was described and patented by Burridge P.W. in 2014 in which he demonstrated that a drastic reduction of the number of components for the hPSCs differentiation produced contractile sheets of up to 95% of Troponin T positive CMs, using a xeno-free medium which is chemically defined and composed by only three elements: the basal medium RPMI, L-ascorbic acid 2-phosphate and rice-derived recombinant human albumin [66].

To conclude, the principal limitations of the strategies here described include: presence of xeno-contaminants (e.g. the stromal feeder cells), undefined medium components (presence of FBS, composition of media supplements…), differences in expression of cytokines of endogenous signalling pathway and, above all, the CMs produced are largely immature necessitating additional studies to determine which, if any of these approaches, could eventually be promoted to clinical practice.

In light of these considerations, synthetic modified mRNAs, described in the previous Paragraph, although in its infancy, could represent a useful and valuable tool for programming cell fate because these modified nuclei acids directly act on cell trascriptome to finely regulate protein expression and could solve the concern regarding cell maturation by forcing the expression of late maturation genes.

1.4.1. Challenges and limitations of the developmental status of hPSCs-derived CM

As mentioned in the above Paragraph, the CMs produced to date from hPSCs are largely immature and most analogous to fetal stages of cardiac development. For this reason, several research groups recently studied and characterized deeply the structural, functional and molecular features of hPSC-CMs (Figure 1.10). While adult human CMs (aCMs) are rod shaped with lengths in the 100 μm range, hPSC-CMs are smaller in size (10 to 20 μm in diameter) showing a round shape [67].

hPSC-CMs show poor contractile proteins organization and very low myofibrillar density with incomplete and randomly distributed structures [67][68]. Moreover, as compared to aCMs contractile apparatus, the hPSCs-CMs sarcomeric length is markedly shorter. Although the sarcomeric organization tends to mature with long-term culture, hPSC-CMs continue to show underdeveloped or absence of T-tubules, or M bands formation, demonstrating their inability to reach the necessary level of maturity comparable to functional adult CMs. While aCMs tend to be multinucleated, hPSCs-derived CMs are mononucleated [16][67][69].

The mitochondrial volume of mature aCMs represents over 35-40% of total cell volume [16][70]. Moreover, while aCMs mitochondria are aligned with myofibrillar proteins to provide the necessary functional energetic units for energy production and excitation-contraction (EC) coupling, in hPSc-CMs, the number of mitochondria is lower; moreover, the organelles are misaligned with sarcomeres and mostly concentrated all around the peri-nuclear area. aCMs derive their energy primarily from oxidative metabolism; in contrast with hPSC-CMs that are predominantly glycolytic, indicating once more their immature and fetal like phenotypes [16][67][72].

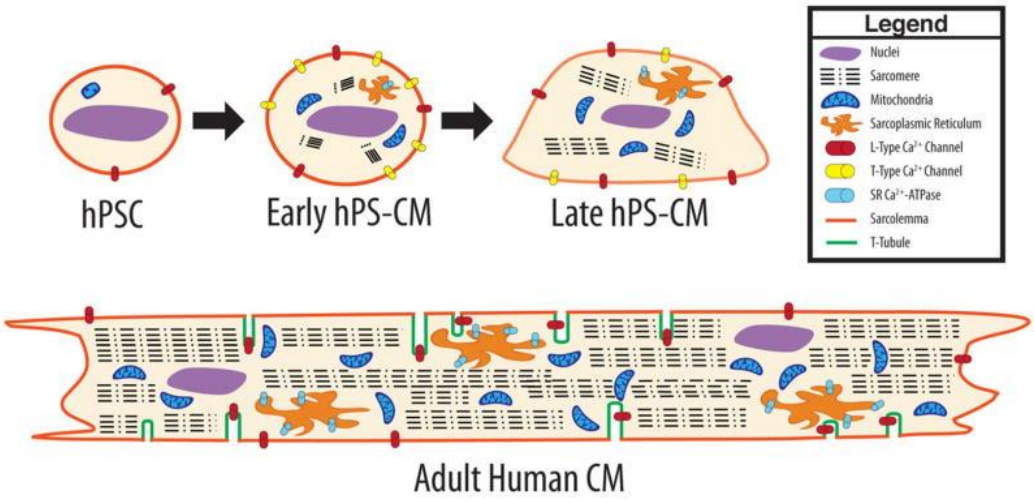

Figure 1.10: *Comparison between early hPSC-CM, late hPSC-CM and adult CM morphology during in vitro maturation process. Note the differences in shape, sarcomeric area and receptor expression between late hPSC-CM and early hPSC-CM. aCM is larger, with multiple nuclei, large sarcomeric area and large number of mitochondria (adapted from [69]).*

Three major subtypes of hPSC-derived CMs can be derived, that present atrial, ventricular-, or nodal-like phenotype as determined by electrophysiological analysis of action potentials (APs)[21][71]. The 3 principal strategies, previously described, for deriving CMs from hPSCs create a mixture of these three cell types [21]. Most reported AP characteristics, well reviewed by Robertson C and collaborators in 2013, are less mature than aCM: precisely, maximum diastolic potential (MDP) for adult ventricular CM is -85mV, whereas in early hPSC-CM it is approximately -30mV; in late hPSC-CM can improve at a maximum of -60 to -75mV. The maximum rate of depolarization (d_v/d_t or v_{max}) in aCM is extremely fast, ranging from 300V/s; on the contrary, early hPSC-CM displays slow depolarization speeds (2V/s, improving to 10-40 V/s in late hPSC-CM).

Mature aCMs are electrically quiescent but excitable upon stimulation while hPSC-CMs display a greater degree of automaticity because they contract spontaneously and simultaneously [69]. hPSC-CMs express frequently abnormal levels of the major ionic currents normally present in aCM (calcium channels, hyperpolarization-activated cyclic nucleotide-gated channels HCN, and Na^{2+}/Ca^{2+} exchangers NCX [69][73][74][75][76]). hPSCs-CMs expressed the potassium currents genes, considered responsible for arrhythmias so these cells could be apllied for anti-arrhythmic drug screening [77]. Calcium-induced calcium release (CICR) from the sarcoplasmic reticulum (SR) of aCMs is responsible of the major total total Ca^{2+} release (70%). On the contrary, hPSC-CMs possess very little SR development and function, similar to fetal CMs in which SRs are smaller in volume and possess limited capacity to load Ca^{2+}. Consequently, an abnormal diffusion of Ca^{2+} in the cell reduces the contractile synchronicity necessary for the generation of large contractile forces [69]. Figure 1.11 shows differences between early-, late hPSC-CMs and adult CMs phenotype.

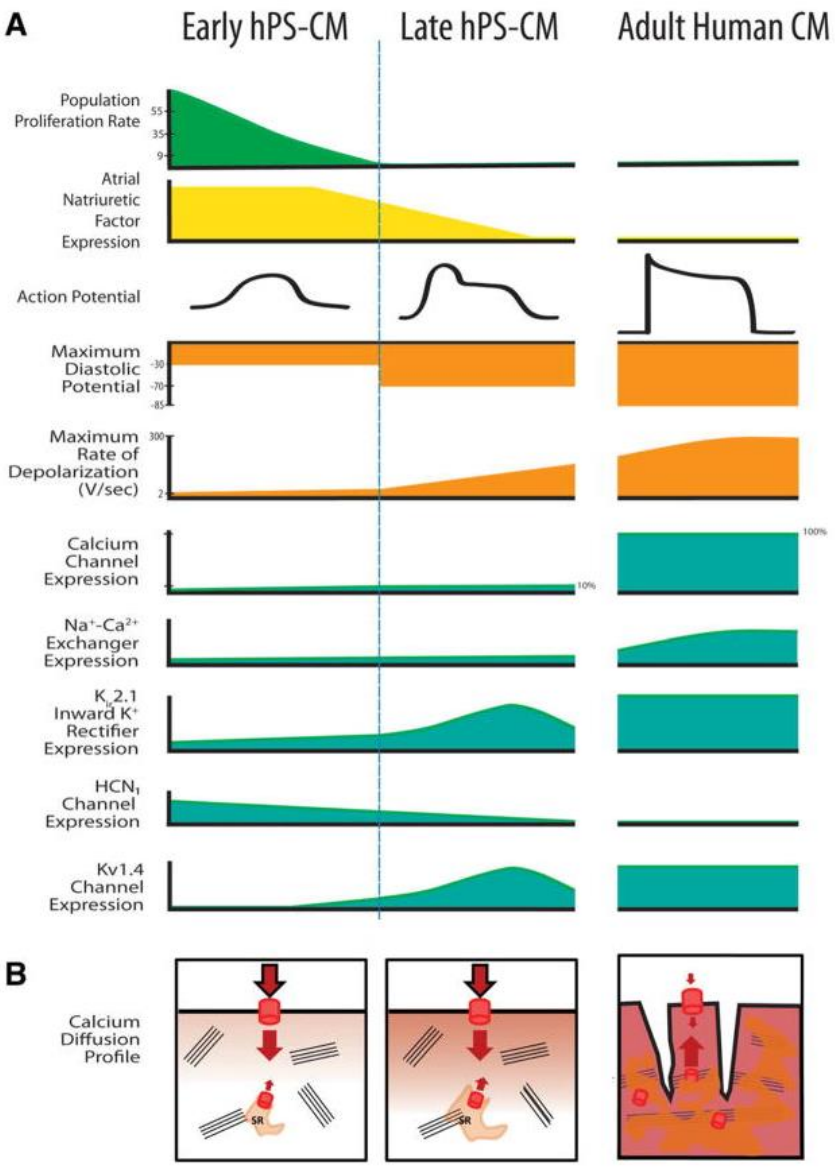

Figure 1.11: *Comparison of early hPSC-CM, late hPSC-CM and aCM.* ***A.*** *Overview of the major changes observed with increasing culture time; action potential (orange), key ion channels (blue).* ***B.*** *Comparison between calcium influx profiles for early and late hPSC-CM with aCM (adapted from [69]).*

From the study of the gene expression profile from the microarray analysis the upregulation of genes involved in cell-cell communication and signal transduction as well as host defence responses are observed in aCMs and fetal CMs but not in hPSC-CMs[69][78]. In contrast, hPSC-CMs show overexpression of genes involved in cell developmental processes, indicating their developing state. Other genes, especially those involved in structure, function and maturation, show increased expression proceeding from fetal to aCMs, rendering them useful as maturation markers. These genes include: the light

chain of myosin *MYL2, MYL7, MYL3* and *MYL11(or MLC);* the cardiac troponin genes *cTnT2 (TNNT2), cTnI3 (TNNI3)* and *cTnC1 (TNNC1).* Calcium handling genes resulted upregulated in hPSC-CMs [79]. The main features discussed that distinguish hPSC-CMs from aCMs are summarized in Table 1.2.

Table 1.2: *Main reported differences between immature hPSC-CMs and aCMs extracted from literature.*

Cardiac feature	hPSC-CMs	Adult CMs	Reference
Morphology	Multi-angular, round shape	Large, rod shape	Robertson, C. *et al.*, 2013
Number of nuclei	Mononuclear	Multinuclear	Robertson, C. *et al.*, 2013
Proliferation rate	Low	None	Robertson, C. *et al.*, 2013
Contraction	Spontaneous	Only induced	Ma, J. *et al.*, 2011
Action potential features	Low diastolic potential (-30mV to -75mV) Slow depolarization rate (2V/sec to 40V/sec)	Diastolic potential (-85mV) Depolarization rate (300V/sec)	Ma, J. *et al.*, 2011
Metabolism	Glycolytic	Oxidative	Cao, F., *et al.*, 2008
Ionic currents and Ca^{2+} handling machinery	Expression frequently at abnormal levels	Correct expression levels	Cao, F., *et al.*, 2008
Gene expression pattern	• Downregulated: cell communication, signal transduction and host defence responses genes • Upregulated: Ca^{2+} handling genes • Overexpressed: cell development genes	Upregulated: cell communication, signal transduction and host defence responses genes	Synnergren, J. *et al.*, 2008

Although the discovery of hiPSCs has represented a great breakthrough with the opportunity to publish numerous successful studies, their clinical application is still quite far to be used in the preclinical phase of human trials. Further optimization together with a great effort are necessary to overcome the major challenges of hPSCs for cardiac regenerative medicine applications prior the translation into clinic [80]. The major safety concerns on using hPSC-CMs include: A) the potential for teratoma formation; B) arrhythmogenesis, and C) rejection. While rejection represent the most frequent issue in transplantation/implantation

medical interventions and the use of hiPSC-for autologous applications can avoid immunological response, the first two mentioned concerns are related to the culture purity and the immature stages of hPSC-CMs, described previously. In fact, the persistence of a minimal pluripotent residual of $OCT4^{+ve}$ can bring to unpredictable teratoma formation and malignant transformation *in vivo*. Moreover, since hPSCs are able to differentiate into various subclasses of hCMs with different electrophysiological properties, there is a risk of arrhythmogenesis [73]. Although current methods can generate CMs population with a purity of up to ~99%, it is still difficult to remove the residual undifferentiated cells. Moreover the purification process has to be highthroughput, non-destructive, efficient, appropriately selecting and cost-effective [81].

Scientists continue to study for refining or developing novel approaches to improve cardiac differentiation of hPSCs but the final and great challenge in this field remains the morphological and electrophysiological CMs maturation *in vitro* as a tool to better understand the mechanisms of cardiac development and accelerate the application of hPSCs to the clinic.

1.5. Aim of the Thesis

As described previously, the major concern of current protocols for deriving CMs from hPSCs is their early and immature phenotype. In light of the considerations illustrated in this introductive Chapter, this work couples three of the major strategies discussed: (I) the monolayer-based cardiac differentiation of hPSCs that relies on the perturbation of Wnt/β-catenin signaling pathway, considered to date as the gold standard for producing a high yield of CMs; (II) the programming of hPSCs fate using the synthetic modified mRNA (mmRNA) technology and (III) the integration of these two strategies into an *ad hoc* microfluidic (μF) platform, fabricated in our BioERA laboratory, to finely drive the cardiac commitment with high efficiency.

In particular, this thesis aims at developing an efficient and robust method for cardiac differentiation of hPSCs in microfluidics, through the overexpression of a defined set of cardiomyogenic TFs, which play key role in cardiac development and function. As a proof-of-concept, this strategy has the purpose of forcing the endogenous TFs expression via the mmRNA administration to drive cardiac differentiation toward cell maturation. The

combination of cardiac TFs and signaling pathway perturbation will be investigated to improve CMs formation from hPSCs. Moreover, in order to improve the delivery of the cardiac TFs, the microfluidics technology was exploited to perform an efficient differentiation of hPSCs in a high controllable microenvironment that allows high efficient, combinatorial and multiparametric analysis at one time, in a cost effective manner.

In conclusion, the approaches studied in this PhD project represented safe and efficient strategies for cell fate programming, holding great promise for cardiac research, disease modelling and regenerative medicine and for producing clinically useful CMs.

Chapter 2.
Human Pluripotent Stem Cells for Cardiomyocytes generation

This Chapter focuses on human pluripotent stem cells (hPSCs) used in this work, describing the human embryonic stem cell (hESC) lines and the human induced pluripotent stem cell (hiPSC) clones produced in our laboratory. The main characteristics of these cells are elucidated with their culture, maintenance and expansion procedures. Moreover, a hESC line, dual reporter for two cardiac transcription factors (TFs), is described in details and employed in all the experiments performed as a useful tool for monitoring the progression of cardiac

differentiation. It is then introduced the first experimental approach in conventional culture for the differentiation of hPSCs into beating CMs. To date, the monolayer-based strategy here applied, is considered the gold standard for the fast generation of a high yield of CMs in approximately 15 days and the results obtained from 2 hESC lines and 4 hiPSC clones are showed. CMs obtained are characterized for the expression of cardiac-specific markers and the cell-cell communication is studied with a functional test.

2.1. Human Stem Cells

Stem cells are primitive, undifferentiated cells characterized by their capacity to self-renew indefinitely and give rise to other stem cells or to specialize and form cells of somatic tissues [82][83].

The self-renewal ability allows the maintenance of the undifferentiated state while the plasticity is involved in stem cells differentiation into a wide range of cells. The degree of potency (Figure 2.1) is commonly used to make a hierarchical classification of cells into:

- totipotent stem cells that can generate all cells of an organism, together with the extraembryonic cell types (zygote);
- pluripotent stem cells (PSCs) that have can give rise to cells of the three germ layers: endoderm (interior stomach lining, gastrointestinal tract, the lungs), mesoderm (muscle, heart, bone, blood, urogenital tract), or ectoderm (epidermal tissues and nervous system); (ESCs, Embryonic Stem Cells; iPSCs, induced-Pluripotent Stem Cells, ICM, inner cell mass of the blastocyst-stage embryo);
- multipotent progenitor cells differentiate into limited cell types (tissue-specific stem cells, HSCs, Hematopoietic Stem Cells);
- unipotent cells generate only a single cell type (hepatoblasts differentiate into hepatocytes) [84].

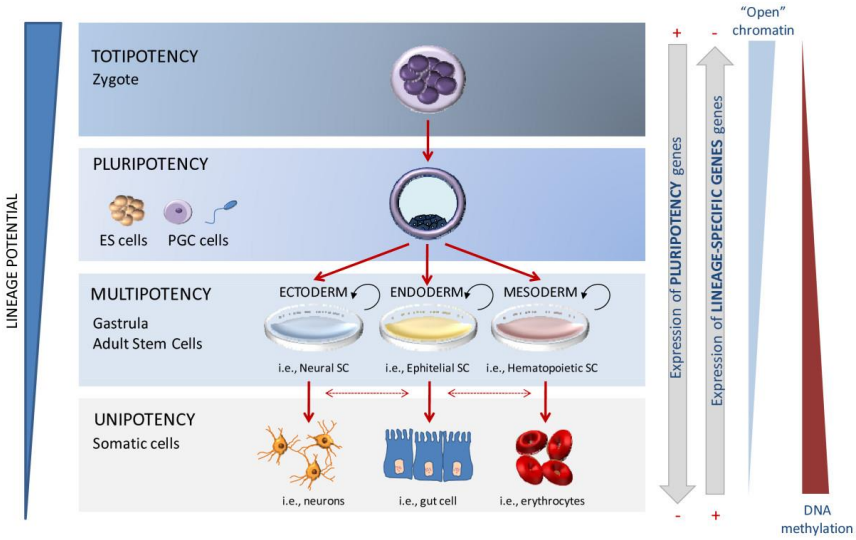

Figure 2.1: *Hierarchical classification of cells based on the degree of pluripotency with the related gene expression and epigenetic patterns involved. At the top, there is the totipotent cells at the morula stage. Proceeding down the lineage potential, pluripotent cells loose the capacity to form extraembryonic tissues.. Multipotent stem cells can originate multiple cell lineages, while, at the end, unipotent cell can only differentiate to somatic cell (adapted from [85]).*

The self-maintenance capacity depends on two main mechanisms of cell division: the symmetric proliferative division to maintain the stem cell pool that, in case of necessity can expand, whereas the symmetric differentiative division makes the stem cell pool depleted in order to generate differentiating progenitor and/or postmitotic cells. Moreover, stem cells can divide symmetrically or asymmetrically in order to regulate the number of stem cells and their differentiating progeny, both in developing embryo and adult individuals [86].

In conclusion, stem cells allow tissues to maintain a proper architectural, cytological and biochemical structure and identity in order to guarantee the correct functionality of the different organs in an entire complex organism [82].

2.2. Human Pluripotent Stem Cells: human Embryonic Stem Cells and human-induced Pluripotent Stem Cells

Pluripotent Stem Cells include human Embryonic Stem Cells (hESCs), derived from the inner cell mass (ICM) of the blastocyst of a human embryo, and human induced-Pluripotent Stem Cells (hiPSCs), obtained from the reprogramming of adult somatic cells with specific factors.

In November 1998, a group in the United States guided by Thomson J. published the first data describing the isolation and derivation of human

Embyonic Stem (ES) cell lines from blastocyst [42]. They derived hESCs from the ICM of a 5-days fertilized blastocyst of fresh or frozen embryos. The blastocysts were then extracted and cultured in presence or absence of mouse supportive layer cells. Once the clonal expansion started, only the cell colonies showing undifferentiated state (high ratio of nucleus to cytoplasm and prominent nucleoli), high clonal capacity, pluripotency and normal karyotype were picked and expanded. As explained in Paragraph 2.1, hESCs are able to form all somatic tissues with the exception of extraembryonic ones required for complete development (placenta and membranes) for this reason they are incapable to give rise to a complete new individual [87]. hESCs are considered immortal because they express high levels of telomerase, the gene protein product that assures the preservation of telomere ends at each cell division, avoiding cells senescence. Pluripotency state of these cells was verified by their capacity to aggregate in Embryoid Bodies (EB), in which cells differentiate into cells from the three embryonic germ layers. Furthermore, when injected into severe combined immunodeficient mice (SCID), the hESCs lines produced teratomas containing endoderm (gut epithelium); mesoderm (cartilage, bone, smooth muscle and striated muscle); ectoderm (neural epithelium, embryonic ganglia and stratified squamous epithelium)[42][88]. Thanks to these abilities, hESCs are a promising candidate for the generation of tissues useful in regenerative medicine approaches, as well as a valuable tool for disease modeling and drug screening to identify new chemical entities (NCEs) that can be developed as novel therapeutics.

However, the use of human embryos for deriving hESCs is currently under a high ethical and political debate in the world. Despite the great potential offered by the use of hESCs for treating diseases and many other applications above mentioned, their use remains controversial because implies the destruction of early embrios [83][88]. In fact, hESCs are currently discussed by the biologists as well as by the medical profession, media, ethicists, governments and politicians: surely, these cells possess a great clinical potential for tissue repair and/or replacement but the major ethical concern is that hESCs are derived from human pre-implantation embryos. To date, most embryos used for the generation of hESC lines came from spare ones conserved for in vitro fertilization (IVF), but also the creation of embryos for the unique derivation of hESCs is under debate.

In 2006 and 2007, another breakthrough in science, first on mouse and then on human cells, was reported by researchers at Kyoto University in Japan by

Yamanaka S and coworkers. In contrast to hESCs, these cells, called induced Pluripotent Stem Cells (iPSCs) were derived by the reprogramming of somatic cells to a pluripotent state forcing the overexpression of a key set of transcription factors (TFs) indispensable for pluripotency maintenance. This process does not destroy human embryos *ex utero,* avoiding a great portion of the ethical and political debates surrounding hESCs generation [43][44]. Thanks to this discovery, Yamanaka S. was awarded with the 2012 Nobel Prize for the ability to reprogramme mature, differentiated cells to a pluripotent state.

iPSCs are obtained with the introduction of a specific combination of pluripotency genes, also named "reprogramming factors" (RFs) or"Yamanaka's factors" , into a differentiated somatic cell type. Yamanaka's factors were the following genes: Oct4 (Pou5f1), Sox2, c-Myc and Klf4. iPSCs were firstly generated from mice fibroblasts in 2006 by researchers of Yamanaka's group to identify the genes important for inducing an embryonic state in adult cells. Before the identification of the 4 RFs above mentioned, Yamanaka's team tested 24 genes that were identified in literature as essential in embryonic stem cells and delivered them into fibroblasts using retroviruses. They arrived at the identification of the set of 4 candidates by removing one factor step-by-step. These cells are defined as the first-generation of iPSCs and displayed typical pluripotency features such as self-renewal and ability to form all three germ layers derivatives both *in vitro*, within EBs, and *in vivo* teratomas. In 2007, another milestone was achieved by deriving iPSCs from the reprogramming of human adult cells [43][44] with two independent research teams studies published one by Thomson J. at University of Wisconsin-Madison, and the other by Yamanaka S. himself and colleagues at Kyoto University. With the same principle adopted by Yamanaka in 2006 in mouse models, his group successfully converted human fibroblasts into hiPSCs using these 4 genes: OCT3/4, SOX2, KLF4 and c-MYC, delivered with a retroviral vector [44]. On the other hand, Thomson and colleagues used lentiviral systems for delivering OCT4, SOX2, NANOG plus LIN28 [89][90]. Moreover, in 2012, researchers from Austria, Hong Kong and China published a work in which they were able to generate hiPSCs using a protocol that reprogrammed the exfoliated renal epithelial cells present in urine to a pluripotent state. This method is less invasive and more compliant, compared to the extraction of cells from, for example, skin biopsies, providing an alternative way to derive hiPSCs from healthy and diseased individuals [91]. Figure 2.2 summarizes the strategies to generate hESCs and hiPSCS.

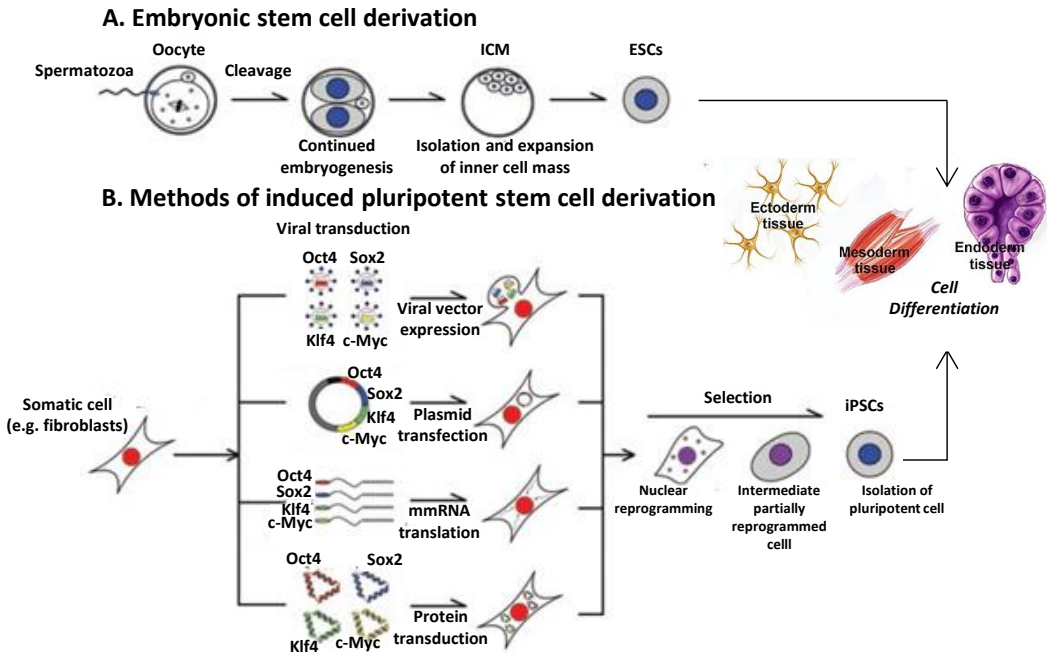

Figure 2.2: *Protocols for ESCs (**A**) and iPSCs derivation (**B**) (modified from [88]).*

However, these first reprogramming methods based on viral vectors were characterized by low efficiency, yielding iPSCs in less than 1% of the starting somatic cell used; moreover, these approaches are accompanied by the great obstacle for future therapeutic applications represented by the modifications of the genome. The use of synthetic modified mRNA (mmRNA), pioneered by Warren L. in 2010 is an appealing tool for cell fate manipulation because allows the modulation of cellular protein expressionon daily, with repeated transfection of selected combinations of TFs, circumventing at the same time, additional stages of purification from residual vector traces [49][50].

The technologies presented and discussed in this thesis have been performed using both hESCs and hiPSCs in order to develop more relevant *in vitro* studies.

2.3. hPSCs culture, passaging and expansion

In this work, the following hPSCs were employed: hESC line HES2 and hESC line MESP1$^{mCherry/w}$/NKX2.5$^{eGFP/w}$ dual reporter [92][93]; mmRNA Clone 1; mmRNA Clone 7; mmRNA Clone A and mmRNA Clone G. The designation and origin of the hPSCs lines and clones employed in this thesis are listed in the Table 2.1.

Table 2.1: *List of hPSCs employed in this work*

	Line/Clone	Type	Vector	Status	Reference
hESCs	HES2	WiCell bank	-	Healthy	Giobbe, G.G. *et al.*, 2015
	hESC MESP1$^{mCherry/w}$/NKX2.5$^{eGFP/w}$	R. Passier's Laboratory, Leiden University	Recombineering modification of bacterial artificial chromosome	Healthy	Den Hartog, S.C. *et al.*, 2015
hiPSCs	mmRNA-Clone 1	N. Elvassore's BioERA Laboratory, Padova Univerisity	mmRNA transfection	Healthy	Luni C. *et al*, 2016
	mmRNA-Clone 7		mmRNA transfection	Healthy	
	mmRNA-Clone A		mmRNA transfection	Healthy	
	mmRNA-Clone G		mmRNA transfection	Healthy	

For more details on the culture settings of the hiPS employed, please see the publications produced by the colleagues of BioERA laboratory Giobbe G.G *et al.* and Luni C. *et al*. in 2015 and 2016 respectively [94][95].

hPSCs were cultured in 0,5% v/v matrigel reduced factor (MRF 50%; BD) coated 6-well plates, maintained and expanded in StemMACS™ iPS-Brew XF medium (Miltenyi Biotec), a feeder-free and xeno-free medium which formulation supports rapid adaptation of feeder-based cell cultures to a feeder-free environment and shows compatibility with commonly used matrices like MRF or vitronectin.

hESC line HES2 (from National Stem Cell Bank, Madison, WI and used in the work published by the colleagues Giobbe G.G. *et al*. in 2015 [94]) was initially expanded in gelatine-coated Petri dishes, in co-culture with mouse embryonic fibroblasts (MEF, Chemicin) mytomicin C-inactivated, for various passages in expansion medium (DMEM F-12 , Invitrogen; 20% Knock-Out serum, Invitrogen; 10% MEF conditioned medium, 20ng/mL basic Fibroblast Growth Factor bFGF, Invitrogen; 0,1% mM β-mercaptoethanol, Invitrogen; 1% non-essential amino acids, NEAA, Invitrogen; and 1% Pen/Sterp, Invitrogen). These cells were then seeded in 6-well plates with 0,5% v/v MRF coating and maintained in StemMACS™ iPS-Brew XF feeder-free medium.

hESC line MESP1$^{mCherry/w}$/NKX2.5$^{eGFP/w}$ dual reporter [92][93], kindly gifted by Robert Passier, was generated by Passier's laboratory (Leiden University Medical Centre, the Netherlands) through the modification of the bacterial artificial chromosome RP11-975L13 (Lifesciences) by recombineering (Gene Bridges),

leading to this dual reporter system for the early cardiovascular lineage markers MESP1 and NKX2.5 (described in Paragraph 2.4) [92][93].

The human induced pluripotent stem cell clones used in this PhD thesis are classified with different names indicated in the work published by Luni C. *et al* in 2016 (μF#501 for mmRNA Clone 1 and μF#505 for mmRNA Clone 7, Well#401 for mmRNA Clone A and Well#405 for mmRNA Clone G;) [95] but for simplicity, the denominations adopted routinely in our laboratory are reported in Table 2.1.

hiPSC mmRNA Clones 1, 7, A and G were generated in our BioERA laboratory through the reprogramming of human fibroblasts with synthetic modified mRNA, according with the protocol described by Warren, L. *et al*., in 2010[49][50], both in multiwell plates and in microfluidic devices developed in BioERA lab [95]. The reprogramming to pluripotency was performed by Giulitti S. and Luni C. of our BioERA laboratory and the details of the protocol is reported in their work [95]. The reprogramming of target fibroblasts (BJ, Miltenyi Biotec or HFF-1, ATCC) was performed both in presence of feeder cells (NuFF-RQ, newborn foreskin fibroblasts AMS Biotechnology) or in feeder-free conditions. Briefly, in case of reprogramming with feeder cells, NuFF were seeded in gelatine-coated plates and, after 24 hours, the target fibroblasts (BJ or HFF) were seeded on feeder cells at different densities in DMEM (Life Technologies) supplemented with 10% fetal bovine serum (FBS, Life Technologies). When starting the reprogramming transfections on day 0, the medium was switched to Pluriton reprogramming medium (Stemgent) supplemented with 200ng/ml of the protein for interferon inhibition B18R (eBioscience). The transfections were conducted for 12 consecutive days using mmRNAs encoding OCT4, SOX2, KLF4, c-MYC, NANOG, LIN-28 and nuclear GFP (Milteny Biotec) according to the StemMacs mRNA reprogramming kit (Miltenyi Biotec), respecting the correct stoichiometry of each mmRNA indicated in the data sheet. All the mmRNAs (concentrated 100ng/μL) were diluted 5X in the transfection mix made by pooling two solutions composed by the transfection buffer (TB) and the transfection reagent (TR) of the reprogramming kit. After 15 minutes of equilibration at room temperature, the transfection mix was then added to the culture medium. For the progressive NuFF death observed during the experiments, from day 6 NuFF conditioned B18R-supplemented Pluriton was always used. Feeder-free reprogramming was performed with the same scheme above described by solely transfecting BJ or HFF fibroblasts using B18R supplemented Pluriton until the end of the

experiment. At the end of the transfection regimen, hiPSCs obtained were maintained in culture with Pluriton for 2 days while some experiments were stopped to verify the pluripotency *via* immunofluorescence staining against the pluripotency markers NANOG and TRA1-60 [95]. hiPSCs colonies were then picked and cultured on 0,5% v/v MRF coated plates in feeder-free StemMACS™ iPS-Brew XF medium (Miltenyi Biotec). In Figure 2.3 are reported bright field images of hESCs and hiPSCs colonies in feeder-free culture on MRF-coated plates. hPSCs colonies grow in colonies showing defined edges.

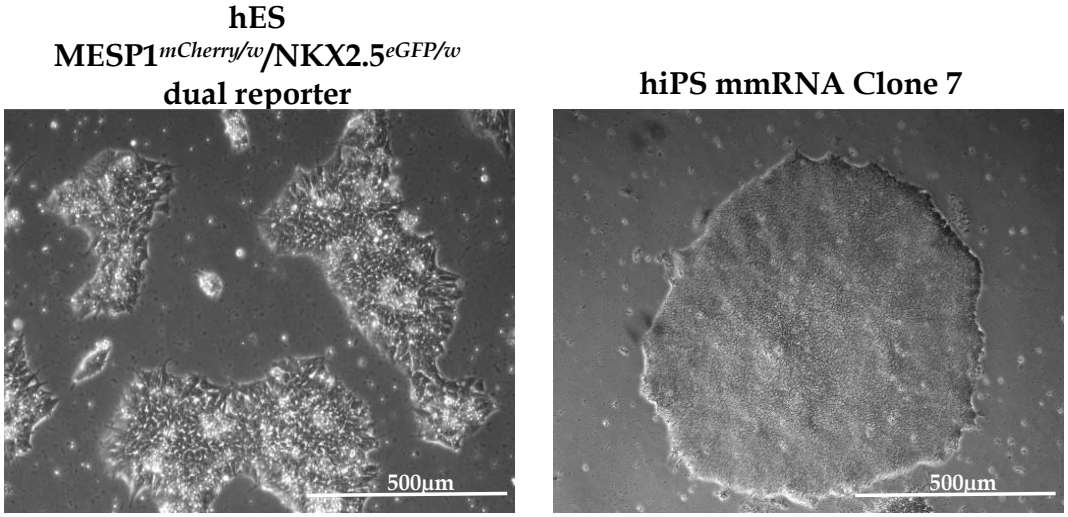

***Figure 2.3**: Bright field images of hESCs (MESP1mCherry/w/NKX2.5eGFP/w dual reporter) and hiPSCs (mmRNA Clone 7) colonies grown on MRF-coated plates. Note the homogeneity and compactness of pluripotent stem cells; undifferentiated colonies presented different dimension showing defined and bright edges with regular shape.*

hPSCs medium was changed daily and, for passaging, two methods were adopted: mechanical and with dissociating buffer. The first one was performed under the stereomicroscope inside the biological safety cabinet to dissect undifferentiated colonies into several pieces using a cutting glass pipette, specifically modified for this procedure; this is considered a gentle method, useful to remouve also the differentiated parts in the culture. The picked colonies were them replated onto 0,5% v/v MRF-coated six-well plates.

The second strategy consisted on the treatment with Gentle Stem Cell Dissociation Reagent (Stem Cell), an enzyme-free method recommended for the ease of use, high cell recovery and for preserving the integrity of cell surface proteins that aid in the reattachment of cells to the matrix. Briefly, medium was aspirated from the well and cells were rinsed with phosphate-buffered saline (PBS, Gibco). Cells were then incubated with the dissociation reagent for 2-4 minutes at

room temperature. The dissociation reagent was removed and stem cell medium was added; gently the colonies were detached by scraping with a cell scraper, taking care to minimize the breakup of colonies. Carefully, the cell aggregate mixture was pipetted up and down and replated at the desired density onto a new 0,5% v/v MRF-coated six multiwell plate. The split ratio could vary between 1:3 and 1:10, depending on the different rate of cell growth, so the split ratio need to be adjusted. Ususally it is recommended to observe the last split ratio and adjust it, taking into account the aspect of the hPSC colonies. If the cells look healthy and colonies have enough space, the cultures can be split every 4-7 days.

A daily check of hPSCs is recommended for both medium refresh and for preventing possible differentiation. When differentiation emerges, two strategies for its removal are possible: "pick-to-keep" (PTK) and "pick-to-remove" (PTR). If only few undifferentiated colonies are present, "pick-to-keep" is preferred, in which the differentiated cells are left on the plate and discarded. On the contrary, if there are mostly undifferentiated colonies, the few differentiated cells undergo the "pick-to-remove" methodology in which they are picked, removed and discarded. Representative pictures of the two strategies mentioned for the removal of differentiated cells are reported in Figure 2.4.

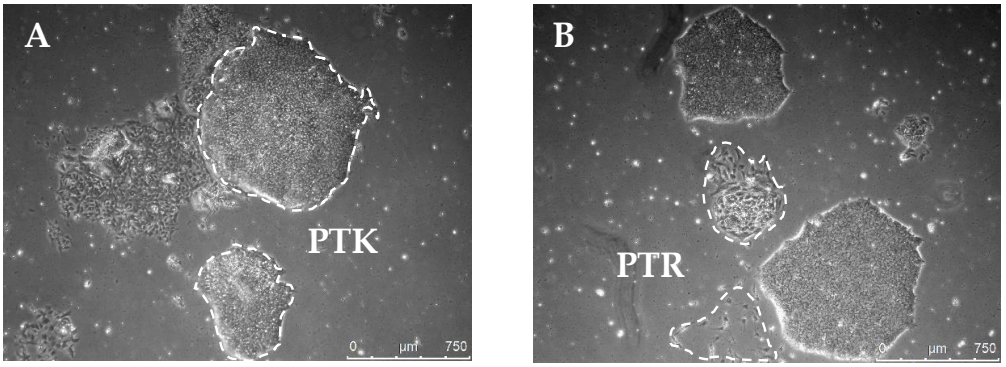

Figure 2.4: *Example of cell differentiation in hiPS (mmRNA Clone 1) culture.* ***A****. White dotted line marked the hiPS colony for the "pick-to-keep" (PTK) strategy in presence of consistent differentiation in the plate.* ***B.*** *White dotted line indicate the differentiated cells that will be removed with the "pick-to-remove" (PTR) strategy in presence of mostly undifferentiated cells.*

The two hESC lines (HES2 and hES MESP1$^{mCherry/w}$/NKX2.5$^{eGFP/w}$ dual reporter) and the four hiPSC clones (mmRNA Clone1, 7, A and G) were successfully cultured and maintained and the pluripotency state was routinely verified by immunofluorescence staining against pluripotency markers: OCT4,

NANOG, c-MYC, KLF-4, TRA1-60, TRA1-81, TRA2-49 (alkaline phosphatase ALP or AP) and SSEA4, as reported in the panel of Figure 2.5, confirming that our cells were *bona fide* pluripotent stem cells. All the immunofluorescences were performed according to the standard 5 steps protocol: fixation, permeabilization, blocking, incubation with primary protein-specific antibody followed by secondary fluorescent-labeld antibody. The details for each antibody with the related 5 steps used are listed in Table 2.2.

The species-specific secondary antibodies employed were from Life Technologies and were visualized by Alexa Fluor-488 (green) or Alexa Fluor-594 (red) and from Jackson ImmunoLab Cy3 (red) fluorophores. Nuclei were counterstained in blue with Hoechst (Sigma Aldrich). Leica DMI6000B epifluorescence microscope, provided with a mercury short-arc reflector lamp or Leica SP5 confocal microscope, equipped with Argon laser were used for taking pictures.

Table 2.2: *Summary of all the primary antibodies employed in this thesis for pluripotency characterization, with all the parameters of the assay listed.*

<table>
<tr><th>Antibody</th><th>Manufacturer</th><th>Fixation</th><th>Permeabilization and Blocking</th><th>Dilution</th><th>Incubation</th></tr>
<tr><td>Oct4</td><td>Santa Cruz #sc5279</td><td rowspan="8">4%PFA, 10min, RT</td><td rowspan="4">PBS-0,1% Triton X
10% FBS</td><td>1:200</td><td rowspan="4">12 h, 4°C</td></tr>
<tr><td>Nanog</td><td>ReproCell #RCAB0004P-F</td><td>1:100</td></tr>
<tr><td>Klf-4</td><td>Santa Cruz #sc20691</td><td rowspan="2">1:250</td></tr>
<tr><td>c-Myc</td><td>Santa Cruz #sc764</td></tr>
<tr><td>TRA1-60</td><td>Cell Signaling #4746</td><td rowspan="4">PBS
10%FBS</td><td rowspan="4">1:200</td><td>60 min, 37°C</td></tr>
<tr><td>TRA1-81</td><td>Millipore #MAB4381</td><td>60 min, 37°C</td></tr>
<tr><td>TRA2-49</td><td>Millipore #MAB4349</td><td>60 min, 37°C</td></tr>
<tr><td>SSEA4</td><td>Santa Cruz #sc21704</td><td>60 min, 37°C</td></tr>
</table>

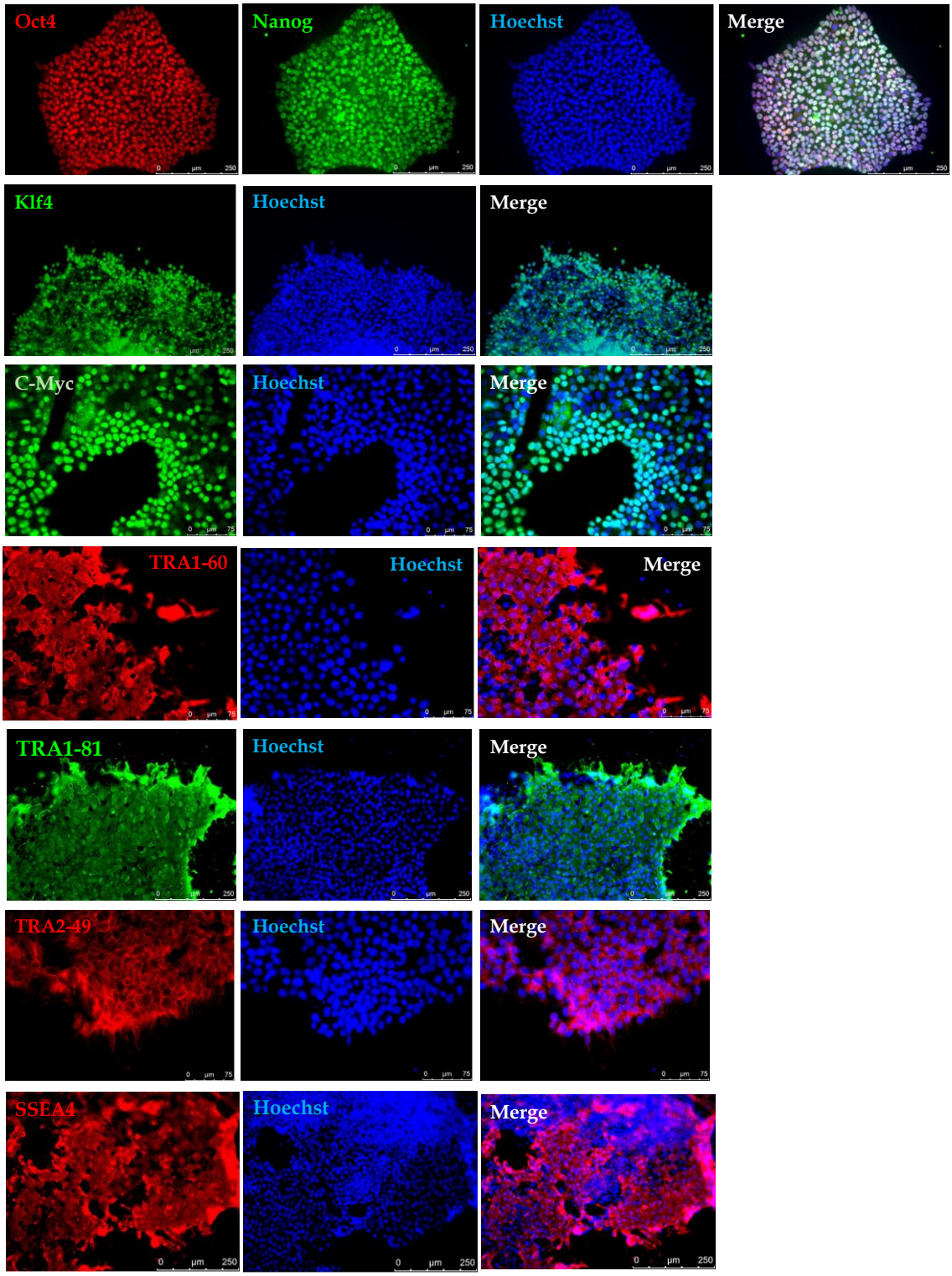

Figure 2.5: *The correct pluripotency maintenance of hPSCs employed in this work was verified by immunofluorescence staining of Oct4 and Nanog (mmRNA Clone 7), Klf4, c-Myc (mmRNA Clone 1), TRA1-60 (mmRNA Clone G), TRA1-81 (mmRNA Clone A), TRA2-49 (hESCs line HES2) and SSEA4 (hES MESP1$^{mCherry/w}$/NKX2.5$^{eGFP/w}$ dual reporter) expression. Nuclei were counterstained with Hoechst. Scale bar 250µm.*

Undifferentiated hPSCs cells express high levels of alkaline phosphatase (AP), responsible of the self-renewal potential of the cells (Figure 2.6). hPSCs were stained using the AP staining kit (Stemgent), undifferentiated cells appeared red or purple, whereas differentiated cells appeared colorless.

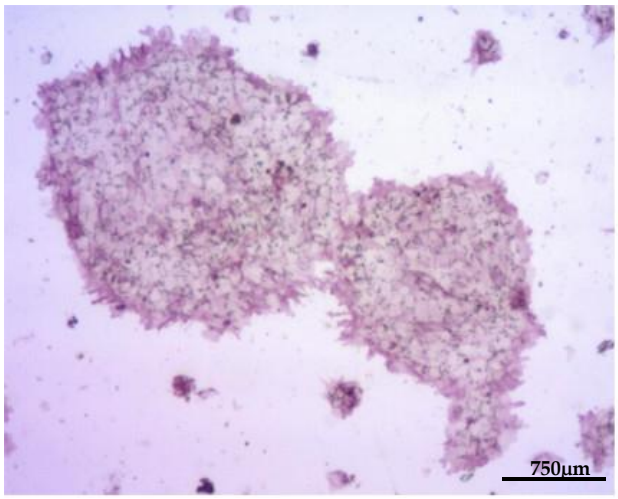

Figure 2.6: *AP activity on mmRNA Clone1. The pluripotent status of stem cells can be characterized by a high level of AP expression. Note that AP positive colonies appear purple.*

2.4. A Dual Reporter MESP1$^{mCherry/w}$/NKX2.5$^{eGFP/w}$ human embryonic stem cell line as a tool to monitor the progression of cardiac differentiation

Passier R. and colleagues of Leiden University in the Netherlands in 2014 developed a new cellular tool to visualize the course of early cardiac mesoderm and cardiomyocyte differentiation *in vitro:* they generated a fluorescent dual MESP1$^{mCherry/w}$/NKX2.5$^{eGFP/w}$ reporter line in hESCs to unravel the developmental signals orchestrating the formation of cardiac progenitors and their subsequent specification toward cardiac differentiation. The use of fluorescent reporter lines, in fact, helps reserchers to properly monitor cells behaviour during, for example, hPSCs cardiac differentiation *in vitro* or to track cells *in vivo* experiments [93]. In Figure 2.7 is reported a schematic representation of human fluorescent reporter lines applications.

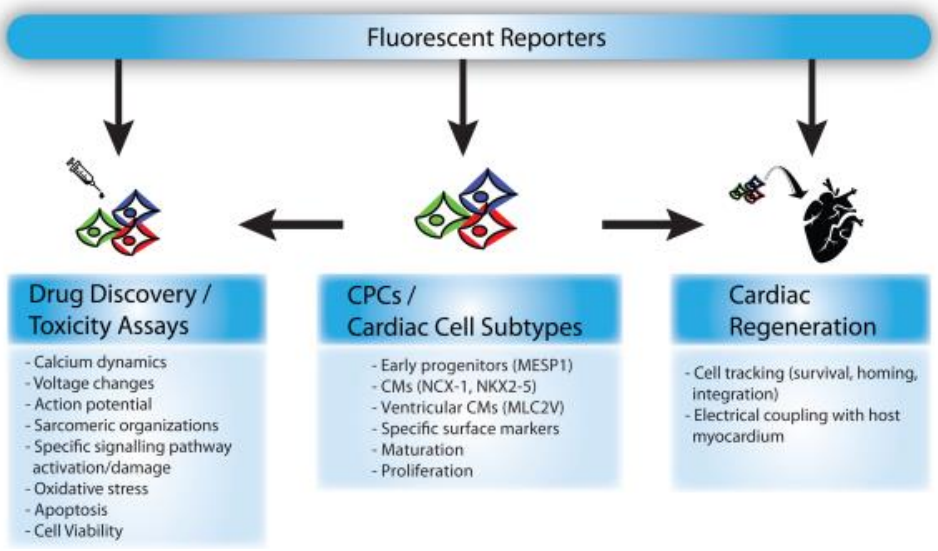

Figure 2.7: *Schematic overview of functional applications of human fluorescent reporter lines for monitoring the cardiac differentiation process and for cardiac disease and toxicity studies. Abbreviation: CPC, Cardiac Progenitor Cell (adapted from [93]).*

As already mentioned in Chapter 1 (Paragraph 1.2.1), MESP1 is an early pivotal TF expressed in embryonic precardiac mesoderm. Transcription factor NKX2.5 is expressed in heart precursor cells of the First Heart Field (FHF) and is maintained in the committed cells of the cardiac lineage [92][93]. During the cardiac differentiation of the dual reporter hESCs, cells transiently express MESP1-mCherry (red fluorescence), followed by a constant expression of NKX2.5-eGFP (green fluorescence).

To generate the *MESP1* targeting vector, Passier's group used the artificial bacterial chromosome RP11-975L13, modified by recombineering. Exon 1 sequence was replaced by the mCherry cassette and a selection marker. The modified *MESP1* locus with the surrounding 5′ and 3′ homology arms were then subcloned into the MESP1 targeting vector which was then linearized through Pvul digestion and electroporated into the mono reporter NKX2.5-eGFP hES line generated in 2011 in a previous work, published by the same research group [92][96]. To demonstrate that cardiogenic ability of the dual reporter line to fully recapitulate the timing of expression of the two TFs, Passier and collaborators performed a monolayer cardiac differentiation in the low-insulin, serum-free medium BPEL (BSA, polyvinyl alcohol and essential lipids) in which they added the growth factors BMP4 and Activin-A, the small molecule CHIR99021 to inhibit GSK3-β from day 0 to day 3, followed finally by the Wnt signalling antagonist inhibitor Xav939 from day 3 to day 7 of the

protocol. They clearly detected the mCherry red fluorescence of mCherry on day 3 of differentiation with cells undergoing epithelial-to-mesenchymal transition (EMT). The details on the generation of the dual reporter stem cell line performed by the researcher of Passier's laboratory are reported in Figure 2.8.

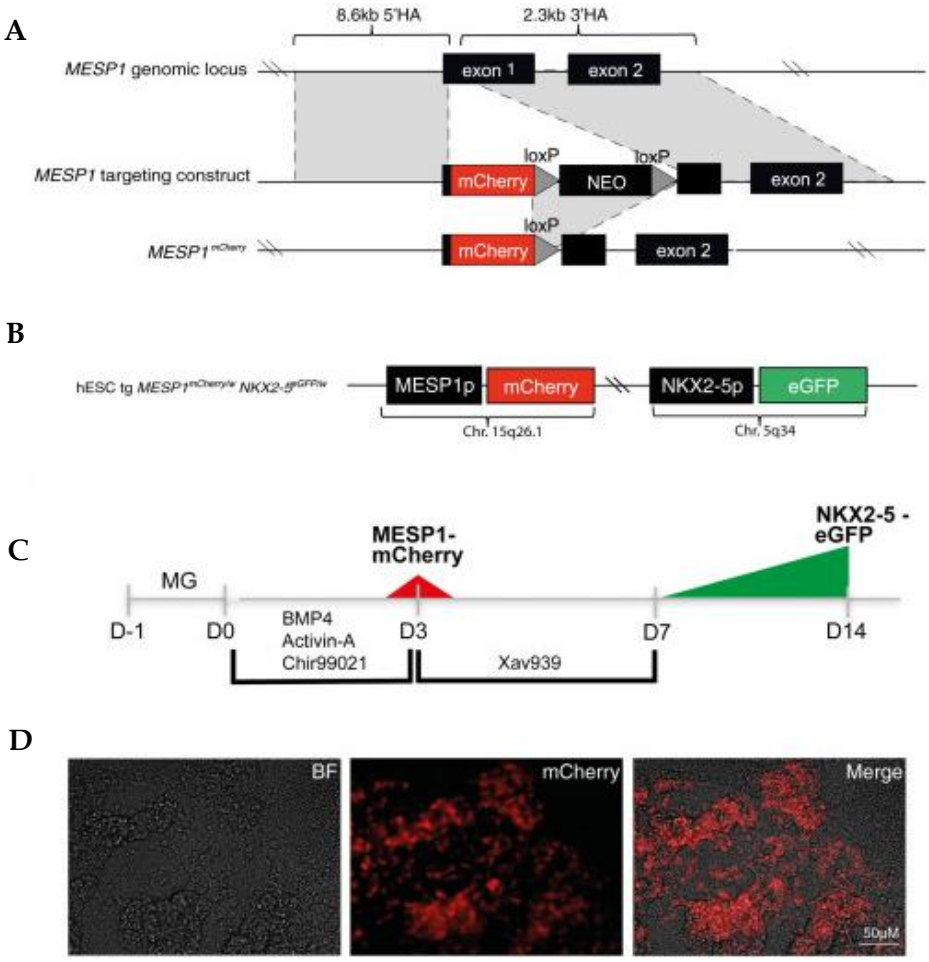

Figure 2.8: *Generation of MESP1$^{mCherry/w}$-NKX2.5$^{eGFP/w}$ dual reporter hESC line by Passier R. et al.* ***A****. Wild-type MESP1 allele, MESP1 targeting construct, and targeted MESP1 allele.* ***B.*** *Dual cardiac fluorescent reporter line. p: endogenous gene regulatory elements of either MESP1 (MESP1p) or NKX2.5 (NKX2.5p).* ***C.*** *Cardiac monolayer-based differentiation in BPEL.* ***D.*** *MESP1-mCherry signal at day 3 of cardiac differentiation. MG, matrigel; Tg, transgenic (adapted from [92]).*

Passier R. and co-workers performed a quantitative PCR (qPCR) gene expression analysis of their dual reporter cells undergoing cardiac differentiation and observed the transient expression of mCherry, with an intense peak on day 3 which mirrored the endogenous *MESP1* expression. In agreement with previous *in vitro* and *in vivo* studies reported in literature, they found that expression levels of mesendodermal genes *Brachyury T* (*T*) and *Eomesodermin* (*EOMES*) showed peak

values at day 2, 24 hours before *MESP1* peak. Expression levels of *NKX2.5* were markedly detectable strating from day 9 of differentiation, just before cells strated to form beating areas, with further increase on day 12 (Figure 2.9).

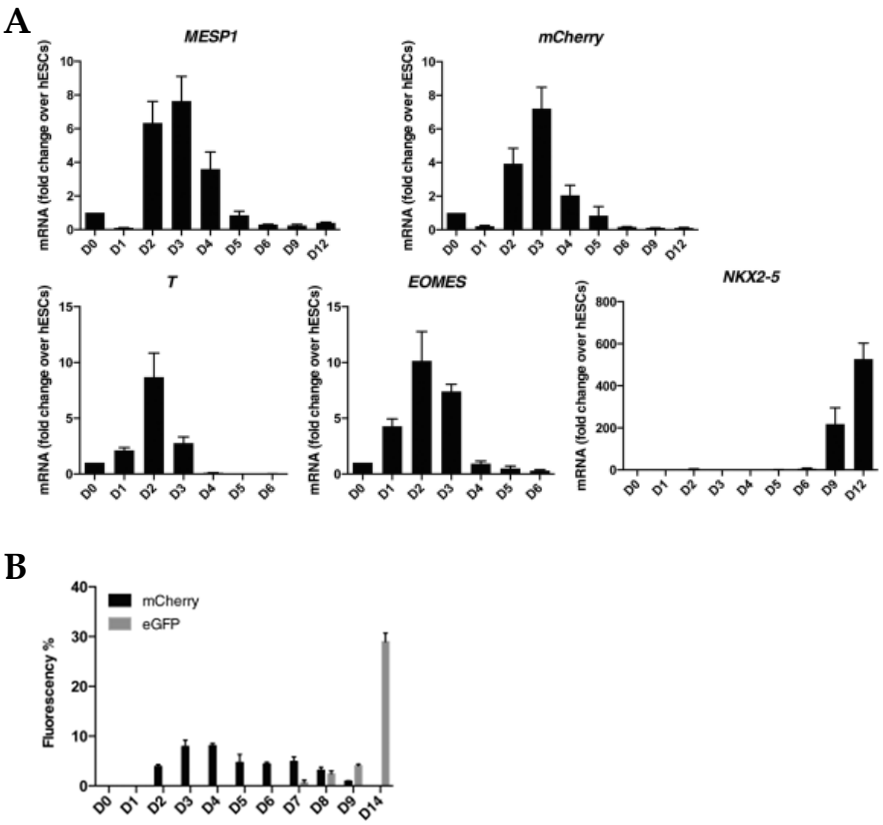

Figure 2.9: *Gene expression pattern analysis performed by the researchers of Passier's laboratory.* ***A.*** *mRNA levels of T and EOMES, MESP1, mCherry, and NKX2.5. Results are normalized for day 0 transcript expression in undifferentiated hESCs (n=3, error bars indicate SEM).* ***B.*** *The quantification of percentages of mCherry and eGFP expressing cells during monolayer differentiation (n=4-8; error bars indicate SEM; adapted from [92]).*

Passier and his group demonstrated the importance of using genetically modified reporter lines as a tool for developing and monitoring protocols that enable a real time observation of the mechanisms of cell differentiation. As demonstrated in their work, in the dual reporter *MESP1*^{mCherry}-*NKX2.5*^{eGFP} line, firstly mCherry started to became visible indicating the mesoderm induction, followed by the later appearance of GFP+ cardiac progenitors and subsequent CMs, unveiling, *in vitro,* previously inaccessible stages of early human cardiac development [92][93][96].

2.4.1. MESP1$^{mCherry/w}$/NKX2.5$^{eGFP/w}$ expression monitoring during monolayer differentiation using Wnt/β-catenin pathway modulators in standard cultures

In this thesis, the dual reporter *MESP1$^{mCherry/w}$-NKX2.5$^{eGFP/w}$* line was used to monitor the progression of cardiac differentiation.

The dual reporter line was differentiated using the monolayer-based cardiac differentiation protocol in standard cultures via the temporal modulation of Wnt/β-catenin pathway that will be described in the next Paragraph 2.5. Briefly, on day 0 of cardiac differentiation was applied the GSK3-β inhibitor CHIR99021 to drive mesoderm induction, followed by Wnt inhibiton with IWP4 on day 3 of differentiation. For every cardiac differentiation experiment, the fluorescence of mCherry and eGFP for the expression of *MESP1* and *NKX2.5* respectively was monitored daily under the fluorescence microscope.

Because the temporal expression window of *MESP1* is very short (2-3days), the mCherry monitoring was performed 3 times/day during the first three days of differentiation. As reported in Figure 2.10, the peak of expression of mCherry appeared on day 3 of cardiac differentiation, accordingly to Passier's work, whereas the *NKX2.5* signal associated to eGFP became visible between day 7 and 8 of differentiation, just 1-2 days before of the detection of beating CMs.

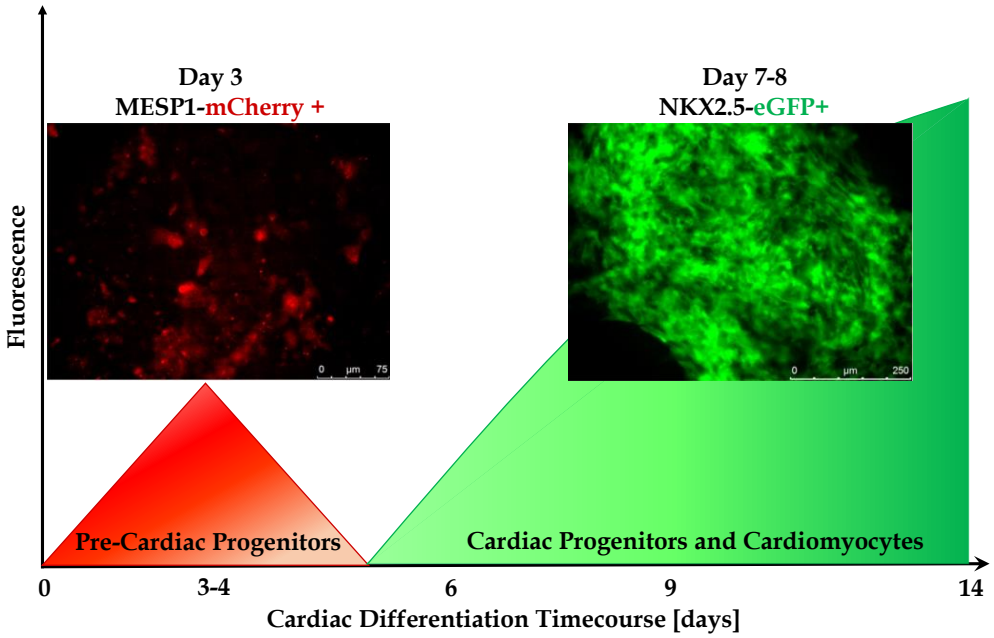

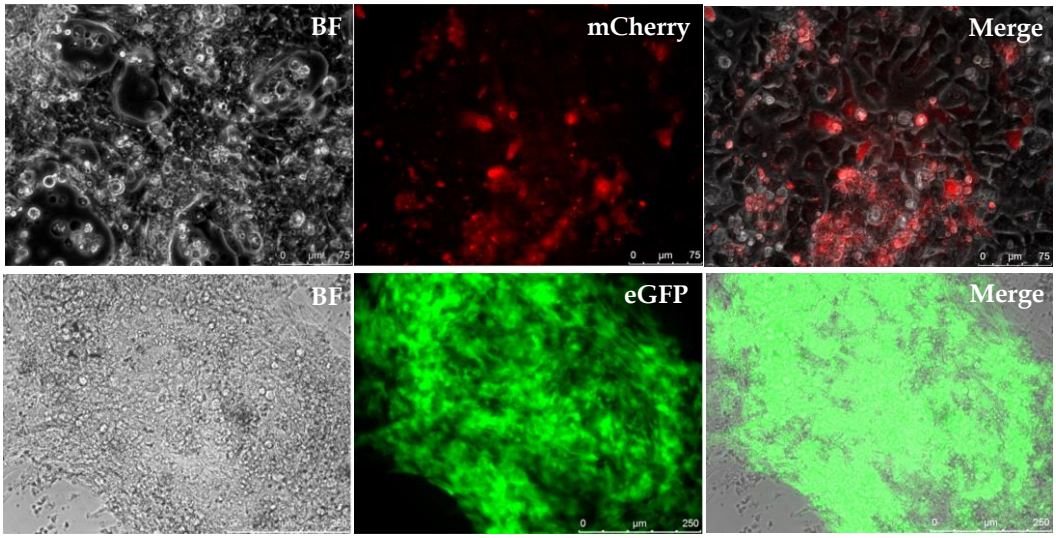

Figure 2.10: *Dual cardiac fluorescent reporter line MESP1^{mCherry}-NKX2.5^{eGFP} in hESCs allows visualization and isolation of precardiac MESP1+ progenitors with a peak on day 3 of differentiation and their further progression to NKX2.5 eGFP+ derivatives starting to be detectable on day 7-8 of differentiation.*

This dual cardiac reporter line allowed the spatiotemporal monitoring of the molecular pathways involved in the switch from hPSCs, pre-cardiac precursors and CMs representing also an useful tool for *in vivo* lineage tracing studies in which, for example, these cells could be implanted in infarcted hearts [92][93][96].

2.5. The gold standard approach for cardiac differentiation of hPSCs in conventional cultures

As described previously in Chapter 1, Paragraph 1.4, recently, significant progress has been made in cardiovascular research to improve the cardiac differentiation of hPSCs. hPSC-CMs were firstly isolated from serum-stimulated EBs in 2001 by Gepstein J.'s laboratory [56], and later derived by co-culture on a feeder layer of mouse stromal cells by Mummery C. and coworkers in 2003 [9]. Early differentiation protocols, presented by Laflamme M.A. *et al.* and Keller G. *et al*., in 2007 strogly improved cardiac purities, of ~30-70% CMs. Additional optimization of these protocols were performed using Activin-Nodal signaling made by Keller's laboratory in 2011 [21][57], culturing cells on extracellular matrix (ECM) proteins by Zhang J.'s laboratory in 2012 [97] and the modulation of Wnt signaling described in 2012 by Palecek S. and colleagues [63][64].

In this thesis was applied the monolayer-based differentiation protocol in standard 24-well plates presented by Lian X, Palecek S. and co-workers in 2012 that efficiently directs hPSCs differentiation to beating CMs in a completely defined, GFs and serum-free culture setting by temporal activation and inhibition of canonical Wnt/β-catenin signaling pathway. This method, described in Figure 2.11., is reported in literature as the most efficient to date for producing a high yield of CMs from hPSCs; in this work, this protocol was used as the gold standard to study cardiac differentiation of hPSCs in conventional culture systems for these reasons:

- it allows a simple and fast CMs generation with high efficiency in approximately 15 days solely *via* small molecules that modulate canonical Wnt/β-catenin pathway;
- the use of small molecules instead of GFs determine a more controllable and reproducible generation of CMs, lowering the intra- and inter-experimental variability observed when using the other methods described for direct cardiac hPSCs differentiation;
- the temporal modulation of Wnt/β-catenin pathway leads to a high yield of CMs (80%-90%) from multiple hPSCs lines;
- CMs produced can be maintained in culture up to 6 months allowing a complete structural, functional and molecular characterization [63][64].

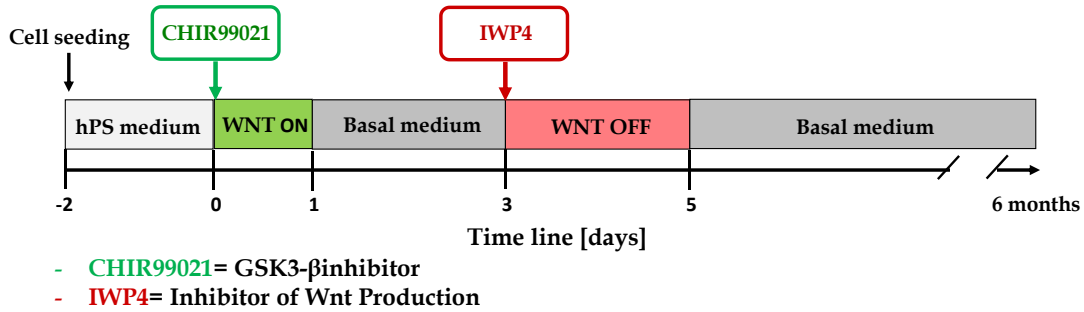

Figure 2.11: *Schematic of the monolayer-based protocol for defined, GFs-free and serum-free differentiation of hPSCs to CMs by temporal modulation of regulators of canonical Wnt/β-catenin signaling pathway. Basal medium indicates RPMI with or without insulin (modified from [63]).*

hPSCs were initially cultured on 0,5% v/v MRF (BD)-coated 6-well plates and maintained in StemMACS™ iPS-Brew XF medium (Miltenyi Biotec) until they achieved the confluence. Differentiation was initiated by seeding hPSCs on 0,5% v/v MRF-coated 24-well plates, removing the hPSCs medium and switching to

RPMI (Life Technologies) with 1X B27 nutrient supplement (Life Technologies) medium lacking insulin (basal medium) and containing a glycogen synthase kinase 3-β (GSK3-β) inhibitor, CHIR99021 for 24 hours. CHIR99021 is an aminopyrimidine considered the most selected inhibitor of the GSK3-β to date, leading to the activation of the canonical Wnt pathway [69]. After 48 hours in basal medium, Wnt secretion was suppressed for 48 hours by adding 10μM of the inhibitor of Wnt production-4 (IWP-4, Life Technologies). IWP-4 was identified with a highthroughput screen for the identification of Wnt/β-catenin pathway antagonists; its mechanism of action relies on palmithylation of Wnt proteins by Porcupine (Porcn) by blocking Wnt secretion and activity; it also blocks the accumulation of β-catenin [98].On day 7 of differentiation, the hPSCs-derived CMs were maintained in RPMI + B27 complete of insulin (basal medium) until use for further experimental procedures.

The cardiac differentiation of hPSCs was monitored daily under microscope, performing a time-lapse analysis for 11 days, and the contractions were recorded (Figure 2.12).

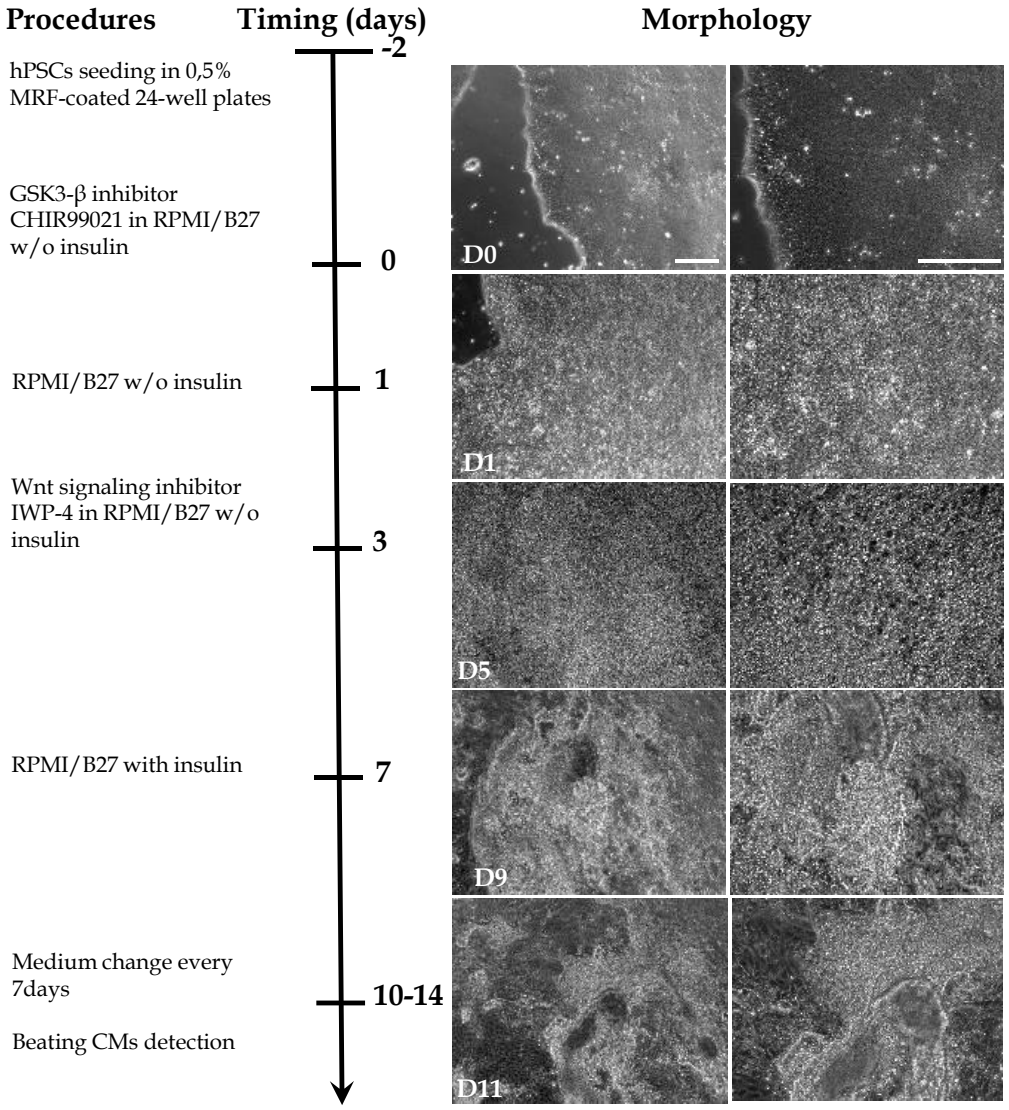

Figure 2.12: *Schematic of the protocol for the differentiation of CMs from hPSCs (in this pictures mmRNA Clone 7) with modulators of canonical Wnt/β-catenin signalling in standard multiwells. Bright-field images of the typical morphology of day 0, 1, 5, 9 and 11 cells shown at 10X and 20X magnifications. Scale bars, 100μm.*

From day 8 to 14, depending on hPSCs line and clone of origin, cells started to contract spontaneously, firstly as isolated points and then the consistent part of the monolayer. Robust spontaneous contractions occurred approximately on day 10-12.

2.5.1. Cardiomyocytes disaggregation for cell characterization

To prepare the sample for the following CMs characterization, cells were firstly detached and disaggregated from the 24-well plate, accordingly to the protocol of Lian X. and colleagues and described in Nature protocols in 2012 [63][64]. Briefly, cells were incubated with 10μM Y-27632 (Tocris), an inhibitor of Rho-associated coiled-coil forming protein serine/threonine kinase (ROCK) for 75 minutes at 37°C, to prevent dissociation-induced apoptosis. Glass coverslip for CMs seeding were coated with 2,5%v/v MRF. After 75 minutes, cells were incubated with the digestion mix composed of 2mg/ml collagenase I (Gibco), 1mg/ml collagenase IV (Gibco), 2U/ml DNase I (Invitrogen) and 10μM Y-27632 in PBS with Ca^{2+} and Mg^{2+} (Life Technologies) for 25 minutes at 37°C, after removing the basal medium and gently washing CMs with PBS. Then the digestion mix was aspirated and cells were washed in PBS and incubated with TrypLE™ Select (Gibco), a cell-dissociation enzyme. CMs were detached vigorously and suspended in single cell suspension. Finally STOP medium (1:1 DMEM and FBS, Life Technologies; with 2U/ml DNase I) was added and cells were centrifuged and resuspended in basal medium. CMs are now ready for quantification by flow cytometry or for seeding them in the MRF-coated glass coverslip previously prepared, for further characterization by immunofluorescence and patch clamp assay described in the next Paragraphs.

2.5.2. Characterization of hPSC-derived cardiomyocytes

At day 14 after differentiation, the cells should show hallmarks of CMs, including spontaneous contraction and cardiac-specific protein expression. CMs obtained were disaggregated as described in Paragraph 2.5.1 and characterized by immunofluorescent staining against nuclear markers GATA4 and NKX2.5 and structural cardiac markers (Figure 2.13) including Troponin T (cTnT), α-Actinin, an embryo/fetal Troponin T (RV-C2) and adult Troponin I (Ti1) isoforms and Myosin Heavy Chain (MYH7 or BA-D5 used in Chapter 4). To determine the expression of proteins involved in cell-cell communication, an immunofluorescence staining for the Connexin 43 (Cnx-43), the major gap junction protein in the heart that promotes electrical coupling and synchronizes contractions of CMs, was performed (Figure 2.13 A and C). All the

immunofluorescences were performed in accord to the five-steps protocol previously described in Paragraph 2.3.

A hES HES2-CMs

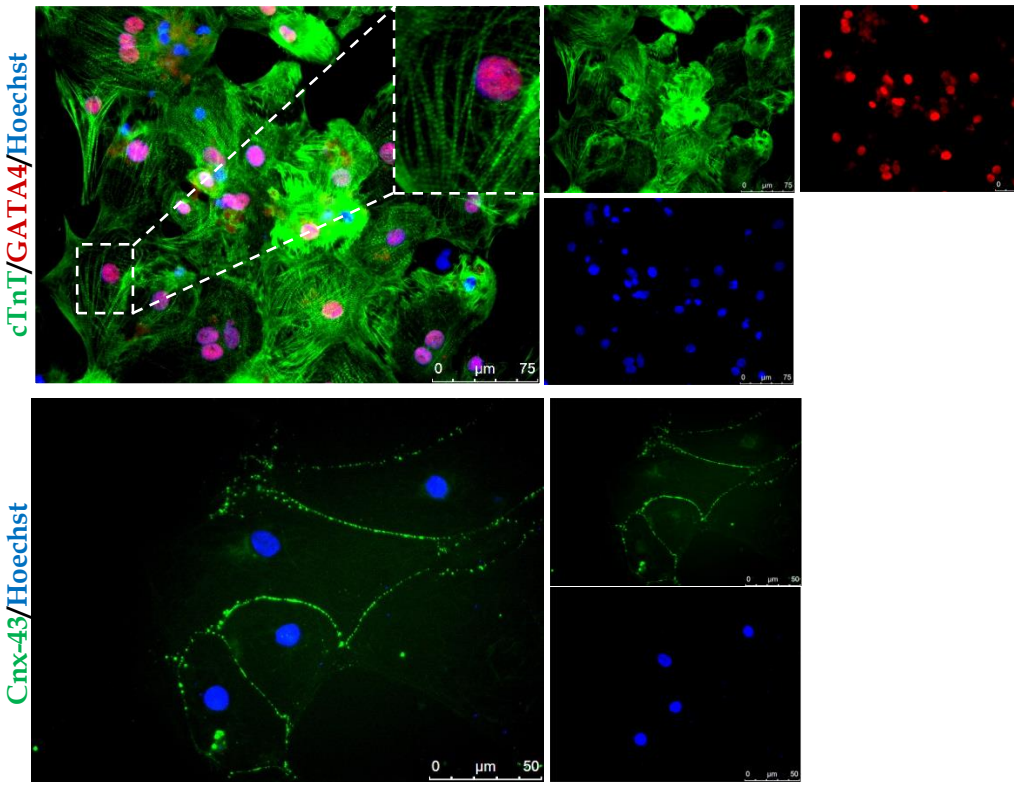

B hES Dual Reporter-CMs

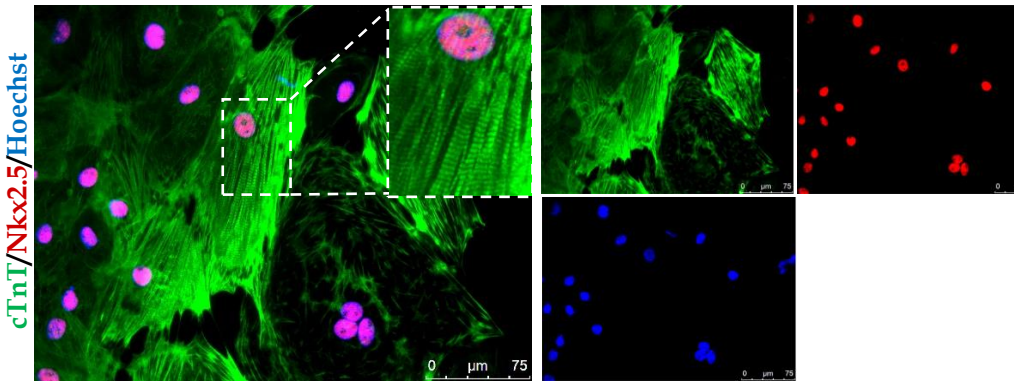

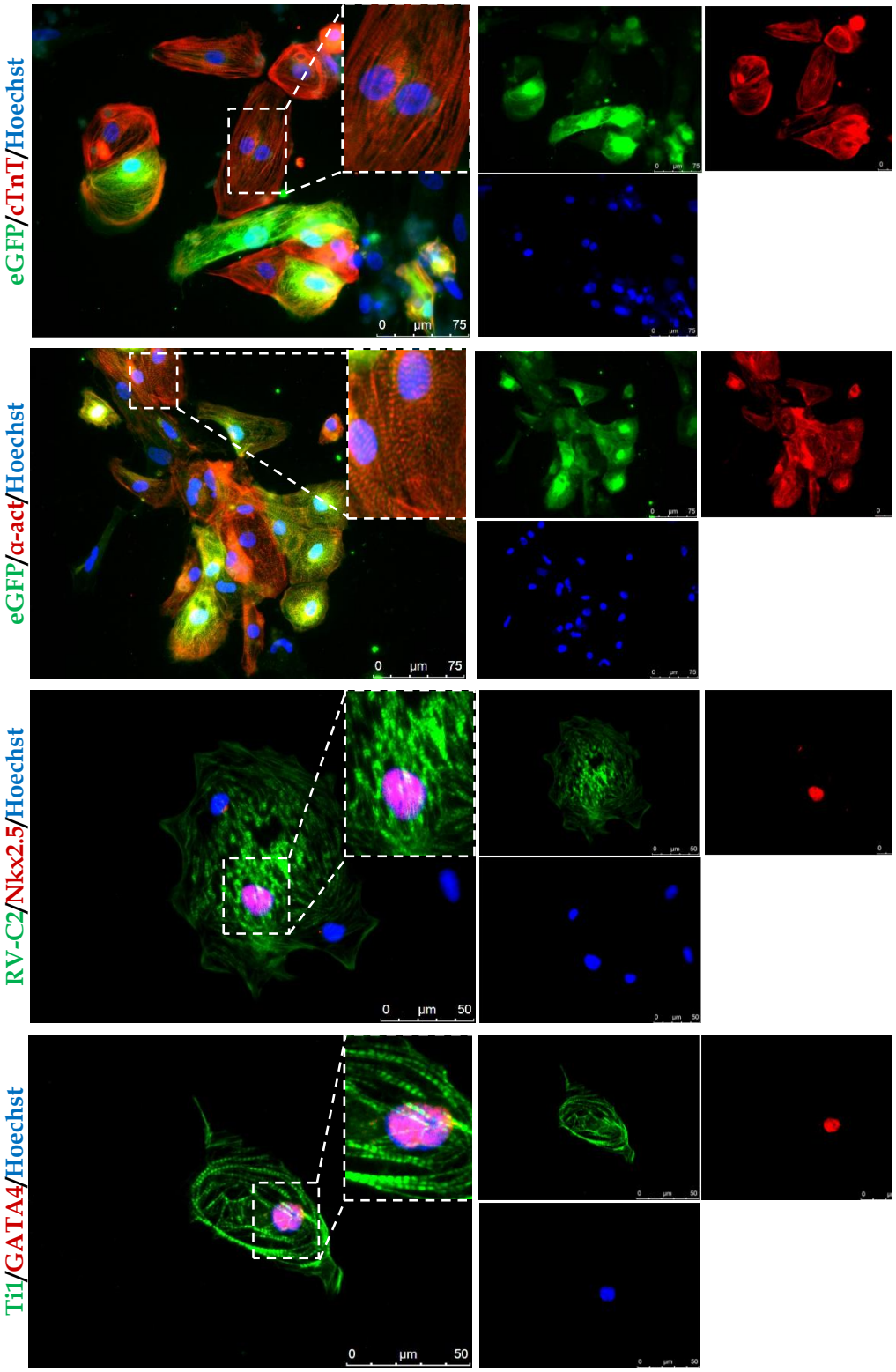
eGFP/cTnT/Hoechst
eGFP/α-act/Hoechst
RV-C2/Nkx2.5/Hoechst
Tf1/GATA4/Hoechst
0 µm 75
0 µm 50

C hiPS-CMs

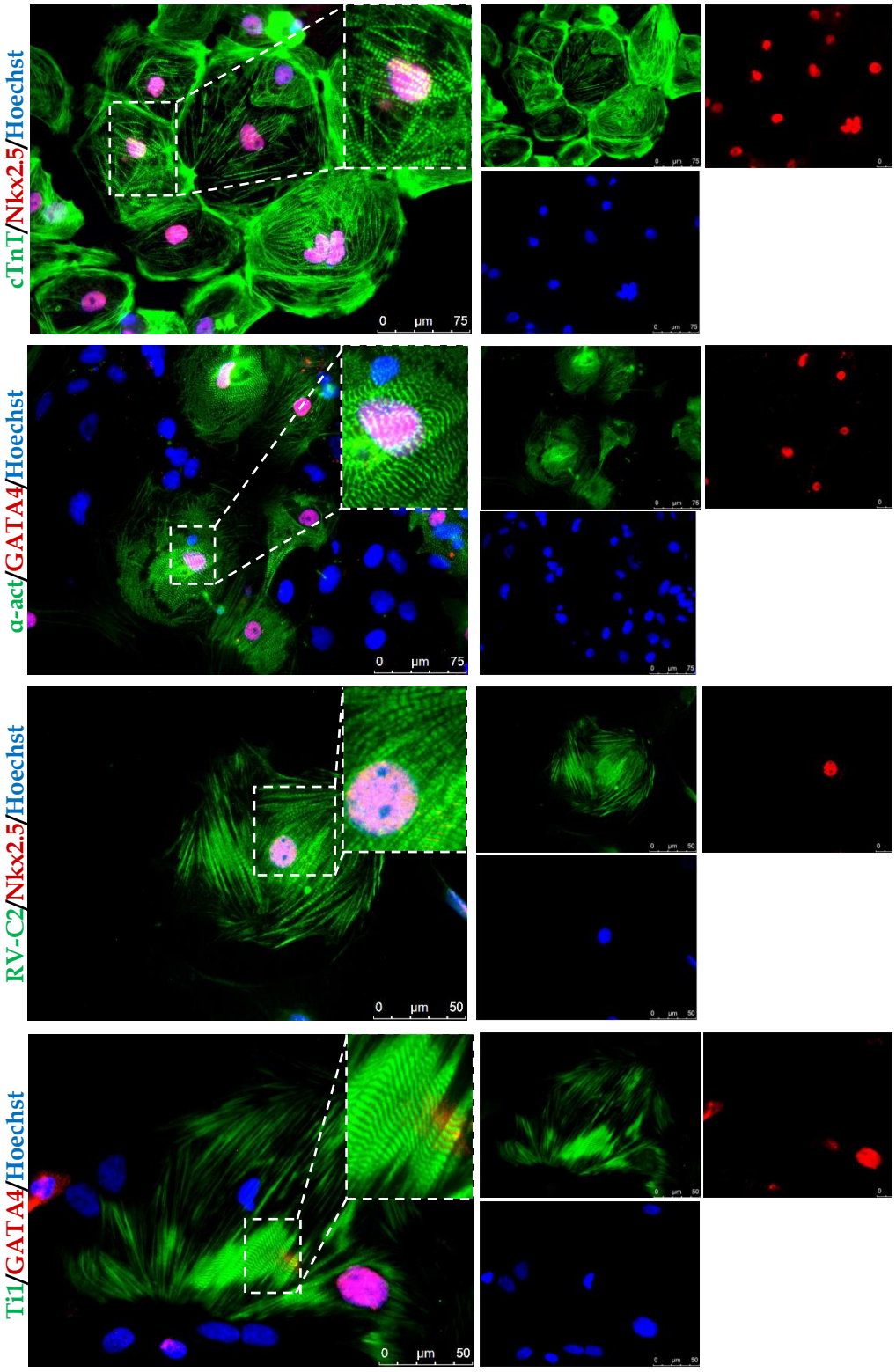
cTnT/Nkx2.5/Hoechst
α-act/GATA4/Hoechst
RV-C2/Nkx2.5/Hoechst
Ti1/GATA4/Hoechst
0 µm 75
0 µm 50

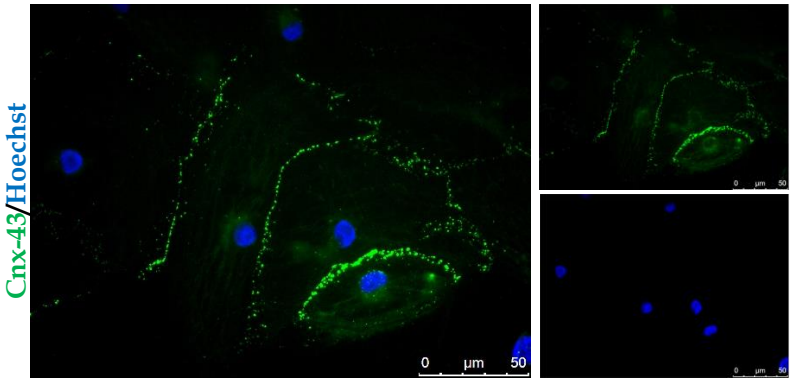

Figure 2.13: *Molecular markers in hPSC-CMs. Expression of cardiac markers in human CMs derived from A. hES HES2 line B. hES MESP1$^{mCherry/w}$/NKX2.5$^{eGFP/w}$ dual reporter (note the expression of eGFP related to the NKX2.5 locus) and C. hiPSCs (mmRNA Clone 7); Immunofluorescence staining showed a remarkable organization of the sarcomeres.*

Supplementary information on antibodies used and immunofluorescence steps are reported in Table 2.3.

Table 2.3: *Summary of all the primary antibodies employed in this thesis for the characterization of the CMs obtained from hPSCs, with all the parameters of the assay listed.*

Antibody	Manufacturer	Fixation	Permeabilization and Blocking	Dilution	Incubation
GATA4	Santa Cruz #sc1237	1%PFA, 10min, RT	PBS-0,1% Triton X 10% FBS	1:50	12 hours, 4°C
Nkx2.5	Santa Cruz #sc8697				
cTnT	Thermo Scientific #MS295P	4%PFA, 10min, RT		1:200	60 min, 37°C
α-Actinin	Sigma-Aldrich #A7811			1:250	
Ti1	DSHB, S. Schiaffino's Lab		PBS-0,1% Triton X 0,5% BSA	1:50	12 hours, 4°C
RV-C2	DSHB, S. Schiaffino's Lab				
BA-D5	DSHB, S. Schiaffino's Lab				
Cnx-43	Millipore #MAB3067	Acetone, 20min, -20°C	PBS-0,25% Triton X 10%FBS, 10 min	1:200	12 hours, 37°C

With this monolayer-based differentiation, it was possible to obtain a high yield of CMs, positive for the principal cardiac-specific markers; in particular, as reported in the magnification of the panels in Figure 2.13, immunostaining showed a remarkable organization of the sarcomere, the contractile unit of this cell type.

CMs obtained were then quantified by counting the cardiac troponin T (cTnT) positive cells from immunofluorescence staining, as reported in the

graph in Figure 2.14 with the related Table reporting the percentages of cTnT^{+ve} cells obtained from each hiPS Clone and hES line.

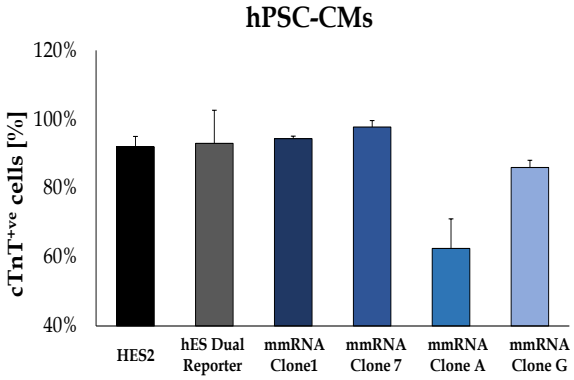

hPSCs	cTnT^{+ve} cells [%]
HES2	92±2%
hES Dual Reporter	93±10%
Clone 1	94±7%
Clone 7	98±2%
Clone A	63±9%
Clone G	86±2%

Figure 2.14: *Percentage of cardiac troponin T (cTnT) positive CMs obtained from the monolayer cardiac differentiation of hPSCs using Wnt/β-catenin modulators with 12μM CHIR99021, (n=3, error bars indicate SEM).*

In Palecek's work, 12μM CHIR99021 was reported as the optimal concentration for cardiac differentiation but he suggested that an optimization of concentrations was required for each hPSCs line used [64].

As observed in the cTnT^{+ve} quantification reported in the graph of Figure 2.14, a hES line and a hiPS clone were selected for their cardiogenic ability to give the highest CMs yield: hES Dual reporter line (93% cTnT^{+ve} cells) and hiPS mmRNA Clone 7 (98% cTnT^{+ve} cells).

To assess the ability of these cells to generate beating CMs, the concentration of CHIR99021 for an optimal GSK3-β inhibition was optimized in a range from 6-12μM and. The CMs obtained were then quantified by counting the cTnT^{+ve} cells from immunofluorescence staining and the graph reported in Figure 2.15 demonstrated that hiPS Clone 7 gave a high yield of CMs from 6 to 10μM CHIR99021, while the hES Dual Reporter line ranged from 9 to 10μM. CHIR99021 10μM emerged as the best concentration for the generation of the highest yield of beating CMs (94% for hES Dual Reporter-CMs and 98% for hiPS Clone 7).

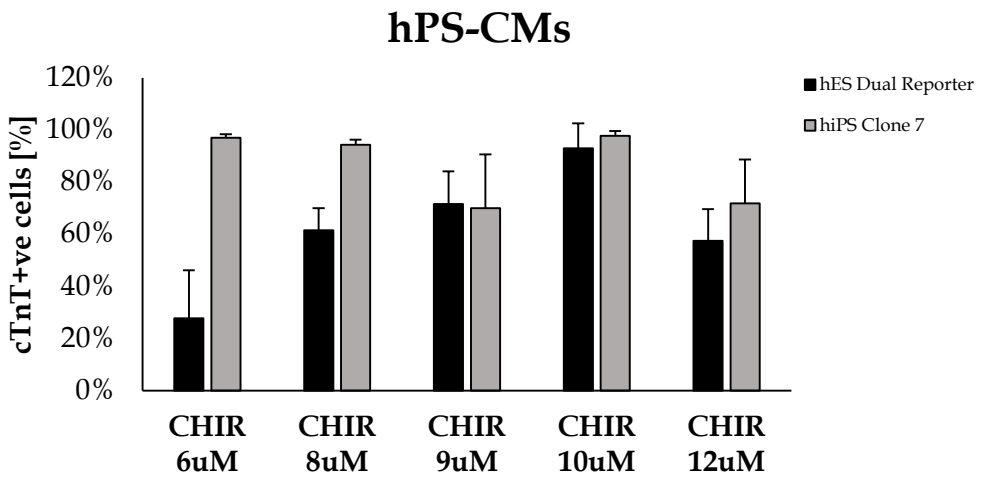

Figure 2.15: *Optimization of CHIR99021 concentration for hiPS mmRNA Clone 7 (grey bars) and hES Dual Reporter (black bars), selected for the following experiments. (n=3; error bars indicate SEM).*

For the following experiments presented in this work, hES Dual Reporter and hiPS Clone 7 were always used and the Wnt perturbation performed using always 10μM CHIR99021.

Furthermore, to make a more complete characterization and to investigate the uniformity of CMs population obtained and the degree of maturation, on day 30 cells were immunostained for two other structural markers: an embryo/fetal isoform of Troponin T (RVC2) and an adult isoform of Troponin I (Ti1).

Cardiac Troponin relies on a complex of three regulatory proteins: Troponin C (cTnC), Troponin I (cTnI) and Troponin T (cTnT), which regulate muscle contraction. The analysis of developmentally regulated and tissue-specific isoforms of Troponins due to the presence of a large number of variants derived from different genes and/or differential gene splicing. In 1988 Schiaffino S. and colleagues, using a monoclonal antibody specific for cardiac Troponin T, obtained direct evidence for developmentally regulated isoform of the embryo/fetal RVC2 in rat hearts [99]. One year later, in 1989 Schiaffino's lab investigated also the developmental switching of Troponin I in rat muscle and identified through immunoblotting and affinity chromatography procedures a distinct cTnI isoform expressed in the adult myocardium [100]. TnI acts by holding actin-tropomyosin complex in place. Because of this inhibitory action, myosin cannot bind actin in when the cardiac cell is relaxed. Immunofluorescence staining for these markers (the antibodies used were

kindly given by Professor Schiaffino S., University of Padova and deposited at Developmental Studies Hybridoma Bank, DSHB) was performed for two cell types: hiPS mmRNA Clone 7, hES Dual Reporter. Embryo/fetal RVC2^{+ve} and adult Ti1^{+ve} cells were quantified and the percentages are reported in Figure 2.16 with the related Table.

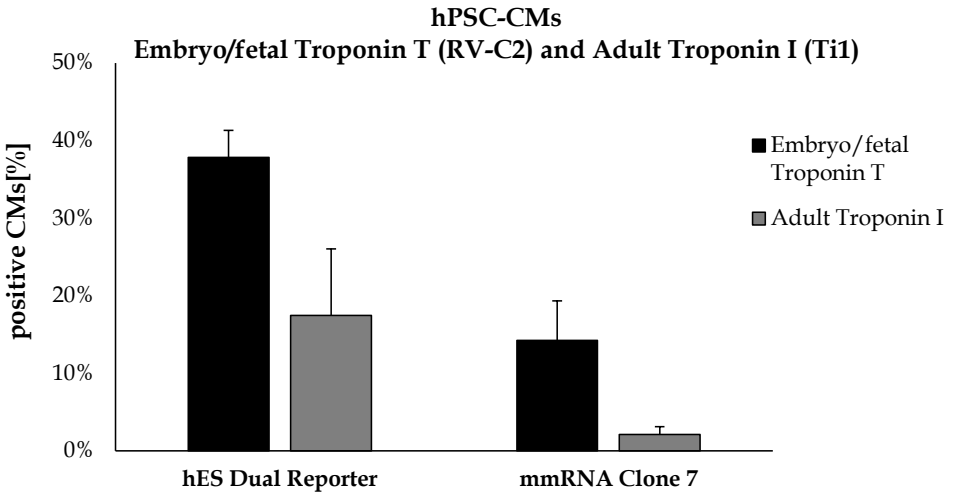

hPSCs	Embyo/fetal Troponin T^{+ve} cells [%]	Adult Troponin I^{+ve} cells [%]
hES Dual Reporter	38±4%	17±8%
hiPS Clone 7	14±5%	2±1%

Figure 2.16: *Percentage of RVC2 embryo/fetal Troponin T and Ti1 adult Troponin I in day 30 CMs obtained from monolayer cardiac differentiation using Wnt/β-catenin modulators, (n=3, error bars indicate SEM).*

As reported in the graph, the hPSC-CMs expressed a higher percentage of the embryo/fetal isoform of Troponin T. Although with this gold standard protocol the cells expressed a good percentage of the adult isoform of Troponin I, it leaves room for improvement regarding cell maturation because it is clear from these results that a random differentiation toward subpopulations occurred and the CMs obtained are partially immature.

2.5.3. Flow cytometry quantification of cardiomyocytes

After the disaggregation on day 14, the percentage of $cTnT^{+ve}$ cells was calculated by flow cytometry analysis of at least 20.000 total cells per test, using indirect immunofluorescence assay. From two wells of a 24-well plate, five samples were prepared for the quantification:

- 2 samples, 1 composed of 1.000.000 cells and 1 of 500.000 cells, incubated with cTnT antibody diluted respectively 1:100 and 1:200 for each sample;
- 2 samples as negative control, 1 composed of 1.000.000 cells and the other with 500.000 cells incubated respectively with 1:100 and 1:200 ßIII-Tubulin antibody (TUJ1, Sigma –Aldrich), a protein involved in neural development and costitutively expressed in neural tissues, absent in CMs;
- 1 sample with 500.000 cells incubated only with the secondary antibody Alexa Fluor-488 to exclude background signals.

All the samples were prepared using the FIX & PERM® Cell Fixation and Cell Permeabilization kit (ThermoFisher) that consists of matched Fixation Reagent (Medium A) and Permeabilization Reagent (Medium B). This kit facilitates antibody access to intracellular structures and leaves the morphological light-scattering characteristics of the cells intact. Moreover, these formulations reduce background staining allowing simultaneous addition of permeabilization medium and fluorophore-labeled antibodies.

Cells were incubated firstly with Medium A for 15 minutes at room temperature and then washed with wash medium (5% FBS in PBS w/o Ca^{2+} and Mg^{2+}). After a centrifugation, the samples were incubated with the primary antibody diluted in Medium B for 20 minutes at room temperature. Another washing with the wash medium and, after a second centrifugation, cells were incubated with the secondary antibody for 20 minutes at room temperature. Analysis were performed at Venetian Institute of Molecular Medicine (VIMM) of Padova on a FACSCanto™II (BD Biosciences) Flow Cytometer System, with the collaboration of Dr. Cabrelle A. The quantifications of cTnT+ cells are reported in Figure 2.17**.**

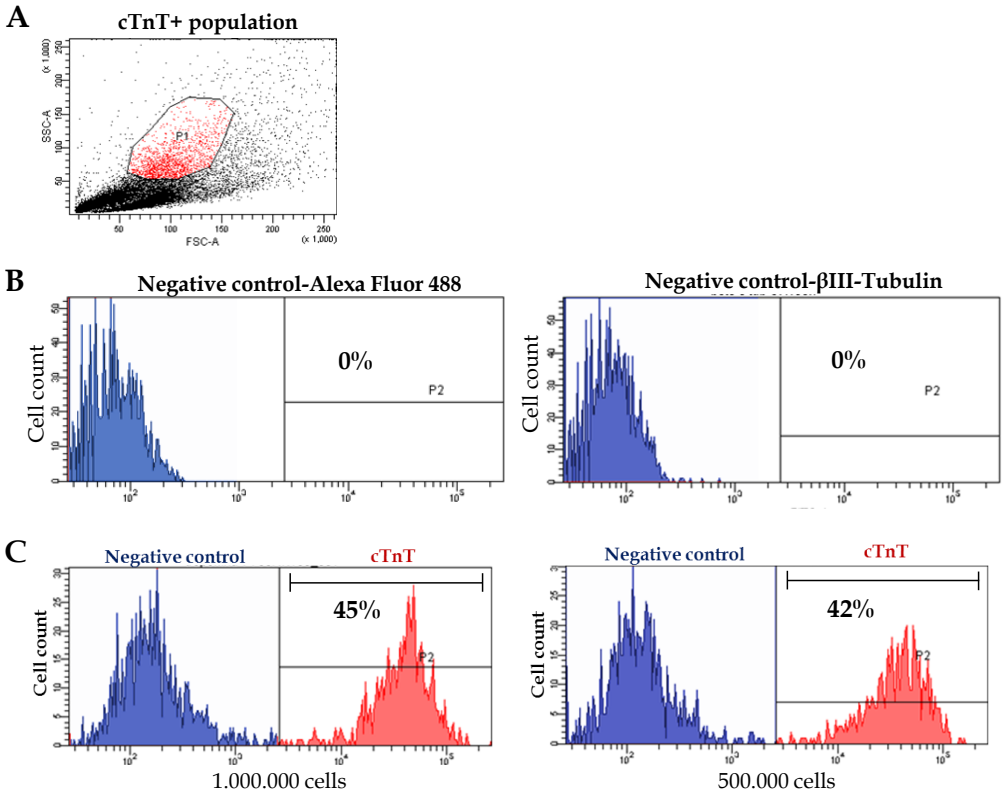

Figure 2.17: *Quantitative flow cytometry analysis of 14 days CMs showed cTnT expression in the sample (hiPSCs mmRNA Clone 7).* ***A.*** *Dot-plot of the sample population. The gate-box identifies the cTnT+ subpopulation in the sample, based on the forward- and side-scatter intensity profile.* ***B.*** *Blue histograms represent the negative control (left panel: secondary antibody Alexa Fluor-488 for the exclusion of background signals; right panel: βIII-Tubulin antibody that is absent in CMs).* ***C.*** *Red histograms represent cTnT expression in samples consisting of 1.000.000 cells (left) and 500.000 cells (right).*

As reported in Figure 2.17**,** CMs quantified by flow cytometry revealed a lower percentage (45 and 42%) of cTnT expressing cells, compared with cTnT positivity resulting from immunostaining and reported in Figure 2.14 of Paragraph 2.5.2, showing a need for an optimization of the sample preparation to correctly quantify the CMs population. In particular, it becomes important the identification of a disaggregation protocol that more efficiently eliminates clusters of cells that can interfere with the analysis at flow cytometer.

2.5.4. Dual-whole cell voltage-patch clamp to study cell-cell communication in gap junctions conductance

2.5.4.1. Cardiac gap junctions

Gap junctions (GJs) in cardiac cells are responsible of the uniform coupling that promotes the rapid, synchronous electrical activation and initiation of contractions [101]. GJs are channels, that directly connect the cytoplasm of one cell with the adjacent one, allowing the passage of ions and small molecules (<1kDa). For each CMs pair, every cell contributed with a hemichannel or connexon, which is formed by the oligomerization of six transmembrane connexins (Cx or Cnx). As illustrated in Figure 2.18**,** these connexins are encoded by a family of closely related, highly conserved genes; their structure relies on of 4 α-helical membrane-crossing segments (M1-M4) separated by 2 extracellular (E1 and E2) and one intracellular loop (CL). Hydrophobic amino acids are predominantly present in the transmembrane segments 1, 2 and 4, while segment 3 is characterized by an amphiphatic character because it is confined in the inner lining of the channel pore [102]. These transmembrane segments are highly conserved, whereas differences in the sequence and lengths of other cytoplasmic domains are unique [103]. In mammalian heart, Cnx 37, 40, 43, 45, 46 and 50 (numbers related to the kDa molecular mass) are present.

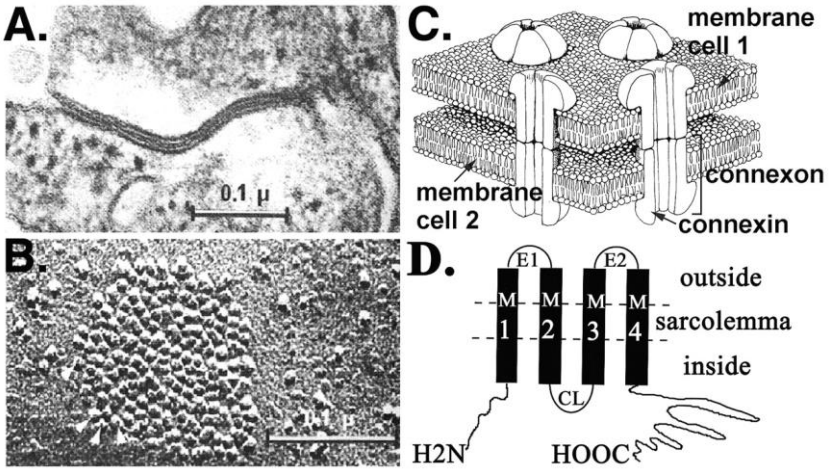

Figure 2.18: *GJ ultrastructure.* ***A.*** *Electron micrograph of two connected cardiac membranes.* ***B.*** *Freeze-fracture electron micrograph of a GJ (round particles are channels).* ***C.*** *Illustration of a part of a GJ.* ***D.*** *Molecular structure of a connexin. M1-M4 membrane spanning regions, E1 and E2 extracellular loops and CL cytoplasmic loop (adapted from [102]).*

Connexin 43 (Cnx 43) is the most abundant cardiac GJ protein and promotes CMs electrical coupling and contractions synchronization. The above mentioned GJs proteins are less abundant and specifically localized in single cardiac districts. GJs are mainly localized at the intercalated disks level, responsible of cell-to-cell attachment *via* desmosomes, strongly connected through adherent junctions with actin filaments [104].

In this work, to determine the expression of proteins involved in cell-cell communication, following the immunofluorescence staining against Cnx 43 showed in Figure 2.13, the dual-whole cell voltage-patch clamp was performed to characterize gap junction conductance (g_j) in CMs pairs. This experiment is described in the following Paragraph.

2.5.4.2. Principle of the method

The voltage patch clamp is an application enabling the measurement of the ion currents passing the membrane of excitable cells, such as CMs. The patch clamp technique is an evolution of the classical voltage clamp presented by the two Nobel Prize in Physiology or Medicine (1991) Neher E. and Sakmann B. in the late 1970s and early 1980s. The development of this functional assay allowed the recording of currents in single ion channel molecules, giving precious insights into the mechanisms involving channels in processes such as action potentials [105]. Principle of the method relies on the highly precise isolation of small "patch" of cell membrane that becomes in contact with the inner part of a glass electrode tip; this near-perfect isolation is achieved through the application, by a specialized technician, of a gentle pipette suction. In order to obtain the gigaseal, the electric resistance of the cell-pipette connection must exceed 1 GΩ. This electrical seal is established by the creation of chemical bonds between cell membrane and the pipette tip; with this configuration, the inside of the pipette is connected uniquely with cell cytosol [106]. The technician generally applies a gentle suction with his mouth to seal the pipette with the cell and he can also position the pipette at a correct distance from the cell with the help of a micromanipulator to precisely identify variations in the electrical resistance between the fluid inside of the pipette and the surrounding fluid.

Several patch clamp configurations are possible after the establishment of the gigaseal: cell-attached, inside-out or, as in the case presented in this work, the whole-cell measurements. The widely applied configuration of the whole-cell

patch clamp is the analysis of voltage-operated ion channels [107]. In the voltage clamp mode used in this thesis, the recorded signal is the transmembrane junctional current and the controlled input is the clamped membrane voltage delivered to the cells examined.

2.5.4.3. Junctional current measurements in a cardiomyocytes pair

This functional assay was performed at the Venetian Institute of Molecular Medicine (VIMM) in Padova with the collaboration of Professor Bortolozzi M., in his *ad hoc* equipped laboratory. In fact, to record and measure current flowing through gap junctions (I_j) of a CMs pair, the following instruments are necessary, as described by Hernandez V. and Bortolozzi M. and co-workers in 2007 [108]: an inverted microscope (BX51, Olympus) for positioning the patch pipettes; a pneumatic table to isolate the system from mechanical vibrations; a Faraday cage providing electrical noise isolation; a perfusion system to deliver the different solutions used and to remove debris and/or dead cells through glass capillaries; these capillaries were fabricated on a vertical puller (PP-83, Narishige) with 1,5mm outer Ø borosilicate glass (Warner Instruments) and filled with an intracellular sterile solution (the composition of ICS, intracellular and ECS, extracellular solutions used in this experiment are reported in Table 2.4 A and B); two patch clamp amplifiers (LIST EPC7); a pulse generator with at least two output channels; a pair of micromanipulators; an oscilloscope; a data acquisition software and data recording computer.

Table 2.4: *Composition and concentrations of: (**A**) intracellular solution (ICS) and (**B**) extracellular solution (ECS) used for the Dual whole-cell patch-clamp measurement of gap junction conductance between a pair of hPSC-derived CMs.*

A. ICS

Intracellular Solution (ICS) mOsM 300; pH 7,2			
Name	**Weight (g/mol)**	**Molarity (mM)**	**Molality (g/L)**
K-ASP	171,20	120	0,517
KCl	74,56	20	0,037
$MgCl_2$-$6H_2O$	203,30	1	0,005
$Cacl_2$	110,99	1,7	0,0047
ATP-K	583,35	10	0,095
EGTA	280,35	10	0,095
HEPES	238,31	10	0,060
Adjusted to pH 7,2 with KOH			

B. ECS

Extracellular Solution (ECS) mOsM 320; pH 7,4			
Name	**Weight (g/mol)**	**Molarity (mM)**	**Molality (g/L)**
NaCl	58,44	135	7,90
KCl	74,56	5	0,40
$CaCl_2$	110,99	1,5	0,16
$MgCl_2$-$6H_2O$	203,30	1,2	0,24
HEPES	238,31	20	4,77
Glucose	180,20	10	1,80
Adjusted to pH 7,4 with NaOH			

The experiment was performed at room temperature.

Glass slide seeded with hPSC-derived CMs was transferred in a 35mm Petri dish (BD Falcon) and cells were perfused with 2ml/min ECS. Patch pipettes were filled with ICS and pipettes resistances were 3-5MΩ when immersed in the bath. To measure junctional conductance (g_j), a CMs pair was identified and each cell was maintained under whole-cell patch-clamp conditions with one of the two amplifiers and kept at the same holding (or resting) potential (Φ_h) of ~ -70mV (-70,8mV) [108].

A first 10mV voltage step (Figure 2.19 A and B) was applied by Bortolozzi M. simultaneously to both patch pipettes to monitor cell parameters; then, to elicit

junctional current (I_j) from cell to cell, five consecutive 10mV voltage steps were applied in cell 1 and cell 2 separately.

To detect single gap junction channel events and thus measure the unitary conductance, the superfusion medium was transiently switched to ECS saturated with 100% CO_2 to produce carbonic acid (H_2CO_3). In fact, g_j between CMs pair is rapidly, substantially and reversibly reduced by sarcoplasmic acidification after CO_2 treatment, as demonstrated by White R.L. and collaborators in 1990 [109]. When it is in the undissociated form, H_2CO_3 is able to permeate the cell membrane, causing a rapid closure of gap junction channels. The reopening of GJs connecting the two adjacent CMs was possible following a rapid wash-out by normal ECS (or NS, normal solution) with cells recovered from cytoplasm acidification, as reported in Figure 2.19 C. This functional assay demonstrated that the CMs obtained with this gold standard protocol in conventional cultures, showed functional features such as the presence of junctional current which responds to external stimuli.

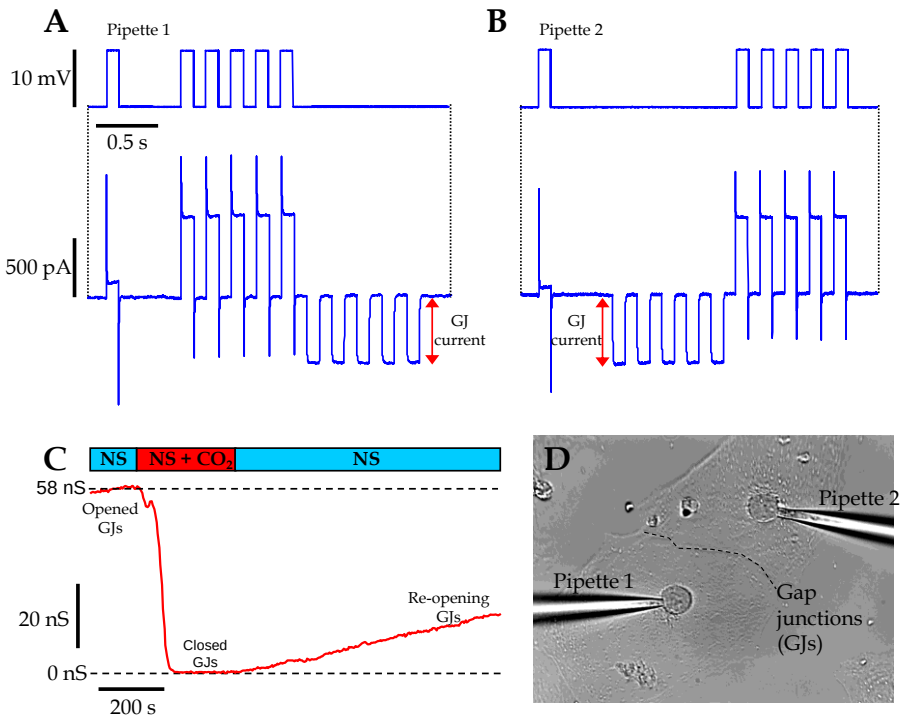

Figure 2.19: ***A*** *and* ***B****: a first 10mV voltage step (top traces) was applied simultaneously to both patch pipettes to monitor cell parameters, followed by five consecutive 10mV steps applied separately to elicit junctional currents (bottom traces) from cell 1 to cell 2.* ***C.*** *Extracellular application of CO_2 to HEPES-buffered normal ECS (or NS, normal solution) rapidly and reversibly acidified the cytoplasm and abolished junctional currents. Following a rapid wash-out by NS, stimulated re-opening of GJs connecting the two adjacent CMs.* ***D.*** *Plasma membrane currents were also observed to have similar behaviour after CO_2 application, likely due to hemichannel closure (data not shown).*

2.6. Conclusions

During this thesis, the protocols and methodologies for hESCs and hiPSCs culture, maintenance and expansion were acquired and 2 hESCs line and 4 hiPSCs clones were successfully cultured and characterized, demonstrating that all the hPSCs used are *bona fide* pluripotent stem cells.

Beating CMs were obtained in standard cultures from hPSCs by the application of a robust and consistent protocol that is currently considered the gold standard for the generation of cardiac cells from pluripotent stem cells. In fact, by the temporal administration of these small molecules, CHIR99021 and IWP4 to modulate canonical Wnt/β-catenin pathway, a high yield of CMs was successfully obtained, ranging from 63% to 98%. The contractions started between 8-14 days, depending on the cells.

To precisely monitor the progression of cardiac differentiation of hPSCs, from pre-cardiac progenitors to CMs formation, a hES line, Dual Reporter for 2 cardiac TFs, MESP1 and NKX2.5, was used and showed a great cardiogenic ability.

Two hPSCs emerged for their ability to give the highest yield of CMs: hES Dual Reporter line and hiPS Clone 7, that were selected for the following experiment described.

To perform an optimal Wnt modulation, as suggested by S. Palecek [63], among the [CHIR99021], ranging from 6-12μM, 10μM was identified as the best concentration which gave the highest percentage of $cTnT^{+ve}$ cells from the 2 hPSCs selected.

Next, a deep characterization of CMs obtained was performed: the expression of cardiac markers was assessed with standard cell imaging technique; a first quantification attempt was performed with flow cytometer and the functional assay patch clamp was adopted to study cell-cell communication. CMs expressed typical nuclear and structural markers, with marked sarcomeric organization. Cell-cell communication analysis showed also the presence of junctional current between a CMs pair, which responds to external stimuli.

However, from the immunofluorescence staining against the embryo/fetal troponin T isoform and the adult isoform of troponin I, a higher percentage of cells expressing the embryo/fetal troponin T emerged, revealing their partially immature phenotype. CMs expressed also a good percentage of the adult isoform but these findings indicate the presence of a heterogeneity of CMs, with the differentiation toward random subpopulation, leaving room for improvement regarding cell maturation.

Chapter 3.
Microfluidic technology for cardiac differentiation of human pluripotent stem cells

This Chapter reviews the microfluidic technology for cell culture in Regenerative Medicine applications, highlighting the state of the art and the related properties and advantages deriving from the convergence of micro-engineering technologies with cell biology. By integrating cell cultures within *ad hoc* microfluidic devices it is possible to derive cost-effective *in vitro* models of relevant human diseases and to perform parallelized, multi-parametric analysis or drug screening assays at one time. Moreover, microfluidics opens the perspective for the development of "tissues- and organs-on-a-chip", reconstructing tissue arrangements and complexity more close to cell microenvironment.

In this Chapter, microfluidics was exploited to precisely drive the cardiac differentiation of hPSCs with high efficiency, exploring the ability to control hPSCs integration, expansion and differentiation into functional CMs. Since hPSCs differentiation into functional tissue-specific cells requires multi-stage process in

which exogenous and endogenous factors balance plays an important role, the optimal frequency of medium delivery and MRF concentration were investigated and identified, allowing proper functional differentiation of hPSCs to CMs.

3.1. Microfluidic technology for cell culture in regenerative medicine research: state of the art

10 year ago it was reported in literature that microfluidics (μF) can revolutionize significantly the way modern biology is conduced [110][111]. This optimism was warranted by the advantages of microfluidics over traditional cell biology assays in standard culture systems. In fact, in biology research, microfluidics could be used to: accelerate complex assays; dramatically reduce volumes and consequently the costs of research materials and reagents; perform parallelized, high-throughput experiments without consumption of precious samples and enable a more precise spatio-temporal control and predictability of the cell microenvironment [112][113]. In fact, the miniaturization of culture settings in microfluidic devices enables the creation of a highly controlled environment for the study of cell-cell and cell-extracellular matrix (ECM) interactions, with real time observation and analysis. The possibility to perform studies at single-cell level can help understanding the knowledge on stem cell niche to preserve cell stemness and to program cell fate[114][115]. As opposed to conventional culture systems, which uses a huge number of cells, microfluidics approaches allows to perform experiment at single-cell level where individual cells can be isolated from a starting population and trapped into ad hoc structure [4]. Microfluidic devices have found applications in the following cell-based *in vitro* systems: single cells studies, cell monolayers, cell tissues and organ-like models also named as "organ-on-chip" [4][114][116][117]. As deeply reviewed by Luni C. *et al* of our BioERA group in 2014, the term "organ" is used to describe the tailoring of microenviroment architecture derived from studies on organ-level functions observed *in vivo*, whereas "chip" refers to the techniques for the design and microfabrication of microfluidic platforms [118]. Figure 3.1 summarizes the applications of μF in regenerative medicine.

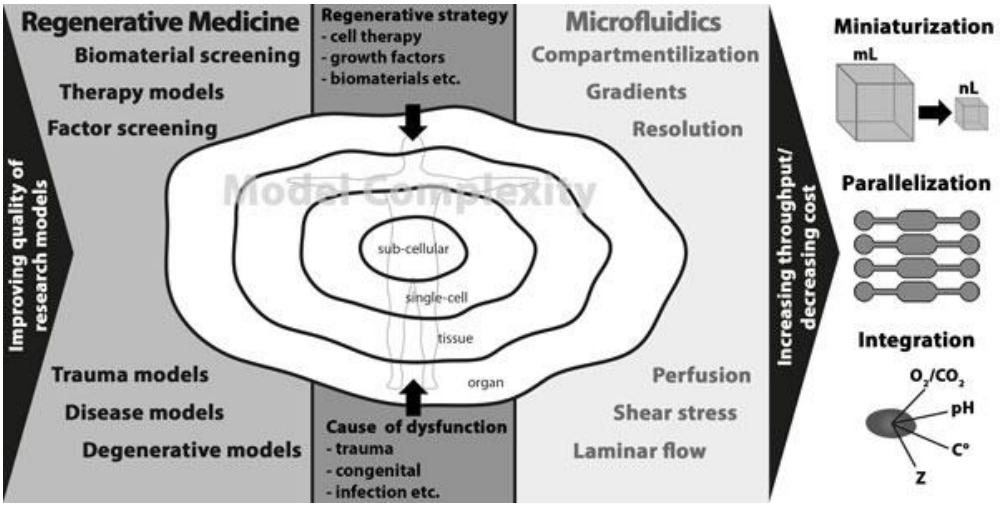

Figure 3.1: *Microfluidics for regenerative medicine (adapted from [4]).*

Governmental authorities are promoting the research that applies microfluidics for *in vitro* tissue-based models-on-a-chip because of the flexibility, reliability, and accessibility of these tools to a larger number of research groups. An example is given by the European commission that promotes "The body on-a-chip" project and the partnership between the principal medical research centers such as the National Institute of Health (NIH), Food and Drug Administration (FDA) and Defence Advanced Research Projects Agency (DARPA) that are collaborating for the realization of platforms for the study *in vitro* of *in vivo* human multi-tissue physiology (from circularoy system to musculoskeletal apparatus) [118].

Three main sources of human biological material can be used for the organ-on-chip studies: *ex vivo* biopsies; primary cells and hPSCs. Biopsies and primary cells best reflect the environment-related diseases because they retain the cellular *in vivo* phenotype. However, they are characterized by scarce availability, isolation difficulties and inability to sustain a long-term culture *in vitro*. Primary cells are derived from biopsies and they can be maintained in culture for a longer timespan but, to preserve their *in vivo* properties, they require a topological organization, such as the recreation of organ-like architecture with bioprinting technologies[118][119]. Finally, the third source is represented by tissues derived from hPSCs, hiPSCs in particular, because they represent an inexhaustible source of human cells, able to differentiate into any tissue in the body. Moreover, hiPS can be derived from skin biopsies and with other less invasive procedures such as blood or urine [91], opening the way for personalized therapy design (Figure 3.2).

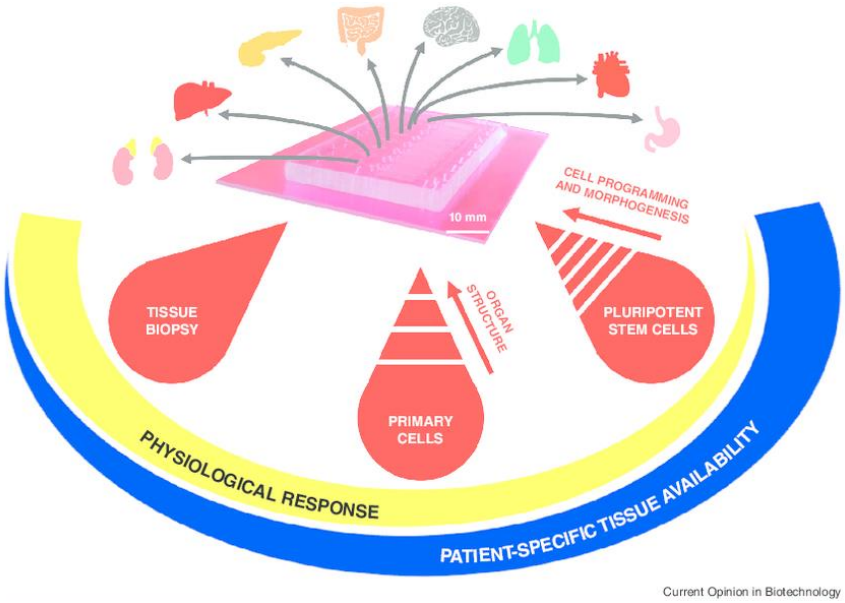

Figure 3.2: *The three major biological sources for organ/tissue-on-chip development. Bioptic tissue (left) and primary cells(center) are difficult to be maintained in culture and require the reconstruction of the in vivo topological organization. hPSCs can differentiate into any tissue of the body (adapted from [118])*

One of the first work using a miniaturized PSCs culture was published by Figallo E. and co-workers in 2007 and described the ability to culture hESCs for 4 days into a specific micro device [120], while Wan C.W. *et al*. in 2011 performed cardiogenesis of murine ES-derived EBs in a microfluidic device [121]. However, few works demonstrated the ability to differentiate PSCs within a microfluidic platform toward multiple lineages such as CMs [118][120].

To conclude, by combining cellular systems with specific microfabricated structures, our BioERA laboratory, have been able to create sophisticated models that emulate the organ architecture, in particular generating functional hepatocytes and cardiomyocytes with high efficiencies [94]. It is important to underline that the creation of organ-on-chip models enables the reconstruction of the organ microenvironment offering a powerful tool to study human physiology and pathophysiology with unprecedented control over the culture conditions, avoiding or limitating animal experimentation [118][122][123].

In this work, μF was exploited to drive the cardiac differentiation of hPSCs in an unprecedented and high controllable microenvironment, aiming at the implementation of the culture conditions during the differentiation with a high efficient and precise delivery of components (small molecules and/or transcription factors, TFs). With the miniaturization of the entire culture system

and more reproducible conditions, in fact, a real-time control over the differentiation process is possible, lowering the intra- and inter-experimental variability observed when using conventional systems. Downscaling the culture settings with μF, best mimics the *in vivo* cellular dynamics occurring in a a tiny soluble environment and in little time interval, enabling high-throughput experiments not achievable and not economically sustainable with macroscopic conventional cultures [118][94].

This Chapter will explore the ability to control hPSCs integration, expansion and differentiation into functional CMs through a microfluidic-based process. The microfluidic-aided cardiac differentiation of hPSCs will be further discussed in Chapter 4 with the association of the synthetic modified mRNA technology for programming hPSCs fate at the microscale with specific cardiac TFs.

3.2. Properties and advantages of microfluidics for cell culture in a high controllable microenvironment

Cells live in a milieu composed of soluble factors, cell-matrix interactions and cell-cell contacts within an environment with specific physicochemical properties given by pH, oxygen, tension, temperature and osmolarity. These elements cooperate for the regulation of cell structure, function and behaviour, influencing the growth, development and repair of tissue. The combination of these biochemical, physical and physiochemical factors make up the cell microenvironment and, for stem cells, it is called stem cell niche, indispensable for the regulation of stem cell survival, self-renewal and differentiation [124][125]. As mentioned before, in order to improve quality of the regenerative medicine research models, it is important to both mimic the cell biological microenvironment, which presents a high level of confinement, and to reach a high level of tissue/organ complexity [4]. Microfluidics, with his miniaturized dimensions, determines a high level of confinement, which resembles the milieu cells experience *in vivo*. Compared to standard cultures, microfluidics is characterized by a convection-free culture system enabling the local accumulation of autocrine-paracrine substances secreted by cells, offering the possibility to automatize the culture and perform parallelized analysis[4][126].

Moreover, the downscaled culture support is characterized by a higher surface/volume ratio, compared with large conventional cultures, offering a more

precise control over the physical parameters (e.g. temperature or gas concentrations in solution) [4][127] and for the delivery of transcription factors when performing reprogramming experiments. In fact, in 2016, Luni C. and Giulitti S. in our BioERA laboratory demonstrated the ability to perform cell reprogramming of human fibroblasts for the generation of hiPS clones with the highest efficiency reported to date using a microfluidic platform (50-fold higher than other published works). They delivered the pluripotency factors as synthetic modified mRNA with daily transfections, the same approach adopted in this thesis to generate CMs from hiPSCs (described in Chapter 4); thanks to the scaling down of the system, there is an optimal balance between endogenous factors and the transfected exogenous ones during cell reprogramming process. These advantages offer consequently reduced consumption of reagents with significant costs reduction, reduced contamination risk and efficient throughput experimentation [95].

The fluid dynamics at the microscale is markedly different from those characterizing the macroscale; for example, the gravity force effects are dramatically reduced in microfluidics while surface tension and capillary forces are dominant in miniaturized systems [110]. Furthermore, the laminar character of the flow in microchannels offer new experimentation configurations, not achievable in conventional culture systems such as the possibility to perform dynamic cultures with cells under continuous perfusion of fresh medium with, for example different flow composition or with the contemporary application of biologically relevant shear stresses[115][128].

In fact, thanks to the laminar flow of medium, microfluidics allows the generation of precise gradients, mimicking the chemical signals cells experinece *in vivo* during embryogenesis as well as during the processes of regeneration and wound healing: gradients of morphogens elicit cell recruitment and stimulate ECM deposition[4][129].

Cells are also influenced by the mechanical properties, with variations of stiffness/softness, of the substrate in which they are put to grow. The first microfluidic systems were initially realized in rigid materials such as silicon and glass; however, these materials required long production procedures and specific cleanroom spaces. Because of the opacity of silicon to visible and UV it is impossible to use it with common microscopy equipment. Glass and silicon are too fragile and require difficult, long and expensive production protocols. Between 1970s and 1980s new elastomeric micromoulding techniques, using polymer materials, were developed by Bell Labs [130]: these polymers could be

photo-curable such as such as SU-8 epoxy, polyimide photoresist, or heat- curable such as the polydimethylsiloxane (PDMS) [110], thermoplastics such as polymethylmethacrilate, polycarbonate, polystyrene (PS), cyclic-olefin-copolymers, or Teflon® [131]. These elastomeric materials allow great flexibility and customization in microfluidic platforms design, taking into account the precise requirements of the cell types studied [132]. PDMS [$(CH_3)_2Si$-O] has two methyl groups attached to the silicon and, as a typical feature of all silicones, it is able to cross-link after the addition of a curing agent containing a catalyst, usually platinum. In this PhD thesis, PDMS has been used for the fabrication of microfluidic devices thanks to its ease to mould without the need of dedicated cleanroom environment and because it is cheap, inert, biocompatible, gas- but not fluid-permeable, optically transparent, allowing the observation of microchannels contents visually and through a microscope [133]. After a simple plasma treatment it is possible to tightly bond PDMS to a glass slide or another PDMS layer for the production of multilayers PDMS devices.

Figure 3.3 describes the most significant advantages and challenges when using macroscopic versus microfluidic cell culture.

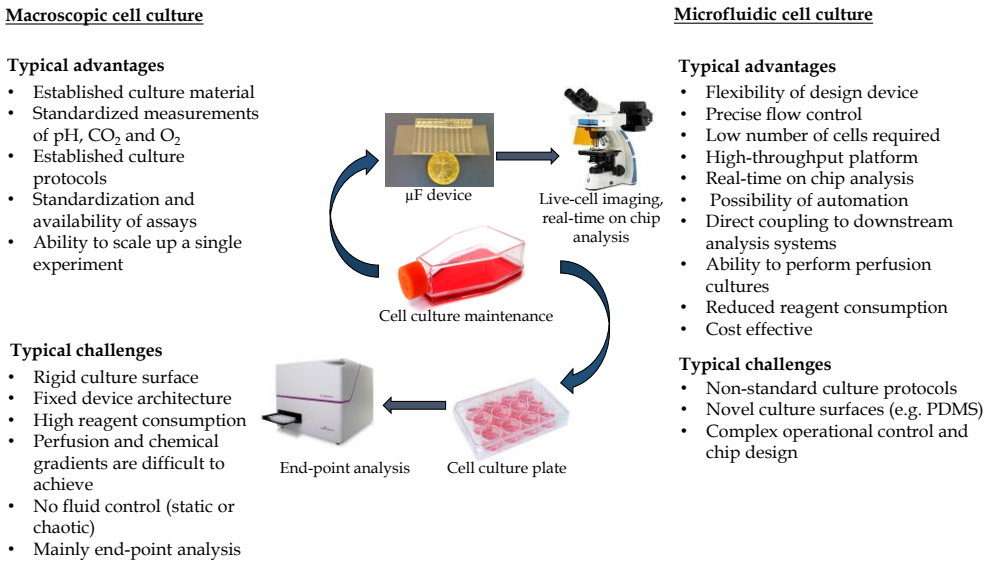

Figure 3.3: *Pros and cons of both macroscopic and microfluidic cell culture (modified from [132]).*

Integrating cell cultures in microfluidic devices requires experience and accurate knowledge of the fundamental principles of cell biology, biochemistry, physics and engineering.

First, in order to develop *in vitro* models more closely to the conditions in which cells reside *in vivo,* it is necessary to know and study the key elements of the cellular microenvironment. Second, it is imperative to have a strong experience in cell culture techniques to facilitate the translation from macro- to microscale. Third, it is indispensable to have a complete background in microfluidics and its state of the art in order to properly design these tools for the required applications [4][111][124].

In conclusion, since culturing and expanding hPSCs at the macroscale is considerably expensive compared to other cell types, the miniaturization of volumes for culture reagents provided by microfluidic technology can guarantee a new system to match the precise requirements of hPSCs in a cost-effective manner.

3.2.1. Facing the soluble control and medium perfusion challenges in microfluidic cell cultures

Although microfluidic posseses several advantages, as described in the previous paragraph, translating cell cultures from the macroscale of standard dishes, flasks and well-plates to microfluidic devices, requires an adaptation of current culture protocols. Microfluidics, compared with standard culture systems, is characterized by reduced media volumes and different frequencies and methods for medium refresh.

It is known that PDMS is permeable to gases such as ambient CO_2 and O_2, allowing to properly buffer the culture medium; however, it is also permeable to water vapour, with subsequent drying problems and significant shift in medium osmolarity [134]. In macroscopic cell culture, medium is typically stagnant, with excess amounts of nutrients diluted in order to feed cells for several days, depending on cell type, cell number and seeding density. On the contrary, microfluidic systems enables medium to flow within the microchannels to create a more realistic cell microenvironment by continuous supply of fresh media with the contemporary removal of waste products [135]. However, the microfluidic cultures present their own challenges.

In vivo cells are continuously subjected to many stimuli coming from endogenous soluble paracrine and autocrine factors (EnF) released by neighbouring cells and by the cell itself respectively; the exogenous factors (ExF) are represented by those delivered with the culture medium.

Furthermore, cells also require and consume energy sources (glucose, glutamine and amino acids) and produce metabolic waste (CO_2 and lactate). A typical microfluidic channel contains a high number of cells to media volume, to better recreate the *in vivo* cell density. On the contrary, in a conventional Petri dish, medium is usually changed every 1-4 days and, for hPSCs culture and expansion, it is suggested a daily medium refresh to prevent the accumulation of toxic signals and stimulate cells with fresh factors [124]. In fact, deprivation of nutrients and accumulation of waste products can elicit cell death or induce unwanted differentiation of the stem cell population. This 24 hours cycle in hPSCs medium replacement in standard culture is necessary to:

- provide the necessary volume to cover the entire culture surface;
- reduce the concentration of medium components due to evaporation at 37°C;
- provide a correct supply of nutrients for the high-demanding hPSCs;
- dilute waste products and debris.

Although microfluidics offers the advantage of delivering, with a homogeneous distribution, tiny amounts of media over a cell layer with high spatiotemporal control, translating a cell culture in a microfluidic chip, would correspond approximately to a total medium exchange frequency every 2-4 hours [124]. For this reason, it is mandatory careful validation experiments and feeding schedule calibrations for every device and cell type used. In Figure 3.4 is reported a schematic of cell niche with the combination of biochemical, physical and physicochemical factors (A) and a comparison of cell environment and medium usage between conventional dishes and microchannels in emerging microfluidic technology (B and C).

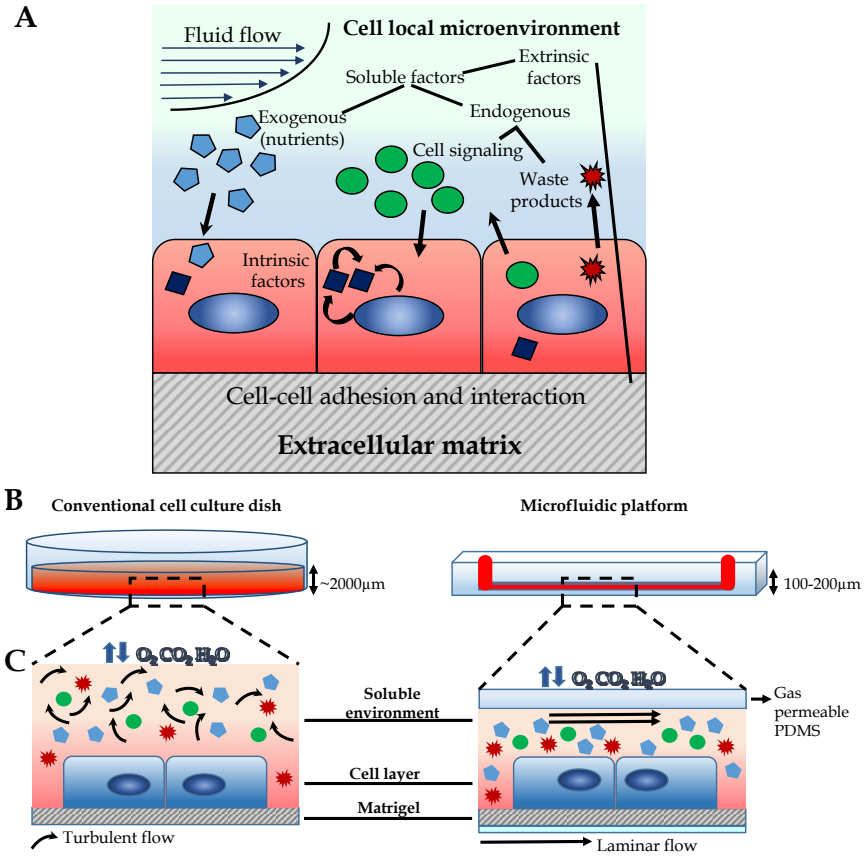

Figure 3.4: *Cell niche and comparison between conventional cell culture environment and a microchannel.* ***A.*** *Cell niche is a microenvironment, which regulates cell fate. Intrinsic signals, and extrinsic factors (cells interactions, adhesion molecules, extracellular matrix, GFs, cytokines and waste products) and exogenous molecules like provided nutrients, interact with cells. In vivo, chemical signals are in the form of gradient, with the characteristics of a laminar flow.* ***B.*** *Longitudinal section of a conventional Petri dish (left) and a channel of a microfluidic chip (right). A standard 35-mm-wide Petri dish requires 2ml (~2000µm height) while a microfluidic chip provides medium exchange into the channels in a range of 100 to 200µm, approximately 1/10 of the 35-mm-wide Petri dish.* ***C.*** *Magnification of microenvironment recreated in vitro at cell layer level with the biochemical signals (cytokines, hormones) and waste products important for cell functions. A correct medium replacement frequency is necessary to avoid nutrient depletion and waste accumulation. Excessive evaporation of O_2, CO_2 and H_2O must be avoided to maintain the correct osmolarity and cells viability. The laminar character of the flow at the microscale generates a precise gradient, supplying fresh nutrients while washing out waste products and debris. In standard cultures these events happen with convective and turbulent flow, not observed in molecular transport in vivo (modified from [95]) .*

With computational modeling and experimental testing, in our BioERA laboratory, Giulitti S. and co-workers in 2013 developed an optimal medium replacement strategy for long-term culture of mouse embryonic stem cells (mESCs) within microchannels of a PDMS microfluidic device. They tested different flow rate, constant, as well as periodic replacement of medium, and reported that slow, continuous perfusion produced deleterious effects on cells while periodic replacement of 8 hours fast pulses of the same media volumes, resulted in uniformly healthy cell growth and survival. This was attributed to

the heterogeneous distribution of nutrients (higher concentration upstream) versus endogenous factors and waste (higher concentration downstream) in slowly perfused culture channels. They concluded that medium delivery strategies are extremely relevant for proper maintenance of cell homogeneity, viability and behaviour in microfluidic cell culture (Figure 3.5) [136].

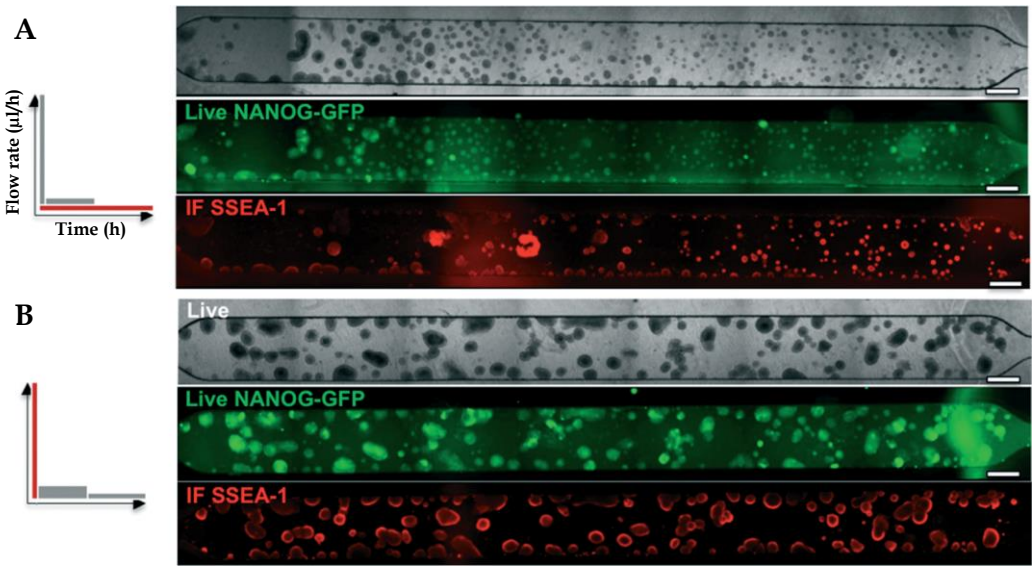

Figure 3.5: *Effects of two different strategies of medium perfusion on mESCs performed by Giulitti S. et al.* ***A.*** *Constant flow rate of fresh medium.* ***B.*** *Periodic medium perfusion in a defined time interval (8 hours). Bright field, live green fluorescent protein reporter (GFP) and immunofluorescence (IF) analysis of pluripotency markers (NANOG-GFP, SSEA-1). After 6 days of culture, IF analysis for pluripotency markers demonstrated that with periodic medium replacement (**B**), cells maintained pluripotency with a homogeneous distribution of compact pluripotent colonies. On the contrary, constant flow rate (**A**), showed heterogeneous and reduced expression of the analysed markers. Scale bars 600µm; (adapted from [136]).*

3.2.2. Effective Culture Time (ECT) for liquid handling at the microscale

Since microfluidic channel relies on few microliters of liquid volume and cells need fresh nutrients before their depletion and waste products accumulation, new fresh culture medium must be supplemented in the chip with a proper refresh rate, higher than conventional culture systems with lower surface/medium volume ratios. Specifically, the maintenance of cell cultures at the microscale relies on media changes at regular time intervals, and failure to do so usually leads to low cell viability and poor quality of cultures. A great challenge when culturing cells in microchannels is the identification of the ideal time interval for medium refresh. To solve this issue Young E.W.K. and Beebe D.J. in 2010 introduced the concept of

the Effective Culture Time (ECT) [124], comparing the time scales of standard dishes and microfluidic platforms. In a macroscopic culture system, cells grow on a surface of area A, in a culture medium with volume V. The medium at the air-liquid interface in standard cultures possesses a height on cell layer of $h=V/A$, corresponding to the channel height in confined microchannels. Height h represented the characteristic length for microfluidic channels because length and width are larger than h, and h represents the limiting dimension for diffusion. When the key biochemical factors in the medium become exhausted, it is necessary a medium exchange. The time interval between every medium refresh is the ECT above mentioned and it depends on: (1) starting nutrients concentration C_0, (2) cell uptake rate of nutrients K_m, (3) nutrients diffusivity D, cell density σ, culture area A and medium volume V. These parameters are connected by the Damkohler number, here explained:

$$Da = \frac{K_m h \sigma}{D C_0}$$

Da is a parameter without dimension for the measurement of the ratio between reaction and diffusion time scales and can be reformulated as:

$$Da = (\frac{h^2}{D})/(\frac{C_0 h}{K_m \sigma})$$

Where the numerator indicates time scale for diffusion $\tau_d=h^2/D$, and the denominator is the reaction time scale τ_r. In microfluidics, h is usually one fifth to one tenth smaller than standard supports, so Da is up to an order of magnitude lower in microchannels. Since τ_r corresponds to ECT in diffusion-dominant systems and τ_r is linearly proportional to h, the ECT is scaled to the height of the microchannel. For example, a typical conventional culture Petri dish of A~ 80cm^2 has a medium V ~ 10ml, with a medium height of $h \approx$ 1,2mm. The height of a microfluidic channel is usually h=200µm, as a consequence, the ECT is ~6 fold lowered, suggesting that medium should be replaced every 8h to maintain the same culture conditions [124]. This observation is in agreement with the experiments conducted by Giulitti S., who optimized medium exchange intervals in microchannels, indentifying an ECT of 8 to 12h (maximum). See Paragraph 3.2.1 for details [124][136].

Depending on cell requirements and microfluidic design, refresh rate of culture medium and liquid handling in our laboratory can be performed:

- automatically, through CAVRO syringe pumps XLP6000 (obtained from Tecan) connected via serial ports to a computer and the

applications are written in LabVIEW (National Instrument) software in order to operate scheduled medium delivery;

- manually with a pipette, by the same operator, at time interval of 12h through the passive pumping.

Syringe pumps are the most common delivery system employed in microfluidics: in the BioERA laboratory, CAVRO pumps are integrated with a multiport head to make every parallel channel independent. LabVIEW software possesses a user-friendly interface to automatically set-up experimental parameters such as frequency of medium changes per day. In Figure 3.6 is reported an automated PDMS microfluidic device used in the lab.

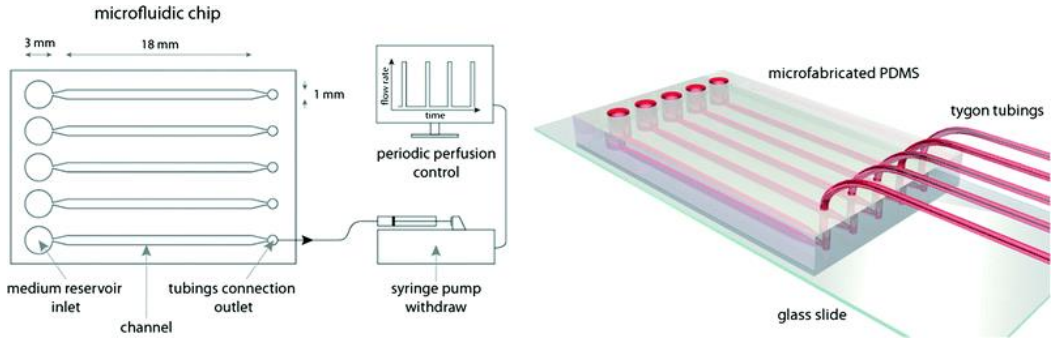

Figure 3.6: *Representation of a microfluidic platform in which every independent chennel outlet has a Tygon tublings connected to a syringe pump. A LabVIEW interface software developed in the laboratory (left) performs periodic perfusion of medium automatically. A complete automatized microfluidic chip is modelled on the right (adapted from [136]).*

When the number of medium change operations are too frequent, the automation of liquid handling is necessary to reduce possible errors by operators (e.g. vehicle contamination, removal of chip from the incubator with loss of temperature and gases…).

An alternative and simple method of fluid replacement is passive pumping and communicating vessels principle. First developed in 2000by Beebe D. group, it relies on the surface tension of different-sized droplets placed at the inlet and outlet ports that drive fluid from one port to the other [137]. The difference in droplet volumes induces a differential pressure between ports that generates flow in the microchannel [124][138]. Figure 3.7 illustrates a schematic of the principle.

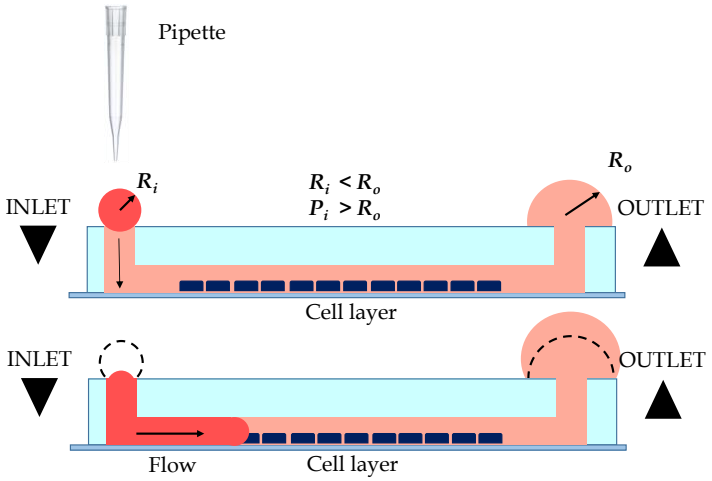

Figure 3.7: *Passive pumping. A smaller droplet with radius R_i at the inlet has an internal pressure P_i greater than one possessed by the larger droplet with radius R the outlet. This phenomenon depends on Laplace's law ($\Delta P=2\gamma/R$. ΔP pressure difference at the droplet liquid-air interface; γ interface the surface tension; inspired from [124]).*

The major advantages of passive pumping are the low cost and the possibility to be performed without connecting to external pump, eliminating the need for tubing and interconnections at the ports. Passive pumping can be performed simply manually by pipetting the appropriate volumes.

In this PhD work, medium refresh was always performed manually at regular time interval of 12h.

3.3. Microfluidic platform fabrication

Microfluidic devices used in this work were fabricated by standard soft-lithography technique, using the know-how of our BioERA laboratory and well described in the work of our colleagues [94][95]; in our laboratory, different types of microfluidic platforms are fabricated, with different characteristics, depending on the application of every research topic. Soft lithography comprises a set of microfabrication techniques for printing and moulding elastomeric stamps with the patterns of interest in bas-relief. As a technique for fabricating microfluidic devices for cell biology research, soft lithography overcomes many limitations of photolithography. In particular, with soft lithography it is possible to pattern biological relevant complex molecules, as well as cells and to fabricate channel structures suitable for microfluidics. In

biology, the production of prototype patterns and structures is convenient, cheap and rapid [139].

An elastomeric stamp made in polydimethylsiloxane (PDMS) is prepared through replica molding by casting a liquid prepolymer and a curing agent solution (Sylgard 184 from Dow Corning) onto a premade master with patterned relief structure on its surface (Figure 3.8).

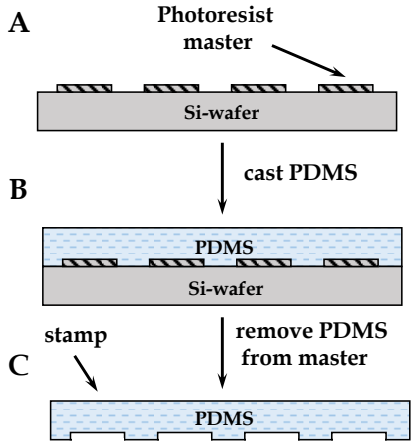

Figure 3.8: *Preparation of polydimethylsiloxane (PDMS) microfluidic chip using replica molding and pattern transfer by microcontact printing.*
A. *Photoresist exposure to UV light on a silicon wafer (Si-wafer) support through a photomask or master. Tthe cured photoresist remains on the silicon support in a bas-relief pattern defined by the master.*
B. *PDMS (Sylgard 184) is used as the elastomer (curing is for 2h at 70°C).*
C. *After baking, PDMS stamp can be peeled off.*

When masters features size is greater than or equal to 20µm, patterns can be drawn in AutoCAD® and printed onto polymer sheets, through commercially available printers. Photomasks are used for selectively polymerizing UV-sensible photoresists, previously spun onto a silicon wafer with defined film-thickness. The viscosity of the photoresist as well UV-light intensity and baking time should be considered for a selective polymerization of the desired structure. As mentioned before in Paragraph 3.2.1, PDMS is chemically inert making microfluidic platform employed in this work biocompatible, and is also highly permeable to gasses (O_2, CO_2, N_2 diffuse rapidly) but not to fluids, allowing fast equilibration time in standard cell culture incubators. It is transparent, for detection analysis instruments like fluorescence microscopy, and allows long-term experiments to be performed. However, appropriate surface functionalization is required for culturing adherent cells such as hPSCs. In fact, PDMS surface properties can be rapidly modified by plasma treatment: air or oxygen-based treatments lead to the formation of OH-groups, which permit covalent bonding between the stamp and glass slides or another PDMS substrate.

Each microfluidic device contains 10 parallel channels (18mm long, 1,5mm wide and 0,2mm high, Table 3.1). Photomask shown in Figure 3.8 and 3.10 (A), was designed in AutoCAD® by the engineers of the laboratory (Michielin F.,

Prevedello L., Giulitti S., Zambon A., Gagliano O.), printed onto a transparent polymer sheet and photolithographically patterned onto a silicon wafer (Si-wafer) with SU8-2100 negative photoresist (MicroChem), to obtain a final thickness of 200µm, according to manufacturer instructions. The master was then treated with hexamethyldisilazane (HDMS) at room temperature for 1 hour under vacuum, in order to facilitate extraction of PDMS mould from silicon wafer. A 10:1 solution of PDMS pre-polymer and curing agent was cast, cured and baked in an oven for a precise time interval. In fact, various baking times are possible: 15 hours at 45°C, 2 hours at 70°C or 1 hour and a half at 85°C. PDMS mold was cut and peeled off from the Si-wafer, punched to obtain liquid inlets and outlets with circular steel punches (Small Part Inc.) and finally sealed to a previously cleaned glass slide (Menzel-Glaser) by plasma bonding with plasma cleaner (Harrick Plasma) for 2 minutes at 30W (Figure 3.9). The ionization of gas within the plasma cleaner produces reactive oxygen species (ROS) that form oxidized activated species on the exposed surfaces treated. Two activated surfaces put in contact lead to the formation of stable chemical bridges between glass/PDMS and PDMS/PDMS

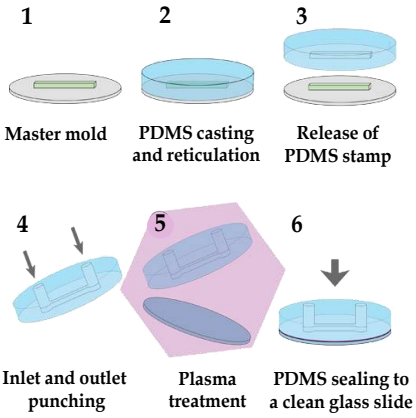

Figure 3.9:
Fabrication of a microfluidic device.
1. *The master mold enables mass-production of microfluidic chips.*
2. *A 10:1 solution of PDMS pre-polymer (liquid) and a crosslinking agent (to cure PDMS) is casted into the mold and heated at 70°C for 2h.*
3. *PDMS is peeled off from the mold.*
Microfluidic device completion.
4. *To allow the injection of fluids, the inlets and outlets of the microfluidic device are punched with a puncher of the desired size.*
5. *Plasma treatment of the face of PDMS block with microchannels and the glass slide.*
6. *The plasma treatment allows PDMS and glass sealing to close the microfluidic platform (modified from [140]).*

In Figure 3.10 (A-E) is shown the complete microfluidic platform made of PDMS on a glass surface.

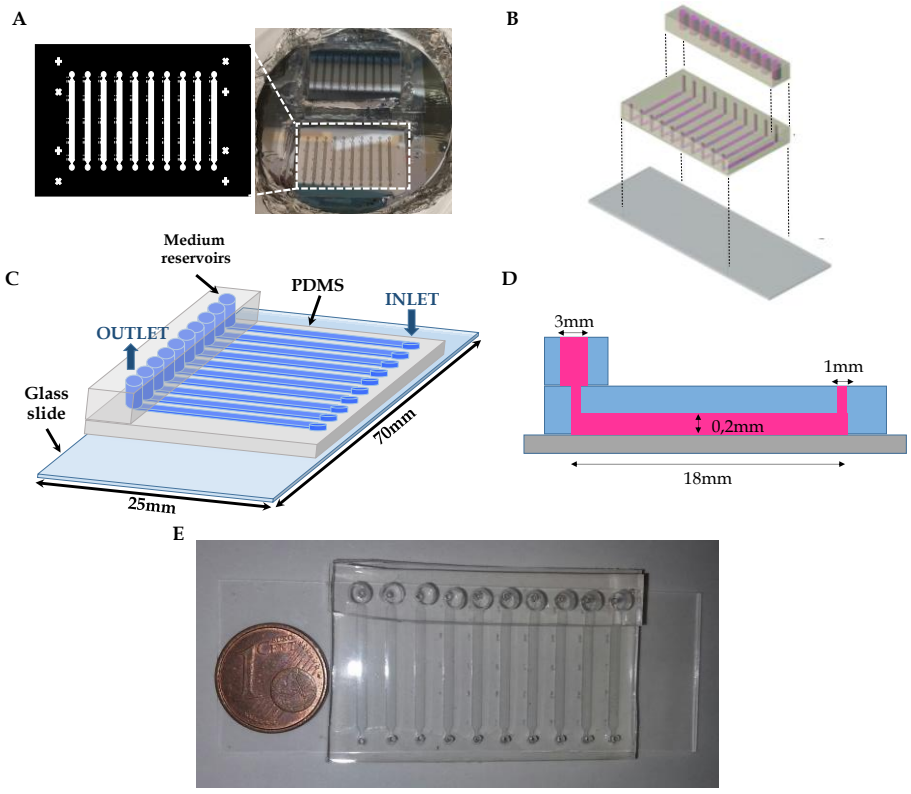

Figure 3.10: *Microfluidic platform for cell cultures integration.* ***A.*** *Photomask with microfluidic channels.* ***B.*** *Schematic of microfluidic platform assembly of the three layers: PDMS reservoirs, PDMS channels and glass slide.* ***C.*** *Tridimensional representation of completed and assembled microfluidic platform with 10 independent channels and medium reservoirs at the outlet of the microchannels with the related dimensions.* ***D.*** *Longitudinal section of a microchannel with the geometrical characteristics.* ***E.*** *Picture of completed microfluidic device used in this work.*

In Table 3.1 are summarized the geometrical characteristics of the device.

Table 3.1*: geometrical features of microfluidic device.*

Microfluidic channel dimensions	
Height	0,2mm
Width	1,5mm
Lenght	18mm
Area	27mm²
Effective Vol.	5,4µl
Total Vol.	12µl

Before cell culture integration, microfluidic devices were rinsed with isopropyl alcohol and sterilized in autoclave, to prevent bacterial contaminations. Glass surface has to be opportunely functionalized with Matrigel Reduced Factor (MRF) in order to promote cell adhesion, survival and growth.

3.4. Cell culture integration into microfluidic platform

As mentioned in previous paragraphs, efficient cell culture integration into microfluidic devices can be achieved through proper supply of nutrients along time.

Part of the research conducted during this PhD is focused on optimizing the best condition for both hESCs and hiPSCs culture, expansion and differentiation into microfluidic device to obtain a robust long-term cell culture platform over several days. The cultivation over this timespan will be fundamental in order to perform the cardiac differentiation and the cardiac programming via transcription factors processes at the microscale; a minimum of two weeks for these experiments is required.

Cell culture in microfluidics is similar to traditional multiwells, concerning the type of medium and reagents used; the unique variables are volumes handling and procedures. When using microfluidics, any type of liquid could be injected or fluxed within the channels. In particular, if the channel is empty, the solution is injected directly from channel inlet while, if only liquid refresh is required, it's sufficient to put a droplet of the solution on the inlet and thanks to passive pumping and communicating vessels principle, the droplet is aspirated through the channel. In the microfluidic platform used in this work, the effective channel volume is 5,4µl but it has been always fluxed a total volume of 12µl to make sure to perform an extensive medium refreshment and waste products removal.

To seed cells at a desired cell density, it is sufficient to apply this formula:

$$V_{res} = \frac{N° \; of \; cells \; \cdot 0{,}2mm}{Density \; (\frac{cells}{mm^2})}$$

Where: V_{res} = Medium volume required for cell resuspension;
0,2mm= medium head within the microchannel.

An early step, before starting the cardiac differentiation-on-chip, was performed by integrating hESCs and hiPSCS grown in conventional 6-well-plates into the microfluidic device described in Paragraph 3.3. Prior to cell seeding, microfluidic channels within the chip were filled with 4°C cold Matrigel Reduced Factor® (MRF, BD) 0,5% v/v in DMEM, incubated at room temperature for at least 1 h and washed with StemMACS™ iPS-Brew XF medium (Miltenyi Biotec). hPSCs were then dissociated with 0,5mM EDTA or with Gentle Stem Cell Dissociation Reagent (Stem Cell) and injected at high density into the channels in medium supplemented with 10μM ROCK inhibitor (Y-27632, CalBiochem) to preserve cell viability. Because of the reduced medium volumes in the microchannels, to prevent a significant evaporation, the microfluidic platform was placed in a 100mm Petri dish and maintained in an isotonic bath with PBS for an optimal humidity of the chamber. For the first experiment of cell culture integration in the microfluidic platform, cells were cultured up to 5 days and then the stemness and the homogeneous morphology was verified through immunofluorescence staining for pluripotency markers. In these culture conditions both embryonic and induced pluripotent stem cells display similar morphology to cells cultured in standard 6-well-plates (Figure 3.11 A). Moreover cells homogeneously express pluripotency markers (OCT4, NANOG and TRA1-60) as revealed by the immunofluorescence staining performed both on hESCs and hiPSCs (Figure 3.11 B).

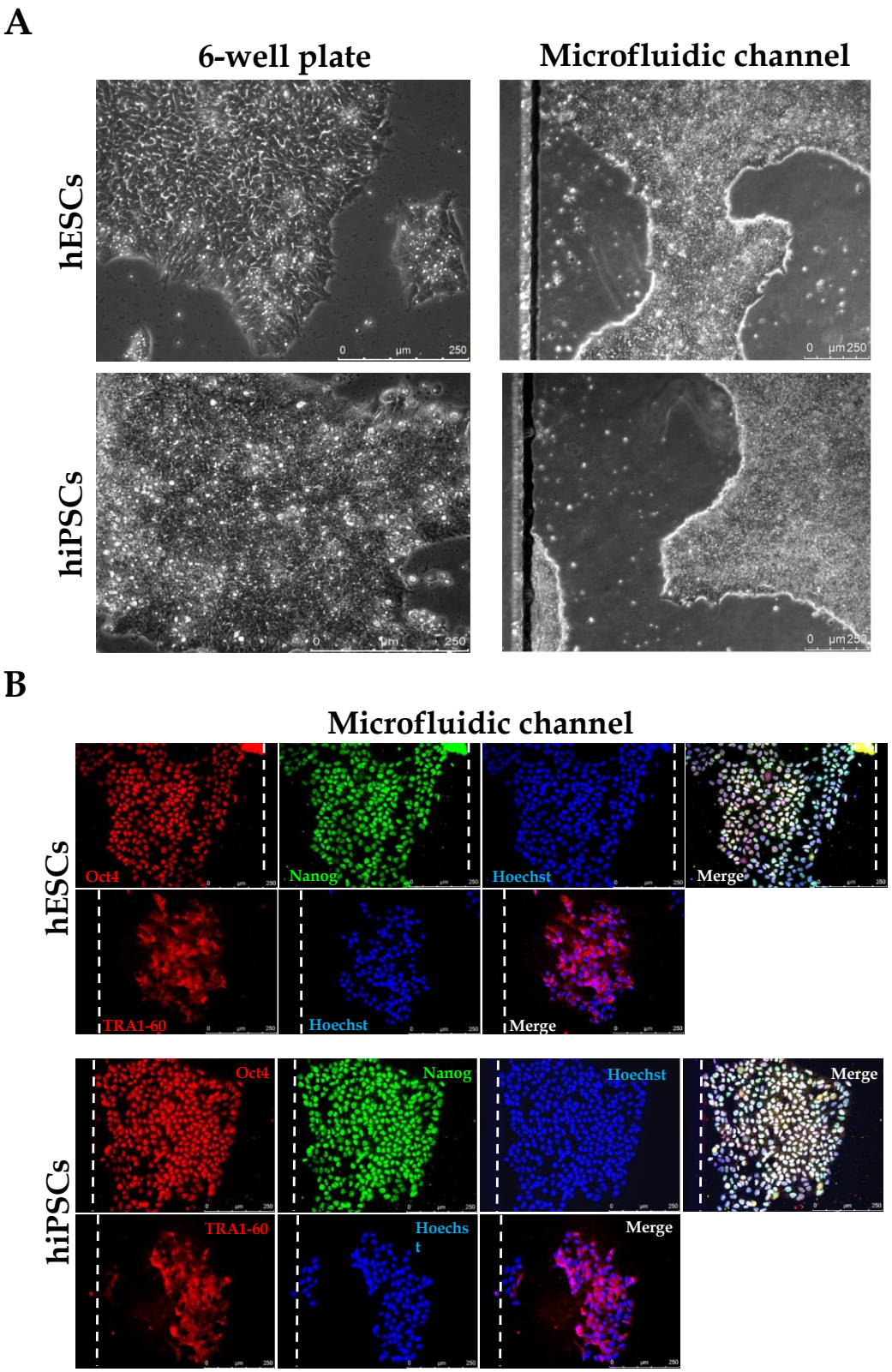

Figure 3.11: *hPSCs culture in microfluidics.* ***A.*** *hESCs and hiPSCs cultured in microfluidic channels up to 5 days display normal morphology as in standard 6-well-plates.* ***B.*** *hESCs and hiPSCs cultured in microchannels homogeneously express pluripotency markers (OCT4, NANOG and TRA1-60) as revealed by immunofluorescence staining. Dotted lines indicate channel outline.*

3.4.1. Cardiac differentiation on-a-chip with Wnt modulators: optimization of the protocol

The focus of this work was on cardiac cells because they are extremely relevant cell candidates for tissue-on-a-chip applications. Cardiac differentiation of human pluripotent stem cells was achieved with an initial optimization and adaptation of the gold standard monolayer protocol based on Wnt/β-catenin pathway perturbations in the microfluidic platform with proper Matrigel Reduced Factor (MRF) concentration for the coating of microchannels, creating an ECM to promote cardiogenesis, and frequencies of medium refreshment.

The optimization of cardiac differentiation protocols reported in literature has focused primarily on finding the optimal application, timing and concentration of growth factors and small molecules to perturbate specific signaling pathways. However, it is well known that cell behavior and stem cell fate decisions importantly depend also on extracellular matrix (ECM) interactions that influence early cardiac development, starting from events such as gastrulation [97]. From the analysis of gene expression profile and activated pathways, it was shown that hESCs and hiPSCs are similar to the cells composing the epiblast of the developing embryo [141]. At the gastrulation stage, some epiblast cells displayed a transition from epithelial to mesenchymal properties (EMT transition) and enter in the primitive streak with the subsequent cardiac commitment, leading to the formation of the heart [142]. During this process, a proper interaction between growth factors, small molecules and ECM becomes necessary [97][143] and ECM represents an adhesive substrate important for promoting these cross-talking events in a spatio-temporal manner.

In 2012 Zhang J. and collaborators developed an efficient cardiac differentiation protocols for hPSCs by using ECM in combination with growth factors involved in cardiogenesis. Briefly, they cultured hPSCs as monolayers on Matrigel, which is an ECM preparation, and subsequently overlayed cells with another layer of Matrigel (0,5% v/v or 1% v/v concentrated). This assembled matrix sandwich promoted the EMT above mentioned, detected by the generation of N-cadherin^{+} mesenchymal cells. From this combination of the matrix sandwich with the temporal application of growth factors (Activin A, BMP4 and bFGF) they generated CMs with high purity (up to 98%) from multiple hPSC lines [97].

In this work, to optimize cardiac differentiation of hPSCs in microfluidics different concentrations of Matrigel Reduced Factors (MRF) were used for channels coating in combination with different medium refreshment frequencies

in order to outline which condition gives a better cell adhesion, proliferation and differentiation. Five microfluidic platforms with 10 independent channels were coated with two different MRF concentrations: platforms A, B, C and D were filled with a solution of 2,5% v/v MRF in DMEM while platform E was filled with a solution of 20% v/v MRF. For each microfluidic platform, two cell types were seeded: hES Dual Reporter and hiPS mmRNA Clone 7. Four different frequencies of medium refreshment were tested:

1. Platform A and E: medium exchange was performed twice a day, every 12 hours;
2. Platform B: medium was refreshed once per day, every 24 hours;
3. Platform C: medium was exchanged with the same frequencies applied in standard culture on 24-well plates;
4. Platform D: the frequencies of medium exchange were adapted from standard culture to microfluidic; when in standard culture medium exchange was performed every 24 hours, in microfluidic it was refreshed every 12 hours while, when in standard culture medium was exchanged every 48 hours, in microfluidic it was exchanged every 24 hours.

The details of the experiment are reported in Figure 3.12.

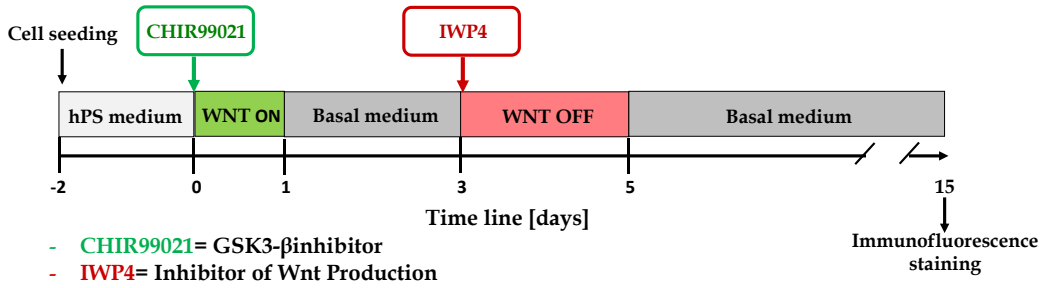

Figure 3.12: *Schematic of the experimental set-up for the optimization of hPSCs cardiac differentiation on-a-chip that is the monolayer based differentiation protocol described in Chapter 2 and published by Palecek's group in 2013 based on the temporal modulation of canonical Wnt/β-catenin signaling pathway (adapted from [63][64]).*

Cardiac differentiation protocol was initiated two days after integrating hPSCs into the microfluidic platforms and cardiac differentiation was monitored daily to analyze the morphology changes in cells during differentiation and to record cell reactions to different medium refreshment strategies. Figure 3.13 shows the time-lapse analysis on days 1, 7 and 15 of cardiac differentiation of hPSCs on-a-chip.

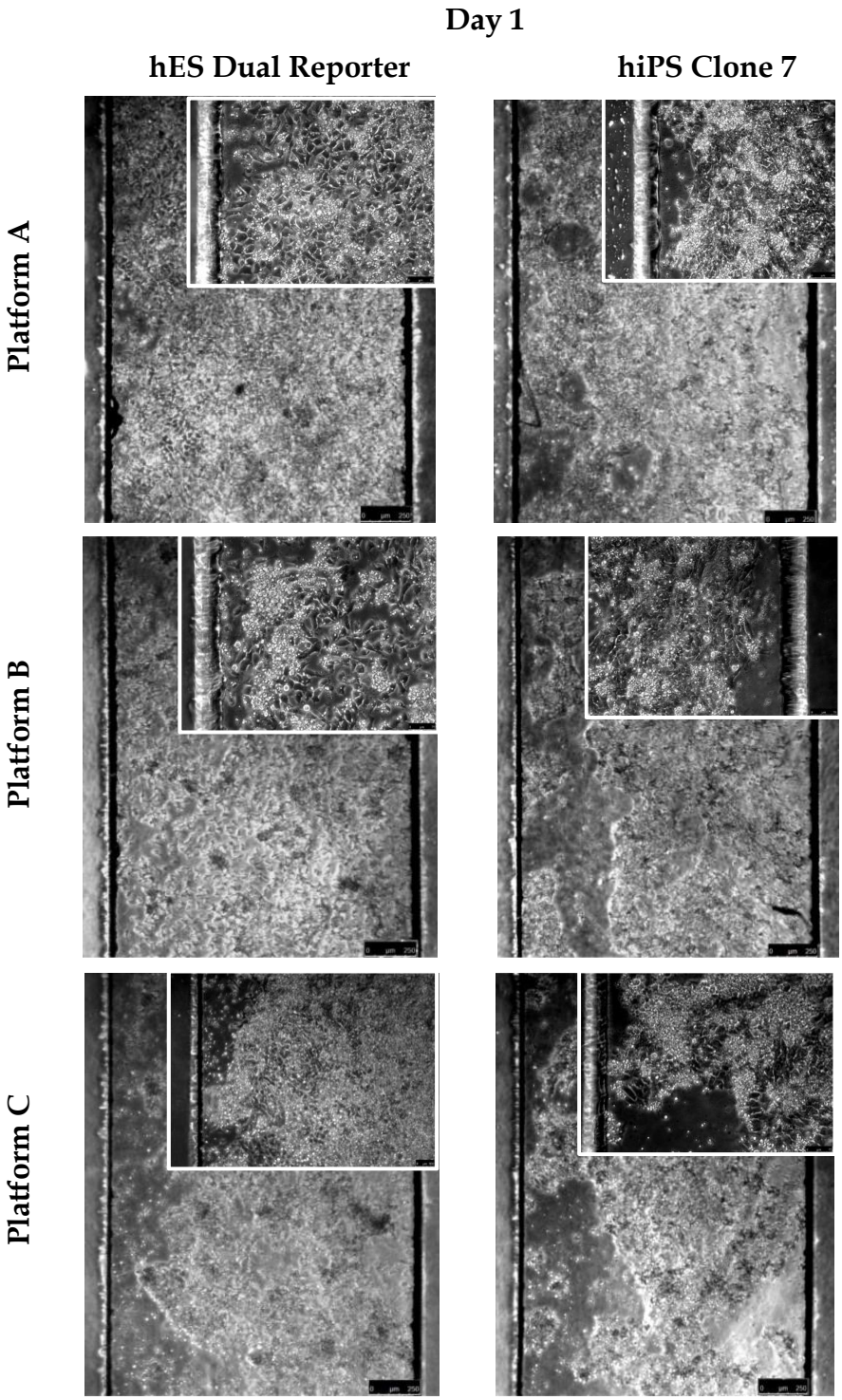
Day 1
hES Dual Reporter
hiPS Clone 7
Platform A
Platform B
Platform C

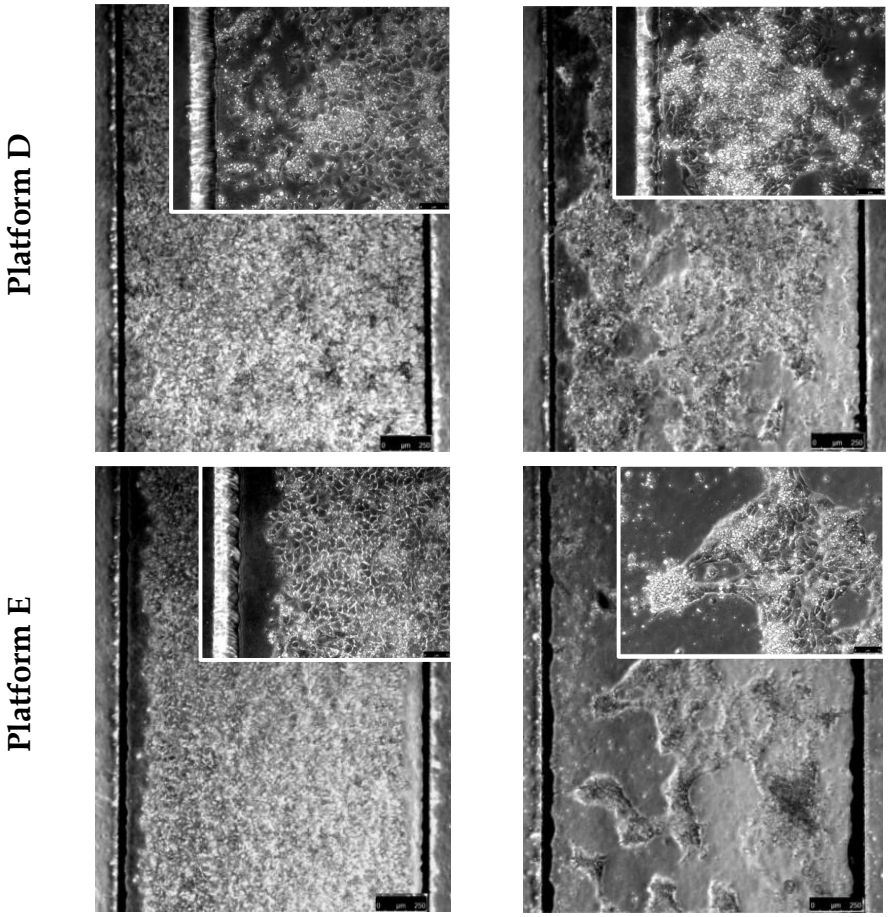
Platform D
Platform E

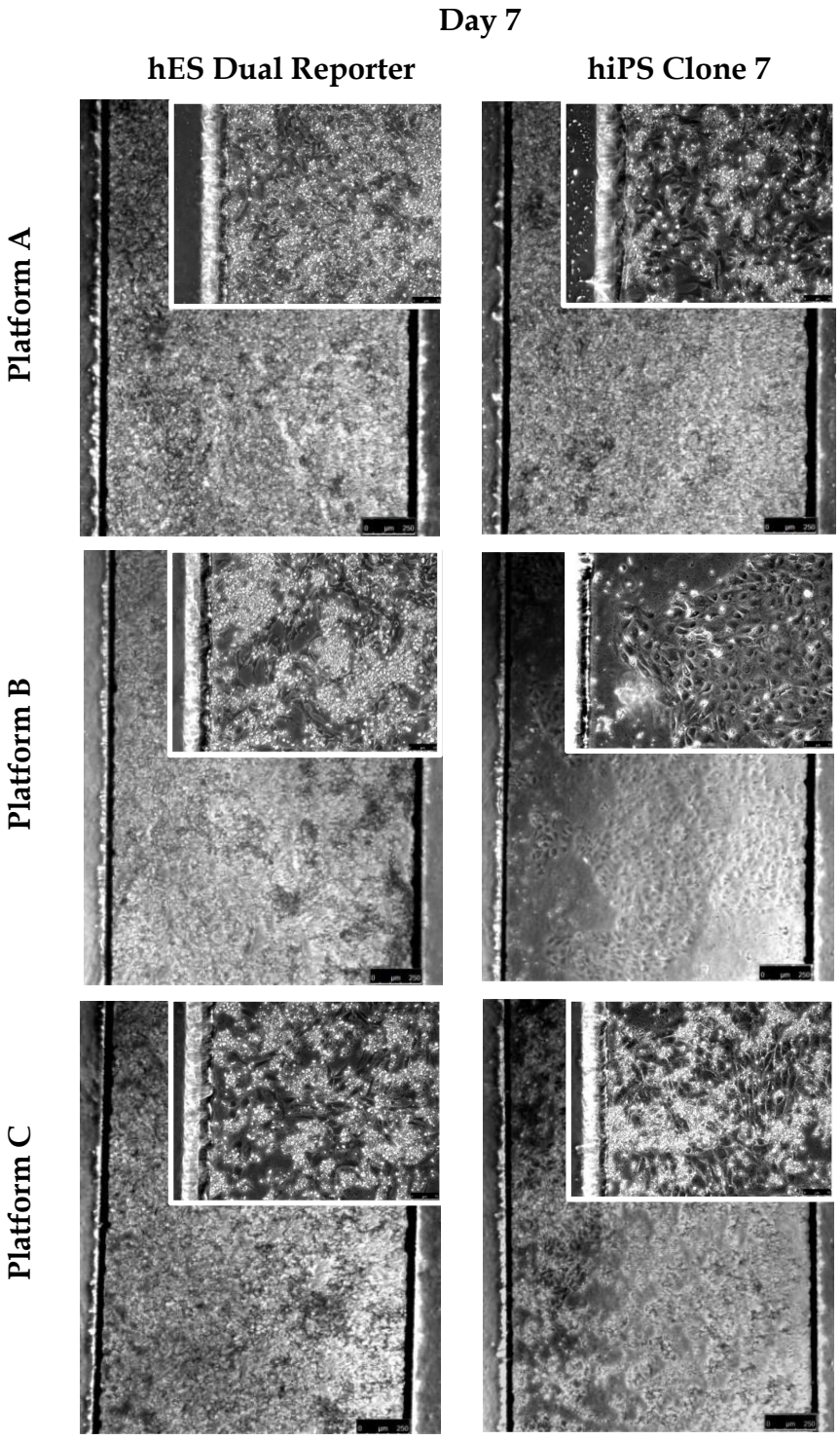
Day 7
hES Dual Reporter
hiPS Clone 7
Platform A
Platform B
Platform C

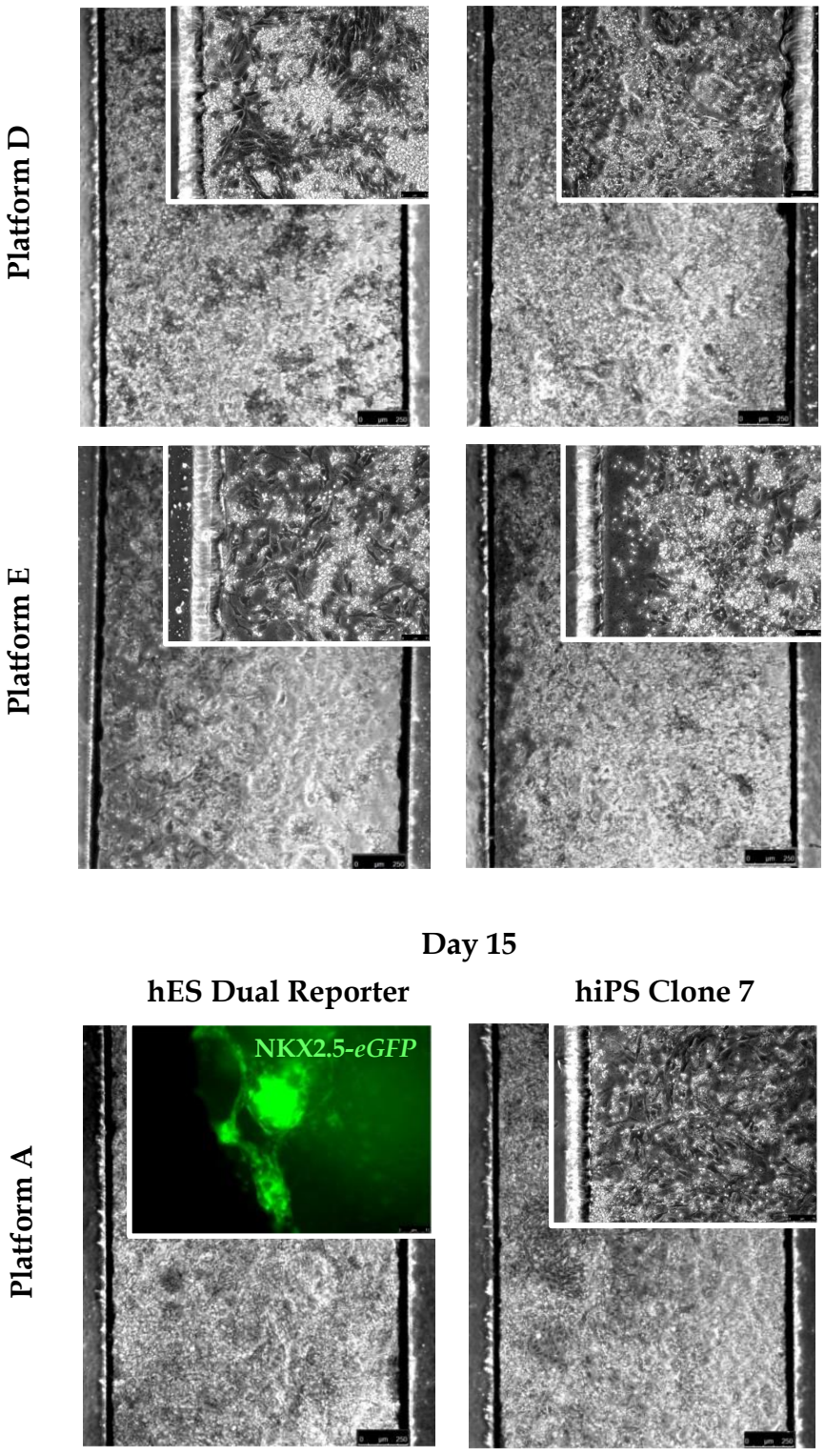
Platform D
Platform E
Platform A
Day 15
hES Dual Reporter
hiPS Clone 7
NKX2.5-eGFP

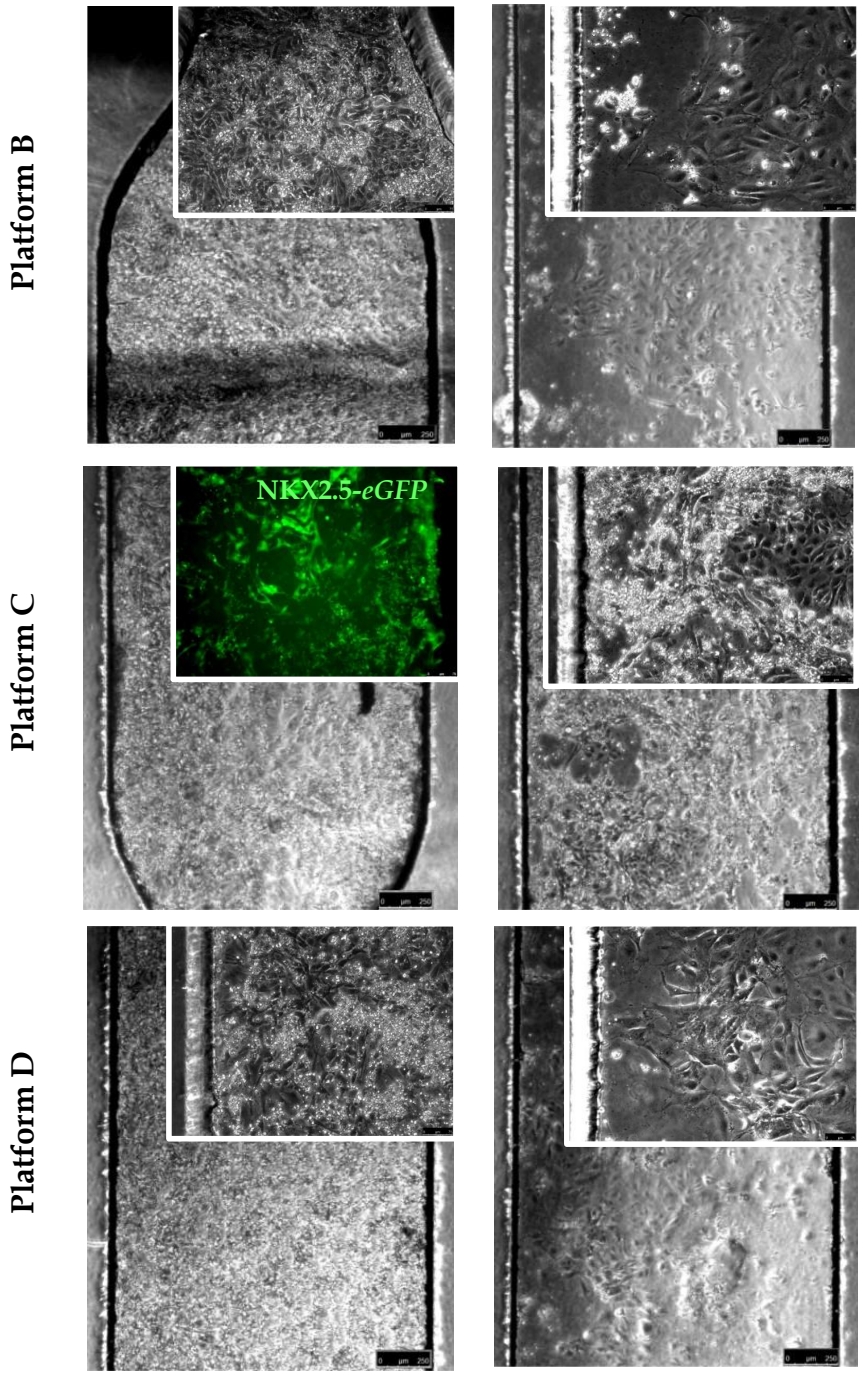
Platform B
Platform C
NKX2.5-eGFP
Platform D

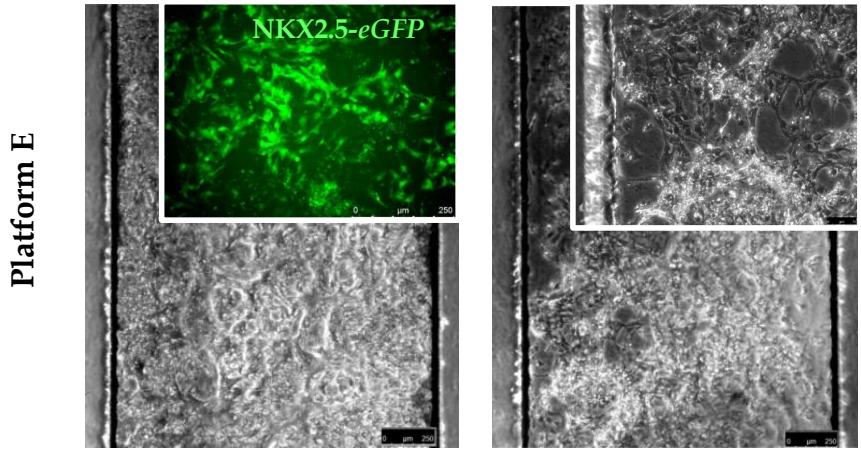

Figure 3.13: *Time-lapse analysis on days 1, 7 and 15 of cardiac differentiation using Wnt/β-catenin pathway modulators of hES Dual Reporter and hiPS mmRNA Clone 7 seeded in five platform with two different MRF coating concentrations and different strategies of medium refreshment. Each picture shows a longitudinal section of a microchannel coupled to the related magnification. Note the sequential changes in morphology, especially for platform A, C and E marked also by the expression of NKX2.5^{eGFP} in Dual Reporter line, indicating the presence of cardiomyocytes. Starting from day 7 of cardiac differentiation, cells seeded in platforms B and D showed a decreased viability and epithelioid morphology with no beating cardiomyocytes formation (no GFP signal was recorded by Dual Reporter line). Culture conditions in platform B and D were then discarded for the following experiments. Scale bar 750µm for the longitudinal section of the microchannel; 250 µm for the magnification of channel section.*

As reported in Figure 3.13, the best conditions for both hESCs and hiPSCs cardiac differentiation on-a-chip was achieved in platforms A (2,5% v/v MRF, medium refresh every 12h), C (2,5% v/v MRF, medium refresh like in standard culture) and E (20% v/v MRF, medium refresh every 12h). This was confirmed by the *eGFP* signal related to NKX2.5 expression in hES Dual Reporter line used to monitor cardiomyocytes formation and only observed in platforms A, C and E. NKX2.5 expression started to became evident on day 8/9 of cardiac differentiation, while the first contractions appeared on day 12/13 for hES Dual Reporter line and 11/12 for hiPS Clone 7. Starting from day 7 of cardiac differentiation, cells seeded in platforms B and D showed an epithelioid morphology with a decreased viability until the end of the experiment: this was probably due to deleterious effects caused by a not optimal medium replacement frequency with subsequent nutrients depletion and waste products accumulation. For these reasons, strategies applied in platforms B and D were discarded for the next experiments.

At day 15 of differentiation, CMs obtained in Platform A, C and E were characterized by immunofluorescence staining against nuclear marker GATA4 and structural marker troponin T (cTnT) and for hES Dual Reporter line was also associated the immunofluorescence against GFP. The immunofluorescence

was performed with the classical five step protocol already described in Chapter 2, Paragraph 2.3. The details of each primary antibody employed are reported in Chapter 2, Paragraph 2.5.2, Table 2.3. The primary antibody against GFP was an anti-rabbit IgG from Thermo Fisher Scientific (A11122). CMs were then quantified by counting the cTnT positive cells from the immunofluorescence, as reported in Figure 3.14.

This experiment allowed the identification of the optimal culture conditions for both hESCs and hiPSCs in microfluidics and their differentiation through the cardiac lineage. In conclusion, among all the conditions tested, the best results were obtained in Platform A in which channels were coated with a solution of 2,5% v/v MRF and medium replacement was perform twice a day, with time interval of 12h. In fact, as reported in the graph, in Platform A, both hESCs and hiPSCs showed a similar behavior in terms of CMs yield. As reported in the immunofluorescence pictures of Figure 3.14 C, cells showed expression of specific nuclear and structural markers GATA4 and cTnT respectively, with marked sarcomeric organization. Moreover, hES Dual Reporter-CMs, stained for both cTnT and GFP reporter for TF NKX2.5, showed contemporary overlaid expression of both marker, confirming that only GFP^{+ve} cells express cTnT, allowing a clear identification of CMs.

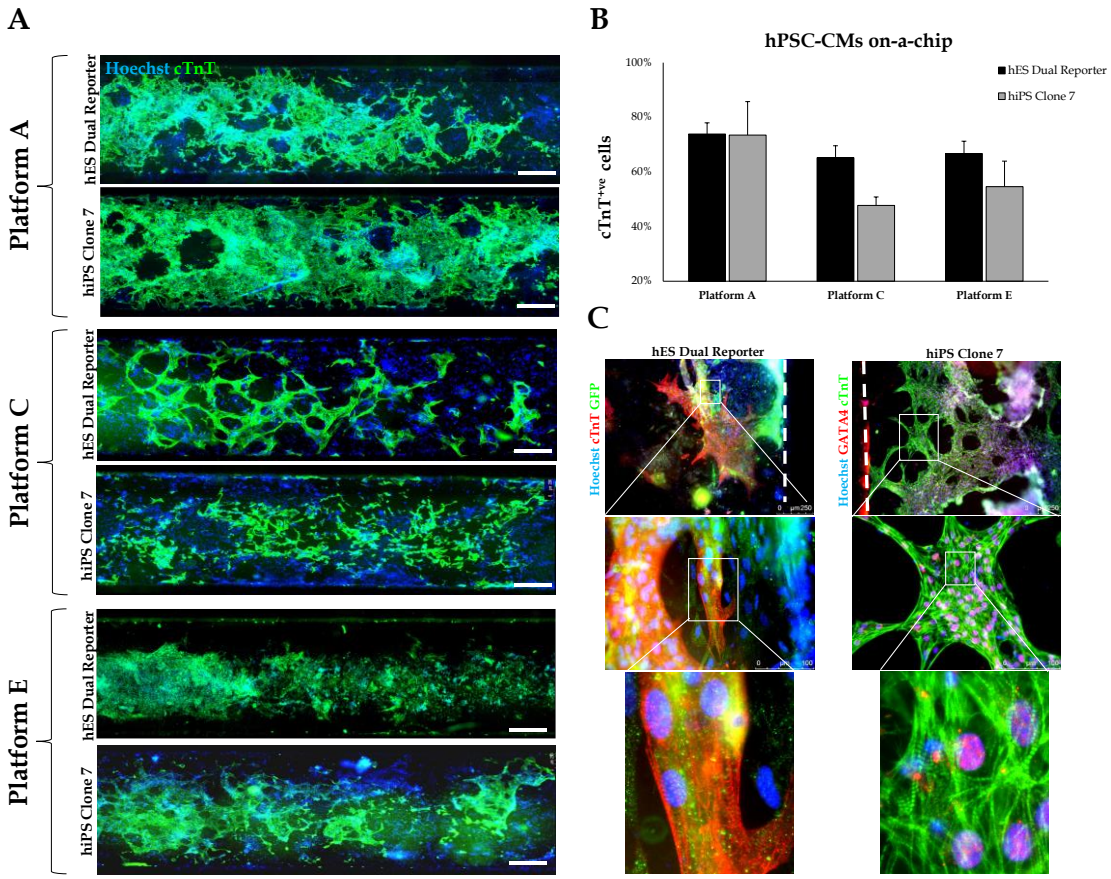

Figure 3.14: *hPSC cardiac differentiation on-a-chip.* ***A.*** *Immunofluorescence staining against cardiac markers cTnT in hES Dual Reporter-CMs and hiPS Clone 7-CMs in Platform A, C and E. Nuclei were counterstained with Hoechst. Representative immunofluorescence pictures of longitudinal sections of microfluidic channels (Scale bar 250µm).* ***B.*** *Quantification of CMs. Percentage of cTnT obtained in Platforms A, C and E. Platform A: hES Dual Reporter-CMs (black bars) 74±4%; hiPS Clone 7-CMs (grey bars) 74±12%. Platform C: hES Dual Reporter-CMs 65±4%; hiPS Clone 7-CMs 48±3%. Platform E: hES Dual Reporter-CMs 67±5%; hiPS Clone 7-CMs 55±9% (n=3; error bars indicate SEM).* ***C.*** *Representative immunofluorescence pictures of channel sections; dotted lines represent channel edge (scale bar 250µm): GATA4 and cTnT for Clone 7-CMs; cTnT and GFP reporter associated to NKX2.5 expression in Dual Reporter-CMs (scale bar 250µm). Note the remarkable organization of the sarcomere in the associated enlargement of the pictures (scale bar 100µm).*

Despite Platform E, characterized by a coating with a solution of 20% v/v MRF and the same frequency of medium refresh of Platform A, gave a high yield of $cTnT^{+ve}$ cells, this condition was discarded because of the difficulty of working with higher MRF concentrations; in fact, at room temperature the 20% v/v concentrated matrix gels rapidly and accumulates at channels edge level, amassing cells in the center, as reported in Figure 3.15.

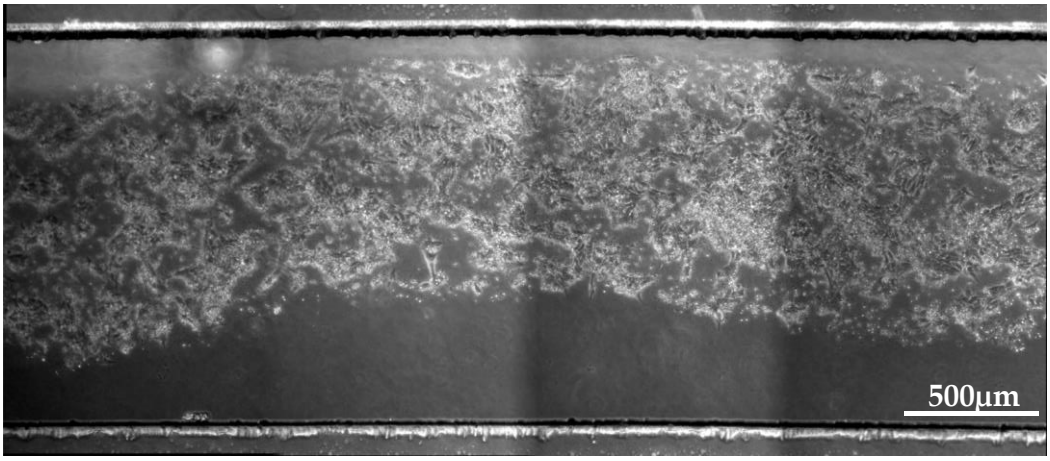

Figure 3.15: *Effect of 20% v/v MRF coating of microchannels in Platform E. When using a higher concentration of MRF, the matrix will rapidly gel at room temperature leading to an accumulation of the cells in the center of the channel.*

These experiments give a proof that a correct matrix concentration for coating and medium refreshment frequency can affect stem cell differentiation. Next experiments, described in Chapter 4, were performed using the same conditions adopted for Platform A with the association of a daily transfection regime using synthetic modified mRNAs (mmRNAs) for the main cardiac transcription factors.

3.5. Conclusions

In this Chapter an *ad hoc* microfluidic device containing 10 independent channels working in parallel was fabricated using the biotechnological state of the art of our BioERA laboratory.

The gold standard CMs differentiation protocol, based on small molecules that modulate Wnt pathway (described in Chapter 2), performed up to now in conventional culture, was successfully integrated in the microfluidic device after step by step optimization derived by the translation from macro- to microscale.

Before starting with the cardiac differentiation protocol, the ability of hPSCs to maintain their stemness and morphology homogeneity in microfluidics was routinely verified, confirmed by the expression of pluripotency markers.

Next, the best conditions for both hES Dual Reprter and hiPS Clone 7 cardiac differentiation were identified, relying on microfluidic channel coating with 2,5% v/v MRF and medium refresh twice a day. The first contractions were detected

between 11-13 days and a high yield of CMs was obtained with cells expressing typical nuclear and structural cardiac markers.

In conclusion, the microfluidic chip employed was used in order to obtain an easy-to-use platform that allow parallelized experiments and the optimization performed enabled a long-term culture over the 15 days required for CMs generation. These achievements represent the basis for the association of the delivery of synthetic mmRNA encoding cardiac TFs to precisely program hPSCs fate and drive cardiac differentiation toward cell maturation.

Chapter 4.
Synthetic modified mRNA for programming hPSCs cardiac fate and driving CMs maturation on-a-chip

This Chapter introduces the novel non-integrating technology of synthetic modified RNA messengers (mmRNA) incorporating specific modifications designed to bypass innate immune response from the cells; this novel approach, pioneered by Warren L. in 2010, can reprogram cells to pluripotency with efficiencies higher than the other reprogramming methodologies [49][50]. Only one proof-of-concept study, published by Warren L. himself, demonstrated the possibility to use mmRNA to drive hPSCs differentiation toward terminally differentiated myogenic cells [49][50].

In this thesis, for the first time, specific mmRNA encoding cardiac transcription factors (TFs) involved in heart development and function, were employed to drive hPSCs cardiac differentiation in our validated microfluidic platform. Thanks to the transient nature of mmRNA and to the possibility to modulate cellular expression simply by adjusting the payload of mmRNA delivery on a daily basis, this novel approach best mimic *in vitro* the developmental signals observed *in vivo* [49][50].

Here, the experimental strategies for TFs delivery were presented, based on the association of Wnt pathway modulators with cardiac mmRNA in microfluidics to investigate how the delivery of TFs in microscale could improve CMs maturation.

mmRNA is a promising tool to finely control gene expression and, thanks to the non-integrating property, to obtain clinical grade CMs that in the next future could potentially be a relevant source of autologous cells for cardiac repair and regeneration.

4.1. Emerging synthetic modified mRNA technology: principle of the method

The possibility to reprogram somatic cells to pluripotency is a powerful tool for studying normal development and generating patient-specific hiPSCs that could be used as disease models or for next future clinically relevant cell-based therapies [49][50].

As described in Chapter 1 and 2, experiments of induction of pluripotency was firstly performed by Yamanaka S. and co-workers *via* the forced expression of 4 transcription factors (TFs), KLF4, c-MYC, OCT4, and SOX2 (KMOS), delivered with retroviral vectors [43][44]. However, the use of virus is entailed

with the risk of viral integration into the genome, rendering this approach not indicated for a clinical use of hiPSCs. Other novel strategies for hiPSCs generation with no risk of genetic alterations are represented by: excisable lentiviral and transposon vectors, transient plasmids, episomal and adenoviral vectors [51][144][145], and DNA-free methods reling on serial protein transduction [146] and transgene delivery with the Sendai virus, characterized by a reproductive cell-cycle completely RNA-based[50][147].

Although DNA transfection-based delivery systems are considered safe, a minimal risk of genomic recombination or insertional mutagenesis is still present while the approaches based on peptide moieties delivery and Sendai virus require long purification procedures [49][50][147]. Importantly, all these methods have shown very low iPSC derivation efficiencies, as already described in Chapter 1, Paragraph 1.3, Table 1.1 [146][149].

In light of these considerations, in 2010 Warren L. and collaborators demonstrated the possibility to derive hiPSCs, with efficiencies superior to established protcols, through repeated transfections of somatic cells with synthetic messenger RNAs incorporating modifications (mmRNA, modified mRNA) specifically designed to avoid innate immune responses. These hiPSCs were named by the author as RiPSCs (RNA-induced Pluripotent Stem Cells). Furthermore, with this simple, nonmutagenic and highly controllable technology, Warren himself used mmRNA to direct the myogenic differentiation of RiPSCs [49][50].

In Figure 4.1 A is reported a table with a list of reprogramming strategies, genomic- and non-genomic-based, with their characteristics on the type of the effector molecule used and its disposition and the related works published; in B the graph simply illustrates the efficiency of each reprogramming methods with the associated safety for future clinical applications.

A

Methods for delivery of iPS cell reprogramming factors			
Genomic			
Method	**Effector molecule**	**Effector disposition**	**Citation**
Retroviral	DNA	Integrated	Takahashi, K. *et al*, 2007
Lentiviral	DNA	Integrated	Yu, J. *et al*, 2007
Lentiviral/cre-lox	DNA	Excisable	Soldner, F. *et al*, 2009
Transposon	DNA	Excisable	Woltjen, K. *et al*, 2009
Non-genomic			
Method	**Effector molecule**	**Effector disposition**	**Citation**
Episomal vectors	Plasmid DNA	Degraded/kicked out	Yu, J. *et al*, 2009
Recombinant proteins	Proteins	Degraded	Kim, D. *et al*, 2009
Sendai virus	RNA	Degraded/kicked out	Fusaki, N. *et al*, 2009
Synthetic nucleotides	**mmRNA**	**Degraded/kicked out**	**Warren, L. *et al*, 2010**

B

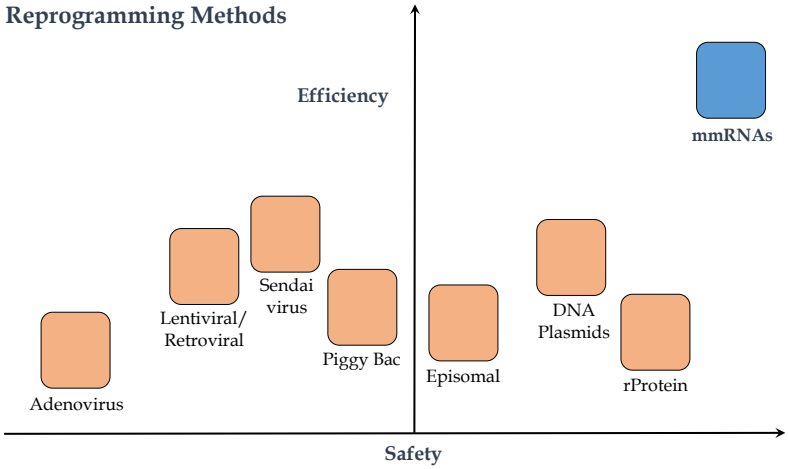

Figure 4.1: A. *Principal reprogramming methodologies used up to date. Retroviral and lentiviral vectors can cause viral integration, with subsequent altered gene function and tumorigenicity when transferred into a host. Lentiviral and transposon-based systems with the transgene excision via the Cre-lox system of transposases, still retain the risk of genomic alterations during transgene insertion and/or excision. Safe methods for deriving iPSCs involve the use of episomal vectors, recombinant proteins and mmRNAs.* ***B.*** *Efficiency of each reprogramming technology versus its safety. mmRNA is the fastest, safest and most efficient method for generating integration-free, virus-free clinically relevant human iPS cells with efficiencies higher than the other approaches here depicted (modified from [150]).*

In Warren's work, the author described the production of mmRNA using *in vitro* transcription (IVT) reactions templated by PCR amplicons. Briefly, for an efficient translation and for boosting its half-life in the cytoplasm, in every mRNA a 5′ guanine cap was incorporated through inclusion of a synthetic cap analog in the IVT reactions [49][151]. Within the templates, the gene-specific open reading frame (ORF) is flanked by a 5′ untranslated region (UTR) with a strong Kozak translational initiation signal and an α-globin 3′ UTR ending with an oligo(dT) sequence for templated addition of a polyA tail [49].

Cytosolic delivery of mmRNA can be performed with cell electroporation or transfection with a lipofectamine-based cationic vehicle to promote endocytosis uptake [50][152][153]. The researchers of Warren's group used a cationic vehicle

for repeated transfection, in order to sustain ectopic protein expression over the days required for cell reprogramming.

In mammalian cells, it is known that interferon- and NF-kB-dependent pathways antiviral responses are triggered by exogenous single-stranded RNA (ssRNA) [49][154][155][156]. Eukaryotic mRNA, *in vivo*, undergoes post-transcriptional modifications, thus, having this in mind, Warren's group synthesized mmRNA incorporating specific modifications of nucleobases to bypass immune responses mediated by RIG-I (the ssRNA sensor) and the inducible endosomal ssRNA sensors TLR7 and TLR8[49][50][157][158]. The nucleobases modifications of Warren's mmRNA are the following: cytidine was substituted by 5-methylcytidine (5mC), whereas uridine was substituted by pseudouridine (psi). Warren L. and co-workers performed cell viability assays on on human neonatal keratinocytes and BJ fibroblasts transfected with unmodified mRNA, mmRNA carrying in turn one of the two modifications and mmRNA with both 5mC and psi; they also analysed a panel of interferon response genes through qRT-PCR and found that the double nucleotide substitution markedly improved cell viability, attenuating interferons signaling as reported in Figure 4.2 [49][50].

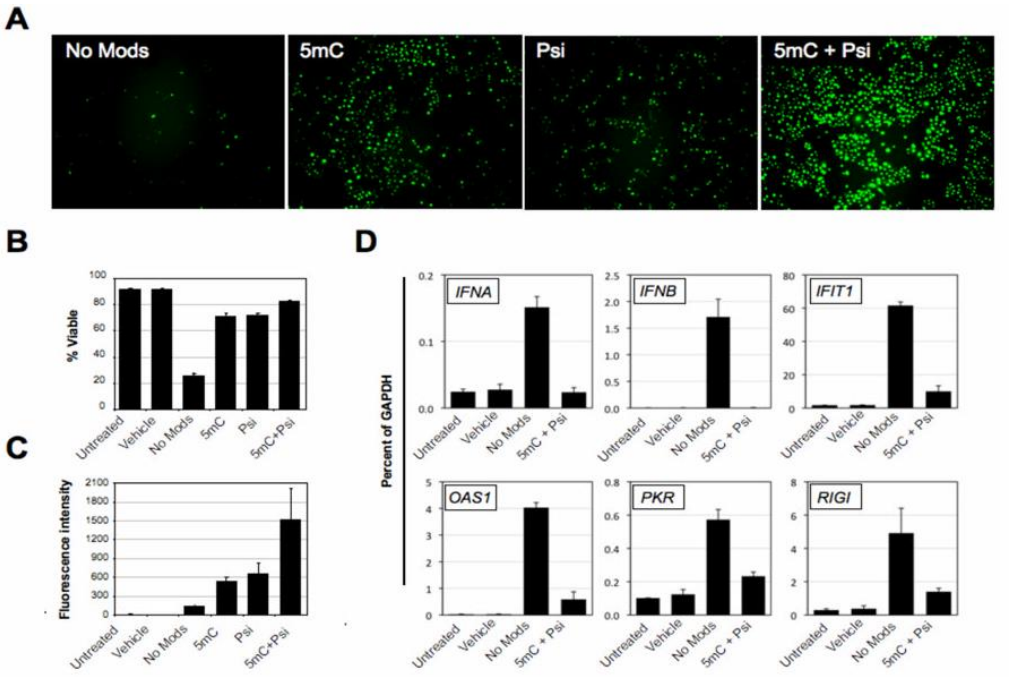

Figure 4.2: *Warren's group attempt to overcome innate immune responses, incorporating modified nucleobases in the mmRNAs.* ***A.*** *Microscopy images of transfected keratinocytes with 400ng/well of synthetic unmodified (No Mods), 5mC modified, psi modified or 5mC+psi mmRNA encoding nGFP.* ***B.*** *Flow cytometry percent viability and* ***C****. Mean fluorescence intensity of the cells shown in A.* ***D.*** *Quantitative RT-PCR data showing expression of 6 interferon-regulated genes in BJ fibroblasts 24 hours after transfection with unmodified (No Mods), or modified (5mC+psi) RNA encoding nGFP (1200ng/well) vehicle and untransfected control cells (adapted from [49]).*

Moreover, to further increase cell viability of RNA transfection, Warren L. and collaborators used media supplemented with a recombinant version of B18R protein, a Vaccinia virus decoy receptor for type I interferons [159]: in fact, coupling mmRNA with B18R, enabled a high, dose-dependent levels of protein expression with high cell viability[49][50]. In Figure 4.3 is illustrated a schematic of mmRNA mechanism of action.

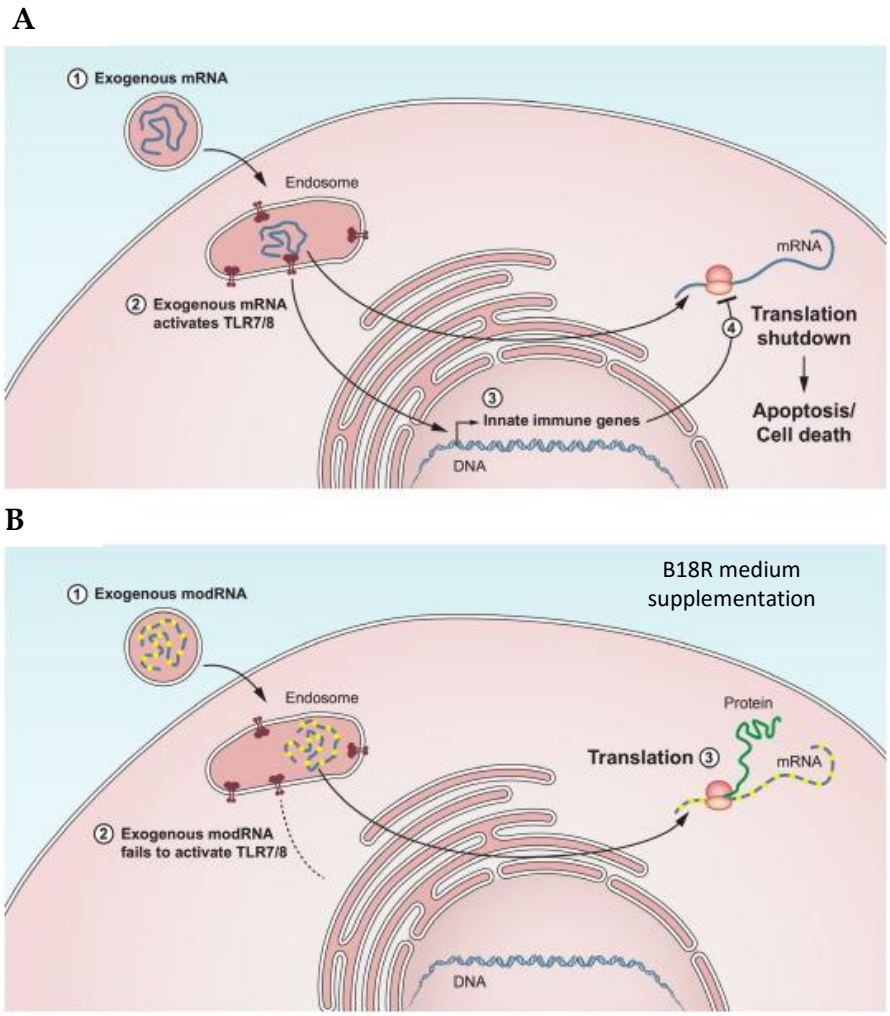

Figure 4.3: *Synthetic mmRNA bypasses Toll-like receptor-induced apoptosis after transfection.* ***A.*** *The exogenous mRNA is detected by Toll-like receptors 7 and 8 (TLR 7 and 8) inducing the expression of innate immune respose genes (type I interferons, RIG-I) and cell apoptosis.* ***B.*** *The double nucleobases modification (psi and 5-mC) changed the secondary structure of the nucleic acid, bypassing immune recognition and mmRNA was then translated. B18R protein addition to the culture medium allowed for high, dose-dependent levels of protein expression with high cell viability (adapted from [160][161]).*

Another important aspect is that this approach is feeder- and xeno-free, rendering it suitable for moving hiPSCs from laboratory to clinic [50].

By combining mmRNA with the soluble interferon inhibitor B18R, it is possible to perform a highly efficient reprogramming of somatic cells to pluripotency, as demonstrated also by a work published in 2016 by our research group BioERA at the University of Padova with the integration of this strategy in micorlfuidics. Giulitti S. and collaborators in fact, showed that downscaling mmRNA reprogramming strategy to microliter volumes generated a favourable environment for the acquisition of pluripotency. With the combination of mmRNA and microfluidics, they achieved an average efficiency of over 120 hiPSC colonies per 100 seeded cells, 50-fold higher than the current data available in literature using conventional multiwells [95].

To promote the application of hiPSC technology for regenerative medicine or disease modeling, it is of paramount importance that the multilineage differentiation potential of pluripotent cells can be achieved. Warren himself have already demonstrated the abilty to differentiate hiPSCs into terminally differentiated myogenic cells using mmRNA, indicating that these modified nucleotides could precisely reprogram as well as program cell fate. To derived myogenic cells they performed a simple *in vitro* hiPSCs myogenic differentiation protocol (FGF withdrawal and serum additions in gelatin-coated plates) followed by 3 days of transfection with a MYOD-encoding mmRNA[49][50]. MYOD was considered a "master regulator" for muscle cell fate and several experiments in literature reported its ability to induce transdifferentiation of mouse fibroblast into myoblasts [162]. At the end of the experiment, Warren's group obtained large, multinucleated myogenin and MyHC (Myosin Heavy Chain) double-positive myotubes, with efficiencies ranging from 35-38% using 1800ng of mmRNA to transfect 10^4 and $5x10^3$ cells. Preskey D. and co-workers in 2015, published another work, reporting the use of synthetic mmRNA to generate hiPS and to drive the transdifferentiation of human fibroblasts into myoblast-like cells. They transfected $5x10^4$ fibroblasts for 4 days using 200ng and 300ng of mmRNA encoding MYOD1 but obtained very low efficiencies, 0,04% and 0,8% respectively [163].

Finally, the use of mmRNA for cell fate manipulation represent a precious tool to modulate cellular expression of specific TFs on daily basis, simply by adjusting the quantities of transcripts at every transfection. At the end of each a TFs transfection, ectopic expression in the targeted cells stops because of the rapid degradation of mRNA in the cytoplasm.

In this Chapter, mmRNA technology is combined with microfluidics to develop an efficient and robust method for programming cardiac hPSCs fate in a high controllable microenvironment that allows cost-effective and combinatorial analysis at one time.

4.2. Changing cell identity with Transcription Factors - state of the art for cardiac regeneration

As already discussed in the previous paragraph, from the pioneering reprogramming experiments performed by Yamanaka, several protocols have been developed to program cell fate in order to obtain for example CMs. In general these approaches relied on the transdifferentiation of somatic cells by forcing the expression of key lineage-specific factors, bypassing the pluripotent state. The first experiment was performed almost 30 years ago, when overexpression of a single gene, the myogenic TF MyoD, was shown to be able to convert fibroblasts into skeletal muscle cells[36][162]. Direct lineage conversion experiments have been reported for a plethora of somatic cell types [163]: hematopoietic system [164][165][166], pancreatic exocrine cells [167], the hepatic system [168] and neuronal lineage [169]. Unfortunately, up to now no single TFs has been identified as "master regulator" for CM development, but it was hypothesized that a combination of specific TFs can be used to instruct the gene expression profile of the transfected cell toward a cardiac fate [36].

Pioneering this field, Srivastava D. and Ieda M. group who performed in 2010 a direct conversion of murine fibroblasts to CMs *in vitro* and *in vivo* with a specific combination of cardiac TFs. They started by testing 14 different factors involved in cardiomygenesis, delivered in mouse post-natal fibroblasts with a mixture of retroviruses [48]. Three were identified and considered sufficient for cardiac programming: *Gata4*, *Mef2c* and *Tbx5* (GMT factors). The conversion into CMs was verified by the up-regulation of a cardiac specific reporter gene, detected in up to 25% of transfected cells. 1 day after the delivery of GMT, cells were transplanted into immunocompromised mouse hearts. However, only 1% of these so-called induced CMs (iCMs) displayed *in vitro* spontaneous contractions, indicating an incomplete conversion into fully mature, functional CMs. Two later studies delivered the GMT cocktail *via* a single polycistronic vector and observed an enhanced differentiation of iCMs from mouse

fibroblasts [170][171]. The second study obtained significantly different results from the pioneer experiment performed by Srivastava D. and Ieda M., with cardiac gene expression found in all the murine fibroblast lines employed, marginally elevated because of GMT transduction, with extremely variable reprogramming efficiencies. Moreover, GMT-overexpressing cells showed no spontaneous action potential *in vitro* and, when transplanted into injured mouse hearts, cells were characterized by poor survival and minimal activation of cardiac genes. The later addition of one more cardiac TF, *Hand2*, to the reprogramming set (GMTH), lead to a low yield of cells positive for both cardiac structural markers *aMHC* and *cTnT* [172].

Since the gene regulatory network that cooperate during human cardiac development is more complex than the mouse counterpart, CMs generation from human fibroblasts needs more TFs than those applied up to date in murine cells. Probably this species-specific requirement is due by differences in gene expression and regulation between mouse and human fibroblasts, showing a different susceptibility in the activation of lineage-specific genes [36].

Nam Y.J. in 2013 demonstrated that both GMT and GMTH combinations were insufficient and unable to reprogram human fibroblasts: he employed a combination of 4 TFs (*Gata4, Hand2, Tbx5; Myocd*) and 2 miRNAs (miR-1 and miR-133), to convert human neonatal and adult fibroblasts into CM-like cells characterized by the expression of sarcomeric structural features. However, a longer time in culture is required for these iCMs to reach a level of maturation, compared to murine cells; moreover these human iCMs displayed low-amplitude calcium transients after electrical stimulation, extremely rare spontaneous contractions and heterogeneity in the cardiac population with different levels of cardiac and non-cardiac genes [47].

Immediately after these first experiments, several groups began to move the reprogramming *in vivo*, by directly injection of cardiac TFs into mouse injured hearts. It was found that GMT delivered with retroviruses in a mouse model of myocardial infarction (MI) reprogrammed resident fibroblasts into CM-like cells [173]. Also in this case, the efficiency was low (~15%) but, *in vivo*-derived iCMs were more fully reprogrammed than *in vitro*-derived ones, resembling the endogenous cardiac cells. These findings indicated that the factors produced within the native milieu, absent in the conventional culture system, influenced cell fate switch. Importantly, performing the cardiac reprogramming *in vivo*, allowed cells to achieve cardiac functionality features coming from a combination of new

muscle formation and environment-dependent effects, such as GFs secretion within the ECM.

Other approaches have been tested, using cell-free methods, taking into account the influence of paracrine factors to activate repair mechanisms in damaged heart. Selected TFs can be vehiculated into the heart with viral and non-viral DNA vectors, small-molecules chemical compounds, recombinant proteins or with the novel non-integrating mmRNA technology. These strategies have been used especially for transdifferentiate CMs into other CMs subtypes, for example to derive conduction system cells using the pacemaker cell-related TF TBX3, revolutionizing current clinical treatment based on the transplantation of costly electronic pacemakers [174]. Other recent studies proposed strategies for First Heart Field (FHF)- and Secondary Heart Field (SHF)-derived cardiac progenitor cells (CPCs) and epicardium-derived progenitor cells (EPDCs) activation and differentiation. In 2013, Zangi L. and colleagues published a work in which they were able to reactivate quiescent murine EPDCs with a direct injection of a mmRNA encoding VEGF-A after MI, driving them away from the fibroblast, scar-forming fate [161]. Figure 4.4 summarized the cell-based and cell-free approaches for human cardiac regeneration and Table 4.1 reported the studies conducted by several research groups.

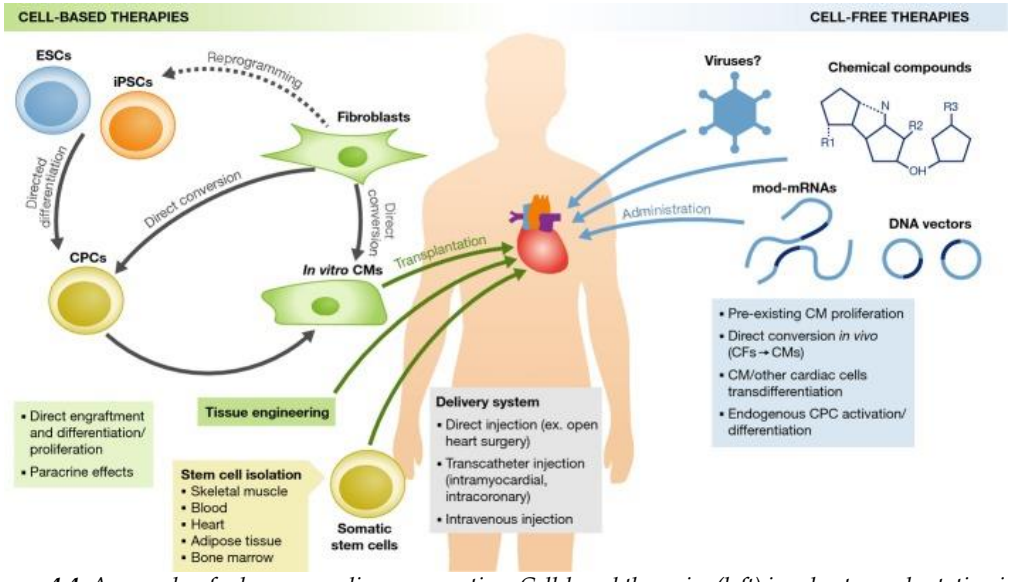

Figure 4.4: *Approaches for human cardiac regeneration. Cell-based therapies (left) involve transplantation into the damaged heart of in vitro-derived CMs differentiated from hPSCs or from transdifferentiated fibroblasts and cardiac progenitor cells (CPC) using specific cardiac TFs. On the right, cell-free therapies rely on the administration of chemical compounds or genes (viral vectors, non-viral DNA vectors or mmRNAs) to stimulate cardiac regeneration (adapted from [36]).*

Table 4.1: *Strategies for directing cardiac cell fate.*

a) Fibroblasts >> CMs							
Reference	Species	Recipient cell type/Organism	TFs/Molecule	Delivery method	Experimental read-out	Efficiency	*In vivo*
Ieda, M. *et al*, 2010	M	Post-natal CFs and TTFs	Gata4, Mef2c, Tbx5	Retrovirus	αMHC reporter/cTnT	5-25%	-
Chen, J.X. *et al*, 2012	M	CFs and TTFs	Gata4, Mef2c, Tbx5	Lentivirus	αMHC /Nkx2.5/cTnT reporters	0-35%	-
Ingawa, K. *et al*, 2012	M	Adult CFs	Gata4, Mef2c, Tbx5	Retrovirus	αMHC reporter	3-7%	-
		MI model			αMHC reporter and α-actinin	1%	+
Qian, L. *et al*, 2012	M	MI model	Gata4, Mef2c, Tbx5	Retrovirus	Postn/Fsp1 lineage tracing, α-actinin and sarcomeric structure	10-15%	+
Nam, Y.J. *et al*, 2013	H	Neonatal FFs, adult CFs and DFs	GATA4, HAND2, TBX5, MYOCD, miR-1, miR-133	Retrovirus	cTnT/Tropomyosin	9-45%	-
b) CMs >> Conduction system cells - Transdifferentiation							
Reference	Species	Genes/TFs	Delivery method	Cell type obtained	Experimental read-out	Efficiency	*In vivo*
Bakker, M.L. *et al*, 2012	M	Tbx3	Lentivirus	Pacemaker cells	Gene expression, electrophysiological parameters	N.D.	-
			Inducible transgene				+
c) CPCs and EPDCs activation							
Reference	Species	TFs/Moleule	Delivery method	Cell activated	Experimental read-out	Efficiency	*In vivo*
Zangi, L., *et al*, 2013	M	VEGF-A	mmRNA	EPDCs to endothelial/ smooth muscle cells	Epicardial lineage tracing with bioluminescence assay	N.D.	-
							+

M, mouse; H, human; CFs, cardiac fibroblasts; TTFs, tail tip fibroblasts; MI, myocardial infarction; CPCs, cardiac progenitor cells; EPDCs, epicardium-derived progenitor cells; N.D., not determined.

4.3. Unsolved issues of human cardiac regeneration

As described previously in Paragraph 4.2, despite the encouraging results obtained from cell-based and cell-free strategies for cardiac regeneration in animal model experiments, much work has still to be done before promoting such approaches to the clinical tests. In fact, the following issues will have to be faced:

- Cell type and scalability: the selection of the ideal cell type is often hard because this cell should tolerate autologous transplantation, show a rapid *in vitro* expansion and ability to differentiate into CMs, properly electrically coupled with the host cells.
- Subtype of CMs: as already explained in Chapter 1 and demonstrated in Chapter 2 and 3, the direct cardiac differentiation of hPSCs allowed the generation of a high yeld of beating CMs; however the resultant population is heterogeneous, characterized by a mixture of atrial,

ventricular and conductive cells. In order to achieve better effects on cardiac function and prevent arrhythmias after transplantation, it may be essential to selectively differentiate the desired cell subtype.

- Electrical coupling: one major concern is the incomplete electrical coupling of the CMs generated, entailing the risk of the development of arrhythmias. Transplanted CMs in fact, have to align, engraft and couple with host cells in ordered fashion.
- Teratoma formation: another caveat related to the transplantation of hPSC-derived CMs is the presence of residual undifferentiated cells.
- Issues on using viral vectors: some viral vectors can integrate into the host genome, with the subsequent risk of tumorigenity. Thus, it is imperative the application of non-integrative methods to efficiently drive cell fate conversion without compromising the safety [36][161].

Latest experimental and therapeutic tools involving the non-integrating mmRNA technology will unveil the mechanisms of human cardiogenesis and repair, providing novel alternatives with the ultimate goal of deriving clinical-grade CMs for cardiac regenerative medicine.

4.4. Experimental setup: programming hPSCs with mmRNA encoding cardiac TFs in microfluidics

The experimental procedures above mentioned reinforce the idea that guided differentiation of hESCs or hiPSCs into clinically relevant populations can be realized *in vitr*o by developmental signals resembling those that instruct cells *in vivo* [21]. The attempt is to trigger hPSCs to mimic the appropriate sequential differentiation observed in the embryo *via* the forced overexpression of key TFs as a powerful way for programming cell fate and identity. As a proof-of-concept, this work aimed at forcing the endogenous protein expression through the administration of mmRNA encoding cardiac TFs to drive cardiogenesis *in vitro* toward cell maturation. The cardiac TFs selected to drive the cardiac differentiation of hPSCs were MESP1, GATA4, NKX2.5, MEF2C, TBX3 and TBX5; this "Cardio mix" will be transfected into cells using a cationic vehicle lipofectamine-based, and to monitor the transfection efficiency, an mmRNA encoding nGFP will be associated in the TFs mixture. All the mmRNA were produced and provided by Miltenyi Biotec (Cologne, Germany). Before

describing the experimental set-up it is important to understand cardiac TFs activity and timing of expression.

- MESP1: is regarded as a regulator of the cardiac TFs cascade to direct the generation of cardiac mesoderm [175];
- GATA4: is essential for proper mammalian cardiac development and for survival of the embryo; it works in combination with NKX2.5 and TBX5 and is expressed in both embryo and adult CMs; promotes cardiac morphogenesis, CMs survival and maintains cardiac function in the adult heart [176].
- NKX2.5: interacts with GATA4 and TBX5 to orchestrate heart development, operating in a positive loop to regulate CMs formation; is also involved in mechanisms that decide ventricle and atrial cell fate [177].
- MEF2C: is involved in cardiac morphogenesis, myogenesis and vascular development; regulates the post-natal growth of the myocardium [178].
- TBX3: in the developing heart is required for pacemaker and conduction system development and is important for functional maturation and post-natal homeostasis of CMs [175].
- TBX5: associates with NKX2.5 and synergistically promotes CMs differentiation [179].

In Table 4.2 are reported the temporal expression windows of cardiac TFs observed during studies on human cardiogenesis performed *in vitro* by Gepstein L. and Burridge P.W. in 2001 and 2014 respectively[56][66][21], while Figure 4.5 is a schematic of the up and downregulation of these TFs during cardiac development.

Table 4.2: *Timing of cardiac TFs of cardiogenesis in vitro [56][21].*

Developmental stage	Genes	Expression window [days]	References
Pluripotency	OCT4, NANOG	Peak D2-3, OFF	- Gepstein, L. *et al*, 2001 - Burridge, P.W. *et al*, 2014
Primitive streak	Brachyury T	Peak D2-3, OFF D5-10	
Cardiac mesoderm	MESP1	Peak D2-3, OFF	
Cardiac TFs	GATA4	Peak D4, ON	
	MEF2C	Peak D6-8, ON	
	NKX2.5	Peak 7-8, ON	
	TBX3	Peak D8, ON	
	TBX5	Peak D8, ON	
Structural Genes - Sarcomere	cTnT (TNNT2)	Peak D8, ON	
	MYH7 (β-MHC)	Peak D14, ON	
Structural/functional Genes – Ion channels	SERCA2A	Peak D6, ON	

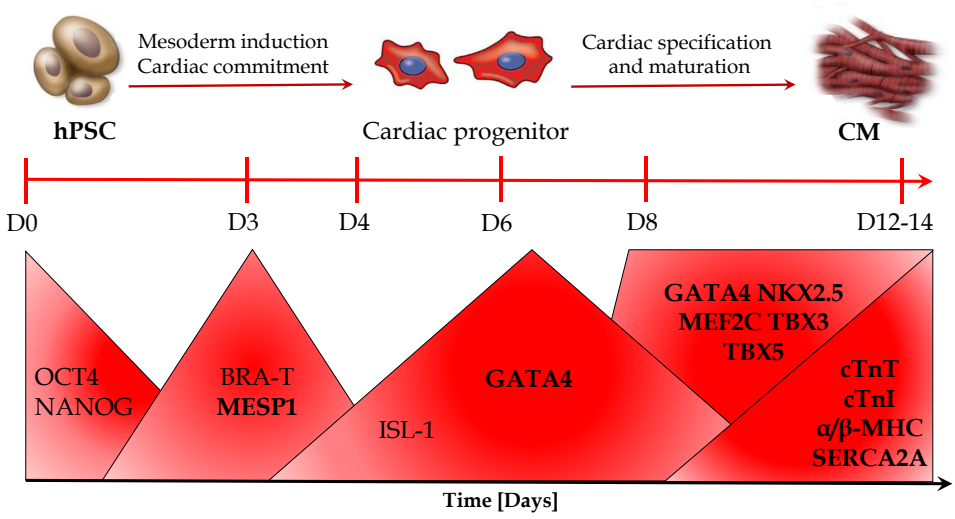

Figure 4.5: *Schematic representation of the waves of expression of the principal cardiac TFs during in vitro differentiation of pluripotent stem cells.*

Taking into account the timing of expression of cardiac TFs and their networking activity studied *in vitro*, an *ad hoc* experimental strategy was designed. Figure 4.6 illustrated a comprehensive scheme of the experimental setup.

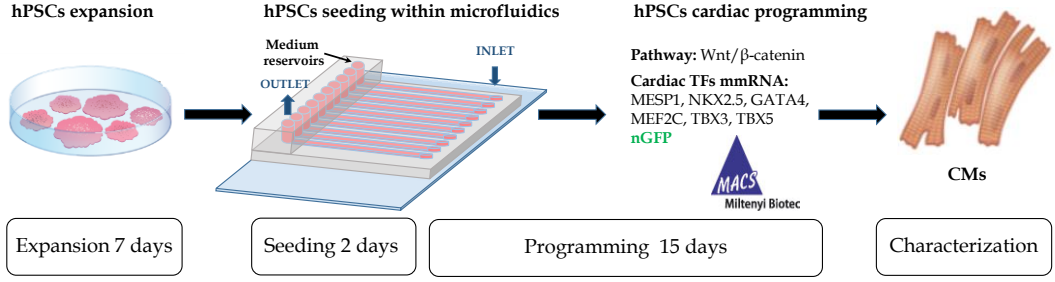

Figure 4.6: *Schematic for hPSCs cardiac programming in microfluidics. After expansion in conventional culture, hPSCs were seeded in microfluidic device and after 2 days, the cardiac programming was initiated associating the Wnt/β-catenin pathway modulation with 6-days of transfection regimen with mmRNA encoding cardiac TFs (Cardio mix). After 15 days, cells were characterized for functional assays and gene expression pattern analysis.*

hPSCs selected for these experiments are: hiPS mmRNA Clone 7 and hES Dual Reporter line for their cardiogenic ability to give a high yield of beating CMs in conventional and microfluidic culture, as described in Chapter 2 and 3. hPSCs were expanded in 6-well plates for approximately 1 week and, when

they reached confluence, cells were dissociated using standard procedures (details in Chapter 2, Paragraph 2.3) and then seeded in the microfluidic device at a density of 700cells/mm^2 in medium supplemented with 10μM ROCK inhibitor (Y-27632, CalBiochem) to preserve cell viability. After 2 days for cell recovery, cardiac differentiation using Wnt/β-catenin pathway modulators was initiated and associated to cell programming with 6 daily transfections with the Cardio mix. Cell were maintained in microfluidic device until day 15 and then, CMs were characterized for their structural, functional and maturation features. The transfection protocol was optimized and then the approaches designed were divided in Part 1 and Part 2 in which two strategies were tested to best mimic the TFs action during cardiac differentiation; the details of each strategy will be elucidated in the next paragraphs.

4.5. Optimization of the transfection with synthetic mmRNA: first steps

In this Paragraph will be elucidated the optimization of the transfection procedure before starting with the hPSC programming using cardiac TFs mmRNAs. In the transfection strategies presented in this work, the mmRNAs were delivered using two transfection kits: StemMacs™ mRNA Transfection Kit (SM; Miltenyi Biotec, Cologne, Germany) and Stemfect® mRNA Transfection kit (SF; Stemgent, Cambridge, USA). These commercial formulations are lipid-based transfection systems, specifically designed for an efficient mmRNA delivery into various cells types; they have been selected for these experiments for the minimal cytotoxicity and high transfection efficiency reported in each data sheet; they were particularly suited for sensitive cell types such as PSCs and complex transfection schedules involving repeated transfections over several days.

For satisfactory transfection results, it is necessary an optimization of the protocol. The use of a nuclear eGFP-mmRNA is indicated as an easy read-out for transfection efficiency and is recommended as positive control when establishing new transfection protocols. Finding the optimal transfection conditions is necessary for driving hPSCS differentiation toward cardiac lineage.

In this experiment, the transfection efficiency of hPSC colonies was evaluated comparing standard 24-well plates with the 10-channels microfluidic device.

When starting mmRNA transfections, it is necessary to establish the optimal cell density to make sure that the majority of the cells will be efficiently transfected. In general, in case of a single transfection, it is recommended to choose a cell density that bring the culture confluence between 50-90% in 24-48 hours while, for repeated transfections for several days, a lower cell density is indicated. As previously mentioned in Paragraph 4.1, to avoid innate immune response, cells were incubated with medium supplemented with B18R 0,2ng/µl (1:2500) 4 hours before the transfection. Both the transfection kits used (SM and SF) are based on two components: the transfection buffer (TB) and the transfection reagent (TR), maintained at +4°C. As reported in Figure 4.7, two solutions were prepared in two separate sterile, RNAse-free 0,2ml tubes (SARSTEDT, Germany): Solution A was prepared by diluting 5-fold 100ng/µl of each mmRNA used in TB; Solution B by adding 10X TR in TB. Solutions A an B were then combined in 3:1 (SM) or 2:1 (SF) volume ratio respectively. The transfection mix was equilibrated at room temperature for 15 minutes (SM) or 20 minutes (SF) to allow the formation of the lipid complex incorporating mmRNA. The transfection mix was added to the cells and incubated for 4 hours at 37°C and 5% CO_2.

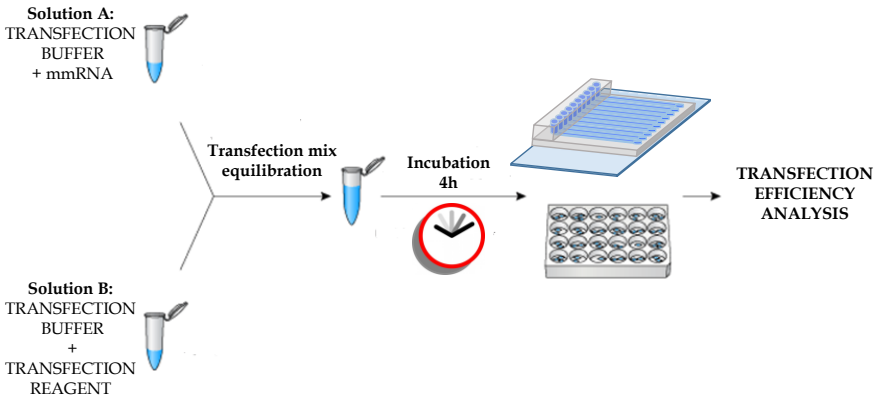

Figure 4.7: *Schematic of the mmRNA transfection using lipid-based systems commercially available (modified from Clontech website).*

The expression of the transfected factor will be detectable 6-24 hours after transfection, peaking after 12-18 hours, depending on the transient nature of mmRNA and protein stability [49]. After 4 hours, transfection was stopped adding new, fresh, prewarmed medium, supplemented with B18R (medium with B18R was used until the end of the transfections plus one additional day).

In conventional culture systems, the transfection mix is added dropwise in the plate, gently move it back and forth to homogeneously distribute the transfection complex while, when using microfluidic device, all the components have to be adapted to small volumes. Moreover, in microchannels it is mandatory to dilute the transfection mix in an appropriate medium volume. In every channel, 12µl of medium were delivered but the effective volume of medium flowing over the cells and covering the channel area of 27mm^2, is 5,4µl, therefore it is necessary to increase the transfection mix/culture medium ratio, compared to conventional 24-well plates, avoiding a significant reagents loss. These adjustments are necessary to increment the transfection efficiency simply by altering the payload of transcripts. For the scale down, ratios between mmRNA, TB and TR were maintained, while only the proportions of medium used for the delivery of transfection mix were reduced.

In this work, 75%, 50% and 25% of medium were used and tested to dilute the transfection mix during cardiac programming in microfluidics, comparing to standard transfections performed in conventional cultures and, for convenience, these percentages corresponded and were always indicated as low dose, middle dose and high dose of transfection mix respectively. These ratios are equal to the following absolute quantities of mmRNA/mm^2 of microchannels: 150pg mmRNA/mm^2; 210pg mmRNA/mm^2 and 380pg mmRNA/mm^2 as reported in the Table 4.3.

Table 4.3: *quantities of mmRNA used in this work, adapted to microfluidics with the related medium volumes.*

Transfection ratios		
Transfection mix dose	**Medium [%]**	**mmRNA[pg/mm^2]**
Low	75%	150
Middle	50%	210
High	25%	380

The selection of the appropriate concentration of the transfection mix, with the related percentage of medium for diluting it, depends on the type of the experiment and will be elucidated in the next paragraph. Commercial kits recommend to use diluted transfections when performing the delivery of mmRNA

for several days, in order to preserve cell viability, since the transfection is a stressful event for the cells and a high dose for several days can cause high mortality; when it is necessary a single transfection for one day, a higher dose can be used for obtaining an immediate gene expression.

4.5.1. Transfection efficiency of hPSCs colonies

In BioERA laboratory, after reprogramming human fibroblast to hiPSCs with high efficiencies, preliminary experiments were performed to study the possibility to use mmRNA transfection to direct cell differentiation toward desired lineages. Evidences from reprogramming experiments, demonstrated a reduced propensity of hiPSC colonies to transfection, until they became refractory to the process. This behavior could depend on cell density within the pluripotent colony and/or a reduced endocytosis. In the first case, cells are less responsive to the transfection because they are closely connected to each other through cell adhesion proteins expression, among which E-cadherin plays an important role. E cadherin is a calcium-dependent cell-cell adhesion molecule involved in epithelial cell behavior, tissue formation, cell survival and pluripotency maintenance [180].

To circumvent these barriers, it was hypothesized that a pre-treatment of hPSC colonies with 0,5mM EDTA before the delivery of a nuclear eGFP mmRNA for 1 day could help mmRNA up-take. EDTA in fact, is a chelating agent that sequesters a variety of polyvalent cations such as Ca^{2+} necessary for E-cadherin, thus allowing a light dissociation of the colony. After this process, EDTA was removed adding fresh medium to restore the physiological Ca^{2+} concentration. With this strategy, weakening cell junctions, the cell surface accessible to medium carrying the transfection reagent increases, allowing a more efficient mmRNA delivery into the cells, as depicted in Figure 4.8.

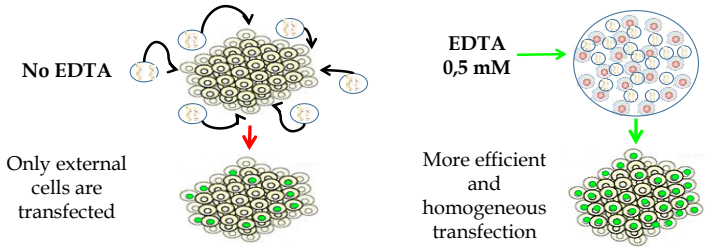

Figure 4.8: *Pretreating hiPS colonies with EDTA 0,5mM before the delivery of nGFP mmRNA allows a homogeneous transfection.*

This experiment was performed comparing the transfection efficiency of hiPS Clone 7 in microfluidic platform and conventional 24-well plate. Cells were seeded mimicking a possible density obtained from a reprogramming experiment established by the expertise in the laboratory: in microfluidics this density corresponds to approximately 20 hiPS colonies/channel while in conventional 24-well is 140 hiPS colonies/well (with~ 460 cells/colony as mean number of cells per colony). The mmRNA encoding nGFP was delivered using Stemfect (SF) transfection kit. The experiment was divided in two groups:

1. hiPS colonies pretreated with EDTA 0,5mM for 2-3 minutes in 24-well plate and 30-40 seconds in microfluidics;
2. hiPS colonies not pretreated with EDTA before the delivery of nGFP-mmRNA, as a control.

From previous experiments in the laboratory, a high and middle doses of transfection mix (75% and 50% respectively) resulted optimal for mmRNA delivery. The quantities of mmRNA used were adapted by the reprogramming expertise of BioERA lab who calculated the mean cell number within a colony and the mean area occupied by the colonies within a channel: high dose 85pg/mm^2 of hiPS colony, middle dose 48pg mmRNA/mm^2 of hiPS colony. In conventional culture, additional quantities of mmRNA were tested using higher doses then those recommended in SF datasheet, 122pg mmRNA/mm^2 of hiPS colony and 1257pg mmRNA/mm^2 of hiPS colony, to make the delivery of nGFP mmRNA sufficient for the transfection of all the colonies.

Transfection efficiency was calculated by counting the nGFP^{+ve} cells versus the total cell number. For a better quantification of cells, it is possible to counterstain nuclei with live Hoechst (Sigma Aldrich) 0,4ng/µl (1:5000) in culture medium, incubated for 10 minutes at 37°C. These data were performed and obtained in collaboration with Dr. Torchio E. who earned her master degree in 2014 [181].

As reported in Figure 4.9 A, EDTA increased considerably the transfection efficiency in hiPS Clone 7: in fact, without EDTA pretreatment, only the edges of the colonies were transfected while colonies pretreated with EDTA showed a homogeneous distribution of transfected cells. The percentage of transfection efficiency was calculated and showed in the graphs in Figure 4.9 B and C.

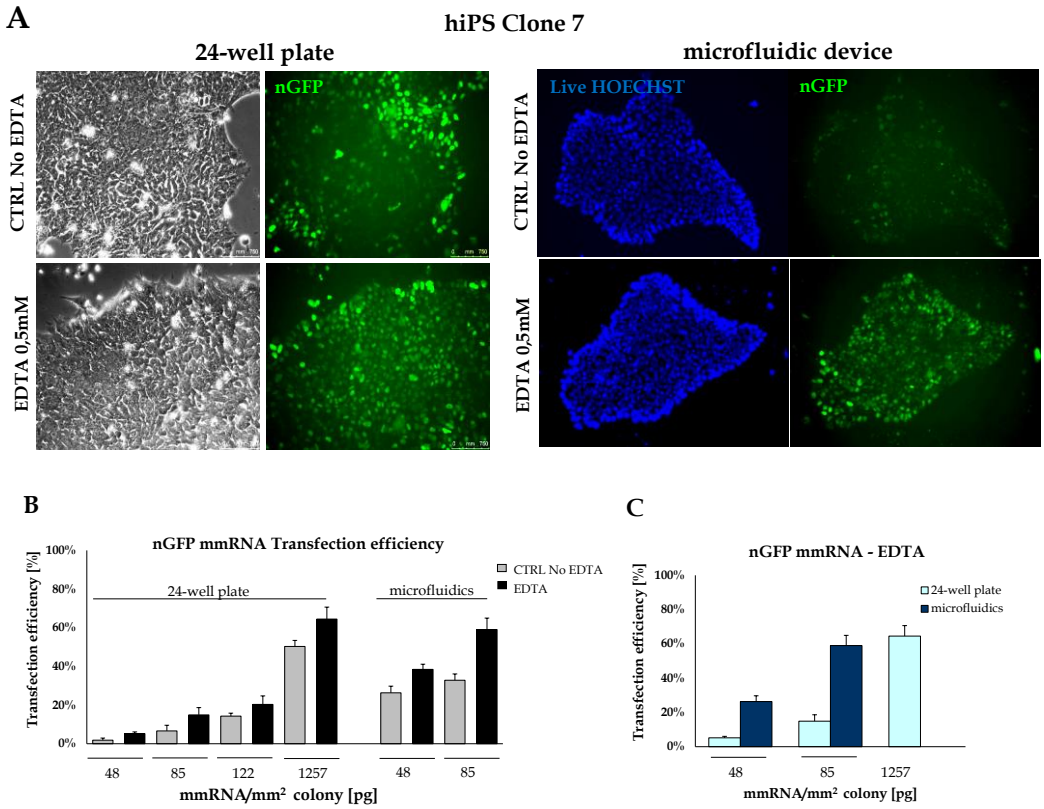

Figure 4.9: *Optimization of mmRNA delivery with EDTA 0,5mM pretreatment.* ***A.*** *hiPS Clone 7 colonies transfected with nGFP mmRNA without (CTRL) and with pretreatment with EDTA in 24-well plate and microfluidic device. In the right panel it is reported the live Hoechst stain for calculating the transfection efficiency. The panels showed cells treated with 85pg mmRNA/mm² of colony. Scale bar 750µm* ***B.*** *Comparison between transfection efficiency of hiPS colonies in conventional 24-well plate and microfluidic device without (grey bars) and with EDTA (black bars).* ***C.*** *Transfection efficiency of colonies pretreated with EDTA both in conventional culture (cyan bars) and microfluidic device (blue bars). n=3; error bars indicate SEM. Data made in collaboration with Dr. Torchio E [181] .*

These findings indicate that not only the EDTA pretreatment allowed a more homogeneous transfection of hiPS colonies with a diffuse protein expression but also the use of the microfluidic platform for mmRNA transfection determined an increase in the transfection efficiency when compared with conventional cell culture systems, as shown in the graphs of transfection efficiency related to the quantity of mmRNA used. Moreover, the same

efficiency was reached in microfluidics using approximately 10- fold lower amount of mmRNA.

To describe at best the optimization performed to obtain such results, a list of key features are listed:

- Robust microfluidics for high transfection efficiency;
- Platform compatibility for mmRNA delivery;
- Scale down of minimum requirements.

Thanks to these characteristics, the platform fabricated in our BioERA laboratory has the potential to become a tool for programming cardiac hPSCs fate, allowing a precise modulation of mmRNA-encoding cardiac TFs delivery to better mimic the processes observed in developmental studies on cardiogenesis. The next step, in fact, is the cardiac programming of hPSCs via the administration of cardiac mmRNAs.

4.6. Part 1: mmRNA-induced overexpression of cardiomyogenic TFs.

Although the mmRNA technology is still in its infancy and very few works are reported in literature, the use of mmRNA is endowed with a number of properties. These properties include the fact that cellular expression of TFs can be modulated on a daily basis, simply by modulating the quantities of mmRNA added to the culture medium. In additon, because of multiple different mmRNAs can be introduced into cells simultaneously, co-expression of multiple proteins can be achieved. Notably, thanks to the transient nature of protein expression mediated by mmRNA it will be possible to activate specific developmental programs[49].

In this thesis, the cardiac programming of hPSCs fate was divided in 2 parts, each one carried out by testing two strategies in parallel. The Part 1, with the related strategies, is illustrated in Figure 4.10 A-C. Control cells were represented by CMs differentiated with the gold standard protocol (described in Chapter 2) based on Wnt pathway modulators, without mmRNA (Figure 4.10 A). The first strategy (Figure 4.10 B) relied on the complete Wnt/β-catenin pathway perturbation with the timed application of CHIR99021 (indicated in the green box) and IWP4 (indicated in the red box) on day 0 and 3 respectively, coupled to 6 days of transfection with the 6 cardiac TFs mmRNAs, while the second one (Figure 4.10 C) was based on the only CHIR99021 administration coupled to mmRNA

transfection, to test the ability of mmRNA to influence CMs formation. The unique variable was the presence or absence of IWP4 molecule; for convenience, the first strategy was named WNT OFF+mmRNA, whereas the second one WNT ON+mmRNA.

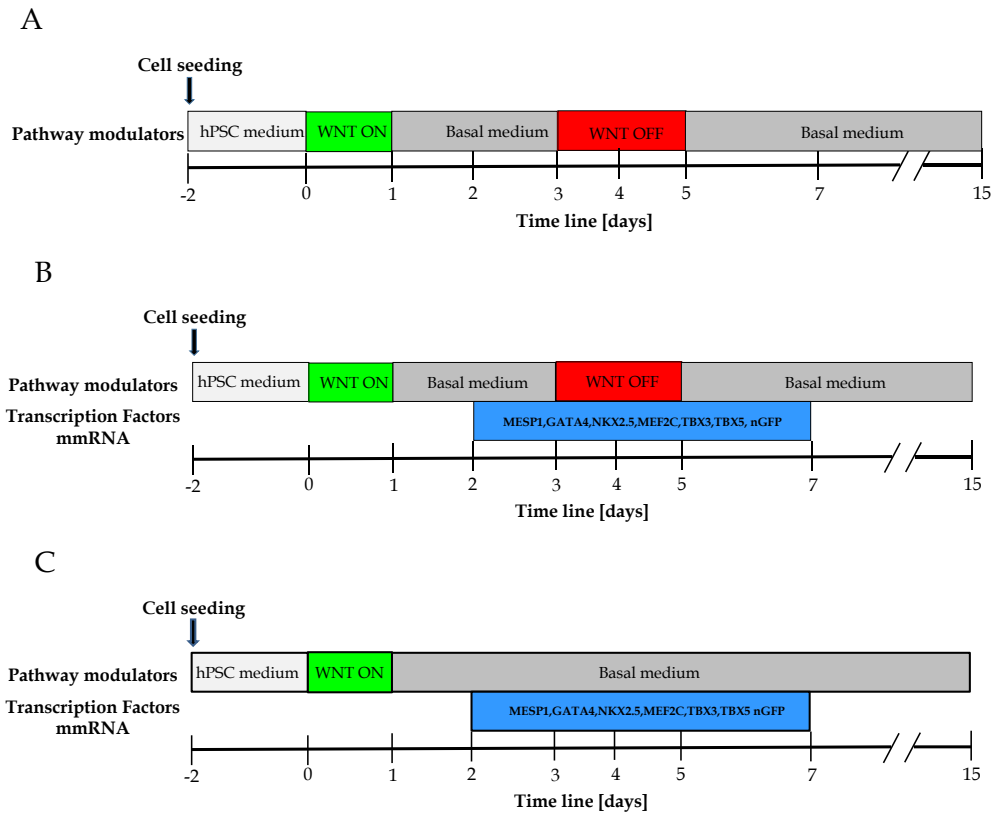

Figure 4.10: *Schematic representation of the two strategies applied in parallel.* ***A.*** *Control platform in which cells were differentiated with the only gold standard protocol with small molecules modulating Wnt/β-catenin pathway.* ***B.*** *Strategy WNT OFF+mmRNA in which the complete Wnt/β-catenin pathway perturbation with CHIR99021 and IWP4 was coupled to mmRNA transfections for 6 days.* ***C.*** *Strategy WNT ON+mmRNA in which only CHIR99021 was administered, in combination with Cardio mix transfections for 6 days.*

For a better understanding, the details of each condition tested with the related acronyms, are reported in Table 4.4.

Table 4.4: *Part 1 experimental conditions*

CTRL	WNT OFF mmRNA	WNT ON mmRNA
Complete Wnt pathway perturbation (**CHIR99021+IWP4**)	Complete Wnt pathway perturbation (**CHIR99021+IWP4**) associated to mmRNA	Only Wnt activation (**CHIR99021**) associated to mmRNA

For the delivery of cardiac mmRNAs, 2 commercial transfection kits were used, StemMacs™ (Miltenyi) and Stemfect® (Stemgent), as already mentioned in Paragraph 4.5. The 6 mmRNAs encoding cardiac TFs were manufactured and provided by Miltenyi Biotec (Germany); as indicated by the datasheet, each mmRNA was diluted at a final concentration of 100ng/µl in RNAse free water (Miltenyi Biotec). When preparing the Cardio mix, the equimolar ratios of MESP1, GATA4, NKX2.5, MEF2C, TBX3, TBX5 and nGFP were 1 : 2 : 1,5 : 1,5 : 2 : 1 respectively. The medium used during the cardiac programming of hPSCs was RPMI with (until day 7) and without insulin (until day 15), supplemented with B18R 4 hours prior to transfections and added fresh every day throughout the experiment. Regarding the experimental procedure, hES Dual reporter line and hiPS Clone 7 were expanded in conventional 6-well plates and then seeded in the microfluidic platform at a density of 700cells/mm^2. Notably, a high seeding density was used since the switch from hPSC medium to RPMI and the exposure to CHIR99021 (10µM) for 24h can cause cell death and/or detachment, as suggested by Lian X. and co-workers in 2012 [63][64]. Preliminary experiments were performed associating simultaneously the application of CHIR99021 with the transfection regimen; however this approach was withdrawn because determined a high mortality of cells. Moreover, since the early cardiac gene MESP1 peaks on day 2-3, activating the cascade of the other TFs, the mmRNAs delivery was initiated on day 2. To avoid stressful events for the cells, a transfection dose ramping of medium for the dilution of the transfection mix was always performed, as reported in the Table 4.5:

Table 4.5: *Transfection dose ramping.*

Transfection dose-ramp	
Transfection days	**Medium/Cardio Mix [%]**
Day 1	Middle dose (50/50%)
Day 2	High dose (25/75%)
Day 3	
Day 4	
Day 5	
Day 6	Middle dose (50/50%)

Cells were transfected for 6 consecutive days for 4 hours, in accord with the datasheet, until day 7 of cardiac differentiation. The cardiac differentiation was monitored daily and the transfection efficiency was assayed through the reporter mmRNA for nGFP. Cells were then maintained in basal medium supplemented with insulin and finally, on day 15 they were characterized by functional and molecular assays.

4.7. Part 1: analysis of the transfection efficiency and CMs characterization

As explained in the previous paragraph, the transfections started on day 2 of cardiac differentiation. During the entire experiment, the change of cell morphology and the transfection time course were monitored and recorded daily and a summarizing panel is reported in Figure 4.11.

For the sake of simplicity, since the unique difference between the two strategies tested is the presence or absence of Wnt OFF (IWP4), the inscription "WNT OFF + "is adopted for the complete Wnt/β-catenin pathway perturbation associated to mmRNA transfections whereas "WNT OFF – " is indicated for the only CHIR99021 administration coupled to mmRNAs delivery in all the pictures and graphs presented.

A

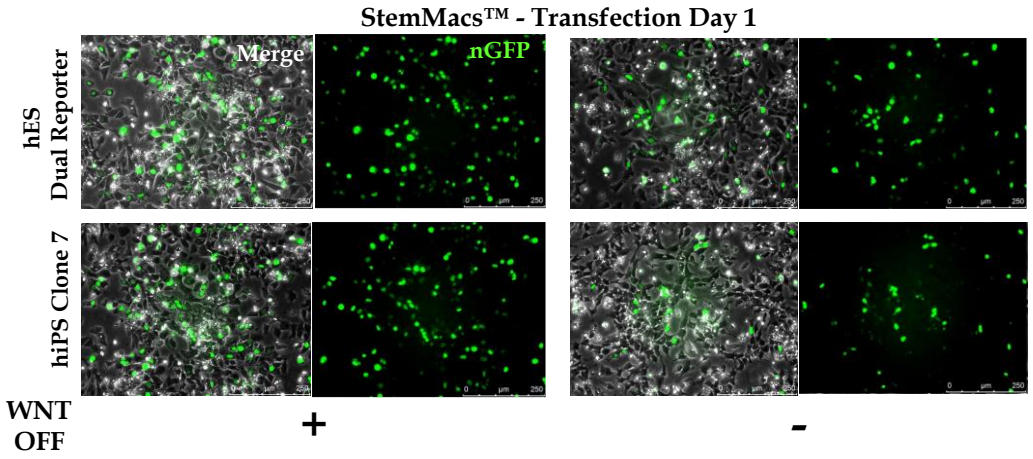
StemMacs™ - Transfection Day 1
Merge
nGFP
hES Dual Reporter
hiPS Clone 7
WNT OFF
+
-

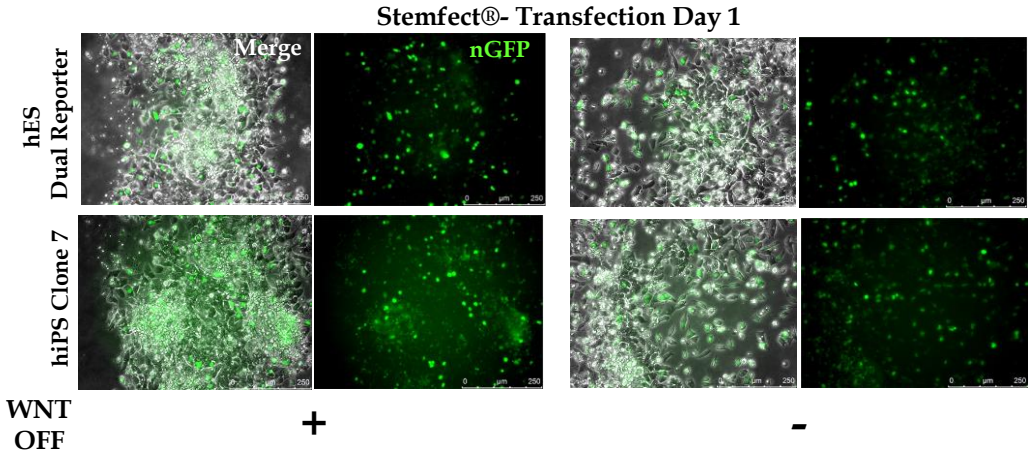
Stemfect®- Transfection Day 1
Merge
nGFP
hES Dual Reporter
hiPS Clone 7
WNT OFF
+
-

B

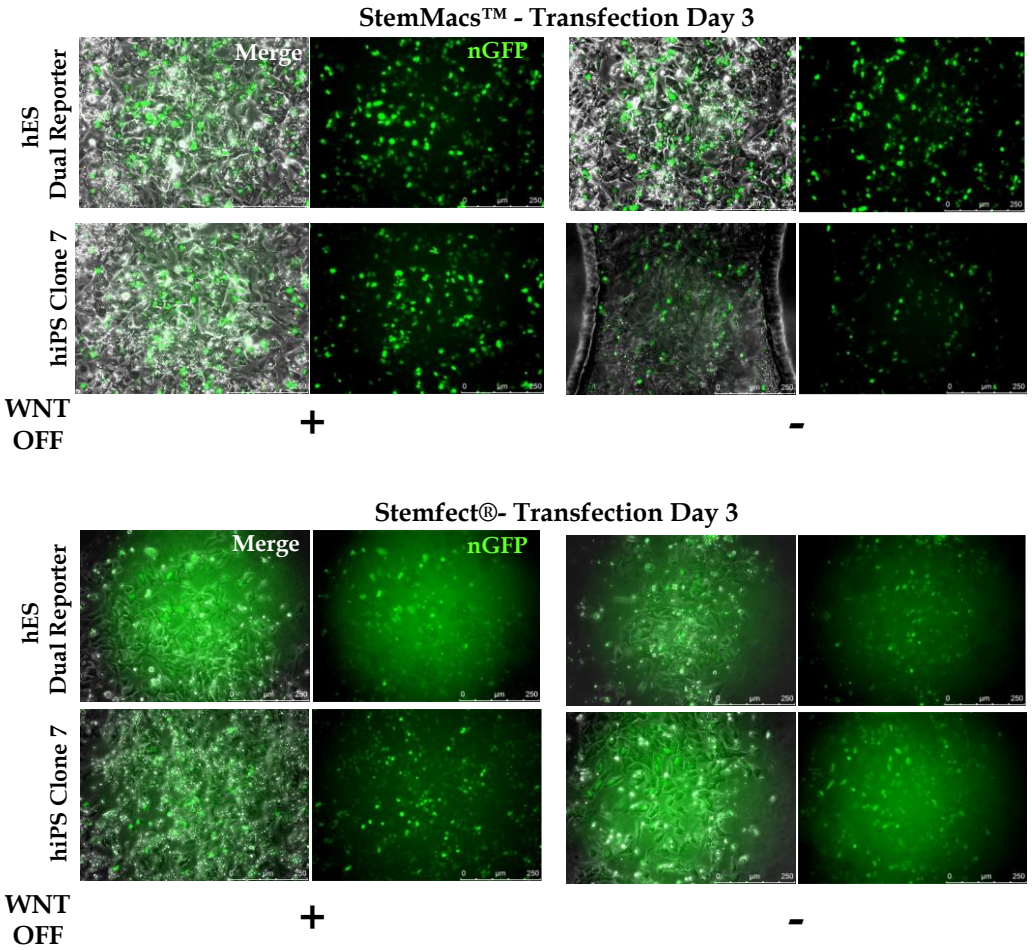
StemMacs™ - Transfection Day 3
Merge
nGFP
hES Dual Reporter
hiPS Clone 7
WNT OFF
+
-
Stemfect®- Transfection Day 3
Merge
nGFP
hES Dual Reporter
hiPS Clone 7
WNT OFF
+
-

C

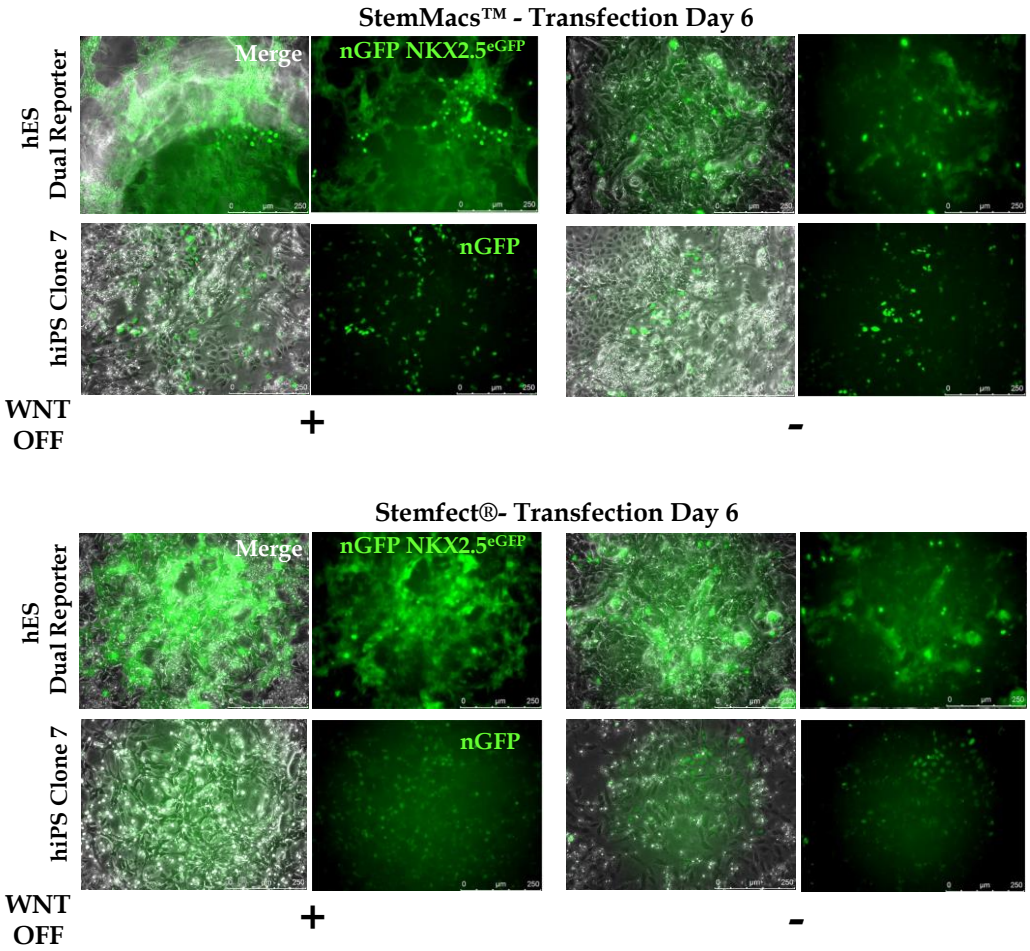

Figure 4.11: *hPSCs programming with mmRNA Cardio mix TFs. The transfection time course was monitored through the expression of nGFP mmRNA in cells seeded at a density of 700cells/mm². **A**, **B** and **C** represent the transfection monitoring on day 1, 3 and 6 respectively, comparing the two transfection kits, StemMacs™ (SM) and Stemfect® (SF) and the two strategies WNT OFF (+) and WNT ON (-) coupled to mmRNA delivery.*

The efficiency of transfection was then calculated and the results are reported in the graphs of Figure 4.12.

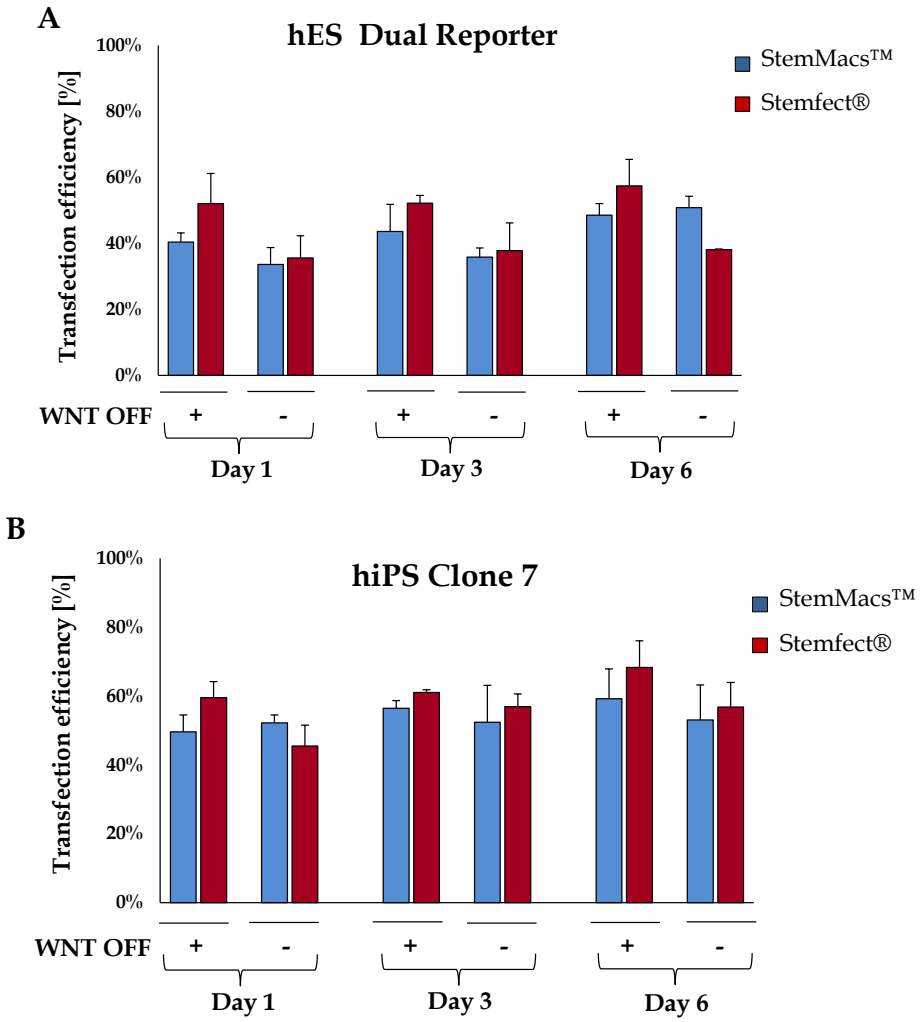

Figure 4.12: *Percentage of transfection efficiency on day 1, 3 and 6 of hES Dual reporter (**A**) and hiPS Clone 7 (**B**) transfected with SM (blue bars) and SF (red bars) and differentiated with the association of WNT OFF and WNT ON. (n=3; error bars indicate SEM).*

From the pictures of the time lapse in Figure 4.11, it is evident that the nGFP signal was more intense when using SM transfection kit. As shown in the graphs of Figure 4.12, SF presented a slightly higher efficiency than SM but these results indicate that both the transfection kits were suitable for repeated mmRNAs delivery in hPSCs showing an increasing in the number of transfected cells. Moreover, to verify a possible toxic effect due to transfection kit and/or to the transfection itself, a LIVE & DEAD cell viability assay (L&D; Invitrogen) was performed after the first transfection. This kit quickly

discriminates live from dead cells by simultaneously staining with green-fluorescent calcein-AM, to indicate intracellular esterase activity, and red-fluorescent ethidium homodimer-1, to identify loss of plasma membrane; Figure 4.13 showed the results obtained from both SM and SF. As demonstrated by this viability assay, no cell mortality nor toxicity were observed. In fact, only few cells were positive to ethidium while the red signals detected were predominantly cell debris.

A

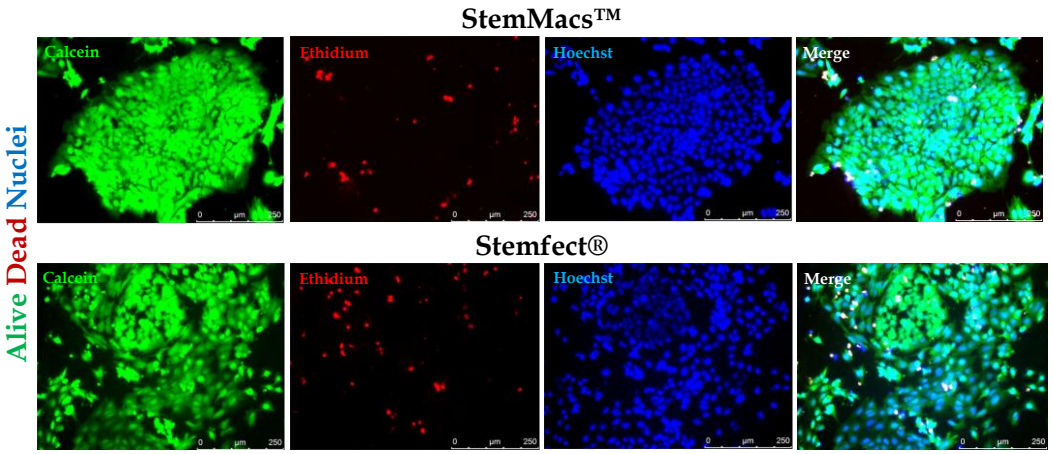

B

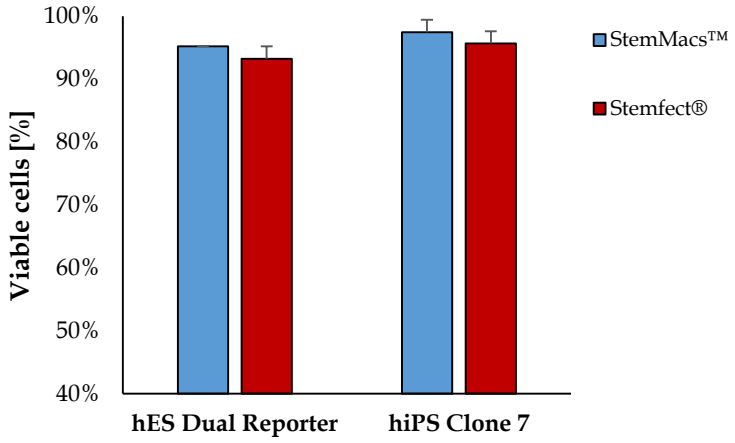

Figure 4.13: A. *Representative picture of L&D cell viability assay on hES Dual Reporter and hiPS Clone 7 after the first transfection, comparing SM and SF transfection kit. Green-fluorescent calcein represents alive cells while red-fluorescent ethidium represents dead cells.* ***B.*** *Mortality quantification by count of ethidium bromide stained nuclei (n=3; error bars indicate SEM).*

During the cardiac differentiation, the temporal expression of MESP1 and NKX2.5 in hES Dual Reporter line was monitored and in transfected cells

MESP1^{mCherry} was detectable on day 2-3 while in non-transfected control cells it appeared one day later, on day 3. NKX2.5^{eGFP} signal, as already reported in the transfection time course of the panel in Figure 4.11, started on day 5-6 whereas in control cells it was observed only on day 8-9, as previously demonstrated in Chapter 3. In Figure 4.14 is reported the expression monitoring of the two cardiac TFs in control cells and transfected hES Dual Reporter, together with the negative control for the GFP signal in hiPS Clone 7 (A-C); the contraction detection in hiPS Clone 7 is reported in D.

A

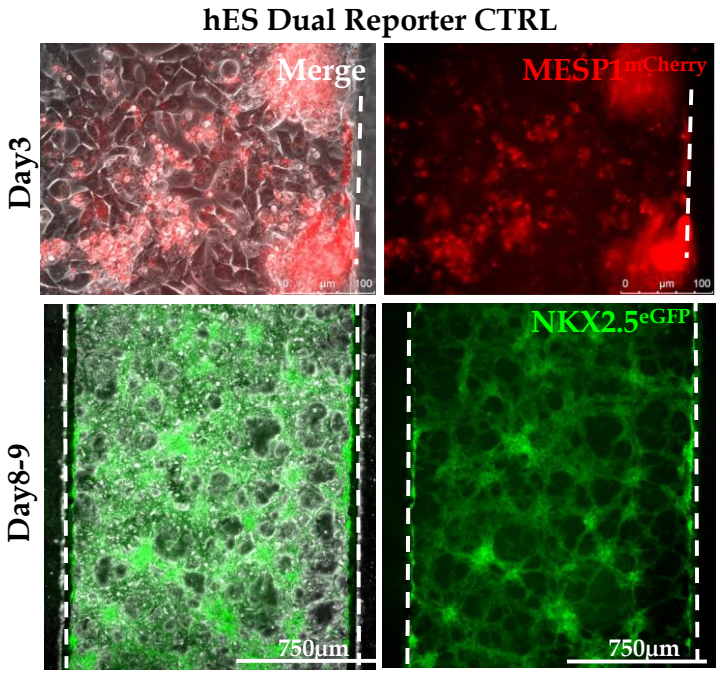

B

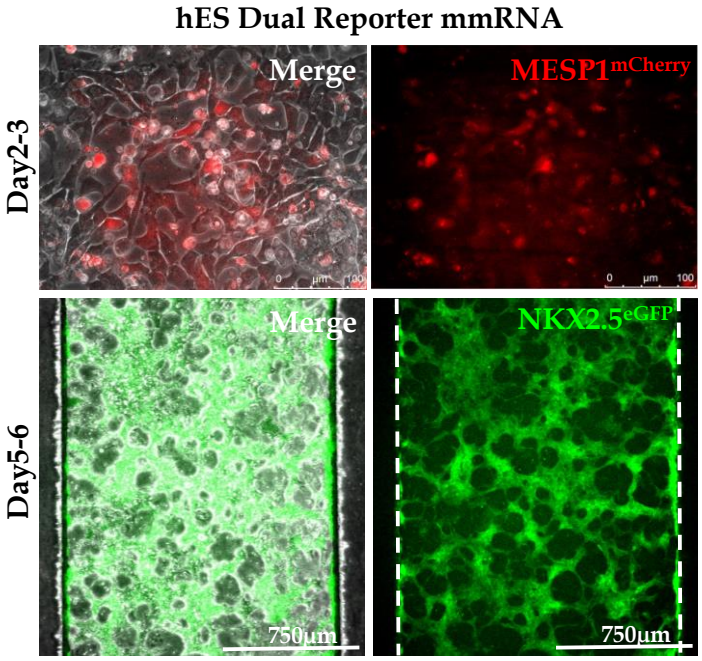
hES Dual Reporter mmRNA
Day2-3
Merge
MESP1mCherry
Day5-6
Merge
NKX2.5eGFP
750µm
750µm

C

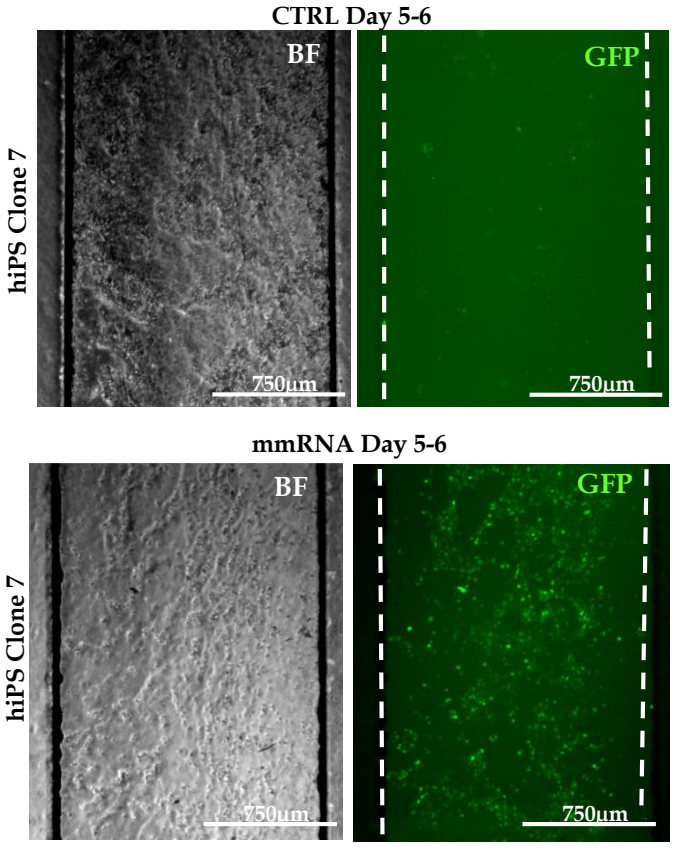
CTRL Day 5-6
hiPS Clone 7
BF
GFP
750µm
750µm
mmRNA Day 5-6
hiPS Clone 7
BF
GFP
750µm
750µm

D

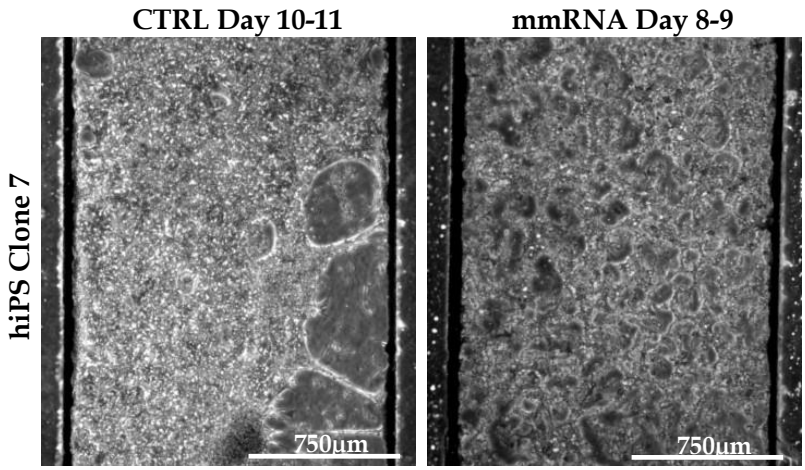

Figure 4.14: *hES Dual Reporter TFs expression monitoring.* ***A.*** *Exemplificative pictures of MESP1^{mCherry} expression recorded on day 3 and NKX2.5^{eGF} (video frame shot) expression on day 8-9 in control (CTRL) non-transfected cells.* ***B.*** *MESP1^{mCherry} expression on day 2-3 and NKX2.5^{eGFP} expression (video frame shot) on day 5-6 in transfected cells (mmRNA).* ***C.*** *Negative control for GFP signal in hiPS Clone 7 to compare the GFP signal associated to NKX2.5 expression in the hES Dual Reporter.* ***D.*** *Video frame shots of the central section of microfluidic channel of contracting hiPS Clone 7 (control CTRL, and transfected mmRNA); dotted lines represent channel edges.*

The first contractions started to became evident 3 days earlier in transfected cells, approximately on day 8-9 while in non transfected control cells they were recorded only on day 10-11, both in hES Dual Reporter and hiPS Clone 7 (Figure 4.14). These findings indicated a possible role of cardiac mmRNA on protein expression.

CMs obtained from both cell types were characterized for nuclear and structural cardiac markers through classical immunofluorescence protocol (the panels are reported in Paragraph 4.11.1, Figure 4.25) and were also quantified by counting the cTnT^{+ve} cells in every microchannel. Figure 4.15 shows the tile scan immunofluorescence staining against cTnT in microfluidic channels while the results from the quantification of troponin T positive cells are summarized in the graphs of Figure 4.16 with the related tables reporting the percentage of CMs obtained from every tested condition.

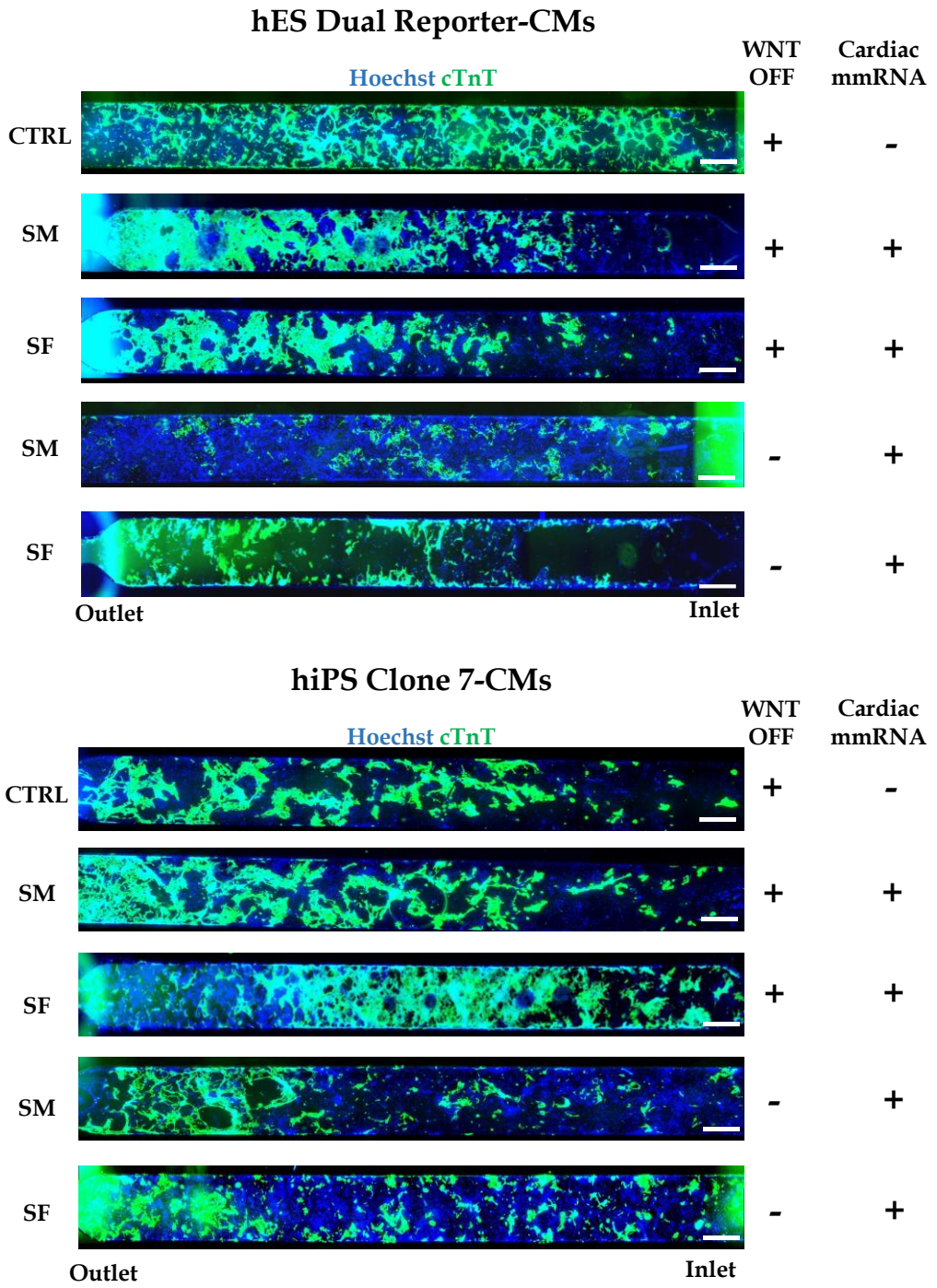

Figure 4.15: *Immunofluorescence staining for cTnT (green) in CMs obtained from hES Dual Reporter (upper panel) and hiPS Clone 7 (lower panel) differentiated in the microfluidic platform. Nuclei were counterstained with Hoechst. The differentiation conditions are reported to the right while to the left are indicated the control cells (CTRL) and the transfection kit tested (SM, StemMacs™; SF, Stemfect®). Scale bar=100µm.*

A

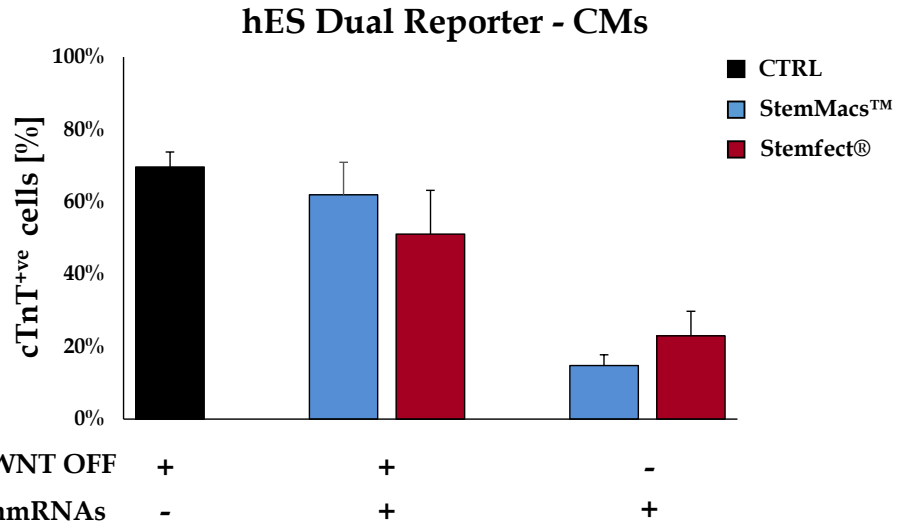

hES Dual Reporter-CMs	cTnT^{+ve} cells [%]	
CTRL	74±4%	
Cardiac mmRNAs	StemMacs™	Stemfect®
WNT OFF mmRNA	62±9%	51±12%
WNT ON mmRNA	15±3%	23±7%

B

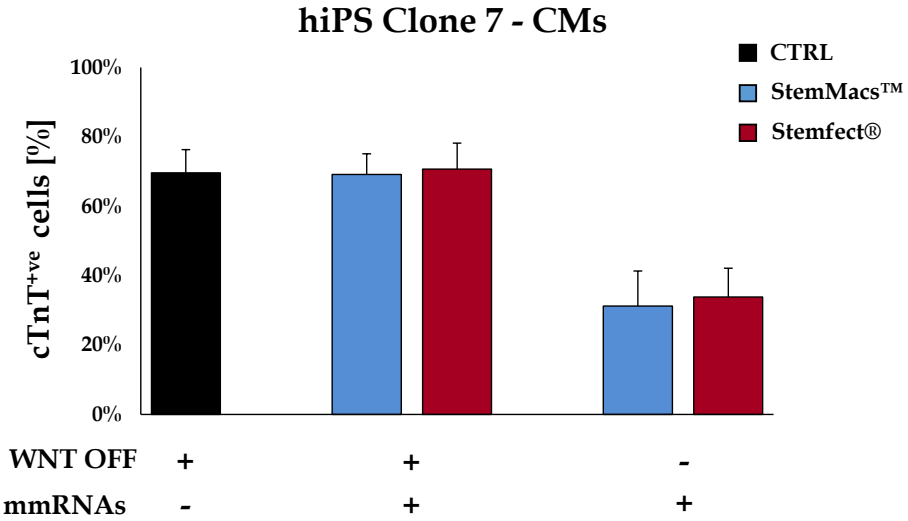

hiPS Clone 7-CMs	cTnT^{+ve} cells [%]	
CTRL	70±7%	
Cardiac mmRNAs	StemMacs™	Stemfect®
WNT OFF mmRNA	69±6%	71±8%
WNT ON mmRNA	31±10%	34±8%

Figure 4.16: *Percentage of cTnT positive CMs obtained with Wnt/β-catenin pathway modulators and cardiac mmRNA delivered with SM (blue bars) and SF (red bars) compared with control CMs obtained with Wnt modulators alone (black bars); n=3; error bars indicate SEM.*

From immunofluorescence panels of Figure 4.15, it is evident that, in some cases, both in transfected as well in non-transfected control cells there is a gradient-like distribution of CMs within the channels, especially concentrated close to channel outlet; this was probably due to medium flow, nutrients and reagents concentration at this level, stagnant in medium reservoirs with subsequent incomplete medium refresh. In the following experiments, this issue was solved by leaving the medium reservoirs empty after every medium replacement.

Furthermore, the cTnT quantification revealed that cardiac mmRNAs coupled to Wnt perturbation (WNT OFF with mmRNAs) lead approximately to the same CMs yield of control non-transfected cells whereas in cells transfected with mmRNAs coupled to the only CHIR99021 administration (WNT ON with mmRNAs), the $cTnT^{+ve}$ cells were significantly lower. These findings indicate that cardiac mmRNAs alone, cannot replace Wnt modulators in terms of CMs yield but the major goal of this work is to drive cardiac differentiation of hPSCs toward cell maturation. In the Part 2, described in the following Paragraph, a new approach is proposed with a further optimization of the transfection with a more precise adjustment on TFs delivery. Moreover, thanks to the more intense nGFP signal observed when transfecting cells with SM, this transfection kit was adopted for the following experiments.

4.8. Part 2: optimization of cardiac TFs delivery to best mimic cardiac development *in vitro*

From the preliminary data obtained in Part 1, the transfection was further optimized and, taking into account the temporal developmental expression of TFs from studies on cardiogenesis *in vitro* (see Figure 4.5, relying on cardiac TFs waves of expression), a new approach was designed and the set-up is illustrated in Figure 4.17 (A-D).

The complete Wnt/β-catenin perturbation (WNT OFF) and the only CHIR99021 administration (WNT ON) were maintained but the transfection regimen was divided in two stages: the first one was defined the "early stage"in which only MESP1 and GATA4 were administered for the first 3 days; during the second "late stage", for the last 3 days of transfection, all the other cardiac TFs were added with the exception of MESP1 because its expression window lasts only 2-3 days. Also in this case, the transfection dose ramp of medium dilution for the Cardio mix was

performed, with the same scheme adopted for the experiments of Part 1: a middle dose was used on day 1 and 6 of transfection while, from day 2 to day 5 a high dose of cardiac TFs was employed to strongly force endogenous protein expression. Two controls were used to compare the effects of mmRNA delivery: the first control was represented by CMs differentiated with the complete Wnt/β-catenin pathway perturbation (WNT OFF) and the second control relied on the only CHIR99021 application (WNT ON). Cells were always seeded at a density of 700cells/mm^2 and the experimental procedure was the same as Part 1.

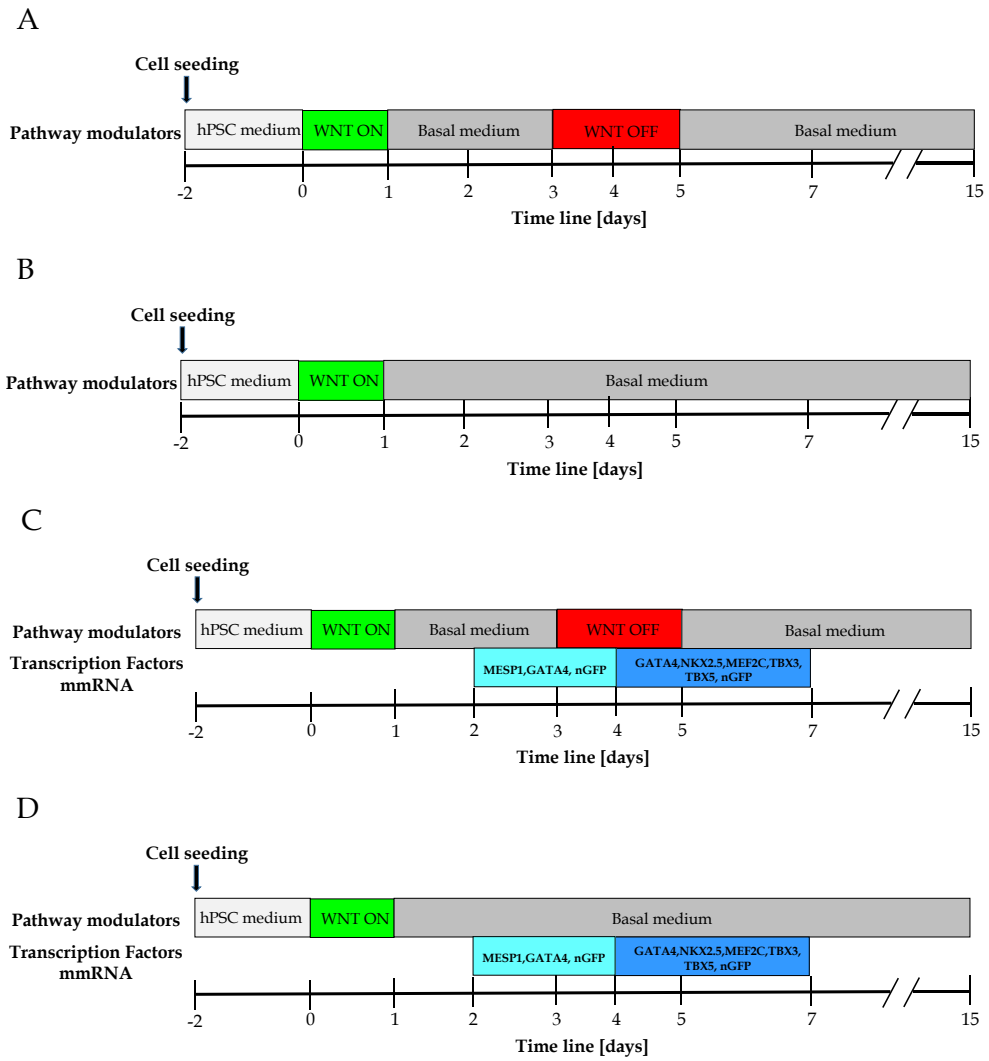

Figure 4.17: *Schematic representation of the optimized delivery of cardiac TFs.* ***A*** *and* ***B****: Control platforms in which cells were differentiated with the gold standard protocol relying on the complete Wnt perturbation (A) or only CHIR99021 administration (B).* ***C*** *and* ***D****. The two strategies tested in parallel in which early stage (MESP1 and GATA4 for the first 3 days) and late stage (GATA4, NKX2.5, MEF2C, TBX3 and 5 for the last 3 days) were associated to complete Wnt perturbation (C) or to CHIR99021 administration (D).*

The details of each condition tested with the related acronyms are indicated in the Table 4.6.

Table 4.6: *Part 2 experimental conditions.*

CTRL WNT OFF	CTRL WNT ON	WNT OFF mmRNA	WNT ON mmRNA
Complete Wnt pathway perturbation (CHIR99021+IWP4)	Only Wnt activation (CHIR99021)	Complete Wnt pathway perturbation (CHIR99021+IWP4) associated to mmRNA	Only Wnt activation (CHIR99021) associated to mmRNA

As already mentioned, for the delivery of cardiac mmRNAs, only StemMacs™ transfection kit was used. At the end of the transfections, cells were maintained in basal medium until day 15 and then, CMs were characterized by functional and molecular assays.

4.9. Part 2: analysis of the transfection efficiency

Since the high transfection efficiency reached with SM transfection kit was already demonstrated in Paragraph 4.7, for convenience, only the pictures of transfection day 6 were reported in Figure 4.18, showing an homogeneous transfection with intense nGFP signal in both hPSCs; in addition, NKX2.5 signal associated to eGFP expression in hES Dual Reporter line was detectable between day 5 and 6, 2-3 day earlier than control cells (Figure 4.20).

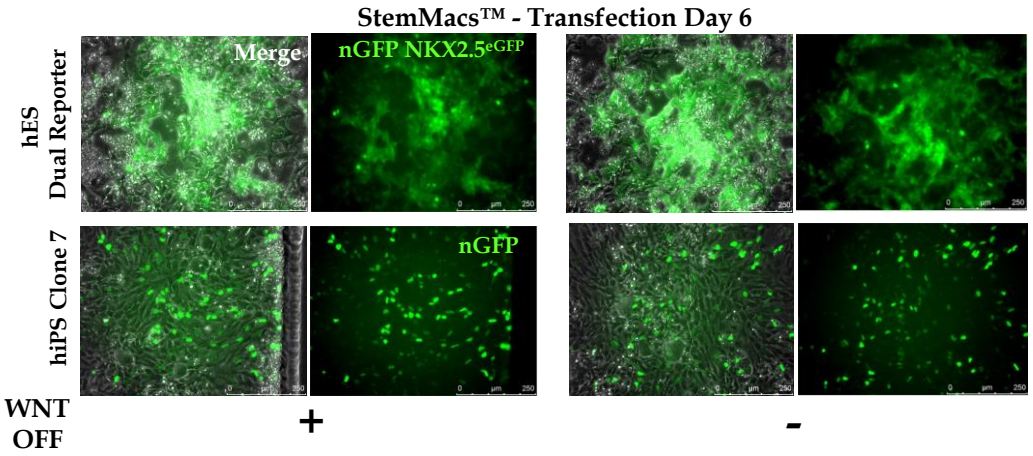

Figure 4.18: *hPSCs programming with early and late stage of cardiac mmRNA delivery using SM transfection kit. Panel of transfection day 6 comparing the two strategies in parallel, WNT OFF (+) and WNT ON (-) coupled to mmRNA transfections.*

Notably, from this panel, also hES Dual Reporter, differentiated with CHIR99021 associated to mmRNA delivery (WNT ON) showed a wide NKX2.5^{eGFP} signal, compared with the panels of Part 1. The percentage of transfection efficiency was reported in the graphs of Figure 4.19.

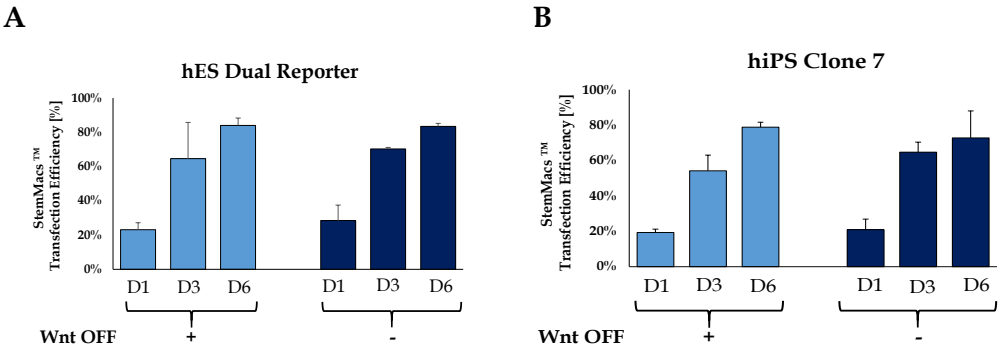

Figure 4.19: *Percentage of transfection efficiency on day 1, 3 and 6 of hES Dual Reporter line* ***(A)*** *and hiPS Clone 7* ***(B)*** *transfected with SM. Light blue bars indicate WNT OFF (+) coupled to mmRNA delivery while dark blue bars indicate WNT ON (-) with mmRNAs; n=3; error bars indicate SEM.*

From these graphs, a high transfection efficiency was reached, increasing day by day, in both hES Dual Reporter and hiPS Clone 7. Also in this case the mCherry signal associated to MESP1 expression in hES Dual Reporter line was monitored and a peak of expression was detected on day 2-3 in transfected cells whereas in control cells it appeared slightly later, on day 3. Representative pictures of MESP1 and NKX2.5 expressing cells together with the negative control for the GFP signal are reported in Figure 4.20 (A-C), with video frame shots of contraction detection in hiPS Clone 7 (D).

A

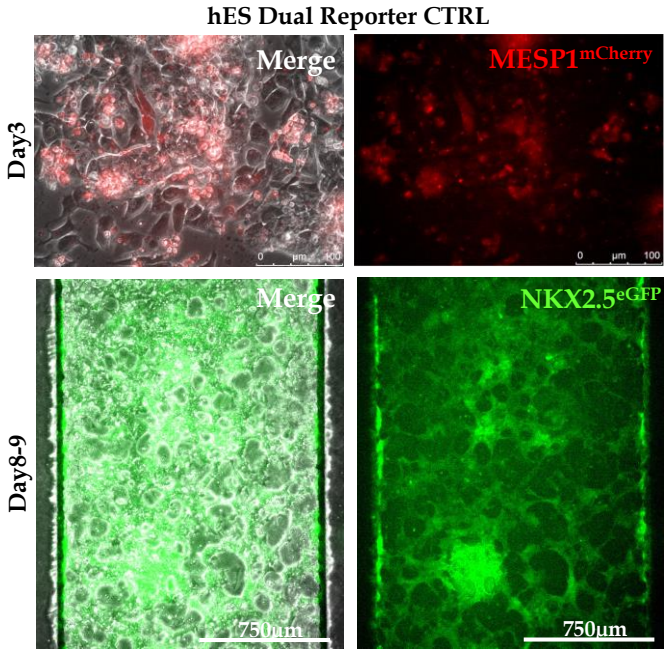
hES Dual Reporter CTRL
Day3
Merge
MESP1mCherry
Day8-9
Merge
NKX2.5eGFP
750µm
750µm

B

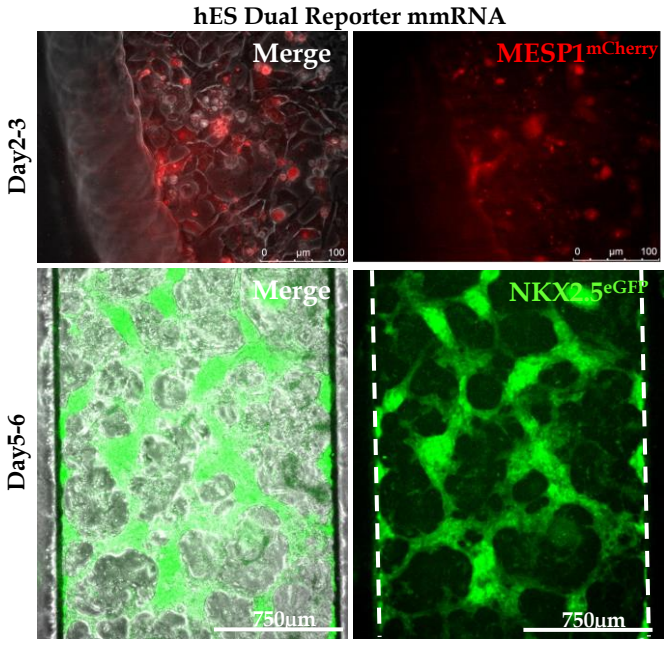
hES Dual Reporter mmRNA
Day2-3
Merge
MESP1mCherry
Day5-6
Merge
NKX2.5eGFP
750µm
750µm

C

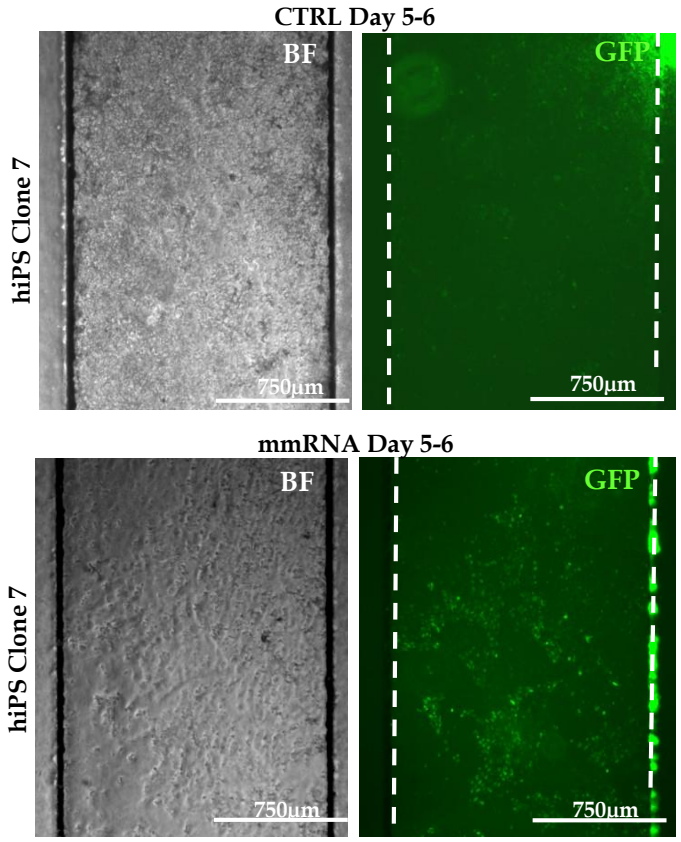

D

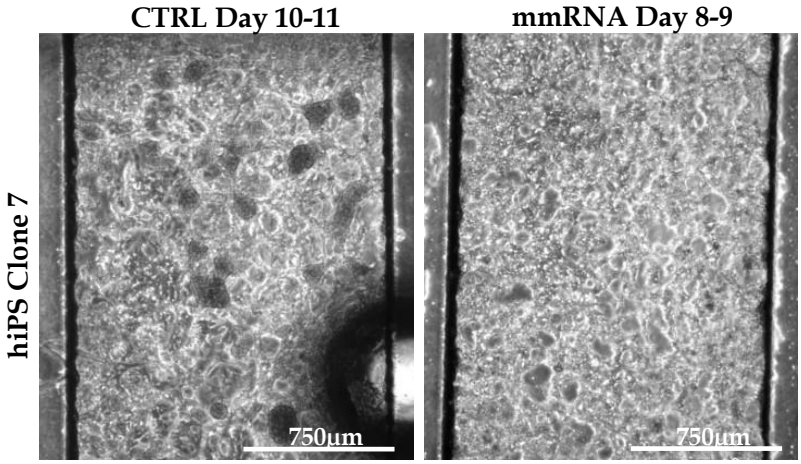

Figure 4.20: *Cardiac differentiation monitoring through the recording of MESP1^{mCherry} and NKX2.5^{eGFP} in control (CTRL) and transfected (mmRNA) hES Dual Reporter-CMs with the negative control for GFP signal in hiPS Clone 7 (**A-C**) and contraction detection in control and transfected hiPS Clone 7 (**D**). hES Dual Reporter NKX2.5 and hiPS Clone 7 pictures are a video frame shots of a central section of microchannel with beating CMs. Dotted lines represent channel edges.*

In Figure 4.21 is reported the tile scan immunofluorescence staining against cTnT performed in the microchannels.

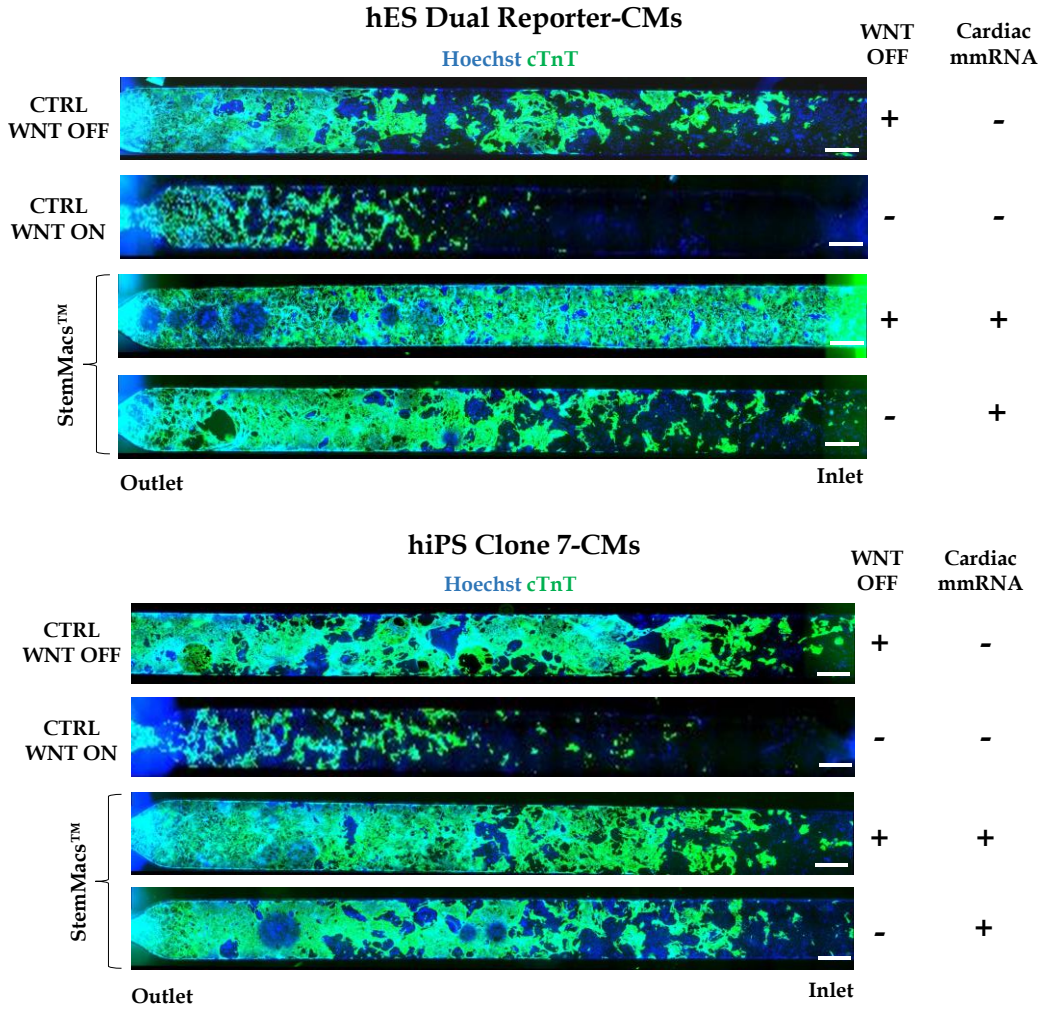

Figure 4.21: *Immunofluorescence staining for cTnT (green) in CMs obtained from hES Dual Reporter (upper panel) and hiPS Clone 7 (lower panel) differentiated in the microfluidic platform. Nuclei were counterstained with Hoechst. The differentiation conditions are reported to the right while to the left are indicated the control cells (CTRL) and the transfection kit tested (StemMacs™). Scale bar=100µm.*

The quantification of cTnT positive cells was reported in Figure 4.22 with the related table summarizing each percentage obtained from every condition tested.

A

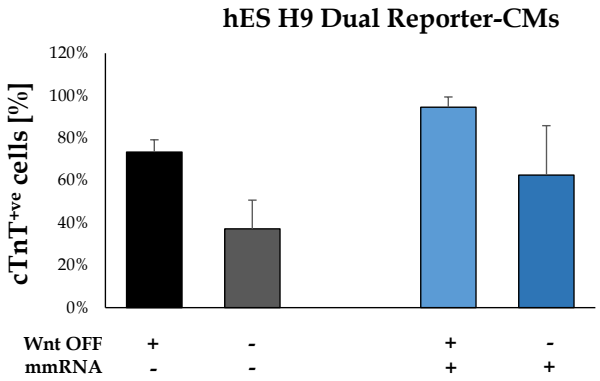

B

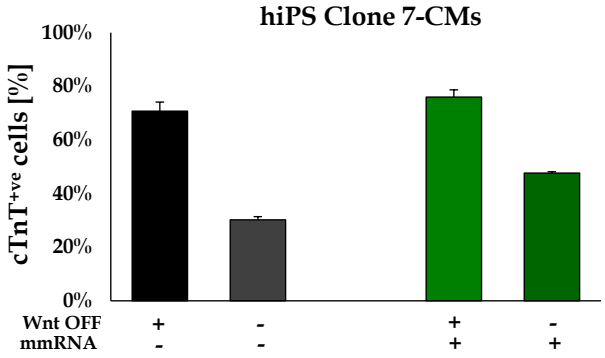

C

	cTnT^{+ve} cells [%]	
	hES Dual Reporter-CMs	**hiPS Clone 7-CMs**
CTRL WNT OFF	73±8%	71±3%
CTRL WNT ON	37±14%	30±1%
WNT OFF mmRNA (SM)	95±5%	76±3%
WNT ON mmRNA (SM)	63±23%	48±1%

Figure 4.22: *Percentage of cTnT^{+ve} cells obtained combining Wnt pathway modulators with early and late cardiac mmRNA delivery (**A.** hES Dual Reporter-CMs: light blue bars for WNT OFF mmRNA, dark blue bars for WNT ON mmRNA; **B.** hiPS Clone 7-CMs: light green bars for WNT OFF mmRNA, dark green bars for WNT ON mmRNA) with StemMacs (SM) compared with control CMs obtained with the only WNT OFF (black bars) or WNT ON (grey bars). In **C** is reported a summarizing table of cTnT percentages; n=3; error bars indicate SEM.*

Notably, from the quantification of cTnT^{+ve} CMs it is evident that this experiment gave a high yield of CMs in cells transfected with the optimized delivery of mmRNA with early and late cardiac TFs, both in presence or absence of Wnt inhibitor (WNT OFF and WNT ON) while, in control cells, the cTnT^{+ve} cells, the yield was lower. Moreover these results, compared with those

obtained in Part 1 are encouraging because with this TFs modulation it was possible to increase the number of CMs obtained by a partial modulation of Wnt pathway, indicating a clear effect of mmRNAs on protein expression. These findings give hope for further optimization of cardiac TFs delivery for cardiomyocytes generation from hPSCs without small molecules.

4.10. Calcium handling regulation in hPSC-derived CMs

4.10.1. Functional characterization of calcium handling in mmRNA-derived CMs

Although the discovery of hiPS derivation technology pioneered by Takahashi and Yamanaka in 2006 and 2007[43][44] lead to the development of a wide variety of cardiac differentiation procedures (as described in Chapter1 and 2), few works reported the description of the functional hPSC-CMs properties with information about their excitation-contraction (E-C) coupling and Ca^{2+} handling properties [182][183]. For this reason, a characterization of the functional nature of CMs obtained from both hES and hiPS is necessary to understand the degree of maturity, before the employment of hPSC-CMs in the emerging field of regenerative medicine. This depends in part on the status of the CMs contractile features and their Ca^{2+} handling dynamics. As already explained in Paragraph 1.1 of Chapter 1, intracellular calcium transients, the cyclic variations in the concentration of cytosolic Ca^{2+}, play a crucial role in the Excitation-Contrction (E-C) coupling, as a result of a spatio-temporal balance between cytosolic Ca^{2+} increase and Ca^{2+} re-uptake by the sarcoplasmic reticulum (SR). In adult CMs, the Ca^{2+}-induced Ca^{2+}release (CICR), starts with a relative small Ca^{2+} influx through the sarcolemmal L-type Ca^{2+} channels that triggers a higer Ca^{2+} release from SR *via* type-2 ryanodine receptor (RyR2). Once recycling the majority of cytosolic Ca^{2+} back to the SR by the SR Ca^{2+}-pump ATPase (SERCA2a) and a small portion of cytosolic Ca^{2+} extruded from the sarcolemma by Na^{2+}- Ca^{2+} exchabger (NCX), a decrease of intracellular [Ca^{2+}] occurs, determining the subsequent myocardial relaxation [183]. However, in literature it has been reported that both hES and hiPS-derived CMs exhibit a fetal and immature calcium dynamics due the underdeveloped SR and the immature expression profiles of proteins involved in calcium handling machinery. Such immature status represents the major concern for the clinical application of these CMs and can leads not only in poor host-graft

electromechanical integration when transplanted, but also leads to lethal arrhythmias [184].

In light of these considerations, at Venetian Institute of Molecular Medicine (VIMM) of Padova, the intracellular calcium pattern dynamics were investigated and recorded under confocal microscope, using a specific Ca^{2+} probe, to investigate an improvement in organization of cardiac structural, functional and maturation features in 15 days mmRNA-derived CMs from hES Dual Reporter line, obtained with the optimized delivery of cardiac TFs described in Part 2. This experiment was performed in collaboration and according with the protocol described by our colleague of BioERA laboratory, Martewics S. who published a work in 2012 regarding the study of CMs calcium dynamics [185].

Briefly, confocal calcium measurements were performed by loading CMs in serum-free 25mM HEPES D-MEM (Life Technologies), supplemented with 2,5μM fluorescent calcium binding dye Fluo-4 AM (Life Technologies). To increase its liposolubility and facilitate the crossing of cell membrane, Fluo-4 was loaded as an acetyl-methyl ester, in presence of 2μM Pluronic F-127 (Invitrogen) as a mild detergent, for 20 minutes at 37°C. Cells were then incubated for additional 10 minutes at 37°C without Fluo-4 for a complete de-esterification of the dye. 20 μM of the anionic transporter inhibitor sulphinpyrazone (Sigma Aldrich) was added in all the media used to limit the dye active extrusion from the cells. As red cell membrane counterstain, 0,2 μM di-8-ANEPPS (Invitrogen) was used in order to distinguish separate cells. Calcium dynamics were acquired in recording solution containing: NaCl 125mM; KCl 5mM; Na_3PO_4 1mM; $MgSO_4$ 1mM; HEPES 20mM; $CaCl_2$ 2mM; glucose 5,5mM, adjusted to pH 7,4 with NaOH (all from Sigma Aldrich). Line scans were acquired with a Leica TCS SP5 confocal microscope equipped with a 63X, 1,4 NA oil immersion objective, with 488nm Ar laser line as an excitation source, 400Hz frequency. To avoid or reduce dye photo-bleaching and phototoxic effects on CMs, the laser power was set at minimum possible. All the experiments were conducted at room temperature within 20-30 minutes from the end of the loading procedures described previously. With this configuration, when Ca^{2+} concentration increases inside the cell, Fluo-4 molecules bind to the ion and emit a fluorescent signal. The increasing (calcium release phase) and decreasing (calcium re-uptake phase) fluorescent signal emitted by the analyzed CMs was recorded for few seconds. Figure 4.23, shows a representative plot of the variation of the intensity signal along time,

providing the shape of the calcium transient from which it is possible to determine these parameters: for the calcium release phase, the time to peak (TTP) value was calculated considering the time that the transient takes to go from the baseline value to the peak of fluorescence intensity; for the evaluation of the calcium re-uptake rate, the half-life of calcium decay rate was used indicating the time that the descending part of the transient takes to go from the peak of fluorescence to a value of 50% of the peak. In the same figure are reported the data acquired from CMs obtained from the hES Dual Reporter line displaying cardiac-like calcium transient. To perform such analysis, cells were differentiated in a microfluidic device containing only 3 or 4 channels in a glass slide of 0,1mm thickness, compatible with confocal microscope equipment. All data handling and computation was performed with Origin 8.1 software.

Intriguingly, as shown in the graphs of Figure 4.23 C, calcium transients significantly shortened ($P<0,001$ and $P<0,01$) in cells differentiated with Wnt modulators (WNT OFF) associated with the optimized delivery of cardiac mmRNA using StemMacs™ transfection kit compared with control cells differentiated with the only application of Wnt modulators. Also in CMs obtained with the WNT ON approach and transfected with cardiac mmRNA the transient is shorter but no significant difference was observed, compared with control cells. These findings clearly demonstrate that the combination of Wnt modulators with the optimized delivery of cardiac mmRNA, that more closely recapitulate the temporal TFs expression observed during cardiac development, can influence CMs intracellular calcium patterns, indicating an improvement in cardiac functional and maturation features.

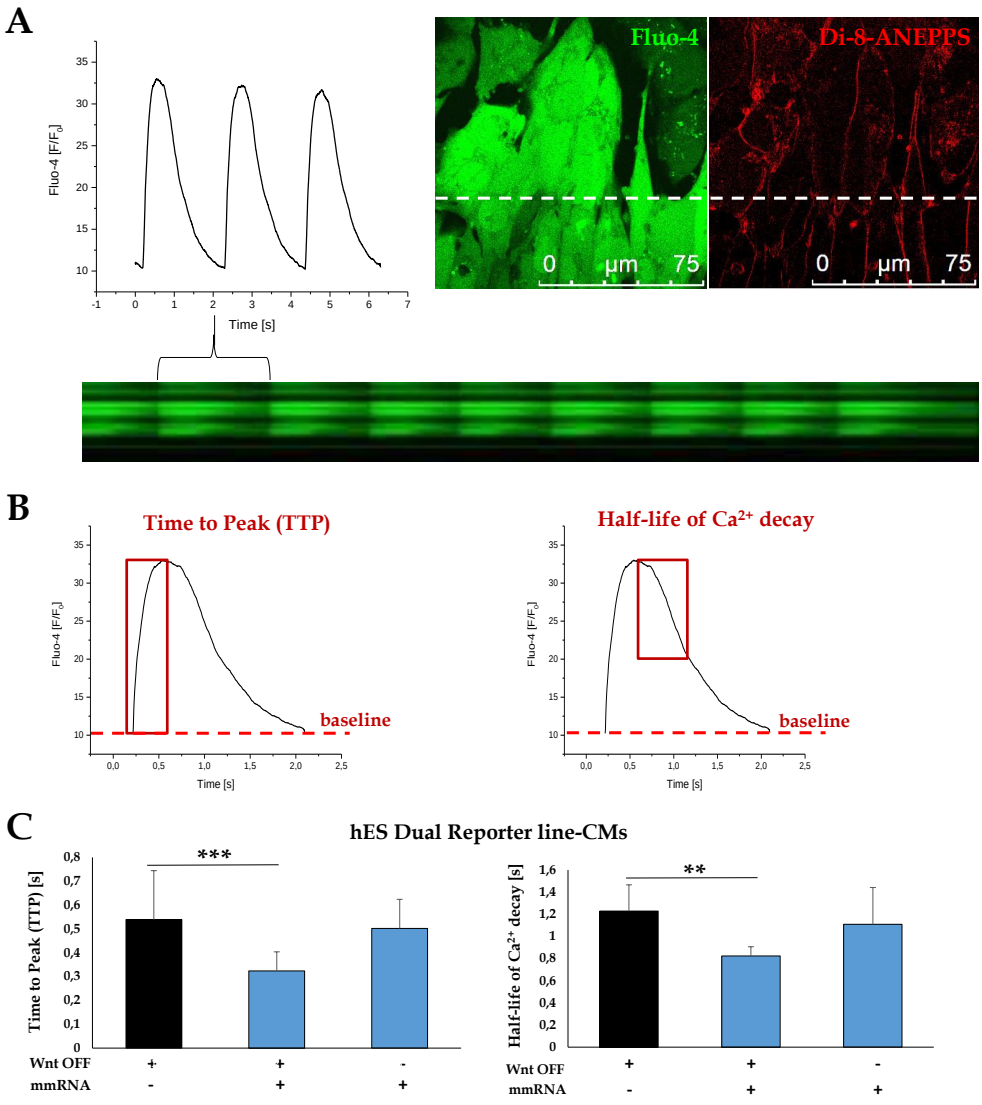

Figure 4.23: *Calcium handling in hES Dual Reporter.* ***A.*** *Representative Ca^{2+} transient profile reporting the fluorescence ratio (F/F_0) versus time (s) with the line scan acquisition of the variation of Fluo-4 intentsity due to cell contraction and relaxation along time (left panel with the plot at the bottom). Representative picture of CMs loaded with Ca^{2+} Fluo-4 (green) allowing the detection of intracellular calcium and cell membranes counterstain with di-8-ANEPPS (red) to distinguish, in this case (dotted lines), 5 separate cells.* ***B.*** *From such curves it is possible to evaluate the time to peak (TTP) and half-life of calcium decay.* ***C.*** *Time to peak (TTP) estimates (left graph) and evaluation of the calcium re-uptake by the half-life of Ca^{2+} decay (right graph) in hES Dual Reporter-CMs differentiated with the association of complete (WNT OFF) or partial (WNT ON) Wnt perturbation with the optimized delivery of cardiac mmRNAs with StemMacs™ (SM, blue bars) compared to control CMs obtained only with the complete Wnt perturbation (black bars). Abbreviations: F/F_0 fluorescence (F) normalized to baseline fluorescence (F_0). Data are presented as mean and error bars represent SEM. Data pairs were compared by Student's t-test. Student's t-test p-values: P<0,001 (***) and P<0,01 (**).*

This increased calcium handling ability, with calcium transient lasting less than 1 second, typical of calcium cycling during contraction, is consistent with maturing CMs features. Moreover, as reported in literature [185][186], the Ca^{2+}

cycling is orchestrated by several molecular components that cooperate for the generation of the Ca^{2+} transient profile. A key element of calcium handling machinery, responsible of the Ca^{2+} re-uptake phase is the cardiac-specific sarcoendoplasmic reticulum calcium ATPase SERCA2. Starting from these observations, CMs obtained by combining Wnt modulators with the optimized delivery of cardiac mmRNA were characterized by immunofluorescence staining to investigate the expression of SERCA2 and a representative picture is reported in Figure 4.24, in association with a co-staining against cTnT showing the sarcomeric organization in the contractile apparatus.

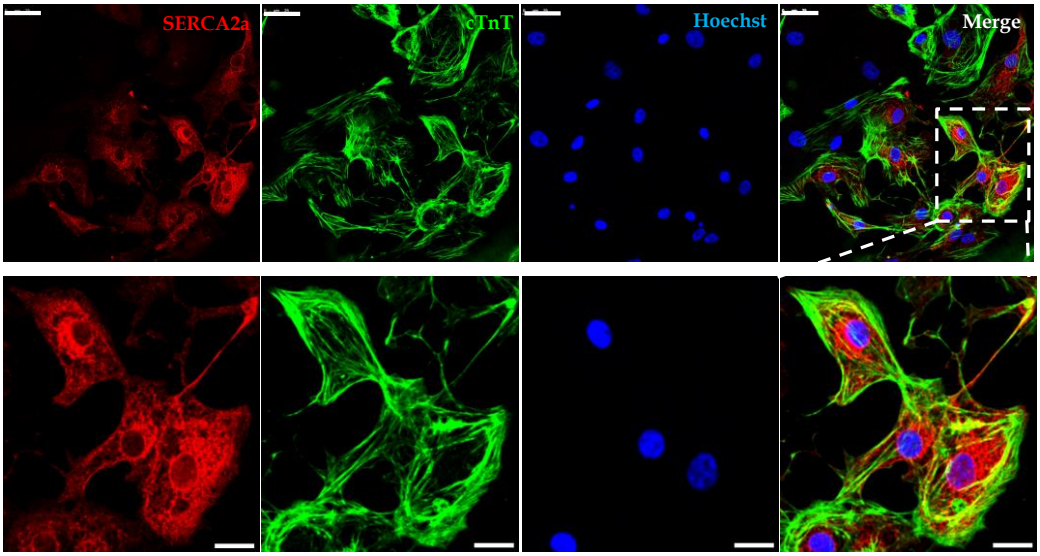

Figure 4.24: *hES Dual Reorter-CMs on day 15. Immunofluorescence staining for Ca^{2+} pump SERCA2a responsible for Ca^{2+} re-uptake showing a spreading localization in the whole cell volume in association with immunofluorescence staining against cTnT demonstrating sarcomeric organization. In the lower panel is reported a magnification of the area selected with dotted line. Upper panel scale bar: 25µm; magnification scale bar: 15µm.*

As observed, the calcium transient shortening in CMs-mmRNA derived is accompanied by the expression of SERCA2a spread in the cytosol indicating an improvement in maturation features of the cells.

4.11. Qualitative and quantitative characterization of Part 1 and Part 2 mmRNA-derived CMs

4.11.1. Qualitative characterization: immunofluorescence staining for cardiac markers

The expression of typical cardiac markers was routinely assessed by immunofluorescence staining in 15 days CMs obtained from both hES Dual Reporter and hiPS Clone 7 from experiments presented in Part 1 and Part 2, as shown in the panel of Figure 4.25, in which nuclear markers GATA4 and NKX2.5 and structural markers cTnT, α-Actinin and MYH7 (Myosin Heavy Chain or BA-D5, kindly given by Professor Schiaffino S., University of Padova) were analyzed. Cells from both Part1 and Part2 exhibited a remarkable expression of typical cardiac markers.

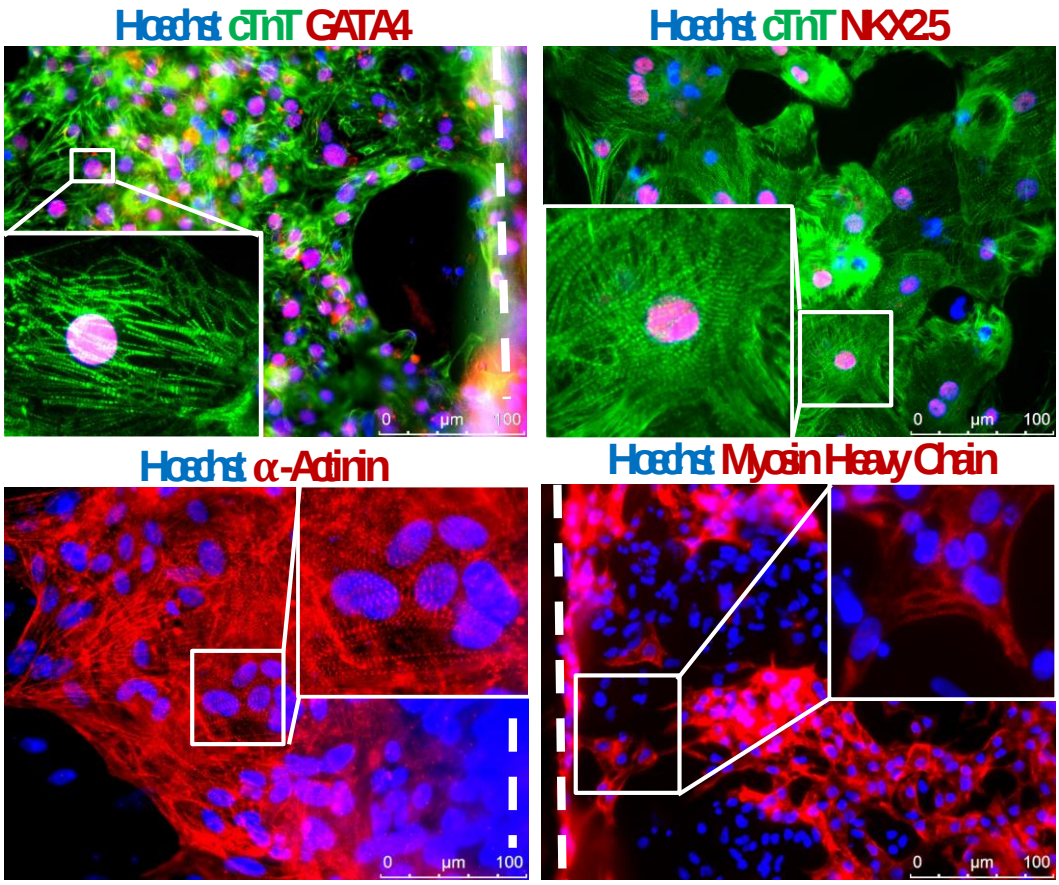

Figure 4.25: *Representative immunofluorescence pictures of 15 days CMs mmRNA-derived expressing nuclear and structural cardiac-specific proteins. Note the sarcomeric organization of the contractile proteins in the related magnification. Dotted lines represent channel edge.*

4.11.2. Quantitative characterization: gene expression pattern analysis

For gene expression analysis, total RNA from 15 days cells in the microfluidic platform was extracted using iScript (BioRAD), a sample preparation buffer designed to efficiently degrade the cytoplasmic membrane while leaving intact the nuclear membrane; thus only the cytoplasmic RNA was extracted, whereas the genomic DNA remains confined within the nuclei, allowing a sensitive quantitative gene expression analysis. This novel reagent accelerates and streamlines quantitative real-time PCR (qRT-PCR) by eliminating the need for lengthy RNA purification. Briefly, microfluidic channels were perfused with D-PBS prior to 10µl of iScript injection and solution was then collected after 1 minute of incubation at room temperature. RNA (0,1µg) was reverse transcribed into cDNA by Reverse Transcription (RT, Life Technologies), according to manufacturer's instructions.

To conclude the characterization of CMs mmRNA-derived, the expression of cardiac TFs involved in cardiogenesis was assessed with quantitative real-time PCR (qRT-PCR) analysis using TaqMan® gene expression assay probes (Invitrogen), accordingly to manufacturer's instructions. The expression of these genes was investigated: the early cardiac markers GATA4 and NKX2.5 and late structural, functional and maturation markers cTnT, MYH7 and SERCA2a, all labeled with FAM™ dye on the 5' end, designed and provided by BioERA lab in Shanghai, ShanghaiTech University. The expression levels of each gene analyzed were normalized to GAPDH, an housekeeping glycolytic enzyme (glyceraldehyde 3-phosphate dehydrogenase), which primer is conjugated with a VIC™ dye on the 5' end, whereas the results were normalized comparing the transcripts with control CMs differentiated with the only WNT OFF and WNT ON approaches. Reaction was done on ABI Prism 7000 SDS, Sequence-Detection-System (Applied Biosystems) machine and results were analyzed with ABI Prism 7000 SDS Software. Data obtained are shown as relative expression fold change of mmRNA-derived CMs compared with control CMs (WNT OFF or WNT ON) and are reported in Figure 4.26 (A-D).

As reported in the graphs, with TaqMan® gene expression assay it was possible to perform an accurate quantitative analysis of multiple early and late cardiac genes at the same time, giving a complete portrait of the CMs-mmRNA derived.

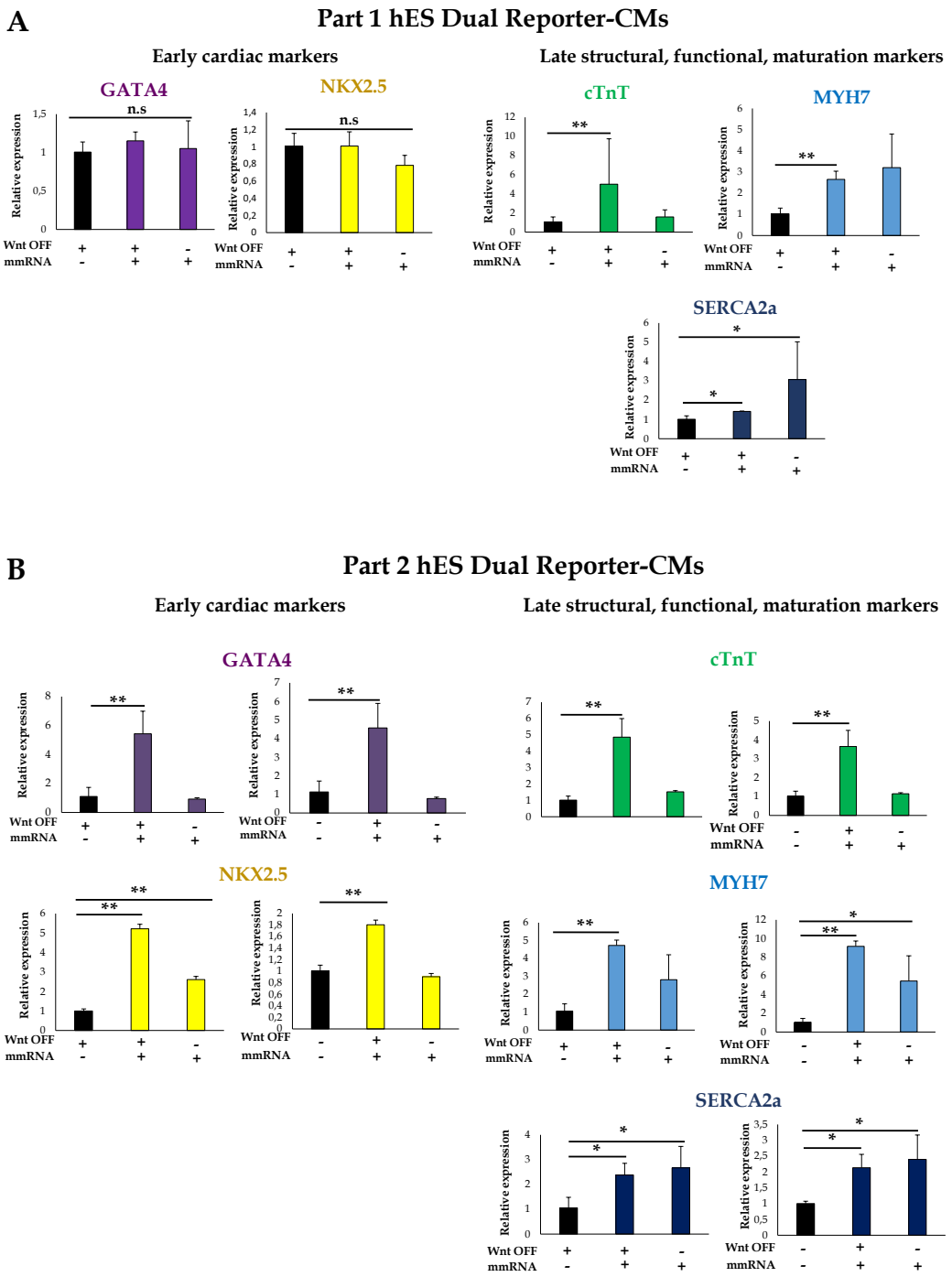
A
Part 1 hES Dual Reporter-CMs
Early cardiac markers
Late structural, functional, maturation markers
GATA4
NKX2.5
cTnT
MYH7
SERCA2a
n.s
**
*
Relative expression
Wnt OFF
mmRNA
B
Part 2 hES Dual Reporter-CMs
Early cardiac markers
Late structural, functional, maturation markers
GATA4
NKX2.5
cTnT
MYH7
SERCA2a
**
*
Relative expression
Wnt OFF
mmRNA

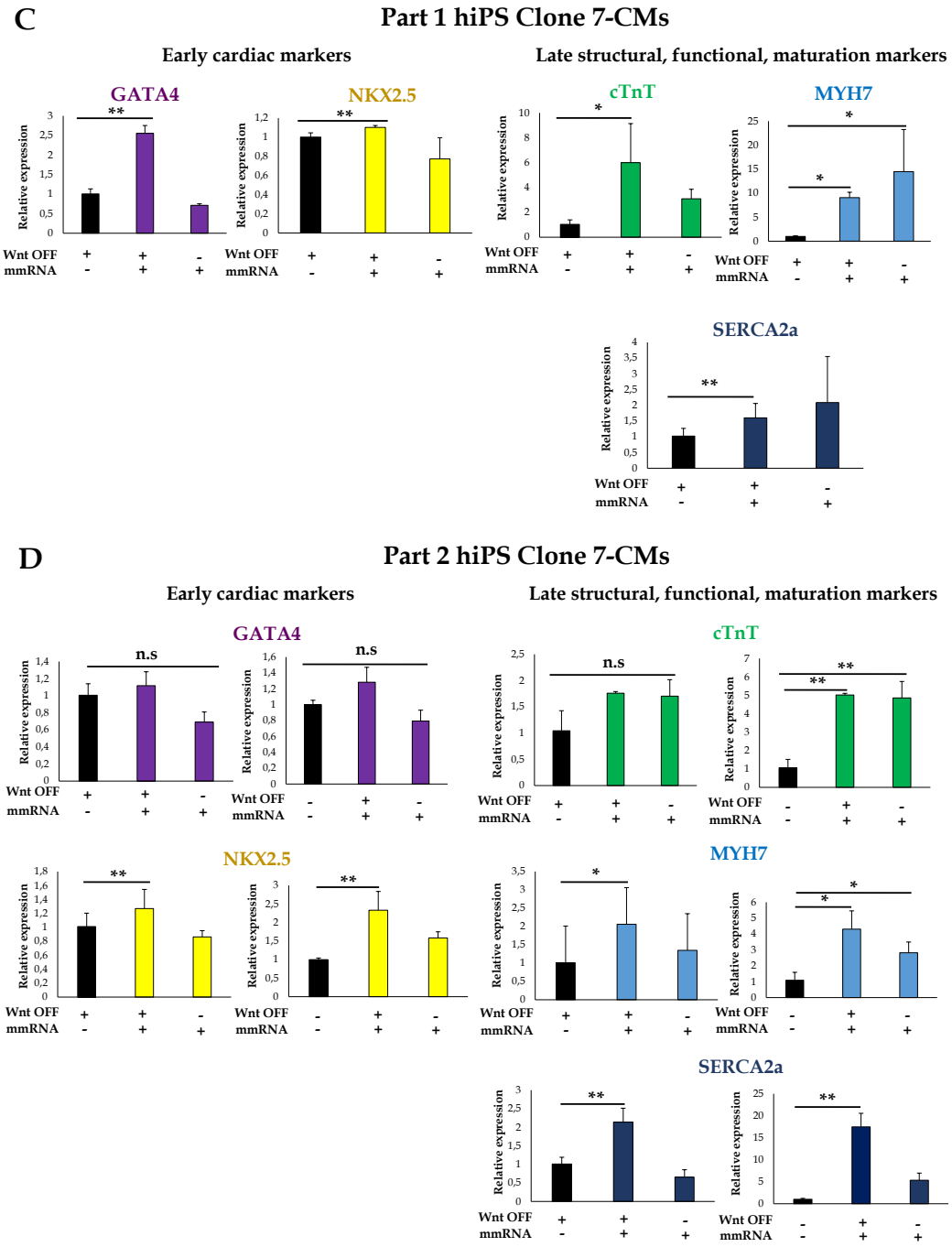

Figure 4.26: *The qRT-PCR analysis (gene expression normalized to GAPDH) of GATA4, NKX2.5, cTnT, MYH7 and SERCA2a in CMs-mmRNA derived obtained from hES Dual Reporter line and hiPS Clone 7 from Part 1 experiments (panels **A** and **C**) in which the TFs were delivered all together in the Cardio mix and the control was represented only by the WNT OFF approach, and Part 2 (panels **B** and **D**) in which the transfection was divided into early and late stage of TFs delivery and the further control of WNT ON was added. Every transcript was compared with control cells (black bars) differentiated with WNT OFF and WNT ON approach. Histograms are based on 3 replicates in the same condition. Data are shown as mean, error bars indicate SEM. Stundent's t-test p-values P<0,05 (*); P<0,01 (**); n.s, non significant.*

This gene expression pattern analysis confirmed that the CMs-mmRNA derived from both Part 1 and Part 2 experiments, expressed significantly higher amounts of cardiac TFs compared with the controls, especially those involved in structure, functionality and maturation and especially when CMs were derived with the mmRNA transfection divided into early and late stages (Part 2 experiments) and associated with the complete Wnt perturbation (WNT OFF). Intriguingly, significantly higher amounts of transcripts were observed also in the majority of CMs differentiated with the partial Wnt perturbation (WNT ON) and mmRNAs, compared with both control cells (WNT OFF and WNT ON), indicating the effect of mmRNA on protein expression.

4.12. Conclusions

In this Chapter was reported, for the first time, the cardiac programming of hPSCs fate with the novel mmRNA technology in microfluidics to generate clinically relevant CMs.

Six cardiac TFs were selected, taking into account their networking cooperation coming from developmental studies on cardiogenesis *in vivo*. The association of this novel strategy with our microfluidic platform, allowed a precise and tiny control and manipulation of mmRNAs and reagents in both space and time.

Before starting the hPSC programming with the mmRNA "Cardio mix", the mmRNA transfection protocol was deeply studied and optimized using only a GFP-encoding mmRNA. It was demonstrated that the integration of the experiments into the microfluidic device, thanks to its high surface/volume ratio, determined an increase in the transfection efficiency using 10-fold lower amounts of mmRNA and reagents compared with standard 24-well plates. Cells were efficiently transfected using two commercial transfection kits based on lipid vehicles and StemMacs™ was identified as the optimal for TFs delivery.

The experimental set-up was developed in 2 parts in which *ad hoc* strategies for the mmRNA Cardio mix delivery were designed and optimized, aiming at recapitulating more closely the cardiac developmental stages observed in the embryo, reflecting the temporal expression windows of each TFs. In particular, by dividing the transfection regimen into an early and a late stage, it was possible to obtain CMs-mmRNA derived with efficiencies that surpass those obtained in control cells differentiated with the only application of small

molecules. CMs-mmRNA derived expressed typical cardiac markers and, importantly, they showed significantly shorter calcium transients, indicating an improvement in cell organization, structure and function toward cell maturation. These results were also confirmed by the analysis of gene expression pattern with qRT-PCR, which showed significantly higher amounts of transcripts than cells differentiated with only Wnt modulators.

Taken together, these experiments provide proof-of-principle that it is possible to program hPSCs fate toward cardiac lineage by combining the novel technology of synthetic mmRNA with microfluidics for precise delivery of specific TFs to obtain clinical-grade cells in a cost-effective manner.

Chapter 5. Conclusions and Future Perspectives

5.1. Conclusions

Cardiovascular disease (CVD) is still one of the main causes of death worldwide and the high burden of the disease, associated with the high costs for the healthcare systems, claim for the development of novel therapeutic strategies [16]. The main issue of current pharmacological or interventional therapies is their inability to compensate the irreversible loss of functional CMs [187]. Because of the limited regenerative capacity of post-natal CMs, and the difficulties to isolate cardiac bioptic tissue and maintain human adult CMs, very limited supplies of these cells are available at present. Furthermore, animal models are surely one of the best tool for *in vivo* heart study of physiology and pathophysiology in the context of a whole complex organism, but they are not fully representative of the human counterpart [41]; from an economic point of view, animals maintenance and experimentations required elevated costs [40].

In this scenario, hPSCs, including hESCs and hiPSCs possess a high potential for cardiovascular research. Thanks to the possibility to be expanded in culture indefinitely while still maintaining their stemness and potency properties, they represent a virtually inexhaustible source of cell from the three germ layers, such as CMs [42]. Moreover, the discovery of hiPSCs first in mouse [43] and then in human [44] by 2012 Nobel Prize Shinya Yamanaka, represents an important breakthrough in science thanks to the fact that these cells can be derived by the reprogramming of adult somatic cell types, bypassing much of the ethical and political debate surrounding hESCs derivation [83]. One exciting advance is the ability to generate patient-specific hiPSCs as an unprecedented opportunity to study disease-specific differences between patients and evaluate novel therapeutic routes.

Substantial efforts has been made by the investigators to develop strategies that efficiently direct the cardiac differentiation of hPSCs, finally aiming at producing clinically relevant cell source [21].

Existing methods for deriving CMs from hPSCs involve stage-specific perturbation of different signaling pathways recapitulating key steps in cardiac development. However, these techniques present the following limitations: high

intra- and inter-experimental variability, low efficiencies, presence of xeno-contaminants, undefined medium components and differences in the expression levels of cytokines of endogenous signalling pathways [63]. Furthermore, new studies have been published, based on the direct lineage conversion of somatic cells through the overexpression of specific cardiac TFs, delivered with integrating and non-integrating vectors, but also these approaches suffered low efficiencies, risk of genomic integration and insertional mutagenesis (integrating vectors) and require stringent steps of purification (non-integrating vectors) [48][51]. In general, the major critical point of CMs produced to date with these protocols, is their early and immature phenotype, most analogous to fetal developing cardiac cells, thus representing an obstacle for future clinical applications [69].

In 2010, Warren L. pioneered a novel, non-integrating strategy based on repeated transfections with cationic vehicles of synthetically modified mRNA (mmRNA), specifically designed to avoid cell innate immune response. He demonstrated the possibility to both reprogram somatic cells to pluripotency with efficiencies significantly higher than established protocols, and to program hiPS differentiation by using a MYO-D encoding mmRNA to derive terminally differentiated myogenic cells [49][50].

In light of these considerations, this PhD thesis focused on the development of an efficient and robust method for cardiac differentiation of hPSCs in microfluidics through the overexpression of a defined set of cardiomyogenic TFs. To this end, the endogenous protein expression was forced by repeated mmRNA transfections to finely drive cardiac differentiation toward cell maturation. In order to improve the delivery of mmRNAs, the microfluidic technology was exploited to perform an efficient hPSCs cardiac differentiation in a high controllable microenvironment that allowed combinatorial, parallelized, multi-parametric analysis at one time in a cost-effective manner.

The work started with the culture, maintenance and expansion of different hESC lines and hiPSC clones that were successfully characterized, demonstrating that all the cells employed were *bona fide* plutipotent stem cells. Among the current strategies available, the differentiation of both hESCs and hiPSCs was achieved firstly by the application, in standard culture systems, of the protocol that to date it is considered the gold standard for simple and fast (~ 15 days) hPSCs differentiation into CMs with variability lower than that observed with the other approaches described (Chapter 1 and 2). This monolayer-based method relies on the administration of small molecules,

CHIR99021 and IWP4 that, in turn, activate and inhibit the canonical Wnt/β-catenin pathway [63][64]. To precisely monitor the progression of cardiac differentiation, a hESC line, Dual Reporter for this two cardiac TFs, MESP1 and NKX2.5 was always used in parallel with hiPS clones. The experimental conditions were optimized, adjusting CHIR99021 concentrations, to perform an optimal Wnt modulation and two hPSCs emerged for their cardiogeneic ability to give the highest yield of CMs. A deep characterization of CMs was performed, from immunofluorescence staining and flow cytometry to double-whole cell-voltage patch clamp; cells showed a remarkable organization of the sarcomeric contractile apparatus, with self contraction capacity and ability to correctly respond to functional test demonstrated by the presence of junctional current, sensitive to external stimuli. However, a first attempt to investigate the degree of maturity of CMs derived with this strategy was performed with an immunofluorescence staining against an embryo/fetal isoform and an adult isoform of cTnT and cTnI respectively, which revealed that a great portion of cardiac cells expressed the embryo/fetal troponin T, indicating their early and immature phenotype. These findings proved also the heterogeneity of CMs obtained, with differentiation toward random subpopulations, leaving room for improvement regarding the ability to homogeneously differentiate and mature cells to obtain completely functional CMs.

As described in Chapter 3, this problem is enhanced in standard culture systems because of the impossibility to precisely monitor and properly mimic cell microenvironment. Microfluidics, with its ability to managed small amounts of fluids in microchannels [3], can help overcome this issue. For this reason, hPSCs culture and expansion and the gold standard protocol for cardiac differentiation were successfully integrated into a microfluidic device fabricated in our BioERA laboratory that allowed parallelized experiments at one time with a precise control of the differentiation process. When translating the gold standard cardiac differentiation protocol from the macro-scale of conventional multiwells to the microscale of the microfluidic platform, a step by step optimization was done, demonstrating how the identification of the correct medium refresh frequency and the optimal MRF concentration for channel coating are essential in directing hPSCs CMs generation.

These achievements represented the basis for the following step of this PhD work, presented in Chapter 4, and describing the association of the delivery of mmRNA encoding 6 cardiac TFs with Wnt modulators in microfluidics. Thanks to the properties of the microfluidic chip, coupled with the transient nature of

mmRNA, with the possibility to modulate cellular expression by daily adjustment of the payload of TFs transfected, a precise spatiotemporal control of the experimental conditions was possible. Also in this case, a first optimization of the transfection process was necessary to study the possibility to integrate mmRNA in microfluidics and was carried out with the initial delivery of a single mmRNA encoding for nGFP. The results obtained demonstrated that the integration of mmRNA technology into microfluidics, thanks to the high surface/voulme ratio, determined an increase in the transfection efficiency compared with standard multiwells, using significantly lower amounts of mmRNA and reagents.

Then, *ad hoc* strategies of mmRNA delivery associated with the complete or partial Wnt perturbation with small molecules, were developed, in order to recapitulate more closely the cardiac developmental stages observed in the embyo, reflecting the temporal expression window of each cardiac TFs. The use of mmRNA to drive the cardiac differentiation of hPSCs allowed the generation of CMs that contract 2-3 days earlier than control cells differentiated with the only application of small molecules. Moreover, with the final approach adopted, based on the division of the transfection regimen into an early and a late stage that better recapitulates TFs expression studied *in vivo*, CMs-mmRNA derived responded to functional test, showing proper calcium dynamics with significantly shorter calcium transients than control cells. These data were also confirmed by the gene expression pattern analysis revealing a significantly higher amount of cardiac transcripts, especially those related to late, structural, functional and maturation genes, indicating a clear effect of mmRNA on cell transcriptome.

In conclusion, the research conducted in this PhD, provide proof-of-principle that it is possible to program hPSCs fate toward cardiac lineage and CMs maturation by combining the emerging mmRNA technology with microfluidics; furthermore the strategies developed allowed the generation of clinical-grade CMs holding great promise for regenerative medicine research and disease modelling.

The results obtained are encouraging compared to the few data available in literature regarding the use of mmRNA. In fact there are only 2 works reporting the generation, in conventional culture systems, of myoblast-like cells, not CMs. The first, published by Warren L. in 2010 demonstrated the ability to direct hPSCs fate to myogenic cells [49][50] while the second one, published by

Preskey D. in 2015 reported the transdifferentiation of fibroblasts to myoblast [163].

In this PhD thesis, having associated the mmRNA with microfluidics allowed a precise and high efficient generation of functional CMs. Moreover, the microfluidic device, fabricated in our laboratory, allowed reproducibility of the experiments, is completely customizable, cost-effective and versatile for a wide range of tests. In fact, the miniaturization can attract the pharmaceutical industry as a tool for the discovery and development of new drugs with more economic procedures, avoiding the non fully predictive animal tests before clinical trials.

5.2. Future Perspectives

Further investigations have still to be done in order to obtain clinically relevant CMs, starting from the optimization of the culture conditions. In all the experiments described in this thesis and, in general in the majority of published works, feeder-free cultures are employed, with cells maintained on Matrigel Reduced growth Factors (MRF) that is an extracellular matrix (ECM) preparation isolated from mouse sarcoma. However, this undefined ECM preparation, based on animal glycoproteins and Growth Factors (GFs) is not ideal for hPSCs culture and subsequent differentiation because of its lot-to-lot variability and the possible introduction of unwanted xenogenic contaminants; these issues are not indicated, especially when the primary objective is to culture these cells for eventual human clinical applications.

A specialized ECM structure, basement membrane, consists of indispensable protein and carbohydrate macromolecules secreted by cells, for mechanical support as well as tissue homeostasis maintenance [188]. Among these biologically active proteins, liminins (lm) play the major role. To this end, for future experiments, feeder-free and xeno-free culture matrices can be adopted, such as those based on recombinant human ECM preparations composed of collagen, fibronectin, laminin or vitronectin, or synthetic commercial reconstituted ECM. Furthermore, the association of a complete chemically defined medium, in which all the constituents are well known, free of animal products (e.g. bovine serum albumin, BSA, MRF or B27 supplement), becomes necessary.

As described in Chapter 2, the gold standard protocol relies on the basal medium RPMI 1640 (which is chemically defined), supplemented with B27, that is a complex mixture of 21 components (many of animal origin) and remains still

unknown the influence exerted by these compounds on hPSCs differentiation. A valuable alternative to circumvent the issue of xeno-contaminants is described by Burridge P.W. in 2014. Burridge's research group developed a cardiac differentiation strategy of hPSCs employing a chemically defined medium ,named "CDM3", prepared with 3 components: the basal medium RPMI 1640, L-ascorbic acid 2-phosphate as an antioxidant, and rice-derived recombinant human albumin as a detoxifier, buffer and ROX binding protein, with cells seeded on a matrix composed of synthesized vitronectin peptide substrate [66].

With these culture conditions, it will be possible to test and compare the ability of cardiac mmRNA to program hPSCs fate toward cardiac lineage alone, without the association of the small molecules CHIR99021 and IWP4, employed up to now.

In addition, current differentiation protocols generated a variable mixture of atrial and ventricular CMs, with small percentages of nodal and conduction system cells [189]. As demonstrated in this PhD work, the forced overexpression of specific cardiac TFs *via* mmRNA delivery can efficiently direct hPSCs fate to beating CMs, which showed an improvement in cell organization, function, structure, and maturation features. Having this in mind and taking into account the possibility to deliver simultaneously several combinations of cardiac TFs-mmRNA, future experiments will address the subtype specification toward different CMs phenotypes such as atrial and ventricular CMs, conduction and endocardial cells, as illustrated in Figure 5.1.

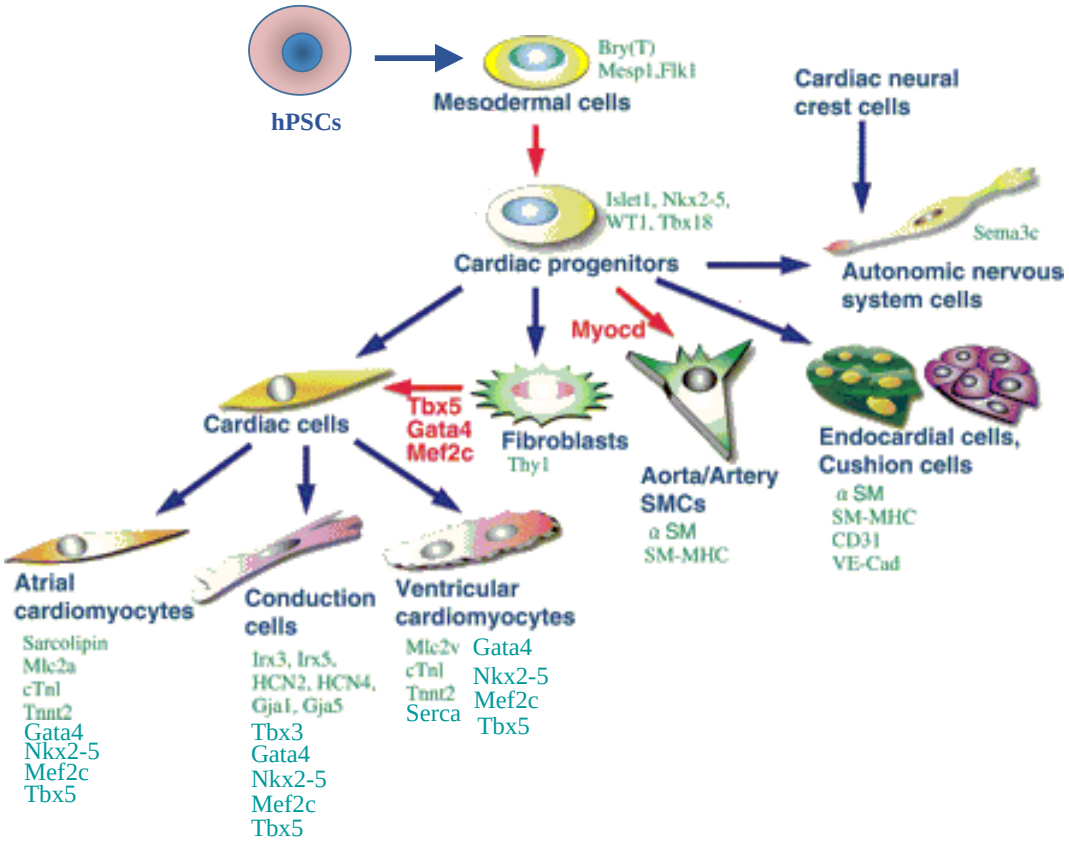

Figure 5.1: *Cardiac cell types derived from multipotent progenitors with the related TFs. Differentiated cardiac cell types are characterized by the expression of specific genes (green). Recently, several works published in literature have identified and studied the delivery of TFs combinations for cardiac transdifferentiation of fibroblasts (red) (adapted from [190]).*

The possibility to modulate hPSCs programming *via* specific mmRNA administration can provide a more homogeneous population of clinical-grade CMs subtypes suitable for future clinical applications and disease modeling with the appropriate cardiac phenotype generated from patient hiPSCs, allowing a more accurate therapy assessment and therapeutic drug discovery.

References

[1]. Appasani K, Appasani R, K. 2011. Stem Cells & Regenerative Medicine From Molecular Embriology to Tissue Engineering. London: Humana Press.

[2]. Laflamme MA, Murry CE. 2005. Regenerating the heart. Nature Biotechnology 23:845-856.

[3]. Whitesides GM. 2006. The origins and the future of microfluidics. Nature 442:368-373.

[4]. Harink B, Le Gac S, Truckenmu R, van Bitterswijka C, Habibovic P. 2013. Regeneration-on-a-chip? The perspective on use of microfluidics in regenerative medicine. Lab on a Chip 13:3512-3528.

[5]. Lewis T. 2016. Human Heart: Anatomy, Function & Facts. Livescience website. www.livescience. com.

[6]. Patton KT, Thibodeau, GA. 1996. Anatomy and Physiology. 8th Edition: MOSBY Elsevier.

[7]. Olivetti G, Cigola E, Maestri R, Corradi D, Lagrasta C, Gambert SR, Anversa P. 1996. Aging, Cardiac Hypertrophy and Ischemic Cardiomyopathy Do Not Affect the Proportion of Mononucleated and Multinucleated Myocytes in the Human Heart, Journal of Molecular and Cellular Cardiology. Journal of Molecular and Cellular Cardiology 28:1463-1477.

[8]. Gerecht-Nir S, Radisic M, Park H, Cannizzaro C, Boublik J, Langer R. 2006. Biophysical regulation during cardiac development and application to tissue engineering. The Internal Journal of Developmental Biology 50(2-3):233-243.

[9]. Bird SD, Doevendans PA, van Rooijen MA, de la Riviere AB, Hassink RJ, Passier R, Mummery CL. 2003. The human adult cardiomyocyte phenotype. Cardiovascular Research 58:423-434.

[10]. Carol CG, Parker B, Antin PB. 2000. To the heart of myofibril assembly. Trends in Cell Biology 10:355-362.

[11]. www.sandiegoalive.net.

[12]. Cheng H, Lederer WJ, Cannell MB. 1993. Calcium sparks: elementary events underlying exitation-contraction coupling in heart muscle. Science 262:740-744.

[13]. Cannell MB, Cheng H, Lederer WJ. 1994. Spatial non-uniformities in [Ca2+]i during exitation-contraction coupling in cardiac myocytes. Biophysical Journal 67:1942-1956.

[14]. Crespo LM, Grantham CJ, Cannell MB. 1990. Kinetics, stoichiometry and role of the Na-Ca exchange mechanism in isolated cardiac myocytes. Nature 345(6276):618-621.

[15]. Austin Community College District website, www.austincc.edu.

[16]. Feric NT, Radisic M. 2016. Maturing human pluripotent stem cell-derived cardiomyocytes in human engineered cardiac tissues. Adv Drug Deliv Rev 96:110-134.

[17]. Porter GA, Hom J, Hoffman D, Quintanilla R, de Mesy Bentley K, Sheu SS. 2011. Bioenergetics, mitochondria, and cardiac myocyte differentiation. Progress in Pediatric Cardiology 31:75-81.

[18]. Navaratnam V. 1987. Heart Muscle: Ultrastractural Studies. Cambridge University Press, New York.

[19]. Mc Culley DJ, Black BL. 2012. Transcription Factor Pathways and Congenital Heart Disease. Current topics in developmental biology. 100:253-277.

[20]. Srivastava D. 2006. Genetic regulation of cardiogenesis and congenital heart disease. Annual Review of Pathology: Mechanisms of Disease 1:199-213.

[21]. Burridge P, Keller G, Gold JD, Wu JC. 2012. Production of de novo cardiomyocytes: human pluripotent stem cells differentiation and direct reprogramming. Cell Stem Cell 10:16-28.

[22]. Buckingham M, Mailhac S, Zaffran S. 2005. Building the mammalian heart from two sources of myocardial cells. Nature Reviews Genetics 6:826-835.

[23]. Kwon C, Arnold J, Hsiao EC, Taketo MM, Conklin BR, Srivastava D. 2007. Canonical Wnt signaling is a positive regulator of mammalian cardiac progenitors. Proceedings of the National Academy of Sciences 104:10894-10899.

[24]. Person AD, Klewer SE, Runyan RB. 2005. Cell Biology of Cardiac Cushion Development. Int Rev Cytol 243:287-335.

[25]. Evans SM, Yelon D, Conlon FL, Kirby ML. 2010. Myocardial Lineage Development. Circulation research 107:1428-1444.

[26]. Arnold SJ, Robertson EJ. 2009. Making a committment: cell lineage allocation and axis patterning in the early mouse embryo. Nature Reviews Molecular Cell Biology 10:91-103.

[27]. Später D, Hansson EM, Zangi L, Chien KR. 2014. How to make a cardiomyocyte. Development 141:4418-4431.

[28]. Noseda M, Peterkin T, Simões FC, Patient R, Schneider MD. 2011. Cardiopoietic Factors: Extracellular Signals for Cardiac Lineage Commitment. Circulation Research 108:129-152.

[29]. Bondue A, Blanpain C. 2010. Mesp1: A Key Regulator of Cardiovascular Lineage Commitment. Circulation Research 107:1414-1427.

[30]. Costello I, Pimeisl IM, Drager S, Bikoff EK, Robertson EJ, Arnold SJ. 2011. The T-box transcription factor Eomesodermin acts upstream of Mesp1 to specify cardiac mesoderm during mouse gastrulation. Nature Cell Biology 13:1084-1091.

[31]. David R, Brenner C, Stieber J, Schwarz F, Brunner S, Vollmer M, Mentele E, Muller-Hocker J, Kitajima S, Lickert H. 2008. Mesp1 drives vertebrate cardiovascular differentiation through Dkk-1-mediated blockade of Wnt-signalling. Nature Cell Biology 10:338-345.

[32]. Naito AT, Shiojima I, Akazawa H, Hidaka K, Norisaki T, Kikuchi A, Komuro I. 2006. Developmental stage-specific biphasic roles of Wnt/beta-catenin signaling in cardiomyogenesis and haematopoiesis. Proceedings of the National Academy of Sciences 103:19812-19817.

[33]. Ueno S, Weidinger G, Osugi T, Kohn AD, Golob JL, Pabon L, Reinecke H, Moon RT, Murry CE. 2007. Biphasic role for Wnt/beta-catenin signaling in cardiac specification in zebrafish and embryonic stem cells. Proceedings of the National Academy of Sciences 2007:9685-9690.

[34]. Kwon C, Qian L, Cheng P, Nigam V, Arnold J, Srivastava D. 2009. A regulatory pathway involving Notch1/beta-catenin/Isl1 determines cardiac progenitors. Nature Cell Biology 11:951-957.

[35]. Qyang Y, Martin-Puig S, Chiravuri M, Chen S, Xu H, Bu L, Jiang X, Lin L, Granger A, Moretti A. 2007. The renewal and differentiation of Isl+ cardiovascular progenitors are controlled by Wnt/beta-catenin pathway. Cell stem cell 1:165-179.

[36]. Sahara M, Santoro F, Chien KR. 2015. Programming and reprogramming a human heart cell. The EMBO Journal 34:710-738.

[37]. Cannon B. 2013. Cardiovascular disease: Biochemistry to behaviour. Nature 2-3.

[38]. Laflamme MA, Murry CE. 2011. Heart regeneration. Nature 473:326-335.

[39]. Jiang J, Han P, Zhang Q, Zhao J, Ma Y. 2012. Cardiac differentiation of human pluripotent stem cells. J Cell Mol Med 16:1663-1668.

[40]. Fiedler LR, Maifoshie E, Schneider MD. 2014. Chapter Four - Mouse Models of Heart Failure: Cell Signaling and Cell Survival. Curr Top Dev Biol 109:171-247.

[41]. Olson H, Betton G, Robinson D. 2000. Concordance of the toxicity of pharmaceuticals in humans and in animals. Regulatoty Toxicology and Pharmacology 32:56-67.

[42]. Thomson JA, Itskovitz-Eldor J, Shapiro SS, Waknitz MA, Swiergiel JJ, Marshall VS, Jones JM. 1998. Embryonic Stem Cell Lines Derived From Human Blostocysts. Science 282:1145-1147.

[43]. Takahashi K, Yamanaka S. 2006. Induction of pluripotent stem cells from mouse embryonic and adut fibroblast cultures by defined factors. Cell 126:663-676.

[44]. Takahashi K, Tanabe K, Ohnuki M, Narita M, Ichisaka T, Tomoda K, Yamanaka S. 2007. Induction of pluripotent stem cells from adult human fibroblasts by defined culture. Cell 131:861-872.

[45]. Ebert AD, Diecke S, Chen IJ, Wu JC. 2015. Reprogramming and transdifferentiation for cardiovascular development and regenerative medicine: where do we stand? EMBO Molecular Medicine 7(9):1090-1103.

[46]. Keller G. 2005. Embryonic stem cell differentiation: emergence of a new era in biology and medicine. Genes & Development 19:1129-1155.

[47]. Nam Y, Song K, Luo X, Daniel E, Lambeth K, West K, Hill JA, DiMaio JM, Baker LA, Bassel-Duby R, Olson EN. 2013. Reprogramming of human fibroblasts toward a cardiac fate. Proceedings of the National Academy of Sciences 110:5588-5593.

[48]. Ieda M, Fu J, Delgado-Olguin P, Vedantham V, Hayashi Y, Bruneau BG, Srivastava D. 2010. Direct Reprogramming of Fibroblasts into Functional Cardiomyocytes by Defined Factors. Cell 142:375-386.

[49]. Warren L, Manos PD, Ahfeldt T, Loh Y, Li H, Lau F, Ebina W, Mandal P, Smith ZD, Meissner A, Daley GQ, Brack AS, Collins JJ, Cowan C, Schlaeger TM, Rossi DJ. 2010. Highly efficient reprogramming to pluripotency and directed differentiation of human cells using synthetic modified mRNA. Cell stem cell 7:618-630.

[50]. Warren L, Ni Y, Wang J, Guo X. 2012. Feeder-Free Derivation of Human Induced Pluripotent Stem Cells with Messenger RNA. Nature. 2(657):1-7.

[51]. Chang CW, Lay YS, Pawlik KM, Liu K, Sun CW, Li C, Schoeb TR, Townes TM. 2009. Polycistronic lentiviral vector for "hit and run" reprogramming of adult skin fibroblasts to induced pluripotent stem cells. Stem Cells 27:1042-1049.

[52]. Fusaki N, Ban H, Nishiyama A, Saeki K, Hasegawa M. 2009. Efficient induction of transgene-free human pluripotent stem cells using a vector based on Sendai virus, an RNA virus that does not integrate into the host genome. Proceedings of the Japan Academy. Series B, Physical and Biological Sciences 85:348-362.

[53]. Davis RP, van den Berg CW, Casini S, Braam SR, Mummery CL. 2011. Pluripotent stem cell models of cardiac disease and their implication for drug discovery and development. Trends Mol Med 17:475-484.

[54]. Mummery C, Ward-van Oostwaard D, Doevendans P, Spijker R, van den Brink S, Hassink R, van der Heyden M, Opthof T, Pera M, de la Riviere AB, Passier R, Tertoolen L. 2003. Differentiation of Human Embryonic Stem Cells to Cardiomyocytes: Role of Coculture With Visceral Endoderm-Like Cells. Circulation 107:2733-2740.

[55]. Filipczyc AA, Passier R, Rochat A, Mummery CL. 2007. Cardiovascular development: towards biomedical applicability. Cellular and Molecular Life Sciences 64(6):704-718.

[56]. Kehat I, Kenyagin-Karsenti D, Snir M, Segev H, Amit M, Gepstein A, Gepstein L. 2001. Human embryonic stem cells can differentiate into myocytes with structural and functional properties of cardiomyocytes. Journal of Clinical Investigation 108:407-414.

[57]. Kattman SJ, Witty AD, Gagliardi M, Dubois NC, Niapour M, Hotta A, Ellis J, Keller GM. 2011. Stage-specific optimization of activin/nodal and BMP signaling promotes cardiac differentiation of mouse and human pluripotent stem cell lines. Cell stem cell 8:228-240.

[58]. Yang L, Soonpaa MH, Adler ED, Roepke TK, Kattman SJ, Kennedy M, Henckaerts E, Bonham K, Abbott GW, Linden RM. 2008. Human cardiovascular progenitor cells develop from a KDR+ embryonic-stem-cell-derived population. Nature 453:524-528.

[59]. Cai W, Albini S, Wei K, Willems E, Guzzo RM, Tsuda M, Giordani L, Spiering S, Kurian L, Yeo GW, Puri PL, Mercola M. 2013. Coordinate Nodal and BMP

inhibition directs Baf60c-dependent cardiomyocyte commitment. Genes & Development 27:2332-2344.

[60]. Laflamme MA, Chen KY, Naumova AV, Muskheli V, Fugate JA, Dupras SK, Reinecke H, Xu C, Hassanipour M, Police S. 2007. Cardiomyocytes derived from human embryonic stem cells in pro-survival factors enhance function of infarcted rat hearts. Nature Biotechnology 25:1015-1024.

[61]. Mummery CL, Zhang J, Ng ES, Elliott DA, Elefanty AG, Kamp TJ. 2012. Differentiation of Human Embryonic Stem Cells and Induced Pluripotent Stem Cells to Cardiomyocytes: A Methods Overview. Circulation Research 111:344-358.

[62]. Paige SL, Osugi T, Afanasiev OK, Pabon L, Reinecke H, Murry CE. 2010. Endogenous Wnt/β-Catenin Signaling Is Required for Cardiac Differentiation in Human Embryonic Stem Cells. PLoS ONE 5:1.

[63]. Lian X, Hsiao C, Wilson G, Zhu K, Hazeltine LB, Azarin SM, Raval KK, Zhang J, Kamp TJ, Palecek SP. 2012. Robust cardiomyocyte differentiation from human pluripotent stem cells via temporal modulation of canonical Wnt signaling. Proceedings of the National Academy of Sciences 109:E1848-E1857.

[64]. Lian X, Zhang J, Azarin SM, Zhu K, Hazeltine L, Bao X, Hsiao C, Kamp TJ, Palecek SP. 2013. Directed cardiomyocytes differentiation from human pluripotent stem cells by modulating Wnt/β-catenin signaling under fully defined conditions. Nature Protocols 8:162-175.

[65]. Xu H, Yi BA, Wu H, Bock C, Gu H, Lui KO, Park J-C, Shao Y, Riley AK, Domian IJ. 2012. Highly efficient derivation of ventricular cardiomyocytes from induced pluripotent stem cells with a distinct epigenetic signature. Cell Research 22:142-154.

[66]. Burridge PW, Matsa E, Shukla P, Lin ZC, Churko JM, Ebert AD, Lan F, Diecke S, Huber B, Mordwinkin NM. 2014. Chemically defined generation of human cardiomyocytes. Nature methods 11:855-860.

[67]. Keung W, Boheler K, Li R. 2014. Developmental cues for the maturation of metabolic, electrophysiological and calcium handling properties of human pluripotent stem cell-derived cardiomyocytes. Stem Cell Research & Therapy 5:17.

[68]. Lundy SD, Zhu WZ, Regnier M, Laflamme MA. 2013. Structural and Functional Maturation of Cardiomyocytes Derived from Human Pluripotent Stem Cells. Stem Cells and Development 22:1991-2002.

[69]. Robertson C, Tran DD, George SC. 2013. Concise review: maturation phases of human pluripotent stem cell-derived cardiomyocytes. Stem Cells 31:829-837.

[70]. Piquereau J, Caffin F, Novotova M, Lemaire C, Veksler V, Garnier A, Ventura-Clapier R, Joubert F. 2013. Mitochondrial dynamics in the adult cardiomyocytes: which roles for a highly specialized cell? Frontiers in Physiology Journal 4:102.

[71]. Moore JC, Fu J, Chan YC, Lin D, Tran H, Tse HF, Li RA. 2008. Distinct cardiogenic preferences of two human embryonic stem cell (hESC) lines are

imprinted in their proteomes in the pluripotent state. Biochemical and Biophysical Research Communications 372:553-558.

[72]. Cao F, Wagner RA, Wilson KD, Xie X, Fu JD, Drukker M, Lee A, Li RA, Gambhir SS, Weissman IL, Robbins RC, Wu JC. 2008. Transcriptional and functional profiling of human embryonic stem cell-derived cardiomyocytes. PLoS ONE 3:e3474.

[73]. Ma J, Guo L, Fiene SJ, Anson BD, Thomson JA, Kamp TJ, Kolaja KL, Swanson BJ, January CT. 2011. High purity human-induced pluripotent stem cell-derived cardiomyocytes: electrophysiological properties of action potentials and ionic currents. American Journal of Physiology - Heart and Circulatory Physiology 301:2006-2017.

[74]. Yanagi K, Takano M, Narazaki G, Uosaki H, Hoshino T, Ishii T, Misaki T, Yamashita JK. 2007. Hyperpolarization-Activated Cyclic Nucleotide-Gated Channels and T-Type Calcium Channels Confer Automaticity of Embryonic Stem Cell-Derived Cardiomyocytes. Stem Cells 25:2712-2719.

[75]. Zahanich I, Sirenko SG, Maltseva LA, Tarasova YS, Spurgeon HA, Boheler KR, Stern MD, Lakatta EG, Maltsev VA. 2011. Rhythmic beating of stem cell-derived cardiac cells requires dynamic coupling of electrophysiology and Ca cycling. J Mol Cell Cardiol 50:66-76.

[76]. Caspi O, Itzhaki I, Kehat I, Gepstein A, Arbel G, Huber I, Satin J, Gepstein L. 2009. In vitro electrophysiological drug testing using human embryonic stem cell derived cardiomyocytes. Stem Cells and Development 18:161-172.

[77]. Kadir SHSA, Ali NN, Mioulane M, Brito-Martins M, Abu-Hayyeh S, Foldes G, Moshkov AV, Williamson C, Harding SE, Gorelik J. 2009. Embryonic stem cell-derived cardiomyocytes as a model to study fetal arrhythmia related to maternal disease. J Cell Mol Med 13:3730-3741.

[78]. Xu XQ, Soo SY, Sun W, Zweigerdt R. 2009. Global expression profile of highly enriched cardiomyocytes derived from human embryonic stem cells. Stem Cells 27:2163-2174.

[79]. Synnergren J, Akesson K, Dahlenborg K, Vidarsson H, Ameen C, Steel D, Lindahl A, Olsson B, Sartipy P. 2008. Molecular signature of cardiomyocyte clusters derived from human embryonic stem cells. Stem Cells 26:1831-1840.

[80]. Yigang W. 2014. Myocardial Reprogramming Medicine: The Development, Application, and Challenge of Induced Pluripotent Stem Cells. New Journal of Science 2014:1-22.

[81]. Ban K, Wile B, Kim S. 2013. Purification of cardiomyocytes from differentiating pluripotent stem cells using molecular beacons that target cardiomyocyte-specific mRNA. Circulation 128:1897-1909.

[82]. Potten CS, Loeffler M. 1990. Stem cells: attributes, cycles, spirals, pitfalls and uncertainties. Lessons for and from the crypt. Development 110:1001-1020.

[83]. Wert Gd, Mummery C. 2003. Human embryonic stem cells: research, ethics and policy. Human Reproduction 18:672-682.

[84]. Mitalipov S, Wolf D. 2009. Totipotency, pluripotency and nuclear reprogramming. Advances in Biochemical Engineering & Biotechnology 114:185-199.

[85]. Berdasco M, Esteller M. 2011. DNA methylation in stem cell renewal and multipotency. Stem Cell Research & Therapy 2:1-9.

[86]. Steinhoff G. 2011. Regenerative Medicine - from Protocol to Patient. Journal of Stem Cells & Regenerative Medicine 7:57-58.

[87]. Reubinoff BE, Itsykson P, Turetsky T, Pera MF, Reinhartz E, Itzik A, Ben-Hur T. 2001. Neural progenitors from human embryonic stem cells. Nature Biotechnology 19:1134-1140.

[88]. Narsinh KH, Plews J, Wu JC. 2011. Comparison of Human Induced Pluripotent and Embryonic Stem Cells: Fraternal or Identical Twins? Molecular Therapy 19:635-638.

[89]. Baker M. 2007. Adult cells reprogrammed to pluripotency without tumors. Nature Reports Stem Cells 124:1038.

[90]. Yu J, Vodyanic MA, Smuga-Otto K, Antosiewicz-Bourget J, Frane JL, Tian S, Nie J, Jonsdottir GA, Ruotti V, Stewart R, Slukvin II, Thomson JA. 2007. Induced Pluripotent Stem Cell Lines derived from Human Somatic Cells. Science 318(5858):1917-1920.

[91]. Zhou T, Beda C, Dunzinger S, Huang Y, Ho JC, Yang J, Wang Y, Zhang Y, Zhuang Q, Li Y, Bao X, Tse H, Grillari J, Grillari-Voglauer R, Pei D, Esteban MA. 2012. Generation of human induced pluripotent stem cells from urine samples. Nature Protocols 7:2080-2089.

[92]. Den Hartogh SC, Schreurs C, Monshouwer-Kloots JJ, Davis RP, Elliott DA, Mummery CL, Passier R. 2015. Dual Reporter MESP1mCherry/w-NKX2-5eGFP/w hESCs Enable Studying Early Human Cardiac Differentiation. Stem Cells 33:56-67.

[93]. Den Hartogh SC, Passier R. 2016. Concise Review: Fluorescent Reporters in Human Pluripotent Stem Cells: Contributions to Cardiac Differentiation and Their Applications in Cardiac Disease and Toxicity. Stem Cells 34:13-26.

[94]. Giobbe GG, Michielin F, Luni C, Giulitti S, Martewicz S, Dupont S, Floreani A, Elvassore N. 2015. Functional differentiation of human pluripotent stem cells on a chip. Nature Methods 12:637-640.

[95]. Luni C, Giulitti S, Serena E, Ferrari L, Zambon A, Gagliano O, Giobbe GG, Michielin F, Knöbel S, Bosio A, Elvassore N. 2016. High-efficiency cellular reprogramming with microfluidics. Nature Methods 13:446-452.

[96]. Elliott DA, Braam SR, Koutsis K, Nq ES, Jenny R, Lagerqvist EL, Biben C, Hatzistavrou T, Hirst CE, Yu QC, Skelton RJP, Ward-van Oostwaard D, Lim SM, Khammy O, Li X, Hawes SM, Davis RP, Goulburn AL, Passier R, Prall OWJ, Haynes JM, Pouton CW, Kaye DM, Mummery CL, Elefanty AG, Stanley EG. 2011. *NKX2-5*$^{eGFP/w}$ hESCs for isolation of human cardiac progenitors and cardiomyocytes. Nature Methods 8:1037-1040.

[97]. Zhang J, Klos M, Wilson GF, Herman AM, Lian X, Raval KK, Kamp TJ. 2012. Extracellular Matrix Promotes Highly Efficient Cardiac Differentiation of Human Pluripotent Stem Cells: The Matrix Sandwich Method. Circulation Research 111:1125-1136.

[98]. Chen B, Dodge ME, Tang W, Lu J, Ma Z, Fan CW, Wei S, Hao W, Kilgore J, William MS, Roth MG, Amatruda JF, Chen C, Lum F. 2009. Small molecule-

mediated disruption of Wnt-dependent signaling in tissue regeneration and cancer. Nature Chemical Biology 5:100-107.

[99]. Saggin L, Ausoni S, Gorza L, Sartore S, Schiaffino S. 1988. Troponin T switching in the developing rat heart. Journal of Biological Chemistry 263:18488-18492.

[100]. Saggin L, Gorza L, Ausoni S, Schiaffino S. 1989. Troponin I switching in the developing heart. Journal of Biological Chemistry 264:16299-16302.

[101]. Lin X, Zemlin C, Hennan J, Petersen JS, Veenstra RD. 2008. Enhancement of Ventricular Gap Junction Coupling by Rotigaptide. Cardiovascular Research 79:416-426.

[102]. van der Velden HM, Jongsma HJ. 2002. Cardiac gap junctions and connexins: their role in atrial fibrillation and potential as therapeutic targets. Cardiovascular Research 54:270-279.

[103]. Bruzzone R, White TW, Paul DL. 1996. Connections with connexins: the molecular basis of direct intercellular signaling. European Journal of Biochemistry 238:1-27.

[104]. Postma S, Rook MB, Jongsma HJ. 2001. Gap junctions in the rabbit sinoatrial node. American Journal of Physiology - Heart and Circulatory Physiology 280:2103-2115.

[105]. Sakmann B, Neher E. 1984. Patch clamp techniques for studying ionic channels in excitable membranes. Annual Review of Physiology 46:455-472.

[106]. Hamill OP, Marty A, Neher E, Sakmann B, Sihworth FJ. 1981. Improved patch-clamp techniques for high resolution current recording from cells and cell-free membrane patches. Pfluger Archiv European Journal of Physiology. 391:85-100.

[107]. Karmazinova M, Lacinovà L. 2010. Measurement of Cellular Excitability by Whole Cell Patch Clamp Technique. Physiology Research 59:S1-S7.

[108]. Hernandez V, Bortolozzi M, Pertegato V, Beltramello M, Giarin M, Zaccolo M, Pantano S, Mammano F. 2007. Unitary permeability of gap junction channels to second messengers measured by FRET microscopy and dual whole-cell current recordings. Nature Methods 4:353-358.

[109]. White RL, Doeller JE, Verselis VK, Wittenberg BA. 1990. Gap junctional conductance between pairs of ventricular myocytes is modulated synergistically by H+ and Ca++. The Journal of General Physiology 95:1061-1075.

[110]. Sackmann EK, Fulton AL, Beebe DJ. 2014. The present and future role of microfluidics in biomedical research. Nature 507:181-189.

[111]. Beebe DJ, Glennys A, Walker MG, Walker M. 2002. Physics and Applications of Microfluidics in Biology. Annual Review of Biomedical Engineering 4:261-286.

[112]. Tehranirokh M, Kouzani AZ, Francis PS, Kanwar JR. 2013. Microfluidic devices for cell cultivation and proliferation. Biomicrofluidics 7:051502-1-051502-32.

[113]. Reyes DR, Iossifidis D, Aurox PA, Manz A. 2002. Micro total analysis systems. Introduction, theory, and technology. Analytical Chemistry 74:2623-2636.

[114]. Le Gac S, van den Berg A. 2010. Single cells as experimentation units in lab-on-a-chip devices. Trends Biotechnol 28:55-62.

[115]. Ranga A, Lutolf MP. 2012. High-throughput approaches for the analysis of extrinsic regulators of stem cell fate. Curr Opin Cell Biol 24:236-244.

[116]. Rouwkema J, Rivron NC, van Blitterswijk CA. 2008. Vascularization in tissue engineering. Trends Biotechnol 26:434-441.

[117]. van der Meer AD, van der Berg A. 2012. Organs-on-chips: breaking the *in vitro* impasse. Integrative Biology 4:461-470.

[118]. Luni C, Serena E, Elvassore N. 2014. Human-on-chip for therapy development and fundamental science. Current opinion in biotechnology 25:45-50.

[119]. Derby B. 2012. Printing and prototyping of tissues and scaffolds. Science 338:921-926.

[120]. Figallo E, Cannizzaro C, Gerecht S, Burdick JA, Langer R, Elvassore N, Vunjak-Novakovic G. 2007. Micro-bioreactor array for controlling cellular microenvironments. Lab on a Chip 7:710-719.

[121]. Wan CW, Chung S, Kamm RD. 2011. Differentiation of Embryonic Stem Cells into Cardiomyocytes in a Compliant Microfluidic System. Annals of Biomedical Engineering 39:1840-1847.

[122]. Huh D, Torisawa Y, Hamilton GA, Kim HJ, Ingber DE. 2012. Microengineered physiological biomimicry: Organs-on-Chips. Lab on a Chip 12:2156-2164.

[123]. Huh D, Matthews BD, Mammoto A, Montoya-Zavala M, Hsin HJ, Ingber DE. 2010. Reconstituting Organ-Level Lung Functions on a Chip. Science 328:1662-1668.

[124]. Young EWK, Beebe JD. 2010. Fundamentals of Microfluidic Cell Culture in Controlled Microenvironments. Chemical Society Review 39:1036-1048.

[125]. Discher DE, Mooney DJ, Zandstra PW. 2009. Growth factors, matrices, and forces combine and control stem cells. Science 324:1673-1677.

[126]. Yu H, Alexanderbc CM, Beebeac DJ. 2007. Understanding microchannel culture: parameters involved in soluble factor signaling. Lab on a Chip 7:726-730.

[127]. Thomas PC, Raghavan SR, Forry SP. 2011. Regulating Oxygen Levels in a Microfluidic Device. Analytical Chemistry 83:8821-8824.

[128]. Shamloo A, Xu H, Heilshorn S. 2012. Mechanisms of Vascular Endothelial Growth Factor-Induced Pathfinding by Endothelial Sprouts in Biomaterials. Tissue Engineering Part A 18:320-330.

[129]. Ashe HL, Briscoe J. 2006. The interpretation of morphogen gradients. Development 133:385-394.

[130]. Masuda S, Washizu M, Nanba T. 1989. Novel method of cell fusion in field constriction area in fluid integration circuit. IEEE Transactions on Industry Applications 25:732-737.

[131]. Mehta G, Lee J, Cha W, Tung Y, Linderman JJ, Takayama S. 2009. Hard Top Soft Bottom Microfluidic Devices for Cell Culture and Chemical Analysis. Analytical Chemistry 81:3714-3722.

[132]. Halldorsson S, Lucumi E, Gómez-Sjöberg R, Fleming RMT. 2015. Advantages and challenges of microfluidic cell culture in polydimethylsiloxane devices. Biosensors and Bioelectronics 63:218-231.

[133]. Chou HP, Thorsen T, Scherer A, Quake SR. 2000. Monolithic Microfabricated Valves and Pumps by Multilayer Soft Lithography. Science 288:113-116.

[134]. Heo YS, Cabrera LM, Song JW, Futai N, Tung Y, Smith GD, Takayama S. 2007. Characterization and Resolution of Evaporation-Mediated Osmolality Shifts That Constrain Microfluidic Cell Culture in Poly(dimethylsiloxane) Devices. Analytical Chemistry 79:1126-1134.

[135]. Kim L, Toh Y, Voldman J, Yu H. 2007. Tutorial Review: A practical guide to microfluidic perfusion culture of adherent mammalian cells. Lab on a Chip 7:681-694.

[136]. Giulitti S, Magrofuoco E, Prevedello L, Elvassore N. 2013. Optimal periodic perfusion strategy for long-term micorlfuidic cell culture. Lab on a Chip 13:4430-4441.

[137]. Beebe DJ, Moore JS, Bauer JM, Yu Q, Liu RH, Devadoss C, Jo B. 2000. Functional hydrogel structures for autonomous flow control inside microfluidic channels. Nature 404:588-590.

[138]. Berthier E, Beebe DJ. 2007. Flow rate analysis of a surface tension driven passive micropump. Lab on a Chip 7:1475-1478.

[139]. Whitesides GM, Ostuni E, Shuichi T, Xingyu J, Donald EI. 2001. Soft Lythography in Biology and Biochemistry. Annual Review of Biomedical Engineering 3:335-373.

[140]. Elveflow Plug&Play microfluidics website, www.elveflow.com.

[141]. Tesar PJ, Chenoweth JG, Brook FA, Davies TJ, Evans EP, Mack DL, Gardner RL, McKay RD. 2007. New cell lines from mouse epiblast share defining features with human embryonic stem cells. Nature 448:196-199.

[142]. Evans SM, Yelon D, Conlon FL, Kirby ML. 2010. Myocardial Lineage Development. Circulation Research 107:1428-1444.

[143]. Rozario T, DeSimone DW. 2010. The extracellular matrix in development and morphogenesis: A dynamic view. Dev Biol 341:126-140.

[144]. Kali K, Norrby K, Paca A, Mileikovsky M, Mohseni P, Woltjien K. 2009.Virus-free induction of pluripotency and subsequent excision of reprogramming factors. Nature 458:771-775.

[145]. Yu J, Hu. K, Smuga-Otto K, Tian S, Stewart R, Slukvin II, Thomson JA. 2009. Human Induced Pluripotent Stem Cells Free of Vector and Transgene Sequences. Science 324:797-801.

[146]. Kim D, Kim C, Moon J, Chung Y, Chang M, Han B, Ko S, Cha EYKY, Lanza R, Kim K. 2009. Generation of Human Induced Pluripotent Stem Cells by Direct Delivery of Reprogramming Proteins. Cell stem cell 4:472-476.

[147]. Fusaki N, Ban H, Nishiyama A, Saeaki K, Hasegawa M. 2009. Efficient induction of transgene-free human pluripotent stem cells using a vector based on Sendai virus, an RNA virus that does not integrate into the host genome. Proceedings on the Japan Academy, Series B 85:348-362.

[148]. Jia F, Wilson KD, Sun N, Gupta DM, Huang M, Li Z, Panetta NJ, Chen ZY, Robbins RC, Kay MA, Longaker MT, Wu JC. 2010. A nonviral minicircle vector for deriving human IPS cells. Nature Methods 7:197-199.

[149]. Keisuke O, Masato N, Hong H, Tomoko I, Yamanaka S. 2008. Generation of Mouse Induced Pluripotent Stem Cells Without Viral Vectors. Science 322:949-953.

[150]. Samedan LTD, Pharmaceutical Publisher website, www.samedanltd.com; magazine 12, issue 151, article 2902.

[151]. Yisraeli JK, Melton DA. 1989. Synthesis of long, capped transcripts in Vitro by SP6 and T7 RNA polymerases. Meth Enzymol 180:42-50.

[152]. Kreiter S, Selmi A, Simon P, Koslowski M, Huber C, Türeci Ö, Sahin U. 2006. Modification of antigen-encoding RNA increases stability, translational efficacy, and T-cell stimulatory capacity of dendritic cells. Blood 108:4009-4017.

[153]. Van den Bosch GA, Van Gluck E, Ponsaerts P, Nijs G, Lenjou M, Apers L, Kint I, Heyndrickx L, Vanham G, Van Bockstaele DR, Berneman ZN, Van Tendeloo VFI. 2006. Simultaneous Activation of Viral Antigen-specific Memory CD4+ and CD8+ T-cells Using mRNA-electroporated CD40-activated Autologous B-cells. Journal of Immunotherapy 29:512-523.

[154]. Diebold SS, Kaisho T, Hemmi H, Akira S, Reis e Sousa C. 2004. Innate Antiviral Responses by Means of TLR7-Mediated Recognition of Single-Stranded RNA. Science 303:1529-1531.

[155]. Ellegast J, Kim S, Brzózka K, Jung A, Kato H, Poeck H, Akira S, Conzelmann KK, Schlee M, Endres S, Hartmann G. 2006. 5'-Triphosphate RNA Is the Ligand for RIG-I. Science 314:994-997.

[156]. Pinchlmair A, Schulz O, Tan CP, Näslund TJ, Liljeström P, Welber F, Reis e Sousa C. 2006. RIG-I-Mediated Antiviral Responses to Single-Stranded RNA Bearing 5'-Phosphates. Science 314:997-1001.

[157]. Nallagatla SR, Bevilacqua PC. 2008. Nucleoside modifications modulate activation of the protein kinase PKR in an RNA structure-specific manner. RNA 14:1201-1213.

[158]. Nallagatla SR, Toroney R, Bevilacqua PC. 2008. A brilliant disguise for self RNA: 5′-end and internal modifications of primary transcripts suppress elements of innate immunity. RNA Biology 5:140-144.

[159]. Symons JA, Alcami A, Smith GL. 1995. Vaccinia virus encodes a soluble type I interferon receptor of novel structure and broad species specificity. Cell 81:551-560.

[160]. Lui KO, Zangi L, Chien KR. 2014. Cardiovascular regenerative therapeutics via synthetic paracrine factor modified mRNA. Stem Cell Research 13:693-704.

[161]. Zangi L, Lui KO, von Gise A, Ma Q, Ebina W, Ptaszek LM, Spater D, Xu H, Tabebordbar M, Gorbatov R, Sena B, Nahrendof M, Briscoe DM, Li RA, Wagers AJ, Rossi DJ, Pu WT, Chien KR. 2013. Modified mRNA directs the fate of heart progenitor cells and induces vascular regeneration after myocardial infarction. Nature Biotechnology 31:898-907.

[162]. Davis RL, Weintraub H, Lassar AB. 1987. Expression of a single transfected cDNA converts fibroblasts to myoblasts. Cell 51:987-1000.

[163]. Preskey D, Allison TF, Jones M, Mamchaoui K, Unger C. 2016. Synthetically modified mRNA for efficient and fast human iPS cell generation and direct transdifferentiation to myoblasts. Biochem Biophys Res Commun 473:743-751.

[164]. Xie H, Ye M, Feng R, Graf T. 2004. Stepwise reprogramming of B cells into macrophages. Cell 117:663-676.

[165]. Laiosa CV, Stadtfeld M, Xie H, de Andres-Aguayo L, Graf T. 2006. Reprogramming of Committed T Cell Progenitors to Macrophages and Dendritic Cells by C/EBPα and PU.1 Transcription Factors. Immunity 25:731-744.

[166]. Szabo E, Rampalli S, Risueno RM, Schnerc A, Mitchell R, Fiebyg-Comin A, Levadoux-Martin M, Bhatia M. 2010. Direct convertion of human fibroblasts to multilineage blood progenitors. Nature 468:521-526.

[167]. Zhou Q, Brown J, Kanarek A, Rajagopal J, Melton DA. 2008. In vivo reprograming of adult pancreatic exocrine cells to beta-cells. Nature 455:109-113.

[168]. Huang P, He Z, Ji S, Sun H, Xiang D, Liu C, Hu Y, Wang X, Hui L. 2011. Induction of functional hepatocyte-like cells from mouse fibroblasts by defined factors. Nature 475:386-389.

[169]. Caiazzo M, Dell'Anno MT, Dvoretskova E, Lazarevic D, Taverna S, Leo D, Sotnikova TD, Menegon A, Roncaglia P, Colciago G, Russo G, Carninci P, Pezzoli G, Gainetdinov RR, Gustincich s, Dityatev A, Broccoli V. 2011. Direct generation of functional dopaminergic neurons from mouse and human fibroblasts. Nature 476:224-227.

[170]. Chen JX, Krane M, Deutsch M, Wang L, Rav-Acha M, Gregoire S, Engels MC, Rajarajan K, Karra R, Abel ED, Wu JC, Milan D, Wu SM. 2012. Inefficient Reprogramming of Fibroblasts into Cardiomyocytes Using Gata4, Mef2c, and Tbx5. Circulation Research 111:50-55.

[171]. Inagawa K, Miyamoto K, Yamakawa H, Muraoka N, Sadahiro T, Umei T, Wada R, Katsumata Y, Kaneda R, Nakade K, Kurihara C, Obata Y, Miyake K, Fukuda K, Ieda M. 2012. Induction of Cardiomyocyte-Like Cells in Infarct Hearts by Gene Transfer of Gata4, Mef2c, and Tbx5. Circulation Research 111:1147-1156.

[172]. Nam YJ, Nam YJ, Luo X, Qi X, Tan W, Huang GN, Acharya A, Smith CL, Tallquist MD, Neilson EG, Hill JA, Bessel-Duby R, Olson EN. 2012. Heart

repair by reprogramming non-myocytes with cardiac transcription factors. Nature 485:599-604.

[173]. Qian L, Huang Y, Spencer CI, Foley A, Vedantham V, Lui L, Conway SJ, Fu JD, Srivastava D. 2012. In vivo reprogramming of murine cardiac fibroblasts into induced cardiomyocytes. Nature 485:593-598.

[174]. Bakker ML, Boink GJJ, Boukens BJ, Verkerk AO, van den Boogaard M, van den Haan AD, Hoogaars WMH, Buermans HP, de Bakker JMT, Seppen J, Tan HL, Moorman AFM, 't Hoen PAC, Christoffels VM. 2012. T-box transcription factor TBX3 reprogrammes mature cardiac myocytes into pacemaker-like cells . Cardiovascular Research 94:439-449.

[175]. Chan SS, Shi X, Toyama A, Arpke RW, Dandapat A, Iacovino M, Kang J, Le G, Hagen HR, Garry DJ, Kyba M. 2013. Mesp1 Patterns Mesoderm into Cardiac, Hematopoietic, or Skeletal Myogenic Progenitors in a Context-Dependent Manner. Cell stem cell 12:587-601.

[176]. Perrino C, Rockman HA. 2006. GATA4 and the Two Sides of Gene Expression Reprogramming. Circulation Research 98:715-716.

[177]. Chen C, Schwartz, R,J,. 1996. Recruitment of the tinman homolog Nkx-2.5 by serum response factor activates cardiac alpha-actin gene transcription. Molecular and Cellular Biology 16:6372-6384.

[178]. Bi W, Drake CJ, Schwarz JJ. 1999. The transcription factor MEF2C-null mouse exhibits complex vascular malformations and reduced cardiac expression of angiopoietin 1 and VEGF. Developmental Biology 211:255-267.

[179]. Hatcher CJ, Kim M, Mah CS, Goldstein MM, Wong B, Mikawa T, Basson CT. 2001. TBX5 Transcription Factor Regulates Cell Proliferation during Cardiogenesis. Dev Biol 230:177-188.

[180]. Qin H, Diaz A, Blouin L, Lebbink RJ, Patena W, Tanbun P, LeProust EM, McManus MT, Song JS, Ramalho-Santos M. 2014. Systematic Identification of Barriers to Human iPSC Generation. Cell 158:449-461.

[181]. Torchio E. Master Degree in Industrial Biotechnology, University of Padova, A.Y. 2013/2014. Riprogrammazione di cellule somatiche umane mediante mmRNA in piattaforme microfluidiche.

[182]. Itzhaki I, Rapoport S, Huber I, Mizrahi I, Zwi-Dantsis L, Arbel G, Schiller J, Gepstein L. 2011. Calcium Handling in Human Induced Pluripotent Stem Cell Derived Cardiomyocytes. PLoS ONE 6:e18037.

[183]. Fu JD, Yu HM, Wang R, Liang J, Yang HT. 2006. Developmental regulation of intracellular calcium transients during cardiomyocyte differentiation of mouse embryonic stem cells. Acta Pharmacologica Sinica 27:901-910.

[184]. Lee YK, Ng KM, Lai WH, Chan YC, Lau YM, Lian Q, Siu CW. 2011. Calcium Homeostasis in Human Induced Pluripotent Stem Cell-Derived Cardiomyocytes. Stem Cell Reviews 7:976-986.

[185]. Martewicz S, Serena E, Zambon A, Mongillo M, Elvassore N. 2012. Reversible alterations of calcium dynamics in cardiomyocytes during acute hypoxia transient in a microfluidic platform. Integrative Biology 4:153-164.

[186]. Bers DM. 2002. Cardiac excitation-contraction coupling. Nature 415:198-205.

[187]. Doppler SA, Deutsch M-, Lange R, Krane M. 2013. Cardiac regeneration: current therapies—future concepts. Journal of Thoracic Disease 5:683-697.

[188]. Vuoristo S, Toivonen S, Weltner J, Mikkola M, Ustinov J. 2013. A Novel Feeder-Free Culture System for Human Pluripotent Stem Cell Culture and Induced Pluripotent Stem Cell Derivation. PLoS ONE 8:76205.

[189]. Blazeski A, Zhu R, Hunter DW, Weinberg SH, Zambidis ET, Tung L. 2012. Cardiomyocytes derived from human induced pluripotent stem cells as models for normal and diseased cardiac electrophysiology and contractility. Prog Biophys Mol Biol 110:166-177.

[190]. van Weered JH, Koshiba-Takeuchi K, Kwon C, Takeuchi JK. 2011. Epigenetic factors and cardiac development. Cardiovascular Research 91:203-211.